Development of Flexible Fibre Biofilm Reactors for Treatment of Milk Processing Wastewater

Mohamed E Essa Abdulgader
B EnvSc
M EnvEng (Hons)

Griffith School of Engineering
Science, Environment, Engineering and Technology
Griffith University

Submitted in fulfilment of the requirements of the degree of
Doctor of Philosophy

December 2010

ABSTRACT

Food processing industries use considerable amounts of fresh water for their industrial purposes. These industries generate large quantities of high strength organic wastewaters which are usually biodegradable and amenable to biological treatment systems. Numbers of biological methods are still in use for the treatment of food processing wastewaters, either anaerobic or aerobic systems. In this research, the performance using newly developed laboratory scale sequencing batch flexible fibre biofilm reactor (SB-FFBR), single stage flexible fibre biofilm reactor (SS-FFBR) and newly developed multiple stage flexible fibre biofilm reactors (MS-FFBR) for treatment of milk processing wastewater were experimentally investigated.

A modified lab scale of 8 L working volume SB-FFBR was operated for a nearly 6-months period for the treatment of milk processing wastewater. The reactor performance was successfully evaluated under different influent COD concentrations and HRTs of 1, 1.6 and 2 days. The use of SB-FFBR proved a good strategy and obtained a successful result for the treatment of milk processing wastewater. A maximum of 97.5% and 99.3% of COD and TSS removal efficiency, respectively, were achieved at low OLR of 0.47 kg COD/m^3.d. However, the minimum COD and TSS removal efficiency of 86.8% and 77.3% were achieved with the increase the OLR to 8.2 kg COD/m^3.d. An inverse relationship was observed between COD and TSS removal efficiencies with respect to OLR. Conversely, a positive relationship was observed between COD and TSS removal rate versus OLR. The influence of SLR on SB-FFBR performance was also evaluated. The kinetic coefficients of COD removal were computed by using a first order substrate removal model at different COD concentrations. The first order kinetic constant, k, was 0.60, 0.65 and 0.357 h^{-1} for 500, 810 and 2000 mg COD/L, respectively. In this study, by using a SEM technique, biofilm morphology of the SB-FFBR was examined to define the nature and the structure of the developed biofilm attached to the flexible fibre. The results showed that use of the flexible fibre as a packing material provides a huge surface area for more microorganism attachment.

A laboratory scale SS-FFBR was used in the treatment of milk processing wastewater with an influent COD concentrations ranges of 800-4000 mg/L (corresponding OLR of 2.4-12 kg COD/m^3.d), and a HRT of 8, 12 and 16 h. A square shape 8-L SS-FFBR was

fabricated using acrylic plastic sheet consisting of 6 flexible fibre bundles. A 95% of COD removal efficiency at an average low influent COD concentration (809 mg/L) was obtained. The COD removal was slightly decreased to 91.7% as the influent COD concentration increased to nearly 4000 mg/L. The effect of OLR on the SS-FFBR performance was experimentally examined with some parameters such as TSS removal efficiency, DO, and turbidity. The SS-FFBR was able to increasingly support high OLR, but with a corresponding slight decrease on the COD removal efficiency, even at the highest OLR of 11.7 kg COD/m^3.d, the SS-FFBR achieved a good performance with 89.9% COD removal efficiency. A 96.7% of TSS removal efficiency was obtained at a low OLR of 1.145 kg COD/m^3.d. However, the removal efficiency of TSS declined to 89.7% at maximum OLR of 11.67 kg COD/m^3.d. In addition, both DO and turbidity increased with increase in the OLR. The aerobic treatment of milk processing wastewater was statistically modelled and analysed with variables, i.e HRT and COD_{in}, using response surface methodology (RSM). The COD removal efficiency increased with increasing the HRT and decreasing the COD_{in}.

A new multistage MS-FFBR with a working volume of 32 L was developed and operated for treatment of milk processing wastewater. The hydrodynamic characteristics and mass transfer coefficients of oxygen were studied. Tracer experiments were performed to obtain the residence time distributions of the MS-FFBR. The results revealed that the reactor's hydraulic regime is a CSTR in series model. The results showed lower K_{La} compared with those reported in literature. This indicated that the fibre packing in the reactor hindered the oxygen transfer to some extent.

A long term performance of the MS-FFBR was examined under different conditions. The reactor performance was assessed based on the contributions of intermediate stages and also final effluent quality of the overall system with ranges of COD_{in} between 1500 to 6000 mg/L (corresponding OLR of 2.4-17.6 kg COD/m^3.d), and a HRT of 8, 12 and 16 h. The stage COD removal efficiency was gradually decreased with an increase in number of stages and about 89.3, 82.2 and 78 % of TCOD removal for HRT of 16, 12 and 8 h HRT were removed in the first stage of MS-FFBR, indicating that the majority of significant TCOD concentration occurs in this stage. However, the first stage had a less contribution at high COD_{in} concentrations, which were about 42, 46.3 and 25% COD removal at 5956, 5827 and 5869 mg/L, respectively. The cumulative TCOD and SCOD removal efficiency increased subsequently as the number of stage increased. As

a result, the first and second stages seemed to contribute more efficiently than other stages. The MS-FFBR was very effective in removing TSS and turbidity. The overall performance of the MS-FFBR was satisfactory. The MS-FFBR could support increasingly high OLR, but with a corresponding decrease in the TCOD, TSS, turbidity. Experimental results indicated that a 94.8% was obtained at 2.4 kg COD/m^3.d, whereas the COD removal efficiency decreased to 69% at the highest OLR of 17.6 kg COD/m^3.d.

Experiments on the MS-FFBR were also conducted based on a central composite face-centred design (CCFD) and modelled using response surface methodology (RSM) with two operating variables, i.e hydraulic retention time (HRT) and influent COD concentration (COD_{in}). The system performance was evaluated by measuring different responses (TCOD, SCOD, $TBOD_5$, $SBOD_5$, TSS removal efficiency, turbidity, pH, SRT and U). By applying RSM, the optimum range of the OLR was found to be between 5.5 and 7.2 kg COD/m^3.d. A mathematical model based on Monod growth kinetics was successfully employed to describe the substrate removal of the process. The kinetic coefficients K_s, K_d, Y and μ_{max}, were found to be 0.133 g COD/L, 0.113 d^{-1}, 0.237 gVSS/gCOD and 0.098 d^{-1}, respectively at 8 h. The biofilm morphology was also conducted in each stage and showed no significant difference.

STATEMENT OF ORGINALITY

This work has not previously been submitted for any degree or diploma in any university and is not concurrently submitted in candidature of any degree. To the best of my knowledge and belief, the thesis contains no material previously published or written by other person except where due reference is made in the thesis itself.

Mohamed E.ESSA. Abdulgader

December 2010

ACKNOWLEDGEMENTS

It has been a most challenging journey for me to complete this thesis and it would not have been possible without the support of several people in Griffith School of Engineering, Griffith University, to whom I would like express my gratitude. First, I would like to thank my principal supervisor, Dr. Jimmy Yu, for his advices, guidance and patience in helping me to finalise my thesis and assisting me to undertake my PhD in the area of environmental engineering. I also give my sincere thanks to Dr. Phillip Williams for his opinions and valuable suggestions that helped to make this work possible. I am very grateful as well to Dr. Ali Zinatizadeh for his constructive comments and generous supports, especially during experimental works.

My deep appreciation also goes to Jane Gifkins and Scott Byrnes for their laboratory assistance and also I would like to show my gratitude to Dr Deb Stenzel for her assistance and generous support of using scanning electron microscopy at Queensland University of Technology (QUT) laboratory. I am likewise grateful to National Foods Company for providing me with samples to work on during my laboratory experiments.

I owe deep thanks to the staff of Griffith School of Engineering at Griffith University for their kind support that facilitated the laboratory work and for providing me with the equipments I needed, from the smallest tools to the largest, and eliminating any difficulties I may have faced during my research and study. I am also indeed grateful to the Libyan Ministry of Higher Education for the financial support and Libyan Peoples Bureau for their concerns through all my study.

Last but not least, my deepest gratitude to my wife for her support, patience and concern, and acknowledges my dear sons Abdulmalik and AbdulMu'ez who have provided me with many enjoyable moments during my study. Special thanks and appreciation go to my father and mother for their love and prayers. Many thanks are also to my brothers and sisters for their concerns. And also, many thanks to my cousin Ali Abdullah Saleh for his efforts to follow up all my documents needed in Libya.

TABLE OF CONTENTS

LIST OF FIGURES

LIST OF TABLES

LIST OF ABBRIVATIONS

2FI	Two Factor Interaction
AAO	Anaerobic-Aerobic-Oxnice
AD	Anaerobic Digestion
AF	Anaerobic Filter
AFB	Anaerobic Fluidized Bed
AFFR	Anaerobic Fixed Film Reactors
AFFR	Anaerobic Fixed Film Reactor
AFR	Air Flow Rate
AJLR	Aerobic Jet Loop Reactors
AL	Aerated Lagoons
AMBBR	Anaerobic Moving Bed Biofilm Reactor
ANOVA	Analysis of Variance
APSBBR	Alternating Pump Sequencing Batch Biofilm Reactor
AS	Activated Sludge
ASBR	Anaerobic Sequencing Batch Reactor
ASFF	Submeraged Fixed Bed Reactro-- Hamouda
ASP	Activated Sludge process
BOD_5	Biochemical Oxygen Demand
CCD	Central Composite Design
CCFD	Central Composite Faced-centred Design
COD	Chemical Oxygen Demand
COD_{eff}	Effluent COD
COD_{in}	Influent Chemical Oxygen Demand
CSTR	continuous Stirred Tank Reactor
CV	Coefficient of Variance
DFFR	Down Flow Fixed Film Reactor
DO	Dissolved Oxygen
DoE	Design of Experiment
DSFF	Down Flow Stationary Fixed Film
F/M	Food: Microorganisms Ratio
FBBR	Fixed Bed Biofilm reactors
FBR	Fluidized Bed Reactors
FFBR	Fixed Film Bioreactor
FFBR	Flexible Fibre Biofilm Reactor
GL	Gigalitres
h	Hour
HRT	Hydraulic Retention Times
IFBR	Inverse Fluidized Bed Reactors
K	First Order Rate Constant
K_{La}	Oxygen Mass Transfer Coefficient
KMT	Kaldnes Miloteknologi
L	Litre
L*W*D	Length*Width*Deep
L/h	Litre per Hour
MBBR	Moving Bed Biofilm Reactor
mg/L	Milligram per Litre
ml/L	Milliliter per Litre
MLSS	Mixed Liquor Suspended Solids
MLVSS	Mixed Liquor Volatile Suspended Solids
mm	Millimetre

MS-FFBR	Multi Stage Flexible Fibre Biofilm Reactor
NTU	Nephelometric Turbidity Units
O & G	Oil and Grease
OLR	Organic Loading Rate
OUR	Oxygen Uptake Rate
PAC	Poly-Aluminium Chloride
POME	Palm Oil Mill Effluent
QF	Feed Flow Rate
R^2	Coefficient of Determination
RBC	Rotating Biological Contactor
RSM	Response Surface Methodology
SBBR	Sequencing Batch Biofilm Reactor
SBBR	Sequencing Batch Biofilm Reactor
SB-FFBR	Sequencing Batch Flexible Fibre Biofilm Reactor
$SBOD_5$	Soluble Biochemical Oxygen Demand
SBR	Sequencing Batch Reactor
SCOD	Soluble Chemical Oxygen Demand
SEM	Scanning Electron Microscopy
SLR	Solid Loading Rate
SRT	Sludge Retention Times
SRT	Sludge Retention Time
SS-FFBR	Single Stage Flexible Fibre Biofilm Reactor
SVI	Sludge Volume Index
$t_{1/2}$	Half Life of First Order Reactor
$TBOD_5$	Total Biochemical Oxygen Demand
TCOD	Total Chemical Oxygen Demand
TF	Trickling Filter
TKN	Total Kjeldahl Nitrogen
TN	Total Nitrogen
TP	Total Phosphorus
TPAD	Two-Phase Anaerobic Digestion
TSS	Total Suspended Solids
U	Substrate Utilization Rate
UAF	Upflow Anaerobic Filter
UAF	Up-flow Anaerobic Filter
UASB	Up-flow Anaerobic Sludge Blanket
UASFF	Up-flow Anaerobic Sludge Fixed Film
UBF	Upflow Anaerobic Bed
VLR	Volumetric Loading Rate
VMSBBR	Vertically Moving Sequencing Batch Biofilm Reactor
VSS	Volatile Suspended Solids
WFR	Water Flow Rate

LIST OF PUBLICATIONS

The following papers also form part of this thesis:

Abdulgader, Mohamed; Yu, Jimmy; Zinatizadeh, A.A.L; Williams, Philip. *Biological treatment of milk processing wastewater in a sequencing batch flexible fibre biofilm reactor*. Asia-Pacific Journal of Chemical Engineering, Vol. 4(5), pp. 698-703, 2009.

Abdulgader, Mohamed; Yu, Jimmy; Williams, Philip; Zinatizadeh, A.A.L. *A review of the performance of aerobic bioreactors for treatment of food processing wastewater*. Proceedings of the International Conference on Environmental Management, Engineering, Planning and Economics, 2007.

Abdulgader, Mohamed; Yu, Jimmy; Williams, Philip; Zinatizadeh, A.A.L. *Biological Treatment of Dairy Wastewater by a Sequencing Batch Flexible Fibre Biofilm Reactor*. Proceeding of the Ninth International Conference on Modeling, Monitoring and Management of Water Pollution, Spain, 2008.

Abdulgader, Mohamed; Zinatizadeh, A.A.L.; Williams, Philip; Yu, Jimmy. *Feasibility of an aerobic sequencing batch flexible fibre biofilm reactor for treatment of milk processing wastewater*. Proceedings of AWA Ozwater 2009 Conference, 2009.

CHAPTER 1 INTRODUCTION

1.1 Background

Increasing industrialization and rapid urbanization have significantly increased the rate of water pollution. Water is an imperative constituent of many food processing industries. Food processing industries occupy a central position economically and are considered one of the fastest growing manufacturing sectors. The amount of water utilises by such industries varies greatly depending on the type of processing. However, they generally consume relatively large amounts when compare with other manufacturing sectors (Dalzell, 1994). The Australian food processing industry uses approximately 215 GL of water annually (Wallis et al., 2007) in various food industries. The total amount of water consumes by the Australian dairy industry is approximately 3000 GL/year, which is equivalent to 13% of Australia's total freshwater resources (Lunde et al., 2003; Prasad et al., 2005). Such a large volume of water is necessary to ensure the quality control and hygiene standards needed by the food processing industry. Water is usually used for cleaning of equipment, operation of utilities such as boilers, cooling tower and pumps, and additional activities, such as toilets and washing facilities. Hence, large amounts of biodegradable wastewaters are discharged as a result of the water used in these industries.

Large quantities of high strength organic wastewaters are generated by food processing industries each year, and consequently may result in significant environmental impacts. It has been reported that approximately more than 80 billion gallons of wastewater are produced annually from processing a variety of fruits and vegetables in the United States (Hang, 2004). The amount of wastewater produced from the dairy industry in the United States averaged of 2.52 kg wastewater/ kg milk of wastewater discharged, while about 1.5 L of wastewater was produced for every litre of raw milk in the Australian dairy industry (Australian Dairy, 2007). These wastewaters may become a major problem for these industries. Waste can be categorized as a complex combination of organic matter either in a soluble or as volatile suspended form and as well as a high level of nutrients. Moreover, the types of the process, the size, age of the plant and the seasons are factors that affect volume and strength of wastewater generated from food processing industries (Gray, 2004). In food processing wastewaters, more than 80% of the total organic matters are soluble (Alvarado-Lassman et al., 2008). The natural organic compounds of food processing wastewater are usually biodegradable and

amenable to biological treatment processes (Yu et al., 2003). Food processing industries are increasingly faced with the problem of treating their wastewaters before releasing them to municipal wastewater treatment plants or to the receiving environment. Consequently, the high cost of wastewater treatment for food industry wastes and increasingly stringent effluent regulations have increased interest in optimizing treatment methods.

1.2 Food Processing Wastewater Treatment Systems

The selection of an appropriate treatment system for food processing wastewater is normally based on the quality of the effluent needed to meet regulatory (eg EPA) standards, the characteristics and strength of the particular wastewater, and operational cost (Metcalf and Eddy, 2003; Sirianuntapilboon et al., 2005). Wastewaters from food processing industries are complex and may require complete treatment using a combination of physical, chemical and biological treatment systems. Various wastewater treatment options are also applied to transform harmful organic and inorganic substances and also when the wastewater is rich in nutrients (El-Gohary et al., 1999; Gavrilescu and Macoveanu, 1999; Metcalf and Eddy, 2003). Chemical and physical treatment processes are occasionally used to reduce the organic content of food processing effluents. However, these processes are insufficient to achieve high organic removal. In addition, they may involve high chemical costs, and difficulties with disposing of the large volume of sludge. Thus, biological systems are typically preferred to treat food processing wastewaters.

Food processing effluents require a dynamic and comprehensive approach for suitable and reliable waste management. Biological treatments become the best process for wastewater treatment as they infrequently contain toxicants or inhibitory compounds (Bertola et al., 1999; Oliva et al., 1995). The choice of either aerobic or anaerobic systems for treatment of municipal and industrial wastewater depends on the characteristics of the wastewaters. The application of anaerobic processes for the treatment of strong organic wastewaters which contain BOD_5> 500 mg/L is desirable (Gray, 2004). Whilst anaerobic reactors are slow, they can be used to treat strong organic wastewaters, such as those discharged by agriculture and food industry wastewater. These systems have disadvantages in producing undesirable gases, such as methane and hydrogen sulfide, which will create more complexity in treating wastewater if there are no facilities to remove or store biogas. Additional expenses and

equipment are required for the plant to remove the gases safely. Anaerobic treatment process equipment must be constantly inspected to ensure that there are no leaks, as oxygen or air leaked into the system would create disturbance in the progress of the treatment. This process has generally been unable to obtain a high quality effluent suitable for direct discharge. The effluent contains solubilised organic matter that is amenable to quick aerobic treatment, which indicates that the anaerobic process cannot comply with standards for discharge into natural water environments and must be always complemented by aerobic processes. Hence, aerobic methods are generally considered to be more cost-effective overall (El Defrawy and Shaalan, 2003; Gray, 2004; Tawfik et al., 2002).

Aerobic processes can be divided into two main types: suspended growth systems and attached growth (biofilm) systems. The conventional activated sludge process (CASP) is one of the suspended growth processes, and is the most extensively applied biological treatment for both domestic and industrial wastewaters due to its simplicity in operation and ability to produce a high quality effluent. However, the process also has many drawbacks. The microorganisms in the aeration tank of the CASP cannot survive a continuous shock loading rate and the process could become operationally unstable (Eckenfelder and Musterman, 1995). The process also generates high amounts of sludge, often with a high bulking problem due to high organic loading, in which the settling of the sludge is reduced (Gray, 2004). In addition, the performance of the process becomes low.

Most recently, biological attached growth systems have gained more attention and have proven to be efficient alternatives for treatment of carbonaceous and nitrogenous pollutants. These have been used for wastewater treatment since the early development of the tickling filter in the nineteenth century (Gray, 2004). The attached growth process can be divided into two types: the fixed support media in which the wastewater uniformly passes over the medium such as in the trickling filter (TF), or moving support media, where the medium moves through the wastewater, for instance the rotating biological contactor (RBC) and fluidized bed reactor (FBR) (Droste, 1997). The development of an active thin layer of microorganisms is identified as biofilm, which plays an important role in the success of any fixed film process. The long residence time of the sludge and the high density of the microorganisms attached to the support media can lead to the process being much more resistant to various shock loads (Gray, 2004).

The attached growth system appears to be more operationally stable when compared with the suspended growth processes. In contrast, biofilm reactors can be more complicated in operation and may require high capital and operating costs.

The trickling filter, rotating biological contactor, and fluidized bed reactor have gained much interest in recent years for treatment of food processing wastewater due to a good performance compared with conventional activated sludge processes. Biofilm bed bioreactors and fixed bed film reactors are also beginning to be used in the treatment of many food processing wastewaters. Application of these technologies for the food processing industry is still in a developmental stage and successful demonstrations are required. Most of these systems are well suited for treating highly soluble waste, but not for handling wastewater containing high levels of suspended solids. Efficient treatment methods are sought to help food processing industries to manage their wastewater efficiently. However, the main drawback of attached growth processes is that a high bulk dissolved oxygen (DO) concentration is needed to drive the diffusion of oxygen into the biofilm (Vanhooren et al., 2002).

This research investigates the performance of sequencing batch flexible fibre biofilm reactors (SB-FFBR), single stage flexible fibre biofilm reactors (SS-FFBR), and a newly developed multistage flexible fibre biofilm reactor (MS-FFBR) for the treatment of milk processing wastewater. This approach can overcome all the problems associated with traditional biofilm systems. The flexible fibres provide a very high surface area for microorganisms to grow on (around 2200 m^2/m^3). It brings together all the advantages offered by activated sludge process as well as biofilm reactors, at the same time avoiding the worst effects from all conventional methods. Sludge bulking in the conventional biofilm reactor can be eliminated through the intensive motion of the fibre caused by air mixing. The flexible fibre biofilm reactors have the potential as an appropriate substitute system for the conventional processes in the treatment of food processing wastewaters, because of their high effluent quality and efficient performance, robustness, moderate cost, ease of construction, low maintenance and simple operation.

The development of effective and simple methods for treatment of industrial wastewater is a challenging task to environmental engineers and scientists. The new wastewater treatment processes should have the capacity to effectively remove the carbonaceous

organic materials, suspended solids, and also nutrients. This research represents a major new technical approach to enhance the treatment capability and the performance of the existing attached growth processes. The major drawbacks associated with the conventional biofilm treatment systems are substrate mass transfer resistance caused by biofilm thickness and occasional instability resulted from sloughing. In this project, our attempt was to present a new treatment approach to overcome the above mentioned problems. Therefore, treatment of milk processing wastewaters or various types of wastewaters using a SB-FFBR has not used before. The literature search showed that this is the first attempt to use and also carry out the kinetics. In addition, a single and multi stage FFBRs were designed fabricated and examined treating milk processing wastewater, and MS-FFBR has also not been experimentally or theoretically studied before. Development of the flexible fibre biofilms provided a large surface area and the biofilm thickness control. In this, the process kinetic analysis as well as process modelling and optimization were successfully performed using RSM and the optimum conditions were determined for scale up purposes.

1.3 Scope of the Study

The main focus of the present study is to assess the treatability and the performance of three types of lab-scale flexible fibre biofilm reactors: sequencing batch flexible fibre biofilm reactors (SB-FFBR), single stage flexible fibre biofilm reactors (SS-FFBR), and a developed multistage flexible fibre biofilm reactor (MS-FFBR) for the treatment of milk processing wastewater. A laboratory scale SB-FFBR (8 L) was fabricated to study its performance for treatment of milk processing wastewater for a period of nearly 6 months. The system performance was assessed under different influent COD concentrations and hydraulic retention time HRT (1, 1.6 and 2 days) using parameters such as COD removal, TSS removal, pH and turbidity. The results obtained were used for kinetics study, employing a suitable kinetics model. Biofilm morphology was also conducted at the end of the experiments.

Long term performance of the SS-FFBR was evaluated for raw milk processing wastewater with an HRT of 8, 12 and 16 hours and influent COD ranges from 800-4000 mg/L. After successful start-up, the steady state reactor performance and the effect of organic loading rate on the reactor performance was evaluated experimentally. The interactive effect of two important process variables on the process responses was investigated using response surface methodology (RSM).

A new developed MS-FFBR was built and operated for treatment of raw milk processing wastewater with an influent COD concentrations ranges of 1500-6000 mg/L (corresponding OLR of 2.4-7.6 kg COD/m^3.d), and a HRT of 8, 12 and 16 h. Long term performance of the MS-FFBR was evaluated under different conditions, and effect of OLR on the reactor performance was also assessed. The aerobic process was modelled using RSM with two operating variable (HRT and influent COD_{in} concentration) and eight responses. A kinetics model using the Monod equation was employed in the kinetics study of MS-FFBR. The SEM technique was used to investigate the morphology of the biofilm in each stage. All above FFBR reactors are developed to examine the effectiveness of this technology in the treatment of high strength milk processing wastewaters.

1.5 Thesis Organisation

This thesis consists of eight chapters. Chapter 1 provides a general introduction, the issues of biological treatment, and scope of the study. The aim and objectives of the study are outlined in Chapter 2. Chapter 3 (Literature Review) presents a comprehensive review of the performance of biological anaerobic and aerobic treatment systems. Process modelling using response surface methodology is also reviewed and, more briefly kinetics analysis of the aerobic biological processes (suspended and attached growth system). Chapter 4 (Materials and Methods) covers the details of the materials and chemicals used, experimental set-up, and details on the experimental procedures, which include studies of the SB-FFBR, SS-FFBR and MS-FFBR performance and analytical techniques.

The results and discussion of this research are divided into three chapters. Chapter 5 presents and discusses the treatment of milk processing wastewater in the sequencing batch flexible fibre biofilm reactor. This chapter covers the performance of the reactor under different HRT and COD_{in}. Chapter 6 introduces the performance of the single stage flexible fibre biofilm reactor for treatment of milk processing wastewater. The effects of the OLR and SLR on the reactor performance are discussed. Chapter 7 illustrates the development and performance of a multistage flexible fibre biofilm reactor (MS-FFBR) for milk processing wastewater treatment. The hydraulic retention time distribution and oxygen mass transfer are also described. The contributions of the reactor stages on the reactor performance are discussed, and then the effects of OLR on the whole system performance.

The details of the process modelling for milk processing wastewater treatment in the SS-FFBR and MS-FFBR process using response surface methodology (RSM) are encompassed in Chapters 6 and 7. The kinetics evaluation of the bioprocess was carried out based on COD removal are indicated in Chapter 7. A brief explanation of the morphological study on the flexible fibre biofilm using SEM techniques is given in Chapters 5 and 7. Chapter 8 (Conclusions) summarises the findings from the current studies.

CHAPTER 2 RESEARCH AIM AND OBJECTIVES

Biofilm systems have found a growing field of applications in industrial wastewater treatment because of the weaknesses associated with using the conventional activated sludge processes. A comprehensive understanding of the factors affecting the performance and treatability is therefore essential in choosing suitable wastewater treatment methods. For this reason a newly developed biofilm reactor needs to be studied. Since the flexible fibre reactors are relatively new as compared to other types of biological processes, our understanding of such a process is still insufficient. To achieve its successful application, it is necessary to assess such a system in greater depth. The aim of this thesis is to develop and evaluate the performance and the treatability of new developed flexible fibre biofilm reactors (sequencing batch flexible fibre biofilm reactor (SB-FFBR), single stage flexible fibre biofilm reactor (SS-FFBR) and multiple stage flexible fibre biofilm reactors (MS-FFBR)) for treatment of milk processing wastewater.

The following objectives were decided on to achieve the overall aim of the research:

- To conduct a comprehensive literature review on the performance of aerobic and anaerobic biological treatment processes utilized to treat various industrial food processing wastewaters;
- To evaluate experimentally the performance of the SB-FFBR in treatment of milk processing wastewater investigating the effect of organic loading rate (OLR) and solid loading rate (SLR) on the SB-FFBR performance under different hydraulic retention times (HRT);
- To establish the kinetic analysis of SB-FFBR and to determine the kinetic parameters of the process;
- To evaluate experimentally the performance of the lab-scale SS-FFBR in the treatment of milk processing wastewater at various operating conditions, and also to study the effects of OLR on COD removal efficiency and effluent quality of the SS-FFBR;
- To investigate the simultaneous effects of the operating variables, HRT and influent COD concentration (COD_{in}) on the process response parameters using a response surface methodology (RSM).
- To design, fabricate and develop a new lab-scale multiple stage flexible fibre biofilm reactor (MS-FFBR) for treatment of milk processing wastewater;

- To study the performance and effectiveness of the lab-scale MS-FFBR experimentally in the treatment of raw milk processing wastewater. The effects and contributions of individual stages on the reactor performance were explored at different ranges of operating conditions; and to evaluate the effect of OLR on the overall MS-FFBR performance;
- To analyse, model and optimize the performance of the lab-scale MS-FFBR in the treatment of milk processing wastewater treatment using response surface methodology (RSM) with respect to the simultaneous effects of two independent operating variables, i.e. HRT and COD_{in};
- To evaluate the kinetic of the treatment process in MS-FFBR and determine the kinetics constants using mass balance based model;
- To study the morphology of the biofilm developed in all stages of the MS-FFBR by using SEM technique and to identify the dominant microorganisms in the biofilm.

CHAPTER 3 LITERATURE REVIEW

3.1 Introduction

Development of new aerobic biological treatment processes to achieve a higher treatment performance with low operational costs is a key objective of biological wastewater treatment. This chapter provides a brief review of several different types of food processing wastewater characteristics, focussing on the performance of aerobic and anaerobic biological wastewater treatment processes. A detailed overview of the performance of aerobic suspended and attached treatment processes treating a wide range of food processing wastewaters is included. A comparison of the performance between suspended and attached growth systems is included. The design of an experiment using response surface methodology (RSM) which was applied in this research to model and optimize the process is also discussed. Finally, a brief review of model development in suspended growth and attached growth processes will provide basic knowledge for the kinetic modelling addressed in this study.

3.2 Food Processing Wastewater Characteristics

Food processing industries typically consume large quantities of water. The average consumption of water expressed as water to product ratio is 10:1 (Dalzell, 1994; Dincer and Kargi, 2001). The main reasons for the production of large quantities of food processing wastewater are the hygiene and quality control requirements. As an example, approximately 1.4 million m^3 of wastewater are generated annually in the USA from 20,000 food processing industries (Oh and Logan, 2005). The chemical and biological components of the wastewater streams of most concern to food processing industries are the high concentrations of carbon, nitrogen and phosphorus, as well as total suspended solids. Wastewater characterization is essential for designing biological treatment systems. This is also important in the evaluation of existing facilities for optimizing performance and available treatment capacity (Metcalf and Eddy, 1991, 2003). The main characteristics of some food processing wastewater are summarized in Table 3.1.

Wastewater characteristics vary significantly between industries. With dairy wastewater, the typical problem is a high concentration of lactose, fats and proteins from milk (Xu and Yu, 2000). The data in Table 3.1 show that dairy wastewater contains a high level of COD typically ranging between 1155-10,000 mg/L, and it could be more than that depending on the nature of the industry. The BOD_5 concentration is

typically 6450 mg/L for milk processing wastewater. The TSS ranges between 340-1730 mg/L. In addition, high concentration of nutrients corresponding to TKN ranging from 14-272 mg/L and TP of 8-70 mg/L are typically present. In meat processing wastewater, the typical characteristics are slightly different from dairy wastewaters. It contains a COD concentration approximately of 4976 mg/L with the TSS concentration at about 1348 mg/L. The nutrient levels of TKN and TP concentration are about 372 mg/L and 10-30 mg/L, respectively. Meat processing wastewater characteristics are significantly different from the other food processing wastewaters. They contain a high concentration of oil and grease, ranging from 110-1228.5 mg/L, as well as blood and faeces (Xu and Yu, 2000).

Some examples of COD concentration are 6000 mg/L in seafood wastewaters, 2000-8240 mg/L in brewery wastewater, 688-1612 mg/L in sugar processing wastewaters, 4800-9025 mg/L in potato processing wastewater, 6953 mg/L in tomato canning wastewater, and in coffee wastewater, the concentration of total COD ranges between 3429-40,000 mg/L. For BOD_5 concentrations, potato processing wastewater contains a range of 1200-3650 mg/L; similarly, tomato processing wastewaters have approximately 6953 mg/L of BOD_5. In coffee processing wastewater, the BOD_5 is in the range of 1837-3242 mg/L. A low level of BOD_5 was detected in sugar processing wastewater, which ranges between 555-1290 mg/L and in meat processing wastewater; the BOD_5 was in the range of 646-1792 mg/L.

The concentration of suspended solids in foods processing wastewater is also significantly different. A high concentration is typical in potato and coffee processing wastewater with a range of 1300-5340 mg/L and 10,000-27,500 mg/L, respectively. Other wastewaters, such as tomato processing wastewaters contain 1380 mg/L, and brewery wastewaters contain SS in the range of 2701-3000 mg/L. The sugar processing wastewaters contain suspended solids concentration of 560-6690 mg/L. The nutrient level in terms of TKN was 540 mg/L in seafood processing wastewater, 151.4 mg/L in tomato processing wastewater, in coffee processing wastewater in the range of 80-120 mg/L, and 0.0196-80 mg/L in brewery wastewaters. In addition, TP is in the range of 8-120 mg/L in seafood processing wastewater, 5.3-124 mg/L in brewery processing wastewater, and 47.5 mg/L in tomato processing wastewater. The level of oil and grease in potato processing wastewater was in the range of 400-1000 mg/L, and it decreased in dairy wastewater in the range of 7-500 mg/L.

Table 3.1: Characterization of food processing wastewater summary

Sources of wastewater	Characteristic of wastewater (mg/L)					
	COD	BOD_5	SS	TKN	TP	Oil and grease
Dairy	1155-10,000	6450	340-1730	14-272	8-70	7-500
Meat processing	4976	646-1792	1348	372	10-30	110-1228.5
Sea food	6000	NA	280	540	8-120	NA
Potato processing	4800-9025	1200-3650	1300-5340	NA	NA	400-1000
Brewery	8240	NA	2901-3000	0.0196-80	5.3-124	NA
Sugar	688-1612	555-1290	560-6690	NA	NA	NA
Tomato canning	6953	3406	1380	151.4	47.5	NA
Coffee	3429-40,000	1837-3242	10,000-27,500	80-120	NA	NA

3.3 Biological Treatment of Food Processing Wastewater

An understanding of the characteristics of each biological process is necessary to ensure that a suitable environment is implemented for the wastewater treatment. Biological wastewater treatment is primarily used to remove dissolved and non-settleable colloidal solids. It is used to stabilize and remove biologically the organic matter and nutrients (N and P) (Droste, 1997; Gray, 2004). Biological treatment depends solely on the microbial growth in the system. Thus it is important for the microorganisms to reproduce and function properly at optimum conditions. There are five major biological wastewater treatment processes, each varying in complexity and efficiency. All these are based on degradation processes occurring naturally (Metcalf and Eddy, 2003) and will be discussed in the following sections.

3.3.1 *Anaerobic Treatment*

Anaerobic processes have been recognized as a viable means for industrial wastewater treatment. These methods involve the degradation of organic and inorganic matter in the absence of molecular oxygen. The anaerobic degradation of high molecular weight organic pollutants in wastewater is usually achieved by a complex group of microorganisms that produce a large amount of biogas such as methane (CH_4) and carbon dioxide (CO_2), as well as smaller amounts of sludge, and other trace biogases as waste stabilization end products (Droste, 1997). The anaerobic biological conversion of organic matters involves three main discrete stages. The first step is hydrolysis, which is an enzyme-mediated transformation of higher-molecular-mass compounds into compounds suitable for use as energy and cell carbon source. The second stage is

acidogenesis (acid formation), which involves bacterial conversion of the compounds produced by the first process into identifiable lower-molecular-mass intermediate compounds. The final step is methanogenesis, whereby the intermediate compounds go through bacterial conversion into simpler end products such as methane and carbon dioxide (Droste, 1997). In practice, about 70% of the methane produced is from acetic acid. The methanogenic step is entirely dependent on the generation of acetic acid (Gray, 2004).

The application of anaerobic processes for the treatment of strong organic wastewaters which contain BOD> 500 mg/L is desirable (Gray, 2004). Treatment of various types of food processing wastewaters has been examined by a wide range of anaerobic methods and approaches (Demirel et al., 2005; Ke et al., 2005; Mittal, 2006; Saravanane and Murthy, 2000). Considerable research and development for performance of various types of high loading anaerobic reactor configuration has been successfully employed for the treatment of food processing wastewaters, including Anaerobic Digestion (AD) (Berardino et al., 2000; Del Nery et al., 2007; Dinsdale et al., 1996); Upflow anaerobic filter (UAF) (Córdoba et al., 1984; Guiot and van den Berg, 19985; Omil et al., 2003; Prasertsan et al., 1994; Veiga et al., 1994), Anaerobic Sequencing Batch Reactor (ASBR) (Dugba and Zhang, 1999; Garrido et al., 2001; Ruiz et al., 2002); Anaerobic fixed film reactor (AFFR) (Borja et al., 1995; Del Pozo et al., 2000); Anaerobic fluidized bed (AFB) (Saravanane and Murthy, 2000), and Upflow anaerobic sludge blanket (UASB)(Oliva et al., 1995; Rintala and Lepisto, 1997; Zoutberg and Eker, 1999). The following sections present an overview of the performance of some of the anaerobic methods used in treatment of food processing wastewaters.

3.3.1.1 Up-flow Anaerobic Sludge Blanket (UASB) Reactor

The upflow anaerobic sludge blanket (UASB) system is commonly used high rate anaerobic treatment process. The UASB reactor as a high rate anaerobic reactor is deemed desirable for high-strength organic wastewater treatment due to its high biomass retention ability and rich microbial diversity (Fang et al., 1989; Grady et al., 1999; Zinatizadeh et al., 2006). The wastewater is introduced at the bottom of the reactor, and is consumed when it passes through the sludge blanket bed. The waste is degraded to CH_4 and CO_2. Gas formation and evolution will give adequate mixing to the sludge bed (Droste, 1997). The UASB process has positive characteristics that tolerate high organic loading rate (OLR), short hydraulic retention time (HRT), and has

low energy demand (Metcalf and Eddy, 2003). The development of granular sludge is the most significant feature of UASB reactors when compared to other anaerobic processes, and it is reported to be more sensitive to waste composition (Droste, 1997; Metcalf and Eddy, 2003). Nutrients, pH, and up-flow velocity also affect the development of granulated sludge. The presence of other suspended solids in the sludge blanket may have an inhibiting effect on the density and formation of granular sludge (Lettinga and Hulshoff Pol, 1991).

The most important features governing reactor heights are the treatability of the wastewater and the efficiency of granular formation. Upflow velocities in typical UASB reactors usually range 1-2 m/h, although Lettinga and Hulshoff-Pol, (1991) and van Haandel and Lettinga (1994), recommend that the average daily upflow velocity should not exceed 1 m/h. The reactor heights should be between 3 and 5 m. The COD loading that can be applied through the UASB ranges from 0.5-40 kg COD/m^3.d and the HRT can be 1 day or less. To maintain process efficiency, biomass settling velocities of 10 m/h are needed (Dalzell, 1994; Xu and Yu, 2000).

The UASB process can be used for strong wastewaters generated from various industrial processes. It is generally an adapted process for the treatment of food processing wastewaters and represents about 2/3 of the digesters built in the world used for wastewater treatment (Cervantes et al., 2006). The UASB is considered to be the best process in treating a number of food processing wastewaters such as those from sugar (Manjunath et al., 1990), potato processing (Kalyuzhnyi et al., 1998; Vegt and Vereijken, 1992; Zoutberg and Eker, 1999), slaughterhouse, meat packing, fish processing (Palenzuela-Rollon et al., 2002; Veiga et al., 1992), coffee (Dinsdale et al., 1997), brewery and winery processing (Cronin and Lo, 1998; Leal et al., 1998; Parawira et al., 2005), fruit juicing, vegetable processing (Lepisto and Rintala, 1997), jam industries wastewater (Mohan and Sunny, 2008), and dairy processing industries (Del Nery et al., 2007; Gavala et al., 1999; Kalyuzhnyi et al., 1997; Nadais et al., 2005; Omil et al., 2003; Onken and Liefke, 1989).

The UASB reactor is a promising option for treatment of fish processing wastewater (Palenzuela-Rollon et al., 2002) with 78±8 % of total COD removed at 5.4±2.3 kg COD/m^3.d, and HRT of 7.2 h, where 61±17% of COD is converted to methane. When used for dairy wastewater treatment, the reactor achieved high COD removal efficiency

(Onken and Liefke, 1989). It was noted that at 3 h HRT, and 2.4 kg COD/m^3.d, the maximum COD reduction ranged between 95.6% and 96.3%. However, the reactor performance decreased when the OLR increased to 13.5 kg COD/m^3.d for 12 h HRT and the COD reductions were about 92-90%. Anaerobic digestion using UASB has been used on jam industries wastewater. The removal efficiency of COD was 82% in 3 days HRT (Mohan and Sunny, 2008).

Treatment of combined dairy and domestic wastewater by using an integrated UASB system with an activated sludge system has been trialled by Tawfik et al. (2008). It is noted that the UASB is unable to treat a mixture of wastewaters which contains different compositions, where it has achieved low removal efficiency 69% of COD 79 % of BOD_5, and 72% of TSS at low an OLR ranging from 1.9-4.4 kgCOD/m^3.d and 24 h HRT (Tawfik et al., 2008). Similarly, Sklyar et al. (2003) treated starch industry wastewater by using a UASB for anaerobic pre-treatment followed by activated sludge process as a post-treatment. They found that the UASB achieved a COD removal of only 85% with an OLR of 15 kg COD /m^3 d and 1 day HRT. Furthermore, Chan et al. (2009) used the UASB and an aerobic CSTR system. An 83-98% reduction of COD with influent COD content in the range of 500-20,000 mg/L at HRT of 11.54 h to 6 days was removed.

3.3.1.2 Anaerobic Filters

Treatment of wastewaters using an anaerobic filter was developed from the submerged attached growth bioreactor (Grady et al., 1999). The filter operated with either up flow or down flow. The packed medium in the anaerobic filter is fully submerged, and the microorganisms are attached in the media to retain biological solids and also to provide mechanisms for separating the solids and the gas produced in the digestion process (Metcalf and Eddy, 2003). The influent enters the reactor at the bottom and circulates through the reactor to maintain the upflow velocity of 19-20 m/h. Most of the biomass, particularly fermentative and hydrolytic bacteria, is developed at the bottom of the reactor, as they receive the raw wastewater directly. Several researchers have studied the application of an anaerobic filter for treatment of various food processing wastewaters, such as seafood and fishery processing wastewater (Mendez et al., 1995; Prasertsan et al., 1994; Veiga et al., 1992); brewery wastewater (Ince et al., 1994; Leal et al., 1998; Yu et al., 2006); soybean processing wastewater (Yu et al., 2002) and dairy processing wastetwer (Garrido et al., 2001; Omil et al., 2003; Veiga et al., 1994).

Anaerobic filter treatment of fishery wastewater and tuna condensate was reported by Prasertsan et al. (1994). The OLR has a great influence on the biodegradation of organic matter in the wastewater, reflected in the biogas productivity, the profiles of pH and volatile fatty acids. The highest COD reduction of 84% was obtained for fishery wastewater at a minimum OLR of 0.3 kg COD/m^3.d and maximum HRT of 36 days. The data showed that with increased OLR, the COD reduction efficiency dropped. The highest loading rate in which the system still maintained its high conversion efficiency (over 78% COD reduction) was 0.99 kg COD/m^3.d at a HRT of 11 days. The tuna condensate contained a high content of volatile acids (3.34 g/L). The COD reduction was maintained at 60% up to an OLR of 1.67 kg COD/m^3.d and sharply decreased thereafter. Biogas productivity was highest at an OLR of 1.3 kg COD/m^3.d, with the pH of the effluent at 7.68. Biogas production stopped completely at an OLR of 2.5 kg COD/m^3.d.

For treatment of seafood processing wastewater, mesophilic and thermophilic anaerobic filters were used (Mendez et al., 1995). Both filters had the same operating parameters with an OLR of 8 kg COD/m^3.d and HRT of 2 days. Around 75, 33 and 78, 83.2 % of COD and TSS removal were achieved for mesophilic and thermophilic, respectively. Leal et al. (1998) noticed an improvement of treatment efficiency of the anaerobic filter treating a brewery wastewater. A COD removal efficiency of 96% was obtained at an OLR of 8 kg COD/m^3.d and constant HRT of 10 h. Recently, the performance of an industrial scale anaerobic filter (AF) reactor and sequencing batch reactor (SBR) for treatment of raw milk discharged wastewater by quality control laboratories was reported by Omil et al. (2003). More than 90% COD removal was attained with an OLR maintained around 5-6 kg COD/m^3.d. In addition, the fat in the dairy wastewater could successfully be degraded by the anaerobic filter reactor. At the same time, the final effluent COD and nitrogen concentrations were below 200 mg/L and 10 mg/L, respectively, which was adequate for discharge.

An investigation was conducted to study the effectiveness of a multi-fed upflow anaerobic filter at room temperature for treatment of a rice winery wastewater effluent. A COD removal of 82% was achieved at an OLR of 37.68 kg COD/m^3.d and short HRT of 8 h (Yu et al., 2006). This type of reactor has proved to be more effective than the single-fed type (Punal et al., 1998) in terms of COD removal efficiency and stability against hydraulic loading shock.

Veiga et al. (1992) carried out both laboratory and pilot studies to treat wastewater from a tuna processing industry in a down flow stationary fixed film reactor under mesophilic conditions. The results showed that the reactor achieved a moderate COD removal efficiency 75% at low OLR of 2 kg COD/m^3.d. The performance of an anaerobic filter in treatment of soybean processing wastewater with and without effluent recycle was investigated by Yu et al. (2002). A COD removal efficiency of 88.1% was obtained when the recycle ratio was 2. It has been demonstrated that the effect of recycle on COD removal is significantly related to the OLR.

3.3.1.3 Anaerobic Fluidized Bed Reactor (AFBR)

A fluidized-bed reactor process or expanded-bed reactor is a recent innovation in anaerobic treatment processes. Most of the media materials used in fluidized reactors are natural materials such as rocks and sand. Granular activated carbon has also been used as a support media in fluidized bed reactors and it promotes more rapid accumulation of biomass during the start-up than anthracite and sand (Droste, 1997). The packing medium size ranges between 0.1-0.7 mm diameters (Droste, 1997). Synthetic materials can also be fabricated into porous structures with a low density. However, the decrease in density can cause the bioparticles to rise and be washed out of the reactor. The liquid pumped through the reactor at up-flow liquid velocities of about 20 m/h is sufficient to give about 100 % bed expansion. The shear force of the liquid as it passes through the fluidized bed is sufficient to limit the growth of the biomass on support media. The process is most suitable for soluble wastewaters due to its inability to capture solids (Malina and Pohland, 1992; Tay and Zhang, 2000). Process COD loading values of 10 to 20 kg COD/m^3.d and HRT ranges from 9 h to 1 day are feasible for the anaerobic fluidized-bed reactor with more than 90 % COD removal, depending on the type of wastewater.

The fluidized bed reactor has been used in many food processing industries. It has been used for treatment of slaughterhouse wastewater (Borja and Banks, 1995), with more than 94% COD removed at an OLR of 27 kg COD/m^3.d. It has been reported that Inverse fluidized bed reactors (IFBR) have the capability to treat brewery wastewater with a satisfactory COD reduction of more than 90% obtained at an OLR of 70 kg COD/m^3.d (Alvarado-Lassman et al., 2008). A laboratory scale anaerobic fluidized bed reactor treating ice-cream wastewater with an influent COD of 5200 mg/L was used by Borja and Banks. (1995). The reactor operated at 15.6 kg COD/m^3.d OLR and a HRT of

8 h, with COD removal of 94.4% achieved at steady state conditions. The effluent quality deteriorated under shock load conditions, but a typical value was regained within 16 h when the temperature returned to normal. Wang et al. (2009) revealed that high strength milk permeate wastewater was easily biodegradable in an anaerobic moving bed biofilm reactor (AMBBR) with COD removal efficiencies in the range of 86.3-73.2% achieved at an OLR of 2.0-20 kg COD/m^3.d.

3.3.1.4 Anaerobic Sequencing Batch Reactor (ASBR)

The anaerobic sequencing batch reactor (ASBR) is considered a suspended growth process with reaction and solid-liquid separation in the same tank. The ASBR consists of four operational steps: (1) feed, (2) react, (3) settle and (4) decant/effluent withdrawal. The critical feature of the ASBR process is the settling velocity of the sludge during the settling period before decanting the effluent. After sufficient operating time, a dense granulated sludge will develop to improve liquid-solids separation rates. At HRT values of 6 to 24 h, the SRT ranged from 50 to 200 days (Metcalf and Eddy, 2003).

The ASBR has been tested for treating food processing wastewaters. A mesophilic laboratory scale anaerobic sequencing batch reactor (ASBR) was used to treat winery wastewater. At 8.6 kg COD/m^3.d OLR and HRT 2.2 days, the reactor achieved 98% of COD removal (Ruiz et al., 2002). In a temperature range between 5 and 20 °C, and at a HRT range between 24 and 6 h, soluble OLR reduction ranged between 62% and 90% for COD removal, and 75% and 90% for BOD_5 removal, respectively. In another study, two-stage thermophilic ASBR systems provided volatile solids removal of 26-44%, while mesophilic ASBR systems achieved VS removal between 26% and 50% for dairy wastewater (Dugba and Zhang, 1999; Dugba et al., 1997). The systems were operated at an OLR range of 2-4 kg COD/m^3.d and HRT of 3-6 days. A brewery wastewater was also treated by an ASBR (Shao et al., 2008). A 1 day HRT and an OLR ranging between 1.5-5 kg COD/m^3.d were used. The COD removal efficiency reached more than 90%. Göblös et al. (2008) showed that a high removal efficiency of COD of 80% and 68% was obtained for pre-fermented and raw wastewater, corresponding to an OLR of 1.6 and 12.8 kg COD/m^3.d, respectively.

3.3.1.5 Anaerobic Fixed Film Reactors (AFFR)

Another type of reactor that has been utilized in anaerobic treatment is the down flow

fixed film reactor (DFFR) (Droste, 1997). Influent is introduced at the top of the reactor and effluent is withdrawn from the bottom. Anaerobic fixed film reactors (AFFR) are cylindrical or rectangular tanks and vertically oriented surfaces are used for bacterial growth. The most commonly used packing materials include corrugated plastic cross-flow or tubular modules and plastic ball rings. Packing heights are in the range of 2 to 4 m and specific surface areas are in the range of 100-150 m^2/m^3 (Droste, 1997; Metcalf and Eddy, 2003). Due to clogging of the packing, the use of a packing material with a high void volume, such as the vertical plastic packing used in tower trickling filters, is recommended. This system is able to treat a high COD loading compared with its volume (Metcalf and Eddy, 2003). However, the disadvantages of this reactor include the cost of the packing material, and the somewhat lower organic loading rates to achieve the same treatment efficiency as the UASB and fluidized-bed reactor processes.

In an AFFR used for treating poultry wastewater, COD removal efficiencies ranging from 85 to 95% were obtained for an OLR of 8 kg $COD/m^3.d$, while the highest OLR at 35 kg $COD/m^3.d$ led to lower removal efficiencies of 55-75% at 35 °C (Del Pozo et al., 2000). Organic loads used in this study were considerably higher than those applied by (Borja et al., 1995) in which the highest load was 25 kg $COD/m^3.d$. In addition, a down flow stationary fixed film (DSFF) was examined for the treatment of tuna processing wastewater. A removal efficiency of 75 % was achieved at OLR up to 2 kg $COD/m^3.d$ (Veiga et al., 1992).

Interest in anaerobic hybrid technology (combination of different anaerobic systems into a single bioreactor) has grown in recent years. This couples the recovery of usable energy with good process efficiency and stability. A laboratory scale hybrid anaerobic reactor has been used to investigate two different types of wastewater (Büyükkamaci and Filibeli, 2002). At first, the reactor was tested by using a synthetic wastewater at different HRT ranging between 0.5-2 days and an OLR 1-10 kg $COD/m^3.d$. It was found that 77-90% COD removal efficiencies were obtained. At a lower OLR of 1 kg $COD/m^3.d$, the reactor achieved 75% of COD removal when meat processing wastewater was treated. A removal efficiency of 78% was obtained when baker's yeast was treated at an OLR of 9 kg $COD/m^3.d$ and HRT of 2 days. A yellow ginger wastewater was treated successfully by using a laboratory scale hybrid biological process (Zhao et al., 2008). A high efficiency of COD removal of 85-95% was obtained.

3.3.1.6 Summary

The performance data of the various anaerobic methods used for food processing wastewater are given in Table 3.2. Treatment of food processing wastewaters using anaerobic treatment processes is widely applied. Anaerobic treatment methods are appropriate for treating several types of food processing wastewater because the anaerobic systems withstand a high organic loading rate. Generating energy in the form of biogas is also an advantage in using these methods for the treatment of food processing wastewaters that contain high amounts of biodegradable organic matter. The presented data in the above literature for anaerobic reactors treating various food processing wastewaters outline the treatment performance in terms of COD removal and tolerance to a high organic loading rate. For instance, the IFBR has the capability to apply an OLR of 70 kg COD/m^3.d with COD removal efficiency higher than 90%. The performance of an UASB reactor is considerably more variable. It reaches about 95% of COD removal at an OLR of 28.5 kg COD/m^3.d for cheese-whey wastewater, while the capacity of the UASB drops to 70% at an OLR of 10 kg COD/m^3.d for coffee processing wastewater. Therefore, in some cases, an UASB has a low performance but is still used in most food processing wastewaters. The rest of the anaerobic methods mentioned in Table 3.2 display a similar trend and performance with regard to COD removal efficiency and organic loading rate.

However, these systems also have disadvantages, due to production of undesirable gases which will create more complexity if not appropriately controlled. Additional expense and equipment are required for the plant to remove the gases safely. Anaerobic treatment process equipment must be continuously inspected to ensure that there are no leaks, as oxygen or air leaked into the system would create disturbance in the treatment progress. Therefore, these processes have generally been unable to obtain a high quality effluent suitable for direct discharge and their effluent contains solubilised organic matter that is amenable to quick aerobic treatments. These factors indicate that the anaerobic process alone cannot meet typical discharge criteria and must be always complemented by aerobic unit as a post-treatment.

Table 3.2 : Summary of performance of various anaerobic methods treating food processing wastewaters

Reactor	Wastewater type	Influent COD mg/L	OLR kg COD/m^3.d	HRT h	COD Removal %	pH	Reference
UASB	Potato	10,500	20	3.5	85	4.5	Vegt and Vereijken, 1992
UASB	Potato-maize	5.3-18.1	14	0.6-1.8	63	6-11	Kalyuzhnyi et al., 1998
UASB	Cheese-whey	5000-7700	1-28.5	2.3-11.6 d	95-99	4	Kalyuzhnyi et al ., 1997
UASB	Brewery	1955±597	1.53		91		Cronin & Lo, 1998
UASB	Brewery	2500-3000	4.9	13.3	89	5-6	Fang et al., 1989
DSFF	Tuna	27000	2	4d	75	5.7	Veiga et al., 1992
UAF	Cheese-whey	50446	5.8	6.9 d	98	7	Veiga et al., 1994
UAF	Winery	7550	4	48	92	5.46	Daffonchio et al., 1998
TPAD CSTR+ Upflow filter	Milk and cream bottling		5	2 (d)	90		Ince, 1998
AF	Dairy	10200	10	24	85	6.9	Cordoba et al .,1984
AF	Raw milk	3000-18000	5-6		90	7-9	Omil et al., 2003
AF	Seafood		0.3-1.8	6-36	85	7.2	Prasertan et al., 1994
Hydird	Synthetic dairy		0.82-6.11	4.1-1.7(d)	90-97		Ramasamy et al., 2004
UAF	Cheese whey	9000	20	AN	87	4-7	Punal et al., 1999
UAF	Winery	8340-25760	37.6	8	82	4.8-5.9	Yu et al., 2006
AF	Seafood		8	2 (d)	75	6	Mendez et al., 1995
ASBR	Winery	19700	8.6	2.2	98	5.5	Ruíz et al., 2002
AF	Brewery	2832	8	10	96		Leal et al., 1998
UASB	Brewery	920-1910	34-39		80	6.7	Ahn et al., 2001
UASB	Cheese	61000	6.2	6 (d)	98	4.7	Gavala et al., 1999
UASB	Vegetable		24		90		Lepistö and Rintala, 1997

Table 3.2. (Continued)

Reactor	Wastewater type	Influent COD mg/L	OLR kg COD/m^3.d	HRT h	COD Removal %	pH	Reference
UASB	Meat	2000	1	2(d)	75		Buyukkamaci and Filibeli, 2002
	Baker's yeast	18000	9	2(d)	78		
UASB	Dairy	19,000	1.5-6.5	12	80	7.5	Nadais et al., 2005
UASB	Tomato	7240	8.5	12	91.3		Gohil et al., 2006
	Tomato	6953	2.5-10	1.3	95.6		Gohil et al., 2006
AF	Food processing		5.6		80		Oliva, 1995
UASB	Potato-chips	4932	8.76		94		El-Gohary, 2000
UBF	Synthetic sugar	2500	5-51	13	96		Guiot, 1985
AFFR	Slaughter house		8	6-31	85-95		Del Pozo, 2000
UASB	Coffee	7400-18000	10	24	70	4.5	Dinsdale et al., 1997
UASB	Fish processing	3000-4000	5-8	11-12	78		Palenzuela-Rollen et al., 2002
UASB	Jam wastewater	19200-26800	6.5	3(d)	82	7.4	Mohan and Sunny, 2008
ASBR	Dairy		1.6-12.8				Göblös et al., 2008
AMBBR	Milk permeate	55200	2-20		86.3-73.2	5.5-6.5	Wang et al., 2009
AFBR	Ice-cream	5200	15.6	8	94.4	5.2	Borja and Banks, 1995
ASBR	Brewery	22500-23500	1.5-5	1(d)	90	3.2-3.9	Shao et al., 2008
IFBR	Brewery	2083	70		90	10	Alvarado-Lassman et al., 2008
Hybrid	Yellow ginger	18000-20000			85-90		Zhao et al., 2008

AF; Anaerobic Filter.UASB Upflow Anaerobic Sludge Blanket. UBF:Upflow anaerobic bed. AFFR; Anaerobic fixed film reactors. DSFF; down stationary fixed film. ASBR; anaerobic sequencing batch reactors. UAF; upflow anaerobic filter. TPAD; two-phase anaerobic digestion. AMBBR; Anerobic moving bed biofilm reactor. IFBR Inverse fluidized bed Reactor.

3.3.2 Aerobic Treatment

Aerobic bioreactors contain mixed populations of microbial cultures, which also acquire a diverse population of grazing organisms. The aerobic bioreactors reviewed in this section can be subdivided into two categories. The suspended growth systems include methods such as aerated lagoons (AL), aerobic jet loop reactor (AJLR), sequencing batch reactor (SBR), and the activated sludge process (AS). Attached growth or biofilm systems include methods such as trickling filter (TF), rotating biological contactor (RBC), fluidized bed reactor (FBR) and fixed film bioreactor (FFBR).

3.3.2.1 Aerobic Suspended Growth Process

Suspended growth processes are the most commonly used methods for treating municipal and industrial wastewaters. In the suspended growth process, the micro-organisms responsible for the biochemical conversion of organic matter are kept in suspension by aeration or agitation in a tank where the wastewater is introduced. The microorganisms consume the organic substances for production of new biomass (cells) and for respiration, which provides the energy for the synthesis and other cellular processes. The performance of aerobic bioreactors used as suspended growth systems is discussed in the following sections.

3.3.2.1.1 Conventional Activated Sludge Process

The activated sludge system is the most extensively used system for the biological treatment of municipal and industrial wastewaters. This process uses the dispersed bacterial floc and other free microorganisms to stabilise wastewater aerobically and these microorganisms are maintained, suspended within the water body (Gray, 2004). It involves two characteristic processes, namely aeration and settling. During aeration oxidation, the microorganisms carry out various biochemical reactions leading to utilization of the organic matter which is oxidized to end-products such as CO_2, H_2O, and NH_4, and new cell biomass. After the aeration process, the mixed liquor is passed into a settling tank to separate the treated effluent. The normal concentration of mixed liquor is in the range 2000-5000 mg SS/L. Some activated sludge is returned back to the aeration tank to keep sufficient microbial biomass active for oxidation of the wastewater. Waste sludge is undergoes dewatering as additional treatment. Continuous recirculation of sludge back to the aeration tank provides a long sludge retention time (SRT) typically many days longer compared with the HRT, typically up to 1 day.

The activated sludge is deemed a very effective process in removing organic pollutants in municipal and industrial wastewaters with generation of a high quality effluent (Eckenfelder and Musterman, 1995). The treatment performance of this system is highly dependent on the concentration of microorganisms and their activity. The settling properties of the biomass can also affect biomass concentration in the aeration tank, as well as final treated effluents. Operating conditions such as SRT, OLR and wastewater composition may influence the character and condition of activated sludge floc (Gray, 2004).

Due to high removal efficiency and capacity, the activated sludge system has been used to treat different types of food processing wastewaters. Among these wastewaters are potato processing wastewater (Menon and Grames, 1995; Nikolavcic and Svardal, 2000), winery and brewery wastewater (Brucculeri et al., 2005; Fumi et al., 1995), fish and tuna processing wastewater (Achour et al., 2000; Garrido et al., 1998), dairy processing wastewater (Garrido et al., 2001; Jung et al., 2002) and other food processing industries (Rusten and Thorvaldsen, 1983). Meat processing wastewater is also treated by such methods (Crandall et al., 1971).

Although the application of activated sludge process is somewhat costly, particularly due to the high energy requirement, it is still acceptable in the treatment of food processing wastewaters. For example, it has been used to treat fruit and vegetable processing wastewater, and a high COD removal efficiency of approximately 90%, at low OLR of 1.1 kg COD/m^3.d, was achieved. However, a low COD removal efficiency of 35% was obtained at high OLR of 2.3 kg COD/m^3.d. In another study, the activated sludge process was used for treatment of dairy processing wastewater (Jung et al., 2002). At high oil and grease concentrations of 400 and 600 mg/L, the process achieved COD removal efficiencies of 86% and 75%, respectively, while at 800 mg/L oil and grease concentration in the feed, the COD removal efficiency of the bioreactor dropped markedly, actually reaching nil values.

The removal efficiency for treating winery wastewater was studied by Fumi et al. (1995). A COD removal of 98% obtained at 0.354 kg COD/m^3.d OLR, producing a small amount of sludge (0.065 kg TSS/kg COD). A COD removal efficiency of 92% at an OLR of 2.4 kg COD/m^3.d was obtained for brewery wastewater (Rusten and Thorvaldsen, 1983; 1983). The possibility of co-treating municipal and winery

wastewaters in a full scale treatment plant was studied by Brucculeri et al. (2005). A COD removal efficiency of 90% was attained, while the observed yield was 0.2 kg MLVSS/kg COD removed.

The performance of the activated sludge process in the treatment of potato processing wastewaters has been investigated. A COD removal efficiency of 94.5% and 86.5% was achieved at 0.396 kg COD/m^3.d and 1.48 kg COD/m^3.d OLR, respectively (Hadjivassilis et al., 1997; Menon and Grames, 1995). Kargi et al. (2000) characterised and treated pickling industry wastewaters in an activated sludge unit. Nearly 96.4% COD removal efficiency was attained with an OLR of 3.6 kg COD/m^3.d and 30 h HRT. In thermophilic conditions, high and stable COD removal was reported at laboratory and pilot scales (Barr et al., 1996; Chiang et al., 2001). The removal efficiency of 95% in COD at an OLR of 4.1 kg COD/m^3.d was obtained. However, performance was different when a mesophilic process was used in the treatment of high oil and grease pet food wastewater. It was also observed that the removal efficiency decreases with food: mass ratio (F/M), with the peak SCOD removal efficiency of 92% occurring at an F/M in the range of 1.3-1.42 mg COD/mg VSS (De Oliveira et al., 2009).

3.3.2.1.2 Sequencing Batch Reactor Process (SBR)

The sequencing batch reactor is an improvement on the fill and draw activated sludge treatment system. In the operation of a SBR system, there are five common operating periods, or repeated cycles. The periods usually carried out in sequence are fill, aeration, settle, draw, decant, as well as an idle period. The subsequent steps of aeration and clarification occur in the same tank (Metcalf and Eddy, 2003; Sirianuntapiboon and Yommee, 2006). There may be a number of variations in each period depending on the treatment requirements and the environmental circumstances that occur in the fill and aeration stage, for example a limitation of carbon oxidation and nitrification. Consequently, the performance of the SBR will lie between that of conventional and completely mixed activated sludge depending on the length of the fill period. The major factors that affect the performance of SBR include OLR, HRT, SRT, DO and wastewater composition and characteristics (Li and Zhang, 2002; Metcalf and Eddy, 2003). In addition, sludge wasting greatly affects performance of the process. Sludge production can be minimized by extending aeration when the system behaves in a similar way to a continuous flow extended aeration system.

A very high treatment capacity and an excellent effluent quality can be achieved by using the SBR. The system is also deemed to be an adequate one to apply for treatment of food processing industrial wastewater. Several researchers (Bandpi and Bazari, 2004; Garrido et al., 2001; Hamoda and Al-Awadi, 1995; Li and Zhang, 2002; Sirianuntapilboon et al., 2005) have studied the performance of the SBR in treating dairy wastewater. Li and Zhang (2002) conducted a study on the SBR performance for treating dairy wastewater with various OLRs and HRTs. At 1 day HRT and 10,000 mg/L COD, the removal efficiency of COD, total solids and volatile solids were 80.2, 63.4 and 66.3%, respectively. Treatment of milk wastewater was also examined in a SBR system by Tam et al. (1986). Wastewater with 919-1330 mg/L COD could be successfully treated with HRT of 20 h. An effluent from a small goat's cheese-making operation containing approximately 1440 mg COD /L was treated by a SBR. COD and SS purification efficiencies of 99% were achieved. In addition, low sludge settling and sludge production yield was noted at 0.2 g SS/g COD, and the SBR worked at an average volumetric loading rate (VLR) of less than 0.4 kg COD/m^3.d (Torrijos et al., 2004). The capability of the SBR for treating dairy wastewater was also confirmed by Bandpi and Bazari (2004) and (Garrido et al., 2001). Removal efficiencies of nearly 80% to more than 90% were achieved for COD concentrations between 1000 and 7000 mg/L.

Some studies have been conducted for the treatment of winery and brewery wastewater using the SBR process (Houbron et al., 1998; Sirianuntapiboon and Prasertsong, 2008; Torrijos and Moletta, 1997; Wang et al., 2007). Torrijos and Moletta (1997) achieved up to 93, 95 and 97.5% of total COD, soluble COD, and BOD_5 removal efficiencies ,respectively, when the average of OLR was 0.8 kg COD/m^3.d. Moreover, the authors found that TSS concentration was low at 3.2 g TSS/L. In another study, a COD removal efficiency of 97% was obtained for treatment of brewery wastewater (Houbron et al., 1998). Wang et al. (2007) reported that at 3.5 kg COD/m^3.d OLR, the COD removal was 88.7% when brewery wastewater was treated by aerobic granulation sludge in a SBR. As reported by Neczaj et al. (2008), two aerobic SBRs can be effective for co-treatment of landfill leachate and dairy wastewater. At an OLR of 0.8 kg BOD_5/m^3.d and HRT of 10 days, a good effluent quality was obtained with a COD and BOD_5 removal efficiency of 98.8% and 98.6%, respectively, and low value of 15 mg/L of SS in the effluent.

A SBR was used successfully for treatment of abattoir wastewater (Cassidy and Belia, 2005). It achieved a higher OLR (2.6 kg COD/m^3.d) and 3 days HRT than those achieved by Mikkleson and Lowery (1992). Without optimizing process conditions, they found that the removal of COD was over 98%, and removal of VSS was over 97%. In this study, they revealed that the conventional SBRs, treating wastewaters with flocculating sludge can be converted to granular SBRs by reducing the settle time. Mikkleson and Lowery (1992) also observed an excellent performance of a SBR in the treatment of meat processing wastewater. Removal efficiencies of 99% BOD_5 and 96% TSS were achieved at 0.28 kg COD/m^3.d OLR and 3.5 days HRT. Furthermore, sludge production and handling were minimised.

3.3.2.1.3 Aerobic Lagoon

Aerated lagoons are one of the oldest and most useful systems used in municipal and industrial wastewater treatment. Aerobic lagoons are simple to build, operate, and maintain, and are generally efficient. Aerobic lagoons have long HRTs; they resist organic and hydraulic shock loading, with no sludge waste recycled (Gray, 2004; Rusten et al., 1992). One of the features of an aerobic lagoon is the use of oxygen simply by exposure of the large surface area of the lagoon to the atmosphere. If the aeration is not adequate, in contrast, additional mechanical aerators are used to provide more oxygen for biological treatment and to keep the biological solids in suspension. By providing oxygen, a good mixing in the lagoon will be achieved to improve the process performance with a good contact between bacteria and dissolved organics (Gray, 2004). However, effluent quality from aerobic lagoons has often been relatively poor, relegating them to use where high quality effluent is not necessary. Food processing wastewater can not be efficiently treated in an aerobic lagoon system in a freezing weather condition (Xu and Yu, 2000).

This process has been used to treat cherry fruit wastewaters (Mauldin et al., 1976), potato processing wastewater (Rusten et al., 1992), and meat processing and slaughterhouse wastewater (Bélanger et al., 1986). In treatment of potato processing wastewater, the process achieved more than 90% COD removal at an OLR of 1.6 kg COD/m^3.d, and 7 days HRT. When the process used in treatment of meat packing wastewater (Witherow, 1973), and at low OLR of 0.0006 kg BOD_5/m^3 .d and 32 days HRT, the COD and BOD_5 removal efficiencies were 70% and 83%, respectively. Bélanger et al. (1986) demonstrated the use of an aerobic lagoon treating slaughterhouse

wastewater. The wastewater contained an influent BOD_5 ranged from 1500-3000 mg/L. At a HRT of 11 days, the system reduced the BOD_5 to below 50 mg/L except in winter when it was little higher.

3.3.2.1.4 Aerobic Jet Loop Reactors

This reactor consists of a cylindrical column with a central aeration tube and a cylindrical degassed tank (Figure 3.1). The mixed liquor is pumped through an ejector venturi nozzle, where the air is drawn into the liquid jet through the air tube by a local pressure drop at the nozzle tip (Bloor et al., 1995; Petruccioli et al., 2002). The use of a vertical aeration reactor for biological treatment of wastewater is becoming an interesting alternative as a means of good oxygen transfer. High biological conversion capacity and turbulence mixing is secured. It is claimed that AJLRs have higher oxygen transfer rates at a low energy cost. In addition, aerobic jet loop reactors are generally categorized by reduced reactor volumes required, meaning limited area needed, resulting in significant reduction in the cost of installation and maintenance (Ana et al., 2004; Bloor et al., 1995). Basically, the reactor is fed with wastewater from a reservoir into the suction side of the recycled pump. The degassing tank is connected to a settling tank where the disposed liquor is collected. The sludge is also returned back and excess sludge disposed from the bottom of the sedimentation tank. The high concentration of suspended solids and non flocculating motile bacteria, however, may cause a cloudy effluent.

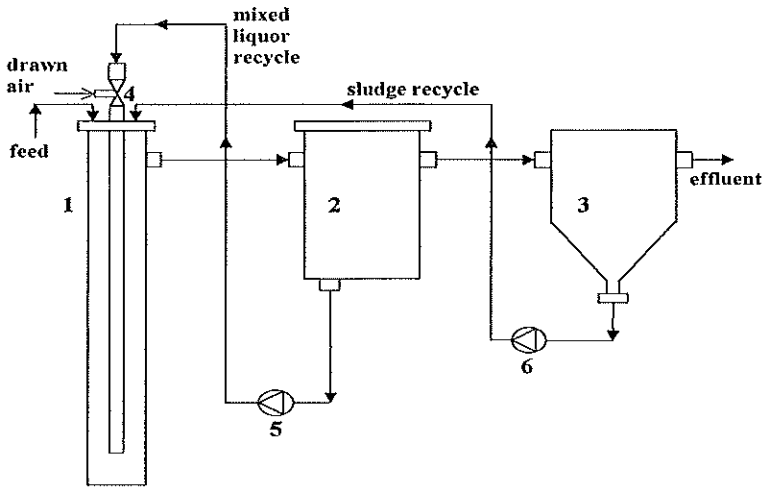

Figure 3.1: Aerobic jet-loop reactor (Petruccioli et al., 2002)

1: column reactor, 2: degassing tank, 3: settling tank, 4: ejector ventur, 5: centrifugal pump, 6: peristaltic pump

An AJLR for the treatment of winery wastewater was studied and a high capacity for COD removal efficiency on average greater than 80% was achieved corresponding to maximum productivity of 20 kg COD/m^3.d OLR and 0.8-1 day HRT (Ana et al., 2004). The performance of the AJLR resulted in maximum COD removal efficiency of 94% with an OLR range of 0.4-5.9 kg COD/m^3.d (Petruccioli et al., 2002). Bloor et al. (1995) obtained a high reduction of soluble COD of 97% at a high OLR of 50 kg COD/m^3.d, with high nutrient (C: N: P 100:5:1), a high F/M ratio of 5-8 kg COD/kg MLVSS .d and also low sludge age of 0.6 days. Xue et al. (2004) studied the feasibility of the reactor to treat food processing wastewater at 2 h HRT. The authors observed that at 3.5 h HRT, the reactor achieved a COD and BOD_5 removal, complying with discharge criteria.

The use of the reactor is not confined to the food processing wastewater only, but is also used in treating synthetic domestic wastewater with a range of COD concentrations (Naundorf et al., 1985). The results showed a maximum COD volume loading and COD sludge loading of 27 kg COD/m^3.d and 5 kg/d per kg MLSS respectively, which were 10-20 times higher than those of a traditional wastewater treatment process. Approximately more than 90% and 85% of BOD_5 and N removal efficiencies were acquired. The authors also observed that oxygen uptake rate (OUR) of the JIBR reactor was 39.13 mg/L.h (Xue et al., 2004). Similarly, around 80% of BOD_5 removal efficiency at 0.5-2 h HRT was obtained (Liu et al., 2005). As noted from Bloor et al. (1995) and Naundorf et al. (1985) achieved an organic loading rate of 28 kg BOD_5/m^3.d for domestic wastewater.

3.3.2.1.5 Summary of the Performance, Advantages, and Disadvantages of Aerobic Suspended Growth System

Table 3.3 presents various biological treatment methods for food processing wastewaters under the operating parameters and removal efficiencies described above. In suspended growth processes, several operational parameters may affect the process performance. The effect of the organic loading rates on the COD removal efficiency for AJLR, AS and SBR reactors can be analysed. For SBR, it is clearly shown that the COD removal efficiency decreased as the organic loading rate increased. It can be noted that both the ASP and SBR achieved a high COD removal efficiency at an OLR less than 4 kg COD/m^3.d. The same trend is observed for AS. However, due to insufficient data in the AJLR case, the trend is not as clear. It is important to note that the process efficiency is also dependent on other operational conditions and control parameters. In

SBR, at a low OLR of 0.4 kg COD/m^3.d, the COD removal efficiency was about 99.5%. Similarly, in AS, the removal efficiency was 98% at 0.354 kg COD/m^3.d OLR. On the other hand, 70% of COD removal was obtained at an OLR of 2.4 kg COD/m^3.d. In general, SBR and AS achieved similar performances. These processes are efficient and achieve a high COD removal efficiency at low OLR. Most of the suspended growth systems have shown similar performances despite the variation in the process conditions, such as the food to microorganisms ratio (F/M), dissolved oxygen concentration, amount of sludge recycled and sludge age (Abdulgader et al., 2007).

Generally, all aerobic methods are effective and viable alternatives in treatment of various food processing wastewaters. Biological methods reduce COD value to 50 mg/L in some of the suspended growth systems (Metcalf and Eddy, 2003). However, some drawbacks may be inherent. For instance, all of the aerobic suspended processes have a problem of producing a large of amount of sludge which requires additional handling. They also have high operational costs. In lagoon systems, accumulation of the sludge creates a serious problem.

Table 3.3: Summary of performance of aerobic suspended growth methods treating food processing wastewater

Reactor	Wastewater type	Influent COD mg/L	OLR kg COD/m^3.d	HRT (h)	COD Removal %	References
SBR	Dairy	10,000	10	1 d	86.3 %	Li and Zhang, 2002
SBR	Dairy	1000	1.4	NA	90 %	Garrido et al., 2001
SBR	Dairy	1541	3.082	14	94 %	Hamoda and Al-Awadi, 1995
SBR	Dairy	445	1.78	6	90 %	Bandpi and Bazari, 2004
SBR	Abattoir	7685	2.6	72	98.6 %	Cassidy and Belia, 2005
SBR	Cheese Dairy	14400	0.4	NA	99.5%	Torrijos et al., 2004
SBR	Winery	2000	0.8	23	93 %	Torrijos and Moletta, 1997
SBR	Dairy	7500	2.5	3-8	87	Sirianuntapihoom et al.,2005
AS	Winery	4600	0.354	13 d	98 %	Fumi et al.,1995
AS	Food processing	8960	4.1	NA	95 %	Chiang et al., 2001
AS	Food processing	760	2.3	8 h	35%	Yu et al., 2003
AS	Pet food	13700	3.76	5 d	90%	Liu et al., 2004
AS	Fish meal	480-1600	3.8	0.42 d	60-90	Garrido et al., 1998
AS	Tuna processing	1007.1	1.2	2.2 d	85 %	Achour et al., 2000
AS	Potato processing	2063	0.396	5.2d	94.60%	Menon and Grames, 1995
AS	Potato Chips	540	1.48	NA	86.5%	Hadjivassilis et al., 1997
AS	Coffee Berry	2000	1.54	31	88%	Oliveira et al.,2000
AS	Brewery	1200	2.4	12	92%	Vriens et al., 1983
AS	Dairy	2521	NA	NA	86%	Jung et al., 2002
AS	Pickling wastewater	4500	3.6	30	96.4	Kargi et al.,2000
AS	Potato chips	4932	18.2	6	86	El-gohary et al., 2000
AS	Food processing	3353	2.8	17-66	70	Rusten and Thorvaldsen, 1983
Aerated lagoon	Potato processing	5680	1.6	5.5-28d	91	Rusten et al., 1992
AJLR	Brewery	NA	50	4	97%	Bloor et al., 1995
AJLR	Winery	800-1200	0.4-5.9	2.1-4.4d	94%	Petruccioli et al.,2002
AAO	Dairy	2053	0.293	7 d	93.5%	Donkin and Russell, 1997
AAO	Food processing	1757	1.48	28.5	94.2%	Mulkerrins et al., 2004

AS; Activated sludge process. SBR; Sequencing Batch Reactor; AAO, anaerobic- aerobic-oxnice. AJLR; aerobic jet loop reactor.

3.3.2.2 Biofilm (or Attached Growth) Systems

For over a century, biofilm systems have been used in wastewater treatment originating from the operation of trickling filters. In the middle of the twentieth century, the development of new biofilm reactor configurations increased (Rodgers and Zhan, 2003). A biofilm system can be defined as a complex coherent structure of cells and cellular products, such as extra-cellular polymers (Nicolella et al., 2000). Biofilm processes have been shown to be an attractive alternative to upgrade activated sludge processes, due to their high loading capacities and short retention time. Heterotrophic bacteria are the most common organisms in the developed biofilm, responsible for breakdown of the organic substances in aerobic conditions (Gray, 2004). The basic concept of the biofilm structure and an overview performance of biofilm reactors such as the trickling filter (TF), rotating biological contactor (RBC), fluidized bed reactors (FBR), and fixed bed biofilm reactors (FBBR) are described in the following sections.

3.3.2.2.1 Biofilm Structure and Characteristics

Biofilms are very complex structures, both physically and microbiologically (Grady et al., 1999). They are characterised by a dense layer of bacteria, and are able to adhere to a medium and to form a fixed film in which the bacteria are protected against sloughing off (Henze et al., 1995). The basic conceptualization of a biofilm system is shown in Figure 3.2. Generally, the biofilm can be divided into two zones: the base film is more anaerobic than the surface film (aerobic). Both zones contain an assemblage of microorganisms and other particulate materials bound together by a matrix of extracellular polymers. The thickness both of the zones depends mostly on the hydrodynamic and operating conditions characteristic of the system, but also on the nature of microorganisms in the biofilm. Tyagi and Vembu (1990) stated that the biofilm thickness can vary from a few microns to more than 1 mm, and the density of the biofilm can vary from 30 to 100 mg/cm^3. Because of mass transfer limitations, the most active part of the biofilm is the top aerobic layer with the thickness ranging from 50 to 200 μm. Subsequently, the substrate removal in the biofilm takes place within the thickness range of 70 to 150 μm (Atkinson et al., 1974).

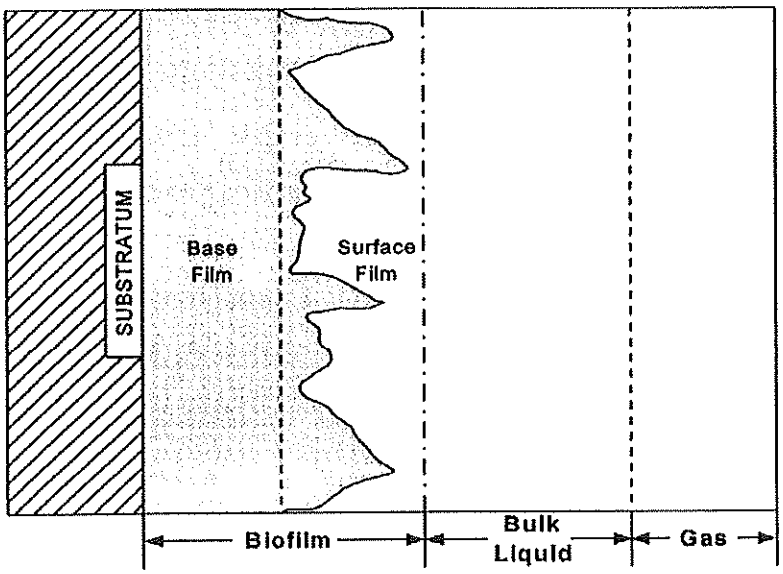

Figure 3.2: Basic conceptualization of a biofilm (Grady et al., 1999)

The appearance of the structures of the heterogeneous biofilm is nonuniform, consisting of cell clusters attached to each other as well as to the existing solid support with extracellular polymeric materials (Grady et al., 1999). The distance between cell clusters forms vertical and horizontal voids, acting as channels. Both biomass distribution within the biofilm and the physical factors, for instance, porosity and density, are uniform. Voids have an important role in wastewater treatment as the liquid can flow through them. Thus, due to the diffusion and advection, mass transfer can happen in the biofilm. Diffusion commonly dominates, however, and occurs from almost any direction into a cell cluster rather than only from the liquid-biofilm interface. It has been hypothesized that the biofilm structure is not a chance occurrence. Nevertheless, it represents an optimal arrangement based on the flux of several nutrients (Grady et al., 1999).

3.3.2.2.2 Trickling Filters

Trickling filters have been one of the most common reactors used for treatment of municipal and industrial wastewaters (Grady et al., 1999; Metcalf and Eddy, 2003). Wastewater treatment occurs normally as it is continuously and uniformly distributed over a support media where biofilm grow. Oxygen via ventilation provides aerobic treatment (Dalzell, 1994). The common packing media of trickling filter is rock, but plastic media may be used in order to increase surface area / volume and hence improve treatment performance. Although bacteria are the dominant microorganisms, a variety

of microorganisms exist in the biofilm. Slough off occurs especially because of a lack of substrates, as well as the bulk weight of the film which is not able to resist the shear force of liquid flowing over it. Clarifiers can be used to separate treated wastewater from the solids. In addition, a part of treated effluent is returned to dilute the feed wastewater, as well as to keep the biofilm layer wet (Droste, 1997; Metcalf and Eddy, 2003). Basically, trickling filter is a heterogeneous bioreactor and organic materials are decomposed by aerobic microorganisms in the outer part of the biofilm layer. Therefore the biofilm may become thick if there is a high organic loading rate, sufficient oxygen and moderate hydraulic loading.

Few investigations have been made of the performance of trickling filters and their ability in the treatment of food processing wastewater. Treatments of synthetic dairy wastewater by trickling filters have been conducted (Raj and Murthy, 1999; Rusten et al., 1996). Satisfactory results were obtained, with 92% of COD removal at 6.3 kg COD/m^3.d OLR and 5 m^3/m^2.d hydraulic loading rate. A decline of removal efficiency from 91.4 to 85.0% was noted because of increase of influent substrate concentration from 686 to 1271 mg/L. It was also observed that the effluent suspended solids concentration increased with increasing organic loading rate. Moreover, a significant effect of hydraulic loading rate on the treatment capacity of trickling filter was observed.

3.3.2.2.3 Rotating Biological Contactor

Rotating biological contactors (RBC) are also known as biodiscs and rotating biological discs. The RBC system consists of a variable number of closely spaced circular discs, typically of polystyrene or polyvinyl chloride. It is usually attached to a horizontal shaft of, for example, 7.5 m length and 3.2 m in diameter (Chan et al., 2009; Metcalf and Eddy, 2003). The selection of biodisk material is important as the biofilm growth varies with different types of materials (Apilanez et al., 1998; Najafpour et al., 2002). The disks are 30-45% submerged in a tank containing wastewater and rotated slowly at 2 to 6 rpm through the wastewater. Submergence to 70-90% may be an alternative design, providing the advantages of less loading on the shaft and bearings, large media volume available and fewer RBC units required (Metcalf and Eddy, 2003). One important factor which has to be considered in the RBC is oxygen mass transfer coefficient. As illustrated by Kim and Molof (1982), the experimental value of oxygen transfer coefficient is in the range between 49 to 87 % theoretical value.

The wastewater passes between the discs, flowing parallel to the adjacent faces of the discs that support the attached biological growth. The discs rotate slowly, imparting a lifting action to the wastewater through the drag forces generated. Thus the contact between wastewater and discs is not a single pass between adjacent surfaces, but a rapid circulation of wastewater many times over several quadrants of the disc before it leaves the tank. Ultimately, a slime layer is formed over the entire wetted surface of the discs. Increase of the biofilm thickness and mass transfer limitations prevent substrate or oxygen being transported to the bottom layers of the biofilm. A limiting biofilm thickness is achieved such that there is no improvement in the rate of organic matter removal. The disc's rotational speed can be increased to increase the level of shear and aeration. As the biofilm thickness achieves a certain range, it will be sloughed off the discs (Droste, 1997).

Some studies have been attempted to enhance the performance of rotating biological contractors (RBC) for food processing wastewater in terms of carbonaceous substrate removal, and organic nitrogen oxidation or both (Hamoda and Al-Sharekh, 1999), but their performance seems insufficient (Bull et al., 1982; Frigon et al., 2009) compared to other biofilm systems. However, other methods have been used successfully. Some of these are briefly outlined here. Treatability of food canning industry wastewater with an influent COD concentration of 6200 mg/L was evaluated in a three stage RBC. An overall 93.7 % COD removal efficiency was achieved at HRT of 40 h, and 3.84 kg COD/m^3.d OLR. The authors observed that COD removal efficiency decreased with an increasing a number of stages and increased OLR. In the first stage, approximately 88% of COD were removed at rotation speed of 11 rpm and 36% submergence (Najafpour et al., 2006). Using the same experimental setup, a poultry processing wastewater was treated (Najafpour et al., 2002). A removal efficiency of 91% at 2.2 kg COD/m^3.d OLR and 1 day HRT was achieved. Further, a RBC system was successfully used to treat a very high strength organic wastewater from a palm oil mill industry. An 88 and 89% of COD and SS was removed with 55 h HRT, respectively (Najafpour et al., 2005).

A strong acidic, high COD and BOD concentration (97,000 and 73,000 mg/L) wastewater from an onion pickling industry was treated by a RBC. The authors concluded that the RBC system can efficiently treat very high concentrations (Wilson, 1997; Wilson et al., 1988). Additionally, Duarte and Oliveira (2009) carried out a study to assess the possibility of treating dairy processing effluent by a RBC. At an OLR of

4.06 kg COD/m^3.d, nearly 97 % of COD was eliminated from the influent concentration of 2000 mg/L. They also investigated using a five stage RBC. It was found that most of the COD and BOD removal took place in the first three compartments while the last two stages behaved as polishing chambers. The feasibility of using a RBC for treatment after an aerobically treated slaughterhouse wastewater effluent was tested by Torkian et al. (2003). The overall results showed that there was a trend of decreased removal efficiency at higher OLRs. The results indicated that most of the organics were removed in the first three stages, with less contribution from the rest of the stages of the RBC reactor. At 5.3 g SBOD/m^2.d, 85% of removal efficiency was achieved. The removal efficiency decreased to 74 % when the OLR increased to 17.8 g SBOD/m^2.d. In treating a corn processing wastewater, Luna-Pabello et al. (1990) achieved 71% of COD removal at an OLR of 1.5 kg COD/m^3.d, with BOD_5 removal efficiency 74%.

3.3.2.2.4 Fluidized bed Reactors

The application of fluidized bed reactors in the treatment of wastewater can be traced to the 1940s. In the early 1970s, there were developments in the use of support media (USEPA, 1993). Currently, in the United States and Europe, it is estimated that there are more than 80 two-phase FBBRs (Lazarova and Manem, 2000). The fluidized bed reactor has been used in many fields of biotechnology and has gained a considerable application in the biological treatment of wastewater, where biofilm grows and is attached to small plastic carrier particles which are suspended in the water (Bjorn Rusten et al., 1998; Sokol, 2001; Souza et al., 2004). The particles are fluidized by drag forces associated with the upward flow water. Bioparticles are generally produced where the plastics carrier is covered by a biofilm. In addition, some bioparticles are developed without the presence of a carrier particle. Due to the retainment of such biofilm in the FBR system, a low suspended solid concentration in the effluent is obtained in the range of 15-20 mg/L (Metcalf and Eddy, 2003), where final clarification is used.

The use of the FBR system has been proved successful in the biological treatment of industrial effluents, particularly food industry wastewater (Andreottola et al., 2002; Rusten et al., 1992; Rusten et al., 1996; Sokol, 2001). The high rate of success of FBR technology is due to the higher specific surface area of the support media used and density of biomass concentration maintained in the system compared with conventional biofilm reactors. Li et al. (1987) reported the successful laboratory-scale trial of aerobic

fluidised beds (AFB) to treat pig slaughterhouse wastewater in Taiwan. Removal efficiencies of 90% BOD_5 and 70% for fat were achieved at an OLR of 20 kg BOD_5 /m^3 .d, respectively. High recirculation ratios were needed to ensure a residence time in the reactor of greater than 30 minutes and pure oxygen was used to aerate the reactor. The AFB offers potentially effective, but expensive, treatment where space is a critical issue, but it remains untried at a large scale.

Grabas (2000) treated meat processing wastewater by laboratory scale moving bed biofilm reactors. The results of the study showed that a considerable portion of the organic matter was removed in the first stage at 4 h HRT and COD loading of 10 kg COD/m^3.d. The system achieved a good performance when the two reactors were connected in series. Sixty to 75% COD removal efficiency was obtained at an OLR of 14 kg COD/m^3.d. Such a system has found to be stable and competitive using a Kaldnes Miljoteknologi (KMT) that has a specific surface area of 350 m^2/m^3. Similarly, Rusten et al. (1998) achieved up to 95% of removal efficiency of filtered COD at a total volumetric organic loading rate range between 30-45 kg COD/m^3.d. Such a high performance can be attributed to the high specific surface area (250 m^2/m^3) of the carriers. Moreover, increasing the number of stages may enhance the performance of the treatment process.

Depending on organic loading rate and media used, FBBRs show uneven performance in dealing with other types of food processing wastewater. Rusten et al. (1992) applied a moving bed biofilm reactor (MBBR) system filled with biomass support media made of polyethylene (KMT) elements in the treatment of wastewater from the dairy and food processing industries. The system showed high and significant removal efficiency over 80% at a volumetric OLR up to 12 kg COD/m^3.d. Adopting Flocor-RMP plastic media, it was possible to obtain COD removal efficiencies of over 80% with an OLR of 5 kg COD/m^3.d (Andreottola et al., 2002). To obtain a removal efficiency of more than 80%, the applied load was lower in the case of FLlOCOR-RMP system compared to the KMT system due to the specific surface area of FLlOCOR (160 m^2/m^3). Rusten et al. (1992) recommended that the surface area of the biofilm carriers should be calculated based on the internal surface area because microscopy has shown no sign of biofilm growth on the outside of the smooth plastic elements due to the erosion of biofilm caused by the frequent collision between the particles.

The performance of an aerobic fluidized bed reactor was evaluated to treat dairy wastewater (Ødegaard et al., 1994; Resmi and Gopalakrishna, 2004; Souza et al., 2004). The studies observed that the COD removal efficiency decreased as the organic loading increased. At an OLR in the range of 2.2-10.2 kg COD/m^3.d, the removal efficiency varied from 94.4 to 82.1 % at 6 h HRT (Resmi and Gopalakrishna, 2004). At the same time, the COD decreased to an average of 67.6% and 48.7% when the OLR was increased at 26.5 kg COD/m^3.d, and 50 kg COD/m^3.d at HRT 25 and 41 min, respectively (Souza et al., 2004). Green (2004) investigated the feasibility of treating dairy wastewater by a vertical bed reactor with a passive aeration system. This achieved an average removal of 67% and 47% of BOD_5 and COD, respectively. The overall COD removal in the complete operational cycle was at 0.467 kg COD/m^3.d.

A number of investigators have assessed the performance of FBR systems. For instance, Ødegaard et al. (1994) conducted a study on a moving bed biofilm reactor. This showed that at one of the reactors, 90% of the total COD was removed when the loading was 36.7 g COD_T/m^2.d. In another study, Øchieng et al. (2002) studied the effect of hydrodynamics on biodegradation of brewery wastewater on the performance of a fluidized bed bioreactor. Similarly, Øchieng et al. (2003) performed a study on treatment of mixed industrial wastewater (petroleum and brewery wastewaters), finding that at an OLR of 1.375 kg COD/m^3.d and 1 day HRT, a 74% COD reduction from brewery effluent was achieved. Similarly, Sokol (2001) obtained a 95% removal efficiency of total COD removal in the aerobic treatment of brewery wastewater in a gas–liquid–solid fluidized bed bioreactor with low density KMT® biomass support.

3.3.2.2.5 Fixed Bed Biofilm Reactors

Submerged fixed bed biofilm reactor systems are a new generation of attached growth bioreactors. This is also categorized as a hybrid biological bioreactor, due to the integration of suspended and attached growth processes. An activated sludge process is used, with process with packing materials fixed in the aeration tank to increase the cultivation on the surface of the media and to increase the concentration of biomass in the reactor (Grady et al., 1999; Metcalf and Eddy, 2003). Fixed (or stationary) film biological processes have been tested to treat wastewater over many years. In fixed film processes, the microorganisms grow in a thin film on support media while removing organic matter from the liquid flowing past them (Grady et al., 1999). These processes are intended to improve the performance of suspended growth process, such as the

conventional activated sludge process (Gebara, 1999), the sequencing batch reactor (Sirianuntapilboon et al., 2005), and other aerobic biofilters (Kantardjieff and Jones, 1996; Rusten and Thorvaldsen, 1983).

The performance of a multistage submerged fixed bed reactor (ASFF) was assessed using sugar processing wastewater by Hamoda and Abd-El-Bary (1987). The system exhibited a good COD removal efficiency of up to 97% at a low OLR of 3.6 kg COD/m^3.d and 6 h HRT. However, an 88% of COD removal efficiency was achieved at an OLR 6.48 kg COD/m^3.d (90 g/m^2.d) (Hamoda and Abd-El-Bary, 1987). In another study a moderate COD removal efficiency (73%) was achieved by Hamoda and Al-Sharekh (1999) by using the same system. The authors concluded that the ASFF process is able to handle a continuous organic loading increase from 50 to 120 g BOD_5/m^2.d. An effluent quality with COD and SS concentration less than 30 mg/L was obtained.

A high removal efficiency ranging between 85-99 % was achieved when Andreottola et al. (2002) used a pilot scale sequencing batch biofilm reactor (SBBR) for treating winery wastewater. The authors confirmed the applicability for the treatment of winery wastewater at an OLR up to 8.8 kg COD/m^3.d. More recently, some advance treatments were applied under a full scale of two-stage fixed bed biofilm reactors used for treatment of winery wastewater. In this system COD removal efficiency of 91% was obtained. The fraction of non-biodegradable soluble COD could interfere with or affect the removal of total COD, as the elimination of this fraction could not be achieved by a simple biological process. The average OLR was 1.57 kg COD/m^3.d, and the effluent COD concentration of 212 mg COD/L for most of the operational period. Significantly, the TSS removal efficiency of the entire system was 78% (Andreottola et al., 2005).

Fixed bed biofilm reactors were also developed to treat dairy wastewater (Rodgers, 1999; Rodgers and Burke, 2001; Rodgers et al., 2006; Rodgers et al., 2004). According to Rodgers et al. (2006), a novel lab-scale horizontal flow biofilm reactor proved excellent in removing COD, ammonium nitrogen (NH_4-N) and total nitrogen (TN). The COD removal efficiency was about 96.3% when the OLR in the entire system was 1.96 kg COD/m^3.d (56.9 g COD/m^2.d), and it also achieved 2.2 g COD/m^2.d for the total sheet surface area. The possible reason for this finding was attributed to assimilation and volatilization, which also contribute to 100% of the NH_4-N removal from the

system. It was noted that no clogging occurred in the system of plastics sheets. As a result, the solids accumulation rate in the system was low at 0.1 g S/g COD_f.

Rodgers and Burke (2001) developed a new experimental biofilm system for carbonaceous oxidation by using both corrugated cross flow plastic modules and a vertical honeycombed module. The system achieved over 7 kg COD/m^3.d of COD removal rate for both modules, with a filtered COD effluent concentration of less than 191 mg/L at a HRT of 1.1 h. The corrugated cross flow media with high specific surface area experienced clogging and reduction in performance; however, the honeycombed media remained unclogged and performed well. A similar technology was also used by Rodgers (1999) and achieved a filtered COD removal rate of 3.8 kg COD/m^3.d with 42 mg/L filtered COD effluent concentration, which corresponds to 92 % COD removal efficiency at a HRT of 2.9 h.

Rodgers et al. (2005) and Sirianuntapilboon et al. (2005) operated their experimental setups as a sequencing batch reactors (SBR) biofilm systems. Rodgers et al. (2005) revealed that the performance of a pilot scale vertically moving biofilm (VMSBBR) was clearly affected by some operational parameters. The authors observed that at an OLR of 0.9 kg COD/m^3.d, the reactor could remove up to 94.8% of COD_f from influent concentration of COD_f 1096 ±425 mg/L. The reactor showed a greater OLR than the loading on suspended growth SBR systems recommended by Metcalf and Eddy (2003) of 0.1-0.3 kg BOD_5/m^3.d. The authors did not observe any clogging problem, even with the increase in SS. But the SS concentration decreases in the effluent with average 11.2 mg/L, which signifies that the VMSBBR unit demonstrated consistent and high clarification efficiency. Suspended solids can further be decreased to as low as 4.4 mg/L from the sand filter polishing unit. Similarly, it can be suggested that the application of an attached growth process, by installing plastic media (135 m^2/m^3) on the bottom of the SBR reactor to obtain a MSBR system, could enhance the performance of the system (Sirianuntapilboon et al., 2005). MSBR achieved the COD, BOD_5 and oil and grease removal efficiency of 89.3, 83.0 and 82.4%, respectively, at an OLR of 1.34 kg BOD_5/m^3.d corresponding to (2.5 kg COD/m^3.d). In addition, the sludge volume index (SVI) was lower than 100 mg/L at the same OLR. The authors observed a higher performance of the reactor when the OLR decreased to 680 g BOD_5/m^3.d.

Performance of a novel biofilm process to treat wastewaters has been tested by means of laboratory and pilot scale experiments. A sequencing batch biofilm reactor (SBBR) process was examined to remove the nutrients from synthetic milk wastewater (Rodgers et al., 2004). It was found that the SBBR was capable of overall nutrient removal efficiency, as well as of organic matter. It achieved 95.4% total COD removal efficacy at an influent concentration of COD 773 mg/L. The alternating pumped sequencing batch biofilm reactor (APSBBR) was developed and operated at 0.487 kg COD/m^3.d. The COD removal efficiency was 91%. The performance of an aerobic bioreactor in the treatment of slaughterhouse wastewater was also evaluated. Sirianuntapiboon and Yommee (2006) used an inner tube of used tyres as biofilm support media in the SBR, because of the non-biodegrability and reusability without any degeneration. It was observed that the removal efficiency of BOD_5 increases with decrease of the OLR. The system achieved 95.9% of COD removal efficiency at an OLR of 0.6 kg COD/m^3.d and 1.5 day HRT, while BOD_5 removal efficiency increased from 94.3% to 97.9% when an OLR decreased from 528 to 80 g BOD_5/m^3.d. However, the removal efficiency of the MB-SBR was higher than 95% even when the system was operated under a very OLR of 528±50.8 g BOD_5/m^3.d. Bio-sludge quality of such reactors was studied and it was found that SVI decreases with decrease of organic loading, while SRT decreases with increase OLR.

Limited studies have been performed in treatment of food processing wastewater using flexible fibre biofilm reactors (Fang and Yeong, 1993; Huang and Hung, 1987; Yu et al., 2003). The process was developed and investigated for treatment of food processing industrial effluents. Due to the features of the packing media used, the performance of these reactors is increased and is not comparable to any other biofilm reactors. Fang and Yeong (1993) concluded that the novel fibre packing media reactors could successfully treat synthetic dairy wastewater having a COD concentration of 958 mg/L. An average of 95-97% of COD removal efficiency was achieved at a HRT of 4-14 h. Using a similar technology, Yu et al. (2003) have treated food processing wastewater by one and two stage flexible fibre biofilm reactors (FFBR). Their system achieved a high overall COD removal efficiency of up to 96% at a high OLR of 7.7 kg COD/m^3.d, 8 h HRT, and 2700 mg/L influent concentration.

Huang and Hung (1987) did not achieve a high performance with treated brewery wastewater using the same technique. A 73.6% COD removal efficiency at an OLR of

5.2 kg COD/m^3.d and 2 h HRT was lower than those achieved by Fang and Yeong (1993) and Yu et al., (2003). Whose systems achieved about 90% removal of BOD_5. Further, a sludge yield estimated in the range of 0.39-0.49 g VSS/g COD resulted, which was within the range of 0.39-0.52 g VSS/g COD as reported by Huang et al. (1983).

3.3.2.2.6 Summary of the Performance, Advantages, and Disadvantages of Aerobic Biofilm Processes

Table 3.4 summarizes data for various biofilm methods used for the treatment of food processing wastewater. The influence of OLR on the COD removal efficiency of attached growth processes has been reviewed in detail. In general, it is noted that as OLR increases, the COD removal efficiency decreases. Most of the attached growth systems show more than 80% COD removal efficiency at an OLR less than 5 kg COD /m^3.d. On the other hand, at high OLR between 10-30 kg COD/m^3.d, especially in FBR and FBBR reactors, a low COD removal efficiency of less than 75% is observed. The FFBR, in contrast, exhibited a different performance. Due to insufficient data, the FFBR still can show a better capacity for treating food processing wastewaters. The FFBR achieved 96% of COD removal efficiency, with corresponding OLR of 7.7 kg COD/m^3.d, which was not achieved by any other attached growth reactors. This could be because some of the features of FFBR differed from the rest of the biofilm reactors. Meanwhile, FBR, FBBR and FFBR are the only reactors that have organic removal efficiencies of more than 70% in the range of 1-17 kgCOD/m^3.d of OLR. Food processing wastewater is varied in COD concentration, and not all biofilm reactors could resist or treat a high COD concentration at high OLR. This is due to (1) high surface contact per unit of volume; (2) relatively uniform substrate distribution throughout the reactor provided by higher upward fluid movement; and (3) higher process stability resulting from microbial activities of most of the biofilm developed in the reactor (Ochieng et al., 2003).

In comparison with the suspended-growth wastewater treatment systems, advantages cited for the attached growth biofilm systems include (1) less energy required; (2) flexibility and simplicity of operation and low land requirement, (3) avoidance of sludge bulking and better sludge thickening properties; (4) a high specific surface area and compactness of the biofilm media; (5) co-existence of aerobic and anoxic metabolic

activity within the biofilm and (6) high resistance to shock loadings, and lower sensitivity.

However, the limitations of the application of some biofilm reactors are caused by the disadvantages encountered with each system. For instance, the trickling filters are not appropriate because some of the obstacles including relatively high occurrence of clogging, relatively low loadings required depending on the media, and limited flexibility and control. The potential disadvantages of the RBC include shaft breakdown due to the excessive microbial growth on the media, frequent motor drive maintenance, and sensitivity to overloading. RBCs are very expensive compared to other biological units. The FBRs are not used extensively, due to some disadvantages including, significantly greater operating costs because of the high purity oxygen and pumping needed; hard to control biofilm thickness; complicated inlet and outlet design; and a need to separate the biomass from the support media.

Attached growth processes use a wide variety of support media. The characteristics of the support media are very important to the efficiency of the process. Among these features is the specific surface area where microorganisms develop and grow. The specific surface area varies considerably due to the different materials used. The flexible fibre packing media has the highest specific surface area, at more than 2000 m^2/m^3, compared with the media used in other biofilm reactors. On the other hand, the trickling filters have the lowest specific surface area, but are nevertheless somewhat comparable with a fluidized bed reactor and fixed bed reactors. The flexible fibre might thus offer a better treatment potential and thus better quality effluent, because of the larger number of active microorganisms.

Table 3.4: Summary of data for various biofilm treatment processes

Reactor	Wastewater	Influent COD mg/L	Specific Surface area (m^2/m^3)	OLR kg COD/m^3.d	HRT (h)	COD Removal %	References
TF	Synthetic Dairy	471	243	0.62	NA	92	Rai and Murthy., 1999
TF	Synthetic Dairy	1271	243	1.215	NA	85	Rai and Murthy., 1999
TF	Cheese wastewater	2740	90	1.34	NA	88.2	Rusten et al., 1996
TF	Food processing	500	NA	NA	NA	80	El Defrawyand Shaalan, 2003
RBC	Slaughterhouse	2061	128.57	3.8	13	76-59	Torkian et al., 2003
RBC	Poultry	2200	111.458	2.2	24	91	Najafpouret al., 2002
RBC	Corn processing	5200	77.53	1.503	83	71	Luna-pabello et al., 1990
RBC	Dairy	2000	280	4.06	1	97	Durate & Oliveira, 1984
RBC	Fish canning	6200	104.167	3.84	40	93.7	Najafpour et al.,2006
RBC	Food processing	79000	230	NA	NA	NA	Wilson, 1997
FBR	Dairy	500	300	2.2	6	94.58	Resmi and Gopalakrishna, 2004
FBR	Brewery	3300	NA	1.375	24	74	Øchieng et al., 2002
FBR	Synthetic Milk	958	NA	1.5-5.6	4	96	Fang and Yeong, 1994
FBR	Milk	462.4	NA	26.5	25 min	67.6	Souzo et al., 2004
FBR	Dairy	3310	276	12	7	85	Rusten et al., 1992
FBR	Dairy	1410	276	12	3.5-11.2	85	Ødegaard et al.,1994
FBR	Meat processing	1158	350	14	4	75	Grabas, 2000
FBR	Winery	4424.7	NA	3.30	2.2d	88.7	Petruccioli et al., 2000

Table 3.4 (Continued)

Reactor	Wastewater	Influent COD mg/L	Specific Surface area (m^2/m^3)	OLR kg COD/m^3.d	HRT (h)	COD Removal %	References
FBR	Cheese wastewater	3070	335	3.55	NA	96.7	Rusten et al ., 1996
FBR	poultry	NA	250	NA	NA	95	Rusten et al., 1998
FBR	Dairy	2395	160	2.06	NA	89.8	Androttola et al., 2002
FBBR	Sugar	1500	67.2	0.739-17.1	2-8	73.6	Hamouda & Al-Sharekh, 1999
FBBR	Winery	2355.5	140	1.57	2.7d	91	Androttola et al., 2005
BBR	Sugar	900	72	3.6	6	97	Hamouda and Abd-El-Bary, 1987
Packed bed	Slaughterhouse	1508	NA	2.7	1.7 d	74.8	Kantadjieff and Jones, 1996
Packed bed bioreactor	Winery	4494.3	NA	5.77	1.2 d	91.1	Petruccioli et al., 2000
FBBR	Winery	2170	300	6.3	8.9-32	93	Andreottda et al., 2002
FFBR	Brewery	413	2472	5.2	1.9	73.6	Huang and Hung, 1987
FFBR	Food processing	2700	2200	7.7	8	96	Yu et al., 2003
FBBR	Synthetic dairy	2947.4	NA	1.96	36	96.3	Rodgers et al., 2006
FBBR	Synthetic dairy	1096	240	0.9	8	94.89	Rodgers et al., 2005
FBBR	Synthetic dairy	503	67.5	4.16	2.89d	92	Rodgers, 1999
FBBR	Milk	7500	135	2.5	3 -8d	89.3%	Sirianuntapihoom, 2005
FBBR	Dairy	3095	290	0.487	24.5	91	Zhan, 2006
FBBR	Synthetic Slaughterhouse	902.4	NA	0.60	1.5d	95.9	Sirianuntapihoom, 2006
FBBR	Food processing	3353	230	12.7	3.2-21	70	Rusten, 1983

TF:Trickling Filter. RBC: Rotating Biological Contactor. FBR: Fluidized Bed Reactor. FFBR: flexible Fiber Biofilm Reactor. FBBR: Fixed Bed Biofilm Reactor.

3.3.2.3 *Performance Comparisons of Various Aerobic Bioreactors*

The removal efficiency with respect to the aerobic biological treatment processes has been reviewed in detail. Generally, it can be seen that all methods removed high levels of COD effectively. In suspended growth systems, the SBR attained a high average COD removal efficiency at approximately 93%. The aerobic jet loop reactor also achieved a slightly superior average of 95.5% of COD removal efficiency, but this requires caution as there are few studies on this system. The AS shows slightly inferior average COD removal efficiency to other suspended growth process. In attached growth systems, none of the reviewed methods have any considerable difference, and all show the same pattern in COD removal efficiency in a wide average of 78.7-88.4%. Abdulgader et al. (2007) mentioned that the average of the removal efficiency in a rotating biological contactor (RBC) was lower in comparison with other biofilm reactors.

The OLR as applied in a range of biological treatment reactors has also been reviewed. There is a clear and significant trend in the average OLR. The trickling filter has the lowest OLR with an average of 1.05 kg COD/m^3.d. On the other hand, aerobic jet loop reactors recorded the highest average OLR, which is 27.95 kg COD/m^3.d. This is considered an exceptional case because of a few studies conducted on this reactor (Abdulgader et al., 2007). Consequently the studies for the aerobic jet loop reactors may not provide a meaningful comparison. In the FBR, the average OLR is 7.84 kg COD/m^3 .d, a little higher than those in flexible fibre biofilm reactors (7.7 kg COD/m^3.d). However, this may be due to the point with an exceptional high OLR (26.5 kg COD/m^3 .d) but low COD removal efficiency (67%). Similarly, fixed bed reactors also could be operated at low organic loading rate with 4.71 kg COD/m^3.d average. Furthermore, some other methods such as activated sludge reactors, rotating biological contactors, and sequence batch reactors also show a lower average organic loading rate. Therefore, it can be concluded that there is a significant difference between the OLR of suspended growth processes and attached growth processes.

In conclusion, the results from this review indicate that all aerobic bioreactors can be effective in the treatment of food processing wastewaters. However, the COD removal efficiency is generally lower when the OLR are increased. In addition, suspended growth reactors are operated with lower OLR, while attached growth reactors are operated at high OLR, with the exception of the trickling filter and rotating biological

contactor. Therefore, it can be concluded that attached growth bioreactors offer better performance, especially for cases with higher wastewater strengths. The high specific surface area and low sludge production of flexible fibre biofilm reactors are further advantages when compared with other attached growth biofilm systems. The analysis shows that a flexible fibre biofilm reactor is a sound alternative amongst all biofilm reactors from a process and economic perspective.

3.4 Process Modelling

3.4.1 Design of Experiments (DOE)

Design of experiments (DoE) has been very useful in the study of complex processes and to determine the optimum process operating conditions with minimum effort and time. The design of experiments is an optional and more efficient methodology that is increasingly being practised in biological processes. The aerobic biological process involves complex series reactions that normally require a number of assumptions to solve the equations, derived on the basis of physical, chemical and biological concepts. Consequently, the steady state models are basically able to predict the parameters that have been considered in mass balance relations but are unable to estimate other interrelated effluent quality parameters (responses) (Sötemann et al., 2005). To overcome such a problem, process modelling and optimization studies can be performed using response surface methodology (RSM) (Baş and BoyacI, 2007; Zinatizadeh et al., 2006). The following sections discuses the use of RSM in various studies reported in the literature.

3.4.1.1 Response Surface Methodology (RSM)

Response surface methodology (RSM) is a collection of mathematical and statistical methods useful for the modelling and analysis of problems in which a response of interest is influenced by several variables and the objective is to optimize the response (Montgomery, 2005). The RSM is an important branch of experimental design and a critical technology in developing new processes, optimizing the performance, improving design and the formulation of a new product. RSM provides a systematic and efficient research strategy for studying the interaction effects of numerous parameters using statistical methods (Hong et al., 2009). Finally, the overall effects of the parameters on the method can be represented by RSM (Baş and BoyacI, 2007). RSM offers a large amount of information from a small number of experiments. Conventional techniques are extremely laborious and time consuming; in addition, such methods do

not guarantee the determination of true optimum conditions and are unable to detect synergistic interactions between two or more operating variables (Wu et al., 2009).

In recent years, the application of RSM has been used effectively by some researchers to optimize and evaluate interactive effects of independent factors in various fields, such as in chemical and biochemical methods. Wu et al. (2009) have used the RSM to optimize the aerobic biodegradation of dichloromethane (DCM) in pure culture. A successful attempt was made to find out the optimum of medium components and growth condition biodegradation of phenol using *Pseudomonas.Putida(ATCC 31800)* (Annadurai et al., 2008). Zinatizadeh et al. (2009) studied the analysis of the interactive effects of process factors on biological activity of granular sludge grown in UASFF bioreactor. An integration treatment of palm oil mill effluent (POME), involving chemical pre-treatment and anaerobic digestion in UASFF was investigated by Zinatizadeh et al. (2006). The interactive effect of two independent operating variables was modelled and analysed using the response surface methodology; in addition, the optimum region for the reactor operation was located. Central composite design and RSM were used to study the effect of Fenton's peroxidation on the treatment of olive oil processing wastewater (Ahmadi et al., 2005), and selective optimization in thermophilic acidogensis of cheese-whey wastewater to acetic and butyric acids (Yang et al., 2003).

Response surface analysis was also used to evaluate the influence of pH, temperature and substrate concentration on the acidogenesis of sucrose-rich wastewater (Wang et al., 2005). Application of coagulation-flocculation process for treatment of leachate using poly-aluminium chloride (PAC) and alum (Ghafari et al., 2009), and palm oil mill effluent (POME) (Ahmad et al., 2005) was optimized and modelled using response surface methodology (RSM). Some researchers used response surface methodology to optimize the electrochemical oxidation treatment of various types of wastewater such as industrial paint wastewater (Körbahti et al., 2007), textile dye wastewater (Körbahti et al., 2007), whey wastewater (Güven et al., 2008), and pulp and paper industry wastewater (Soloman et al., 2009). Central composite design of experiments was used to study the effect of ozone treatment on acid dye effluent for colour and COD removal and to optimize the variables (Muthukumar et al., 2004).

As stated by Montgomery (2005), in most RSM problems, the relationship between the response and the independent variables is unidentified and may be complicated in most

cases. Thus, the first step in RSM is to find an appropriate approximation for the functional relationship between responses y and the independent variables. Usually, this process uses a low-order polynomial in some region of the independent variables. If the response is well-modelled by a linear function of the independent variables, then the approximating function is a first order model. If there is curvature in the system or in the region of the optimum, then a polynomial of higher degree must be used to approximate the response, which is analysed to locate the optimum, i.e. the set of independent variables, such that the partial derivatives of the model response with respect to the individual independent variables is equal to zero. RSM problems use one or both of these approximating polynomials (Khuri and Cornell, 1996; Mason et al., 2003; Montgomery, 2005). The ultimate objective of RSM is to determine the optimum operating conditions for the system, or to find out the region that complies with the operating requirements.

RSM is used along with the Design of Experiments to obtain the optimum operating conditions. Several different types of design are useful when one is exploring to fit a response surface for the optimum region. Among these designs are central composite design (CCD), Box-Behnken design, Hybrid design and Three-level Factorial design (Montgomery, 2005). The study carried out involved the employment of central composite design to optimize the aerobic biofilm treatment process because of its flexibility and suitability to fit quadratic surface that usually works well for the process optimization.

3.4.1.1.1 Central Composite Design (CCD)

The most popular class of experimental designs that are applied in process optimization and used for RSM design is called central composite design (CCD). The CCD is an effective design that is ideal for sequential experimentation, and allows a reasonable amount of information for testing lack of fit while not involving an unusually large number of design points (Montgomery, 2005). Generally, the CCD consists of 2^k factorial points augmented by $2k$ axial points and a centre point where k is the number of controllable process variables. The levels of the chosen independent variables are numerically expressed or coded as -1 and 1, where 0 is coded as an intermediate level. The CCD has three main varieties, present in most statistical software programmes, and these are rotatable, face-centred and inscribed. These types of central composite design are shown in Figure 3.3. It can be seen that the rotatable design explores the largest

process space and the inscribed designs are rotatable designs, while, the face-centred design is not.

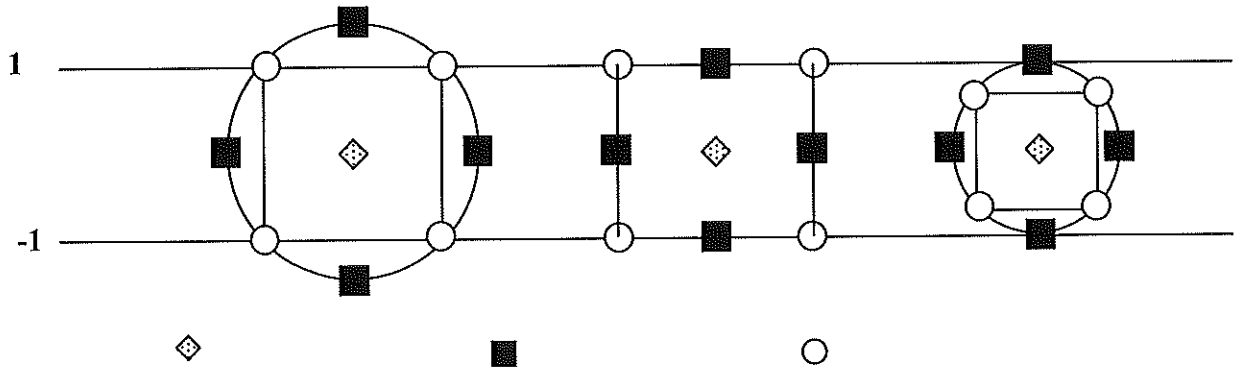

Figure 3.3: Comparison of three types of central composite designs, from left to right: Rotatable, Face-centred, Inscribed (Montgomery, 1991)

In the face-centred design, the axial points occur at the centre of each face of the factorial space, rather than outside the faces as in the case of a spherical region, so $\alpha = \pm 1$. This variety requires 3 levels of each factor. Augmenting an existing factorial with appropriate axial points can also produce this design. In this study, experiments were conducted based on a central composite face-centred design (CCFD). The central composite face-centred design for k=2 and k=3 factors can be shown in Figure 3.4.

After experiments were completed, the coefficients of the polynomial model were calculated using the following equation (Khuri and Cornell, 1996; Zinatizadeh et al., 2009).

$$Y = \beta_0 + \beta_i X_i + \beta_j X_j + \beta_{ii} X_i^2 + \beta_{jj} X_j^2 + \beta_{ij} X_i X_j + \ldots \quad (3.1)$$

where i and j are the linear and quadratic coefficients, respectively, and β is the regression coefficient. The experimental data were analysed and processed for Eq. 3.1 using Design Expert software (Stat-Ease, Version 6.0.6, Inc., Minneapolis, MN) including analysis of variance (ANOVA), which is suitable for experimental design. The quality of fit of the polynomial model equation was expressed by the coefficient of determination R^2, adjusted R^2 and adequate precision. Model terms are selected or rejected based on the probability of error (P) value with 95% confidence level. The fitted polynomial equation was expressed as three dimensional surface plots to visualize the relationship between the responses and the experimental level of each factor used in

the design. The optimum region is also identified based on the main parameters in the overlay plot.

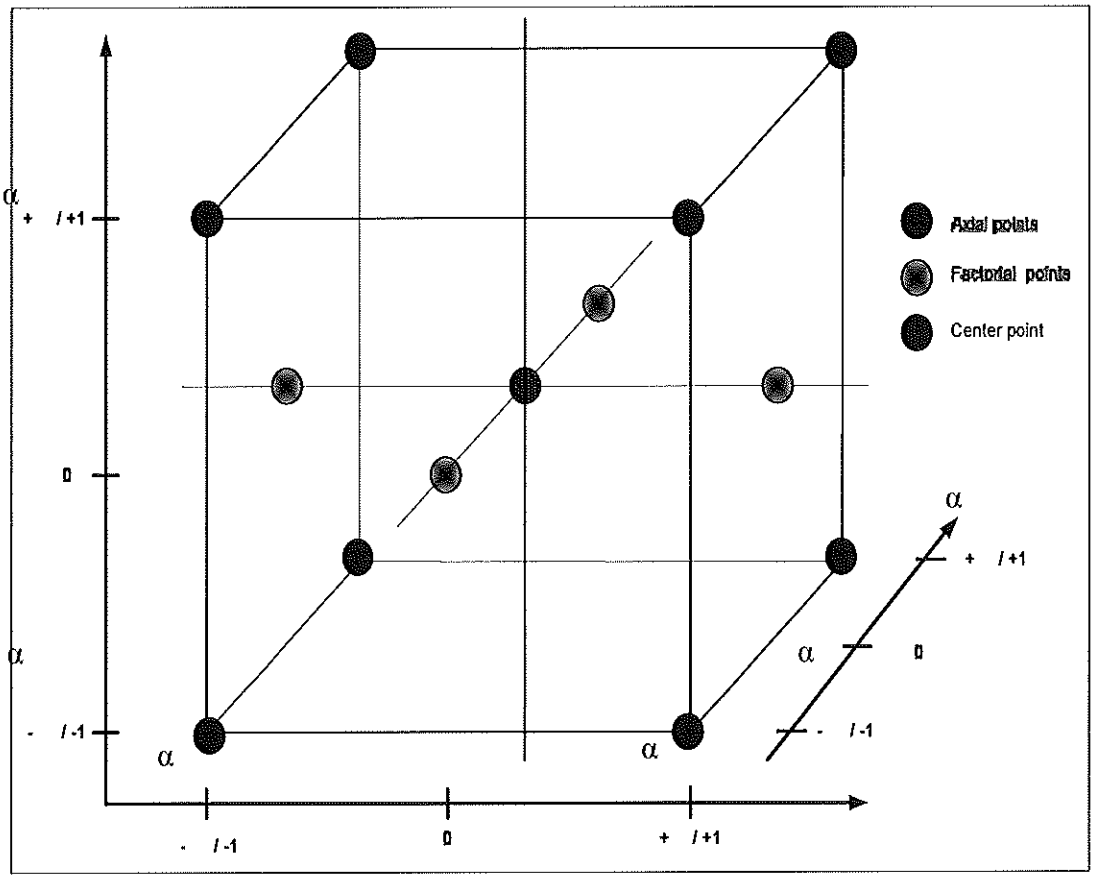

Figure 3.4: Central composite faced-centred design with three variables

3.4.1.1.2 Graphical Presentation of the Model Equation and Determination of Optimal Operating Conditions

The graphical presentation of the predicted model equation can be obtained by the response surface plot and contour plot. The response surface plot is the theoretical three-dimensional plot showing the relationship between the response and the independent variables. The two-dimensional display of the surface plot is called contour plot and in this plot, lines of constant response are drawn in the plane of the independent variables. The contour plots help to visualize the shape of a response surface. When the contour plot displays ellipses or circles, the centre of the system refers to a point of maximum or minimum response. Sometimes, a contour plot may show a hyperbolic or parabolic system of the contours. In this case, the stationary point is called a saddle point and it is neither a maximum nor a minimum point. These plots provide useful information about the model fitted but they may not represent the true behaviour of the system. It needs to

be noted that the contours (or surface) represent contours of estimated response, and the general nature of the system arise as a result of a fitted model, not the true structure (Baş and BoyacI, 2007; Myers and Montgomery, 1995).

3.5 Kinetic Modelling

Kinetics is a useful approach for understanding and designing biological treatment systems. The performance of biological processes used for wastewater treatment depends on dynamics of substrate removal and growth of microorganisms (Wang et al., 2009). During biological treatment of wastewaters, two correlated principles should be taken into consideration. First, metabolically active microorganisms catalyse the pollutant-removing reactions for microbial growth. The substrate removal rate depends on the concentration of the active biomass. Second, the active biomass is grown and sustained through the utilization of its energy- and electron-generating substrates, which are its electron donor and electron acceptor. The production rate of active biomass is proportional to the utilization rate of the substrates. The relationship between the microorganisms and the substrates is the most fundamental factor needed for understanding and exploiting the system for pollution control (Rittman and McCarty, 2001).

A number of models exist in the wastewater treatment in the literature describing activated sludge processes and biofilms systems (Wang et al., 2009). Kinetics modelling of high strength wastewaters by the Monod model has been widely reported in literature (Nakhla et al., 2006). The basic equations that describe the interaction between the growth of microorganisms and utilization of the growth limiting substrate in activated sludge processes are based on the Monod model, which is considered as the most commonly and widely used for determining the kinetics coefficients. The substrate utilization rate in biological systems can be modelled with the following expression for soluble substrates (Metcalf and Eddy, 2003).

$$r_{su} = -\frac{kXS}{K_s + S} \tag{3.2}$$

where r_{su} is the rate of change in the substrate concentration due to utilization, g/m^3.d, k is maximum specific substrate utilization rate, g substrate/g microorganisms .d, X is biomass concentration, g/m^3, S is growth-limiting substrate concentration in solution, g/m^3 and K_s is half-velocity constant, substrate concentration at one-half the maximum specific substrate utilization rate, g/m^3. The biomass growth rate is proportional to the

substrate utilization rate by the synthesis yield coefficient, and biomass decay is also proportional to the biomass present. When the substrate is being used at its maximum rate, the bacteria are also growing at their maximum rate. The maximum specific growth rate of the bacteria is thus related to the maximum specific substrate utilization rate as follows:

$$\mu_m = kY \quad \text{and} \quad k = \frac{\mu_m}{Y} \tag{3.3}$$

where μ_m is maximum specific bacterial growth rate, g new cells/g cells .d, and Y is true yield coefficient, g biomass produced/g substrate consumed. By combining Equations (3.2) and (3.3) the substrate utilization rate will become:

$$r_{su} = -\frac{\mu_m XS}{Y(K_s + S)} \tag{3.4}$$

It is important to note that kinetic expressions used to model substrate utilization and biomass growth rate, are all empirical (based on experimentally determined coefficient values). Besides the substrate limited relationship presented above, other expressions that have been used to develop the substrate utilization rates include the following (Droste, 1997; Metcalf and Eddy, 2003):

$$r_{su} = -k \tag{3.5}$$

$$r_{su} = -kS \tag{3.6}$$

$$r_{su} = -kSX \tag{3.7}$$

$$r_{su} = -kX\frac{S}{S_o} \tag{3.8}$$

It is known that the rate of substrate degradation is usually described by first order reaction rate, which is the rate of reaction directly proportional to the concentration of substrate. This means the first order reaction occurs in the completely mixed bioreactor at the limitation of substrate concentration. However, the zero order reaction is utilized to determine the rate of biodegradation at a rate independent of the concentration of substrates (Kaewsuk et al., 2010).

In the system that has an abundance of substrate concentration and the heterogeneous substrate condition, the reaction is a function of time. A pseudo first order reaction is used to explain the rate of reaction (Schnell and Mendoza, 2004). The mass balance to employ a pseudo- first order reaction can be expressed as:

$$\frac{1}{SRT} = -Y\left(\frac{r_{su}}{X}\right) - K_d = \left(Y\frac{Q(S_o - S)}{VX}\right) - K_d \qquad (3.9)$$

where the term $\frac{1}{SRT}$ is related to μ, the specific biomass growth rate, g VSS/g VSS d, as $\frac{1}{SRT} = \mu$, Q is wastewater flowrate, m^3/d, X is the biomass concentrations in influent settling tank, g/m^3, V is volume of the reactor, m^3, K_d, microbial decay rate, d^{-1}, and r_{su}/X =Q (S_0–S)/VX is the specific substrate utilization rate, g COD/g VSS.d. According to the equation (3.9), a plot of $\frac{1}{SRT}$ versus $\frac{r_{su}}{X}$ must lead to a straight line for every experiment conducted whose intercept and slope will be biomass yield coefficient (Y) and biomass decay coefficient K_d, respectively.

Parameters such as half velocity coefficient (K_s) and maximum rate of substrate degradation (k) defined from Eqs. (3.2) can be linearized into:

$$\left(\frac{X\theta}{S_o - S}\right) = \frac{K_s}{k}.\frac{1}{S} + \frac{1}{k} \qquad (3.10)$$

Kaewsuk et al. (2010) developed and verified the kinetic coefficients of mixed culture photosynthetic bacteria use for dairy wastewater in the membrane sequencing batch reactor using Monod's equation. The kinetic coefficient K_s, k, K_d, Y and μ_m were found to be 147 mg COD/L, 7.42 mg COD/mg VSS/d, 0.1383 day^{-1}, 0.2281 mg VSS/mg COD and 1.69 day^{-1}. The authors found that the kinetics are precise for designing and predicting the performance of the system using mixed culture. A fixed film bioreactor was examined for removing phthalic acid and dimethyl phthalate at various operating conditions by Pirsaheb et al., (2009). In this study, the kinetics parameters μ_m, K_s, Y, and K_d for phthalic acid and dimethyl phthalate were determined using Monod model, and the values were reported as 0.0371 h^{-1}, 8, 0.6112 g VSS/g phthalate and 0.0047 h^{-1}, and 0.0249 h^{-1}, 1.1,0.7875 g VSS/g phthalate and 0.0025 h^{-1}.

The kinetic model based on a mass balance model was investigated to describe the biological treatment of dairy wastewater in parallel batch system (Orhon et al., 1993). The kinetic coefficients with respect to the degradable COD in dairy plant wastewater were computed as μ_{max}=3.3 day^{-1}, K_s=74 mg/L. The kinetics of biomass growth were

presented by the yield (Y_{obs} and Y) and the endogenous decay rate (K_d), which were in the reported range of conventional activated sludge using Monod model (Al-Malack, 2006). Hamoda and Al-Awadi, (1995) presented a mathematical model based on Monod growth kinetics to describe the performance of data of four stages aerated submerged fixed film bioreactor. This study revealed that the Monod model can successfully describe the reactor performance and biomass growth. This is applicable to the first stage only and the later stages can be better described by fist order kinetics.

Two kinetics models (Monod and Haldane models) were investigated to describe the aerobic biodegradation kinetics for high oil and grease pet food wastewater (Nakhla et al., 2006). It has been concluded that the Haldane model gave a better description of the substrates consumption and the biomass growth rates than typical Monod model for the DAF-pre-treated wastewater because of the removal of particulate organic matter and oil and grease in this stage. For the DAF pre-treated batches, Haldane Model kinetic coefficients k, K_s, Y and K_i values of 1.28–5.35 g COD/g VSS.d, 17,833-23,477 mg/L, 0.13-0.41 mg VSS/mg COD and 48,168 mg/L, respectively, were obtained reflecting the slow biodegradation rate. Modified hydrolysis Monod model kinetic constants for the raw wastewater i.e., k, K_s, Y, and K_H varied from 1-1.3 g COD/g VSS.d, 5580-5600 mg COD/L, 0.08-0.85 mg VSS/mg COD, and 0.21-0.66 d^{-1}, respectively.

3.6 Summary of Literature Review

This chapter has conducted a comprehensive review of literature on the performance of biological treatment methods that have been used to treat food processing wastewater. Food processing wastewaters have similar characteristics; therefore biological treatment is always suitable. Choosing a suitable treatment method is important and complex. From the review, it can be seen that biological anaerobic treatment methods are more appropriate in treatment of high strength biodegradable wastewaters such as food industrial effluents. However, not all anaerobic processes achieve a good performance. There are considerable variations in organic loading rates and hydraulic retention times. Although it is a low cost process with less sludge production, there are still some drawbacks that more limited uses in treating high strength biodegradable wastewater. It is a very slow process, in which residence time extends to several days. It generally does not meet the standard discharged criteria and anaerobic methods can be very costly

if heat exchange needs to installed, so that aerobic methods have to be attached as a post treatment for further reduction of biodegradable materials.

The review indicated that aerobic processes can be effective in the treatment of food processing wastewaters. Conventional biological methods (suspended growth process) exhibited their moderate ability for treatment of food processing wastewaters. Although they have some good advantages such as low capital costs and acceptable COD removal efficiency, these systems can not work perfectly or withstand high organic loading rates. Increasingly, a large amount of sludge waste produced during treatment can also be a problem since it will increase the capital cost. Application of attached growth systems for treatment of food processing wastewater has increased due to their advantages, compared with the performance of suspended growth processes. Most attached growth systems are operated at high organic loading rates, with the exception of the trickling filter and rotating biological contactor. This creates a better treatment capacity and low sludge production, especially for cases with high strength wastewater. Introducing rayon fibre as a packing media can enhance the performance of the treatment process, because of the unique features of this material that make it more attractive than any other materials used. The review showed that a flexible fibre biofilm reactor is a sound alternative amongst all biofilm reactors from a process and economic perspective. Thus, using multiple stage reactors could be strongly beneficial in treatment of high strength wastewaters, as it is suggested by many researchers. It would improve and enhance the effluent quality and treatment performance. In spite of these promising results to date, no specific investigation has been reported in the literature especially using multiple stages flexible fibre biofilm reactors for treatment of any sort of food processing wastewater. Major areas for future work are to focus on the performance of MS-FFBR on treatment of food processing wastewater, particularly milk processing wastewater.

CHAPTER 4 MATERIALS AND METHODS

This project was designed to evaluate the performance and effectiveness of newly developed flexible fibre biofilm reactors for treatment of raw milk processing wastewater. In this research and under different operating conditions, three flexible fibre biofilm reactors were developed: Sequencing Batch Flexible Fibre Biofilm Reactor (SB-FFBR), Single-Stage Flexible Fibre Biofilm Reactor (SS-FFBR) and Multiple Stage Flexible Fibre Biofilm Reactor (MS-FFBR). Details of the reactor set-up and other operating conditions, and experimental procedures, are described in the following sections.

4.1 Chemicals and Reagents

The chemicals and reagents used in the study are listed in Table 4.1. The chemicals were used as received without further purification.

Table 4.1: List of chemicals and reagents

Name of chemical	Assay	Supplier	Purpose of use
Distilled water	-	-	Solution preparation
KH_2PO_4	99.5 %	Merck, Germany	BOD_5 test
NH_4Cl	99.0 % ≤	Merck, Germany	
K_2HPO_4	99.0 % ≤	Merck, Germany	
Na_2HPO_4, $7H_2O$	98.0 % ≤	Merck, Germany	
$MgSO_4$. $7H_2O$	98.0 % ≤	Merck, Germany	
$CaCl_2$	98.0 % ≤	Merck, Germany	
$FeCl_3.6H_2O$	99.0 % ≤	Merck, Germany	
KI	99.7 %	Merck, Germany	
NaN_3	99.0 % ≤	Merck, Germany	
$Na_2S_2O_3.5H_2O$	98.5 % ≤	Merck, Germany	BOD test
Hach Kit (0-150 mg/L)	-	HACH Company	
Hach Kit (0-1500 mg/L)	-	HACH Company	COD test
Hach Kit (0-15000 mg/L)	-	HACH Company	
NaOH	99.0 %	Merck, Germany	BOD test and pH adjustment in media
H_2SO_4	96 %	Merck, Germany	pH adjustment and BOD test
HCL	96 %	Merck, Germany	pH adjustment
Glass Microfiber Filter paper Whatman GF/C (pore size 1.2 µm)	-	Fisher Co.	TSS and VSS test

4.2 Wastewater

4.2.1 Source of Wastewater

The wastewater used in this research was collected from the final collection wastewater tank at National Foods Milk Ltd, Brisbane, Queensland, Australia. The factory uses approximately 400,000 litres of water each day over a six days operation. The water is predominantly for cleaning and plant operation. An extensive cleaning begins with flushing out the milk residual from tanks and pipes; general working environment, external surfaces of tanks, lines and machinery. All ends up in the wastewater along with cleaning chemicals.

Raw wastewater samples were continuously collected in 20 L plastic containers from the factory wastewater effluent stream. After the samples were collected, they were directly transported to the laboratory at Griffith University for initial characterization and stored in a cool room at 0-4 °C before being used for further investigation.

4.2.2 Characterization of Wastewater

The characteristics of the wastewater samples were determined in the laboratory at Griffith University. The wastewater investigations were conducted to identify the main parameters, including COD, BOD, total suspended solid, (TSS), volatile suspended solids (VSS), total solids (TS), turbidity, pH and total phosphate (TP). Typical characteristics of raw milk processing wastewater are given in Table 4.2. The composition of raw wastewater shows relatively high total COD concentration averaging between 4000-14250 mg/L, and BOD 3000-8910 mg/L. The BOD to COD ratio was about 0.62. The pH was usually basic due to cleaning operation using sodium hydroxide. The total solids and the total suspended solids in the raw wastewater were 5790-6380 mg/L, and 1420-3540 mg/L, respectively. The wastewater showed a high amount of total phosphate at 37 mg/L.

Table 4.2: Characteristics of raw milk processing wastewater

Parameters	Concentration (mg/L)
COD	4000-14250
BOD	3000-8910
pH	11.70
Total Solids	5790-6380
Total Suspended Solid	1420-3540
Volatile Suspended Solid	1350-3480
Total Nitrogen (as N)	N/A
Total phosphate (as P)	37
Oil and Grease	N/A

N/A=Not Analysed

4.3 Flexible Fibre

The configuration of the flexible fibre used in this study is illustrated in Figure 4.1. The flexible fibre media chosen as the packing material of this study was manufactured from rayon fibre with a specific gravity of 1.02, and a unit weight of 3 kg/m^3. The fibres were bundled and circularly attached to a rope for support at intervals of about 80 mm. The length of the fibre when straightened was about 75 mm and the diameter of the fibre was 0.07 mm. The rope was attached to a support frame and fixed at the centreline of each compartment. The length of the rope used in this experiment was 450 mm. The fibre packing had a specific contact surface area of around 2164 m^2/m^3 of tank volume and a void fraction of more than 99% (Table 4.3). This provided a large surface area for bacteria growth and attachment. The arrangement of packing media in the reactor is depicted in Figure 4.1.

Table 4.3: Fexible Fibre media characteristics (Huang and Hung, 1987)

Parameters	Value
Material	Rayon fibre
Specific weight	1.02
Unit weight (kg/m^3)	3
Void ratio	0.99
Aldehyde content	25%
Anti-pulling strength (g/fibre)	6.8-7.1
Maximum elongation ratio	12%

Figure 4.1: Photo of flexible fibre bundles

4.4 Seed Culture and Acclimation

Suitable inoculums were prepared by acclimatizing the seed with wastewater. Activated sludge samples were used for acclimatization. The activated sludge sample was collected from Logan City Council Wastewater Treatment Plant in Loganholme and Brisbane City Council Wastewater Treatment Plant at Oxley Creek. In both locations, the raw sewage is mainly domestic in origin. The collected sludge from both plants was tested in the laboratory. The total suspended solid was more than 5000 mg/L and SV30 was 180 ml/L. The sludge volume index (SVI) value was accounted to be 77 g/L. Live microorganisms existing in the sludge were also observed. Because of the considerable amount of aerobic bacteria found in activated sludge, it is easy to obtain large amounts from activated sludge plants. Another advantage is that activated sludge contains little sand or soil and is composed mostly of biomass. Thus, there is little problem with a dead space, consisting of sand and grit.

4.5 Air and Temperature

The reactors were supplied with compressed air from the laboratory air tap. All of the experiments were done at room temperature. The temperatures of the biological reactors were not adjusted throughout the study. The wastewater temperature was measured at 20±2 °C in the laboratory.

4.6 Reactor Setup

4.6.1 Sequencing Batch Flexible Fibre Biofilm Reactor (SB-FFBR)

The schematic diagram of the reactor setup used in this study is shown in Figure 4.2. This reactor set-up was previously used by Xu et al. (2001) to treat food processing industrial wastewater. The system included of an equilibrium tank with a capacity of 50L used as storage of wastewater and for pH adjustments. The SB-FFBR reactor was constructed from acrylic having a cylindrical shape (120 mm diameter, 900 mm height) with a working volume of 8 L. Air ceramic porous diffusers were installed at the bottom of the reactor for mixing and aeration. A compressed air source from the laboratory air tap was used to provide the SB-FFBR with air. The continuous air supply was maintained by regulating it at pressure of 10 psi and the air flow rate was controlled by an air flow meter (Model Porter-F65-AV1, Parker Hannifin Corportion, USA) to ensure desired flow of air applied to the biological system. Eight bundles were fixed in the column as a flexible fibre packing media for microorganisms. A general description of the simple flexible fibre packing media was described in Section 4.3. The influent was injected directly from the top of the reactor from the equalization tank. One sampling port was located at the bottom of the column. A peristaltic pump (Cole Parmer, Masterflex, Model 7523-60) with Tygon tubing was used for feeding the wastewater into the reactor. The excess sludge was drawn from the waste sludge port during the draw period.

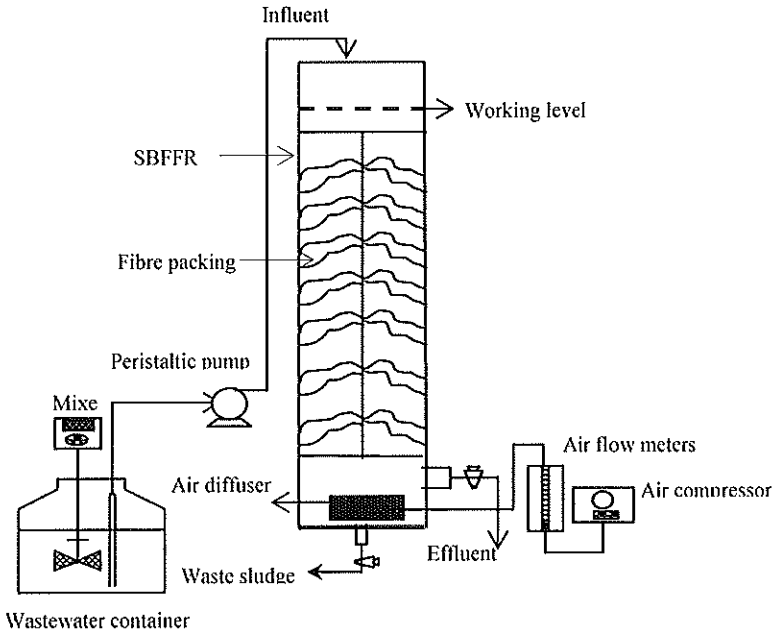

Figure 4.2: Schematic diagram of SB-FFBR experimental setup

4.6.2 Multistage Flexible Fibre Biofilm Reactor

The newly developed multistage flexible fibre biofilm reactor was designed and fabricated in the Griffith University mechanical workshop. The details of the design and the construction are described in the following sections.

4.6.2.1 Reactor Design

The design of the multistage flexible fibre biofilm reactor model is shown in Figure 4.3. The reactor was divided into four equal size compartments (stages) internally connected in series through the baffles. The total volume of the reactor is 40.625 L while an effective working volume is 32 L with dimensions L*W*D of 500 mm 125 mm and 650 mm. The reactor was made of Acrylic (Perspex) with 6 mm thickness (Figure 4.3). Compressed air was introduced by using two identical air diffusers in each stage placed at the bottom of each compartment to maintain adequate dissolved oxygen level and provide a better mixing. In addition, sampling ports were placed near to the effluent hole of each stage. The reactor was operated as a continuous flow system at a constant liquid level and controlled flow rate. A schematic diagram for the experimental setup is illustrated in Figures 4.4 and 4.5.

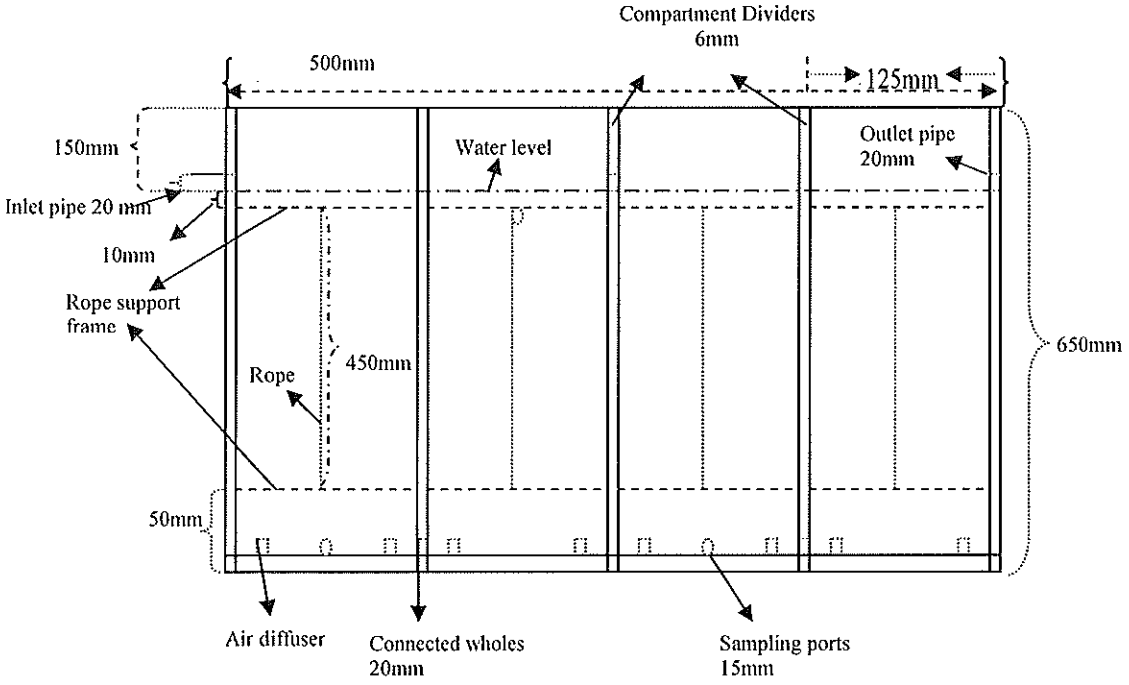

Figure 4.3: Construction details of the MS-FFBR

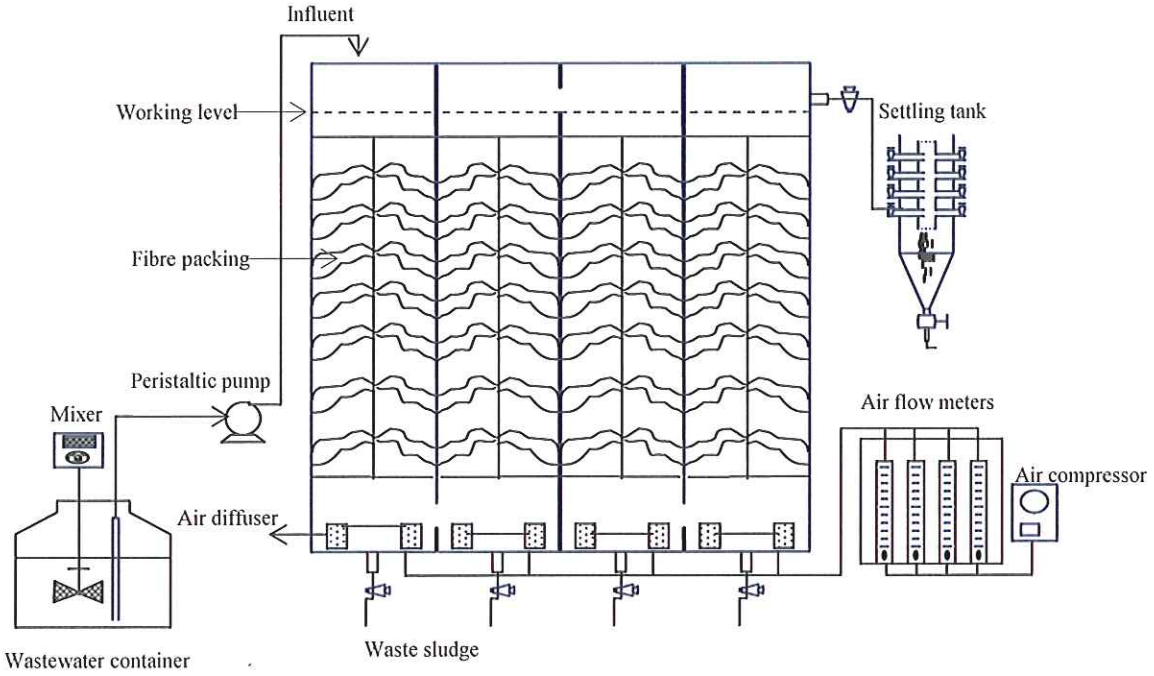

Figure 4.4: Schematic diagram of MS-FFBR experimental set-up

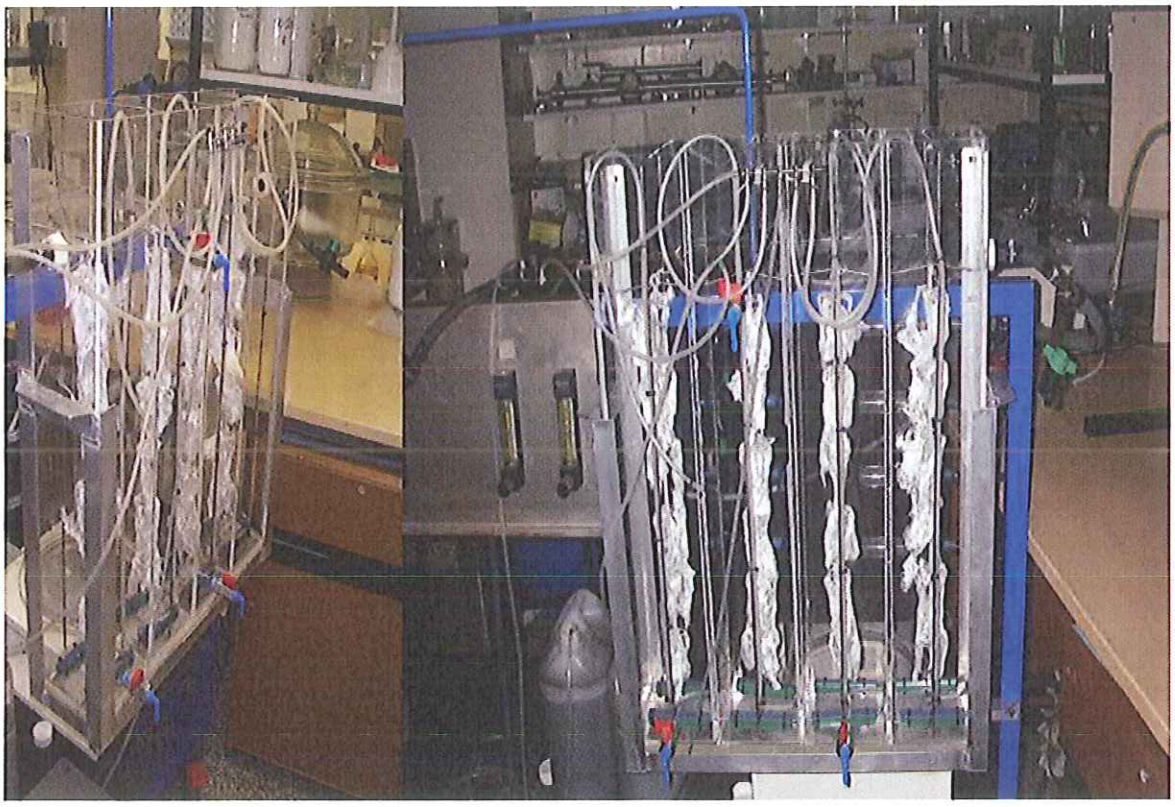

Figure 4.5: Laboratory-scale experimental set-up used in this study

4.6.2.2 Settling Tank Design

A cylindrical settling tank was applied in order to settle the washed out suspended solids (SS) from the reactor and also provide a clear effluent with low SS. The dimensions and schematic diagram of the settling tank are illustrated in Figures 4.6 and 4.7. The total volume of the settling tank was approximately 12.5 L. The total suspended solids and volatile suspended solids were continuously measured in the collected solids and the excess sludge was disposed of as waste.

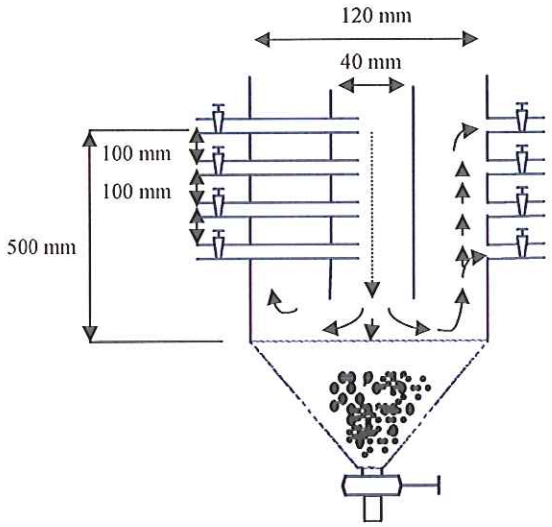

Figure 4.6: Settling tank design

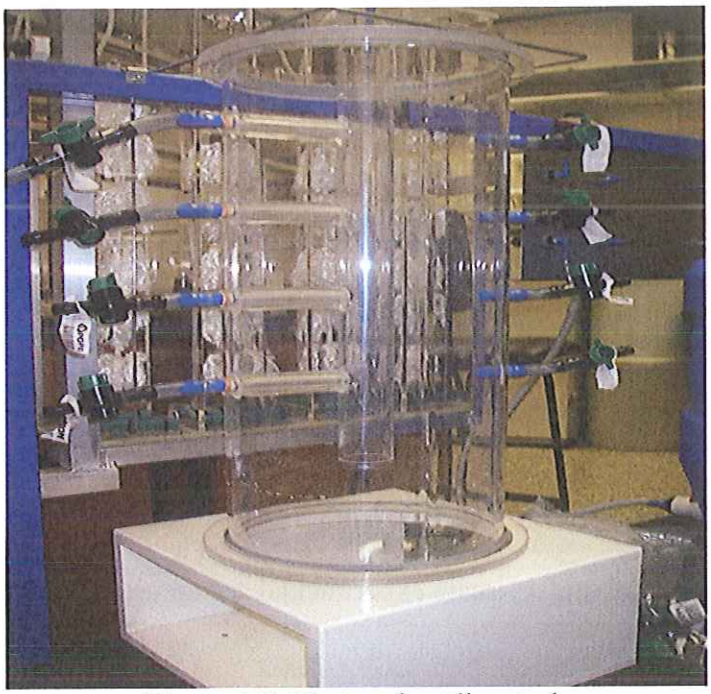

Figure 4.7: Photo of settling tank

4.6.3 Single-Stage Flexible Fibre Biofilm Reactor (SS-FFBR)

In this part of the study, the experiments were carried out in a laboratory-scale single stage flexible fibre biofilm reactor. The schematic diagram of the SS-FFBR is illustrated in Figure 4.8. The square shape SS-FFBR was fabricated using acrylic plastic transparent sheet with a thickness of 6 mm. A transparent malarial was used to build the reactor in order to observe wastewater throughout the experiment. Such material was thick enough to withstand the wastewater working volume pressure on the tank wall. The reactor had an effective working 8 L volume of with a height of 650 mm and width of 125 mm. The reactor was aerated through two air diffusers placed at the bottom. The influent port was located at the top of the reactor with a diameter of 20 mm, while the effluent sample port was in the bottom, also with 20 mm diameter. The reactor was provided with a support frame where the flexible fibre was attached. The reactor was supplied with 7 flexible fibre bundles and attached to 450 mm rope length. A peristaltic pump (Cole Parmer, Masterflex, Model 7523-60) with 16 inches diameter Tygon tubing was used for feeding the wastewater into the reactor. The effluent port was connected to a settling tank with a volume of 12.5 L and HRT used in the settling tank were 12.2, 18.9 and 23 h.

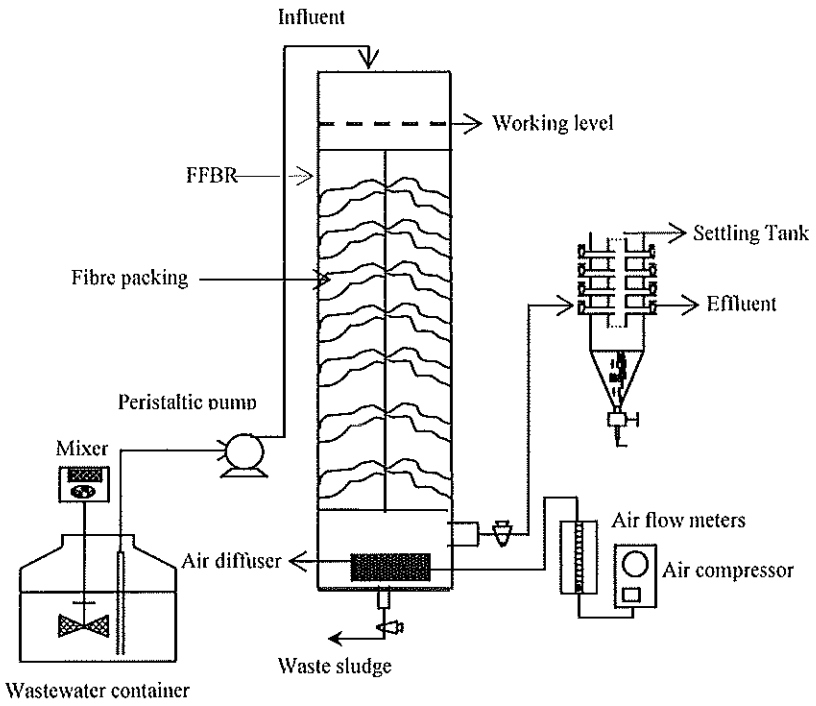

Figure 4.8: Schematic diagram of SS-FFBR experimental set-up

4.7 Definitions of Process Parameters Studied

The following parameters were determined as the process responses in this study.

$$COD(\%) = \frac{COD_{in} - COD_{eff}}{COD_{in}} \times 100\% \quad (4.1)$$

$$SRT = \frac{(V).(\mathrm{X})}{(Q_F).(effluentVSS)} \quad (4.2)$$

$$HRT = \frac{V}{Q_F} \quad (4.3)$$

$$U = \frac{(Q_F).(COD_{in} - COD_{eff})}{(\mathrm{X}.V)} \quad (4.4)$$

$$OLR_{COD} = \frac{(Q_F).(COD_{in})}{(V).(g/kg)} \quad (4.5)$$

$$CODremoved = \frac{(COD_{in} - COD_{eff}).(24)}{(HRT).10^3} \quad (4.6)$$

where COD_{in} is influent COD concentration (mg/L), COD_{eff} is effluent COD concentration (mg/L), SRT is solid retention time (d), X is the biomass concentration in the reactor (mg/L), Effluent VSS is the volatile suspended solid, (mg/L), V is the volume of the reactor (L), Q_F is feed flow rate (L/d), HRT is hydraulic retention time (d), U is specific substrate utilization rate (g COD_{in}/g VSS.d), and OLR_{COD} is the organic loading rate of COD (kg COD/m^3.d).

4.8 Operating Conditions

To gain insight into the development of flexible fibre biofilm reactors, the operating conditions and parameters were monitored. As the experimental strategy of this research was conducted on a sequencing batch flexible fibre biofilm reactor and continuous multi and single stage flexible fibre biofilm reactors, the operating conditions were different. The experimental details are described in the following sections.

4.8.1 Sequencing Batch Flexible Fibre Biofilm Reactor (SB-FFBR)

In this part of the study, the experimental design of SB-FFBR followed a similar strategy to Sirianuntapilboon et al. (2005). Two operating parameters were chosen as variants to study the role of the new SB-FFBR system for treatment of milk processing wastewater. The biological system of the SB-FFBR was studied to assess the effect of

influent COD and HRT on the performance SB-FFBR system. Three HRT values, 1, 1.6 and 2 days, were tested for influent COD wastewater of 610 to 7636 mg COD/L, 726 to 7597 mg COD/L and 8067 mg COD/L, respectively. To achieve a desirable concentration for each run, the raw wastewater was diluted with a tap water. The air flow rate was maintained constant, unless the DO concentration level in the reactor increased or decreased.

4.8.2 Continuous Multi and Single Stage Flexible Fibre Biofilm Reactor

For the single and multistage continuous processes, the response surface methodology (RSM) used in this part of research was a central composite face-centred design (CCFD) involving two different factors, HRT and COD_{in} concentration. The experiments of single and multi stage flexible fibre biofilm reactors were assessed based on the full face-centred CCD experimental plan in order to carry out a comprehensive analysis of the aerobic process. The HRT values for single and multistage were 8, 12 and 16 h were tested for single stage at an influent COD wastewater concentration of 800, 2400 and 4000 mg/L, while the influent COD concentration for multistage were 1500, 3750 and 6000 mg/L to provide a wide range of OLR and to study the performance of the systems. Independent parameters were measured and calculated as a response of the experiments.

4.9 Experimental Procedures

4.9.1 Sequencing Batch Flexible Fibre Biofilm Reactor (SB-FFBR)

The experiments were conducted to determine the treatability of milk processing wastewater in a SB-FFBR and to evaluate the effect of organic loading rate on the reactor performance.

4.9.1.1 Bioreactor Start-up

The inoculum of seeding culture of the SB-FFBR was a mixture of activated sludge sample collected from Oxley Creek and Loganholme Wastewater Treatment Plant. An equal volume of activated sludge from both sources was taken and mixed to ensure a diversity of microorganisms was available. The concentration of suspended solids was 1600 mg/L. The mixtures were then settled by the centrifuge and the supernatant was removed. The settled activated sludge sample was transferred into a 500 mL, conical flask containing 250 mL of raw milk processing wastewater. The mixture was shaken for 24 h to acclimatize with the substrate before being poured into the bioreactor. A

volume of 1L was transferred to the bioreactor. The reactor was fed using a peristaltic pump (Master flex model 7523-60 at 42 mL/min) with wastewater having the initial COD concentration of 500 mg/L and the concentration was gradually increased. Different dilutions of substrate were prepared using tap water. The reactor was operated batch-wise for about a week where 75% of the reactor volume was discharged and a new substrate was added. Before feeding into the reactor, the pH of the feed was regularly adjusted to 7 using HCL or H_2SO_4. No nutrient was added in this experiment.

4.9.1.2 Bioreactor Operation

After the reactor was started, the performance of the SB-FFBR was studied for the treatment of milk processing wastewater. The operation strategies of SB-FFBR are presented on Table 4.4. The operational sequence for different operations during each treatment cycle of SB-FFBR consisted of 5 steps: fill, react (aeration), settle (sedimentation/ clarification), draw (decant) and idle (Droste, 1997; Metcalf and Eddy, 2003). After a successful start-up of the reactor, a fresh raw milk processing wastewater was added using a peristaltic pump (Master flex Model 7523-60) at 42 ml/min for a final volume of 8 L in a period of 2 h (Fill). The system was fully aerated and continued for another 20 h of reaction (react). The air was shut down and the reactor allowed settling down for approximately 1.5 h (settle). Then, for a period of 0.5 h (draw), the effluent was discharged and supernatant was removed from the effluent port based on the replacement volume shown in Table 4.4. The idle step was neglected in this experiment. Then, a fresh raw wastewater sample was introduced into the reactor and the above sequence cycle repeated.

This experiment was operated at different hydraulic retention time HRTs and different influent COD concentrations. In the first set of this experiment, the HRT was maintained constant at 1.6 day throughout the operation. The influent COD concentration started with an average of 610 mg COD/L (OLR=0.38 kg COD/m^3.d) for a period of 10 days until a pseudo-steady-state condition was achieved, then the influent COD concentration was increased step wise to an average 7636 mg COD/L (OLR=4.77 kg COD/m^3.d). At a hydraulic retention time HRT of 2 days, the reactor was initially operated at an influent COD concentration 945 mg/L (OLR=0.47 kg COD/m^3.d). The influent COD concentration was gradually increased to 8051 mg/L (OLR= 4.02 kg COD/m^3.d). For each operating HRT, a pseudo-steady-state condition was reached within an average period of 14 days. The variation of less than 5% in effluent COD

concentration at each cycle was considered as a criterion for steady state conditions. In addition to the above experimental conditions, the performance of the SB-FFBR was investigated at the influent COD concentration at 8193 mg COD/L (OLR=8.19 kg COD/m^3.d). This condition operated for than 20 days, and a fluctuation in the effluent COD concentration was observed. It did not reach a steady state condition, but the effluent COD variation was less than 10% of the influent. The pH adjustment in the reactor was not necessary as it remained constant throughout the experiment cycles. The system was operated at a constant temperature of 22 ±2°C. COD reduction, biomass concentration, pH, TSS, VSS and DO were monitored regularly.

Table 4.4: Operation strategies of SB-FFBR

Parameters	Wastewater Concentration									
	610	2041	4382	7636	945	1913	3450	5450	8051	8193
HRT (d)	1.6	1.6	1.6	1.6	2	2	2	2	2	1
Working volume, L	8	8	8	8	8	8	8	8	8	8
Flow rate L/d	5	5	5	5	4	4	4	4	4	8
Replacement volume L/d	5	5	5	5	4	4	4	4	4	5
Operating cycle time/d	1	1	1	1	1	1	1	1	1	1
Fill up (h)	2	2	2	2	2	2	2	2	2	2
Aeration (h)	20	20	20	20	20	20	20	20	20	20
Settling (h)	1.5	1.5	1.5	1.5	1.5	1.5	1.5	1.5	1.5	1.5
Draw (h)	0.5	0.5	0.5	0.5	0.5	0.5	0.5	0.5	0.5	0.5
Operating period (d)	1	1	1	1	1	1	1	1	1	1
OLR kg COD/m^3.d	0.38	1.27	2.74	4.77	0.47	0.96	1.72	2.72	4.02	8.19

4.9.2 Single Stage Flexible Fibre Biofilm Reactor (SS-FFBR)

4.9.2.1 Experimental Design

In order to describe the interactive effects of HRT and influent COD concentration on the responses, using the one variable at a time technique, 9 continuous experiments on SS-FFBR were conducted at HRTs of 8, 12 and 16 h each with the influent COD concentration was 800, 2400 and 4000 mg/L. For this experimental design, both HRT and influent COD concentration were chosen as independent factors. The parameters that were considered as dependent output responses are TCOD removal efficiency, TCOD removal rate, SRT, turbidity, specific substrate utilization rate (U) and VSS/TSS ratio. The analysis of the data was accomplished by using the general factorial design of response surface methodology (RSM). Table 4.5 describes the conditions used for the

experimental design. The results were analysed using analysis of variance (ANOVA) that was performed by Design Expert Software (version 6.0, State-Ease, Inc., Minneapolis, MN).

Table 4.5: Experimental conditions

Run No.	Factors		
	Factor 1 A:HRT (h)	Factor 2 B:COD_{in} (mg/L)	OLR kg $COD/m^3.d$
1	16	2400	3.6
2	16	4000	6
3	16	800	1.2
4	12	2400	4.8
5	12	800	1.6
6	12	4000	8
7	8	2400	7.2
8	8	800	2.4
9	8	4000	12

4.9.2.2 Bioreactor Operation

This part of the experiments was conducted to evaluate the effectiveness and performance of a SS-FFBR in the treatment of milk processing wastewater. A 500 mL of a mixture of activated sludge was poured into the reactor. The sludge mixture had a VSS concentration of 4189 mg/L and VSS/SS ratio of 0.79. Initially, the reactor was batch-fed daily with diluted milk processing wastewater, starting with a COD concentration of 500 mg/L and the concentration increased gradually to an average concentration of 2417 mg COD/L. This step took about 7 days till the biofilm was developed on the fibre.

Continuous experiments were started by feeding the reactor with an initial influent COD concentration of 2400 mg/L corresponding to an OLR of 3.6 g/L.d and a HRT of 16 h. Different dilutions of raw milk processing wastewater were prepared using tap water. The pH of the feed was adjusted to 7 using diluted HCL and NaOH solutions. In this set of experiments, the steady state condition was not reached till after 20 days due to interruption occurring in the reactor. In order to study the effectiveness of the single stage reactor and the effect of OLR on the system performance, the HRT and wastewater flow rate were maintained constant at 16 h, and 12.96 L/d; the influent COD concentration was changed between 800 mg/L and 4000 mg/L. In addition, the reactor was operated at HRTs of 12 and 8 h and the flow rate of wastewater was kept controlled

at 15.84 L/d, 24.48 L/d, respectively. The wastewater was fed with COD concentrations of 800, 2400, and 4000 mg/L. The biomass concentration in the reactor was evaluated in every experimental run. Throughout the experiments, the influent pH was monitored and kept at 7. The air flow rate of all experiments was adjusted based on keeping the level of dissolved oxygen concentration > 2 mg/L in the reactor. The temperature of the reactor was maintained at room temperature.

4.9.3 Multistage Flexible Fibre Biofilm Reactor

4.9.3.1 Distribution of Hydraulic Retention Time

The residence time distribution experiments were determined by tracer tests. The tracer test is commonly utilized to investigate the hydraulic performance of reactors used for wastewater treatment. This test is usually done by pulse input or C-curve and F-curve.

In the C-Curve test, to evaluate and understand the hydraulic characteristics of multiple reactors in series, a tracer was initially introduced in the first stage of the reactor. The experiment was operated at hydraulic retention times of 2, 4 and 8 h, corresponding to water flow rates of 271 mL/min, 135 mL/min, and 68 mL/min, respectively. In addition, the air flow rate of this experiment was controlled at 564 mL/min, 270 mL/min, and 135 mL/min at HRTs of 2, 4, and 8 h, respectively. The ratio of the airflow rate to water flow rate was 2 in all experiments. A solution of food dyes was pulsed to the influent stream as a tracer. For a completely mixed reactor in series, the theoretical mean residence time was calculated using the following equation (Levenspile, 1992; Metcalf and Eddy, 2003).

$$\bar{t}_i E = \left(\frac{t}{\bar{t}_i}\right)^{N-1} \frac{1}{(N-1)!} e^{-t/\bar{t}i} \tag{4.7}$$

where, $\bar{t}_i$E = mean residence time in on reactor, $\bar{t}_i = N\bar{t}_i$, mean residence time in the N tank system, and N= number of reactors.

In the F-curve test, the experiments were performed with no initial tracer in the reactor. A tracer of concentration C_o was introduced to the entering of the reactor using a step input. The tracer response curve, determined using a continuous injection of tracer, is known as C/C_o. The test was conducted similarly to the C-curve test, however, the air flow rate at the HRT of 4 and 8 h was 807 mL/min, which corresponded to the AFR/WFR ratios of 6 and 11.8, respectively. It should be noted that the theoretical

mean residence time of the F-curve can be obtained by integrating Equation 4.7. In the present study, the integration has been conducted numerically.

The determination of the C-curve and F-curve was experimentally investigated. Pure water was introduced into the reactor at a desired water flow rate and under three different HRTs. The air flow rate was supplied using the central air source in the laboratory. The reactor was free of any suspended materials such as microorganisms for these experiments. The effluent sample absorbance was measured using a spectrophotometer (Shimadzu Corporation, UV 1601) at a wavelength of 629 μm at central interval time. The calibration curve for the tracer experiments is shown in Figure 4.9.

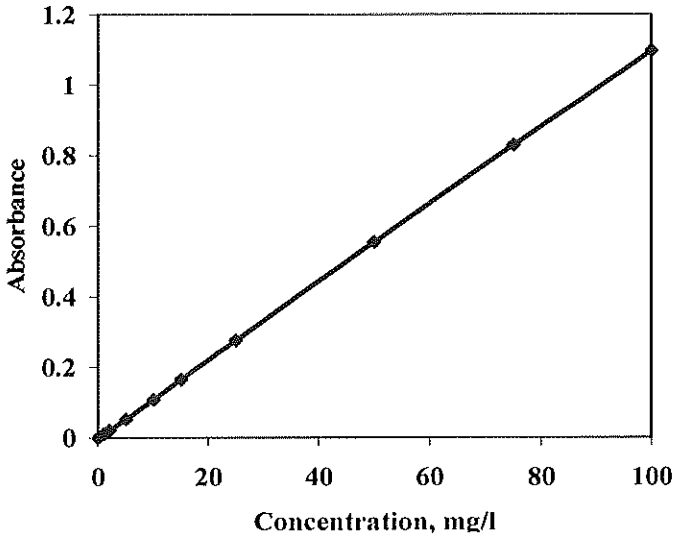

Figure 4.9: Tracers experiments calculation curve

4.9.3.2 Oxygen Mass Transfer

The oxygen mass transfer coefficient (K_{La}) is a useful parameter to characterise a bioreactor's capacity for aeration. To estimate the capability of oxygen transfer into the bulk water for the newly developed flexible fibre biofilm reactor, the measurements of oxygen mass transfer were conducted using clean tap water. The oxygen transfer rate was determined by direct measurement of the rate of increase in the dissolved oxygen concentration in the reactor after it was lowered by passing pure nitrogen gas (oxygen free) through the influent equalization tank and the bioreactor to reduce the amount of oxygen to nearly zero. The flow of nitrogen gas was stopped and this was followed by passing various rates of dry air as sources of oxygen through the air sparger at the bottom of the bioreactor. At the same time, the influent was started by pumping into the

reactor at a water flow rate of 1.0178 L/h for a HRT of 8 h. The experiments were operated at AFR_s of 15 L/h, 48.2 L/h, 94.5 L/h, 142.4 L/h, 190 L/h, and 239.8 L/h, which corresponded to the AFR/WFR 15, 47, 93,140,187 and 235. The dissolved oxygen (DO) concentration in the reactor was recorded with a DO meter every 20 seconds.

As described by Yu et al. (2006), the oxygen mass transfer coefficient K_{La} was developed based on the equation presented in the standard Methods for the Examination of Water and Wastewater (APHA, 1995). The K_{La} values were obtained from the data and calculated using the following Equation (4.8):

$$In\frac{C_s - C_0}{C_s - C} = \left(\frac{F}{V} + K_{La}\right)(t - t_0) \qquad (4.8)$$

where, K_{La}= overall mass transfer coefficient (h^{-1}), C_s= dissolved oxygen (DO) saturation concentration at test temperature and pressure mg/L, C= DO concentration at time, mg/L, t_o= initial time (h), t= time (h), F= water flow rate (m^3/h), and V= Volume of reactor (m^3). The value of C_s varies with oxygen partial pressure in contact with water and temperature. In the laboratory, the atmospheric pressure was 760 torr and the temperature was about 20°C.

This experiment was operated at water flow rate 1.0178 L/h and a reactor volume of 8 L. Hence, the value of F/V was 0.127, which was much less than the K_{La}. Therefore, equation 4.8 can be simplified to the following equation:

$$In\frac{C_s - C_0}{C_s - C} = K_{La}(t - t_0) \qquad (4.9)$$

In the study, dissolved concentration DO was studied versus time. A plot of $t-t_o$ versus $\ln(C_s-C_o)/(C_s-C)$ was made for the FFBR to obtain an overall oxygen mass transfer coefficients K_{La} at different ratios of AFR/WFR. To determine the relationship between AFR/WFR, and value of K_{La}, a correction between AFR/WFR ratio and K_{La} was obtained for the FFBR.

4.9.3.3 Experimental Design and Bioreactor Start up

The experimental conditions of this part of the research are presented in Table 4.6. The HRT and influent COD concentration were chosen as the main independent operating variables. The raw wastewater was diluted using tap water to achieve the influent COD

concentrations of 1500, 3750 and 6000 mg/L. The steady state performance of the MS-FFBR under different COD (1500, 3750 and 6000 mg/L) and HRT (8, 12 and 16 h) was evaluated. The collected data was organized and analysed by general factorial design of response surface methodology (RSM), and the analysis of variance (ANOVA) perform.

The reactor was started up using activated sludge collected from the MLSS tank at Oxley Creek wastewater treatment plant. The concentration of suspended solids was 5000 mg/L. The biofilm of the first stage was first established as in the single stage reactor experiment; Stages 2, 3 and 4 of the reactor were seeded separately with 500 mL each of acclimatized activated sludge. During the start-up phase, the reactor was run at 16 h HRT and an average COD concentration of 800 mg/L for several days, and then the feed concentration was increased step wise to 2800 mg/L. The reactor continued to operate in this condition until the development of the biofilm was perceived at the stages 2, 3 and 4. The pH of the feed wastewater was maintained constant at 7±1. The system was operated under room temperature.

Table 4.6: Experimental conditions

Run No.	Factors		
	Factor 1 A:HRT (h)	Factor 2 B:COD_{in} (mg/L)	OLR kg COD/m^3.d
1	16	3750	5.62
2	16	1500	2.25
3	8	1500	4.5
4	12	1500	3
5	12	3750	7.5
6	16	6000	9
7	8	3750	11.25
8	12	6000	12
9	8	6000	18

4.9.3.4 Bioreactor Operation

In order to study the performance of multistage reactor in the treatment of milk processing industrial wastewater, two interactive variables were considered as presented in the experimental condition in Table 4.6. The experiments were conducted on 9 runs with different hydraulic retention times of 16, 12 and 8 h and influent feed concentration (COD_{in}) of 1500, 3750 and 6000 mg/L, which corresponded to an OLR range of 2 to 18 kg COD/m^3.d. The reactors were first operated in a batch mode for a few days with clean packing media to develop attached microbial films on the flexible

fibre for the stages 2, 3 and 4, while in stage 1, the biofilm developed and existed from the single stage experiments described in the section 4.9.3. After the biofilm was developed, the reactor was fed continuously from the feed storage tank into the top of the first stage at water flow rates of 34 mL/min, 45 mL/min and 67 mL/min that corresponded to HRT of 16, 12 and 8 h, respectively. The effluent from the reactors was withdrawn by gravity. For each run, the wastewater in the equalization tank was freshly prepared to achieve the working concentration of the targeted run, and the raw wastewater was diluted using tap water. Stirring was continuously used by a stirrer located at the bottom of the equalization tank in order to obtain a correct homogenization of the wastewater. Each experimental run lasted between 1-3 weeks to reach the steady state condition. The air flow rate (AFR) varied from one stage to another and was kept constant and increased based on the DO concentration in each stage. In experimental runs 1-5 of the reactor, samples were collected each day from the inlet and outlet of the reactors, while in runs 6-9 the samples were taken daily. Additionally, samples were withdrawn from each compartment to characterise every individual stage. The samples collected in this experiment were then analysed for total and soluble COD, total and soluble BOD, TSS, VSS, turbidity and suspended biomass concentration (MLTSS and MLVSS) in each stage and also in the settling tank of each run. In addition, daily measurements of pH and dissolved oxygen were made. At the end of all runs the total amount of attached biomass concentration to the flexible fibre was measured using procedures described in Section 4.10.8.

4.10 Analytical Procedures

Influent and effluent samples were analysed in each experiment. The parameters analysed were pH, DO, COD, BOD, TSS, VSS, Turbidity and biomass concentration. The analytical testing procedures were in accordance with the standard APHA methods (APHA, 1995). In addition, mixed liquor biomass concentration, and wasted sludge, as well as attached biomass were determined.

4.10.1 pH

The pH is considered one of the important process parameters that have to be frequently monitored in both influent and effluent samples. The pH was measured using a pH meter model 90-FL provided from TPS Pty Ltd (Australia). The pH meter was calibrated with pH 7 and pH 4 buffer solutions before each use.

4.10.2 Dissolved Oxygen (DO)

Dissolved oxygen (DO) measurement in the aeration tank was monitored daily with a DO probe (YSI Model: 5010). The digital DO meter model YSI/5000 was supplied by the YSI Company, USA. The DO concentration was maintained between 3-6 mg/L for all experiments conducted by adjusting the airflow rate. The air flow rates were controlled by an air flow meter model Porter F665-AV1, Parker Hannifin Coporation, USA, and the range of the flow rates operated in these experiments was varied between 0.250-15 L/min. In each measurement, the DO meter was turned on and left for 20 to 30 min for the probe to be polarised. To ensure the accuracy of DO measurements, the DO meter was calibrated before each use.

4.10.3 Biochemical Oxygen Demand (BOD)

The biochemical oxygen demand BOD_5 is the most widely used parameter to determine the strength of organic contaminants in wastewater. In this measurement, the concentration of dissolved oxygen used by microorganisms to oxidize the organic matter is determined. The BOD_5 concentration in the feed and effluent was determined as one of the main parameters for this part. The BOD_5 test was conducted according to the procedures described on Wastewater Engineering Treatment and reuse (Metcalf and Eddy, 2003). The dilution water was aerated for approximately 24 h and nutrient was added to it before beginning this test. A small sample was directly pipetted in a 300 ml BOD bottle. Before the bottle was stoppered, the oxygen concentration in the bottle was measured. Another bottle was incubated for 5 days in the incubator controlled thermostatically at 20 ^{o}C. The BOD_5 test for the influent and effluent samples was carried out consistently. There was no seed used in the test. The initial and the final DO concentration was measured by a DO probe model YSI 5010. The digital DO meter model YSI/5000 was supplied by the YSI Company, USA. The BOD_5 of the sample was calculated from the difference in the dissolved oxygen concentration results obtained and expressed in mg/L.

4.10.4 Chemical Oxygen Demand (COD)

The determination of chemical oxygen demand (COD) was chosen to evaluate the amount of organic matter in the targeted wastewater. Basically, it is a measurement of the oxygen equivalent of the materials present in the wastewater that undergo chemical oxidation with dichromate. The total COD was regularly analysed for influent and effluent samples by a colorimetric method (digestion method) using the Hach kit. High

range vials (0-1500 mg/L and 0-15000 mg/L) and low range vials (0-150 mg/L) were used to determine the COD. For low range vials (0-150 mg/L) and (0-1500 mg/L), 2 mL of samples were add to a test vial with prepared reagents. The vials were then shaken vigorously for complete mixing with the reagents and heated at 150 °C for 2 h using a digester (model 45600, HACH Company, USA). The vials were allowed to cool to room temperature and the COD value of the samples was read from a Hach spectrophotometer (Model DR 2000) at 420 nm for low range, or at 620 nm for high range vials.

4.10.5 Turbidity

The turbidity was one of operational parameters measured for influent and effluent wastewater. It was determined by using a turbidity meter model 2100 A, supplied by (HACH Company, USA), based on the nephelometric method, and the results of the measurements were reported as nephelometric turbidity units (NTU).

4.10.6 Total Suspended Solids (TSS) and Volatile Suspended Solids (VSS)

Total suspended solids (TSS) and volatile suspended solid (VSS) were frequently measured in both sludge and liquid samples according to standard methods (APHA, 1998). For measurement of TSS, VSS and sludge samples, a suitable amount of sample (50 mL) was collected and then filtered through a Whatman GF/C glass microfibre filter paper (pore size 1.2 μm). The filter was then dried at 105°C for 1 h for TSS determination. The filter paper was then desiccated for about 20 min, and dried again at the same temperature. For VSS determination, the sample was burnt at 500 °C for 15-20 min.

4.10.7 Sludge Morphology

Microscopic examination of the developed biofilm in the flexible fibre reactor was conducted at the end of each experimental run. Scanning Electron Microscopy (SEM) was carried out to observe the biofilm morphology at different magnification.

4.10.7.1 Scanning Electron Microscopy (SEM)

The biofilm specimens were taken from three different bundles in the reactor for SEM viewing. The samples were immediately fixed with freshly prepared 3% glutaraldehyde fixative (3% electron microscopic grade glutaraldehyde (ProSciTech, Australia) in 0.1M sodium cacodylate buffer (ProSciTech, Australia) until the time of the scan. Scanning

Electron Microscopy SEM (Model FEI Quanta 200) photography was conducted at Queensland University of Technology (QUT). After washing with cacodylate buffer, samples were dehydrated in an ascending series of ethanol (70%, 90% and 100%), placed into amyl acetate, and then critically point dried with a Denton Vacuum Critical Point dryer. The samples were mounted on a support stub coated with gold-palladium (Biorad SC500 sputter coater) prior to examination and the digital image recorded with a FEI Quanta 200 scanning electron microscope, operating at 10 kV.

4.10.8 Suspended and Attached Biomass Concentration

TSS and VSS in the mixed liquor sample were used to estimate the suspended biomass concentration in the reactor. The experimental procedures were described in section 4.10.6. Because the flexible fibre used in this research as a packaging material does not have thermal resistance, and also with the plastic rings that carry the fibre, the bundle could not be burnt directly at 550°C to estimate the attached biomass concentration. The procedure for estimating the amount of attached biomass on the fibre described as follows. An empty dish was cleaned and dried overnight at 105 °C; the dishes were cooled in a desiccator and then weighed as an initial weight of W_0. The bundles were taken out of the reactor and put into the pre-weight dishes. The dishes were dried at 105 °C, and then cooled in a desiccator, and dried again until they reached a constant weight W_1. An average weight of clean bundle flexible fibre was obtained separately. The attached biomass concentration was then calculated by the difference between the weight of dried bundle and initial weight of dish minus average weight clean bundle fibre divided by reactor volume.

4.11 Data Analysis and Modelling

The data analysis was carried out by using an Excel software package and also general factorial design of response surface methodology (RSM). The Excel software was used for data and regression analysis. Correlation coefficients were used for determining whether there are relationships between dependent and independent variables. Regression of linear or curvilinear was also used for calculating the method to determine the intercept, the slope and relationship of parameters between dependent and independent variables. The Design Expert Version 6.0 Software was also used for data analysis by performing analysis of variance (ANOVA), and also for regression and graphical analysis of the data.

CHAPTER 5 TREATMENT OF MILK PROCESSING WASTEWATER IN SEQUENCING BATCH FLEXIBLE FIBRE BIOFILM REACTOR

5.1 Introduction

This chapter presents and discusses the results on the feasibility of using a modified sequencing batch flexible fibre biofilm reactor (SB-FFBR) for treating raw milk processing wastewater. The start-up phase was briefly described. The operation of the SB-FFBR was started after a visible biofilm appeared on the fibre media. The results of the COD variation, COD removal efficiency and effluent quality will be described in detail, based on the proposed hydraulic retention times (HRT). The effect of organic loading rate (OLR) and solid loading rate (SLR) on SB-FFBR performance will be explained based on 1, 1.6 and 2 day HRT. The kinetics of COD removal will be discussed to model the process. This chapter also includes a detailed explanation of the morphological study on flexible fibre biofilm using SEM techniques.

5.2 Reactor Start up Data

The start up of the SB-FFBR was the first step in this experiment. The reactor was run in SBR mode to acclimatize the microorganisms to the new substrate. The bioreactor was initially inoculated with 1L biomass solution as a seed culture. The biomass solution contained 4.6 g VSS/L, which represents the initial biomass concentration in the sludge sample. The acclimatisation was started by feeding the SB-FFBR with diluted milk processing wastewater containing approximately 600 mg/L of COD. This COD concentration was gradually increased to 1000 mg/L to adapt it to the microorganisms. At this stage, the air flow rate (AFR) was kept consistent and the dissolved oxygen (DO) level in the reactor was recorded to be higher than 2 mg O_2/L. The pH values of influent wastewater were in the range of 6.5-7.5. The effluent quality data of the start up experiments were not recorded, but visually the COD removal efficiency was high. The biofilm was developed and the acclimatisation was achieved after a couple of days. Figure 5.1 presents the developed biofilm during the start up phase. In the meantime, the microorganisms were easily attached on the flexible fibre. To examine the diversity of microorganisms in the reactor by gram stain test (Figure 5.2), a small sample was taken from the developed biofilm. As exhibited in Figure 5.2 the sample contains a diversity of bacteria with different round and rod shapes. A

negative gram stain bacteria with pink colour also existed. However, some of the positive gram stain also appeared in the reactor sample.

Figure 5.1: SB-FFBR during start up process

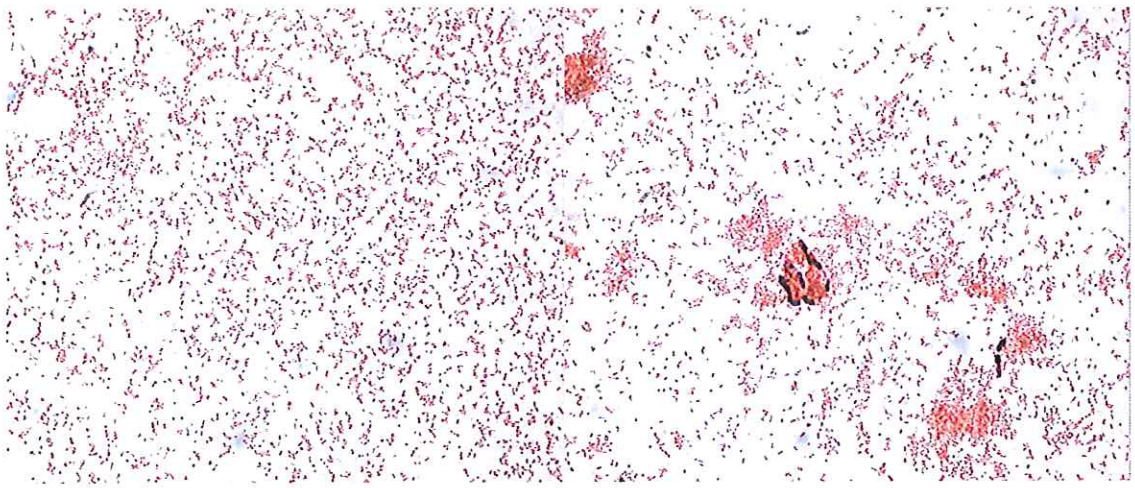

Figure 5.2: Gram stain of bacteria from SB-FFBR

5.3 Reactor Performance at 1 Day HRT

5.3.1 Variation of COD and Solids Concentration

The variation of the influent and effluent COD as a function of operation time under 1 day HRT are depicted in Figure 5.3. The assessment of performance of the SB-FFBR was studied by carrying out 24-h cycles. As can be seen in Figure 5.3, the pattern of influent COD concentration is not constant throughout the cycles, with minimum and maximum values of 6650 to 9070 mg/L, respectively. The average value of the COD concentrations obtained at steady conditions was about 8193 mg/L corresponding to an organic loading rate of 8.19 kg COD/m^3.d. The effluent COD achieved an average value of 1077.1 mg/L. In the first four cycles, despite high influent COD concentrations, the effluent COD concentration decreased to reach 758 mg/L, corresponding to an 89.3% COD removal efficiency. After that, the effluent COD increased because of an increase in the influent COD concentration on the day 9^{th} of the operation. Subsequently, the effluent COD decreased and was almost in steady conditions on day 11 to 16. Even though, the cycles continued for 22 days, the reactor reached a steady condition before this time. The variation of the influent COD concentrations in this set of experiments may be because of changes of the COD concentration in the influent tank and raw samples of wastewater due to the activity of some microorganism. This experiment illustrated that the SB-FFBR system achieved a good performance and effluent quality when treating raw and untreated milk processing wastewater containing a high level of organic and solids. One reason for such good effluent quality is because of the increase in total biomass mass concentration in the reactor that approximately was on average 2000 mg VSS/L during the operation time.

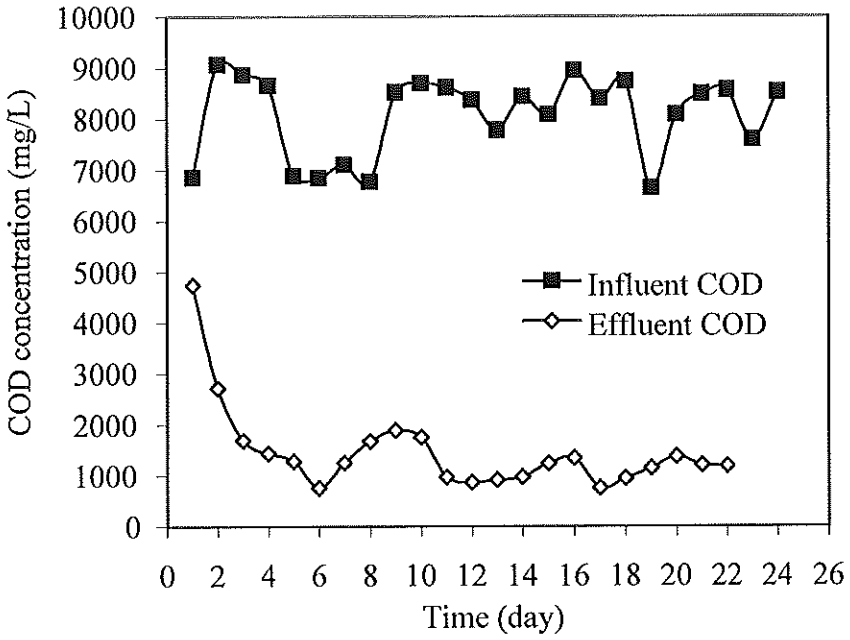

Figure 5.3: Variation of influent and effluent COD in SB-FFBR at 1 day HRT

Figure 5.4 shows the variations of total suspended solids (TSS) and volatile suspended solids (VSS) in influent and effluent streams as functions of operation time. As can be seen, the concentration of TSS and VSS in the influent and effluent are similar. The influent concentration varied in the range 1380 to 2560 mg/L for TSS and 1340 to 2420 mg/L for VSS. In the effluent stream, the TSS concentration was in the range 200 to 3180 mg/L for TSS and 280 to 2820 mg/L for VSS. In the first cycle, the effluent TSS and VSS concentration were high. This may be because of a high death rate of microorganisms as the organic loading rate suddenly increased. The solid concentration decreased gradually and did not show any stability throughout the experiments until the last two cycles. However, the influent solids concentrations (TSS and VSS) were not constant, and that was the main reason behind the fluctuating effluent concentrations. It has been noted that during the draw of the effluent, some of attached biomass was easily separated from the packing media and washed out with the effluent, which may indicate that the support media had reached the biomass carrying capacity. Some portion of reactor biomass was in a suspended form. The suspended biomass also contributes to solid concentrations and the accumulation rate of such solids increased throughout the cycles. The influent VSS/TSS ratio was 0.95, which is a bit higher than the recommended ratio of 0.6-0.7.

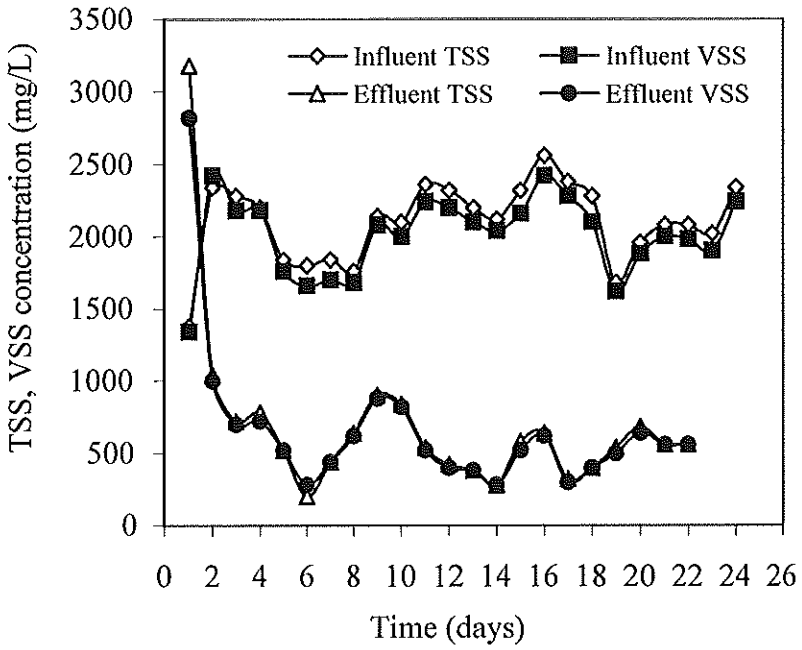

Figure 5.4: Variation of influent and effluent TSS and VSS SB-FFBR

5.3.2 COD Removal Efficiencies and Effluent Qualities

The performance of SB-FFBR was evaluated by estimating COD, TSS, and turbidity removal efficiencies, and the removal efficiency of each cycle of operation was assessed and plotted as a function of time in Figure 5.5. The system showed a significant variation on the COD removal efficiency between 70 to 90 % with an overall average of 86.8%. However, in the first cycle, the COD removal efficiency was only 30%. This was because of the shock loading as the organic loading rate increased during day 1 of the experiments. However, the removal efficiency gradually improved and increased to above 70 % as the organic loading rate was as high as 9 kg COD/m^3.d. Because of the fluctuation in the influent COD concentration, the system did not show stability of the COD removal efficiency until day 16 of the experiment when the reactor reached a steady condition, even though there was still a slight variation in the influent concentration. The achieved COD removal efficiency of 86.8% at steady condition was high at an organic loading rate of 8.2 kg COD/m^3.d. This confirms that the performance of the aerobic reactor becomes virtually independent of OLR applied to the system and relies on the amount of the biomass in the reactor and type of wastewater being treated.

With respect to TSS removal efficiency, the system exhibited a wide variation of removal efficiency, varying between 55.5-89.1% with an overall average of 73%. The removal efficiency of TSS was not constant and varied during cycle operations. It is evident from the results that the system showed inconsistently and unexpectedly low

performance for TSS compared with COD removal efficiency. However, good turbidity removal efficiency was obtained and the result was almost steady during the operation time with an overall average of 97.9%. It is evident from the results that the system was highly capable of treating high organic loading rates and achieving high COD and turbidity removal. However, the solid removal efficiency was lower and variable, due to the fluctuation of the solid loading rates. The lower TSS removal efficiency may also be due to the increase of the washout of the total suspended solids from the reactor.

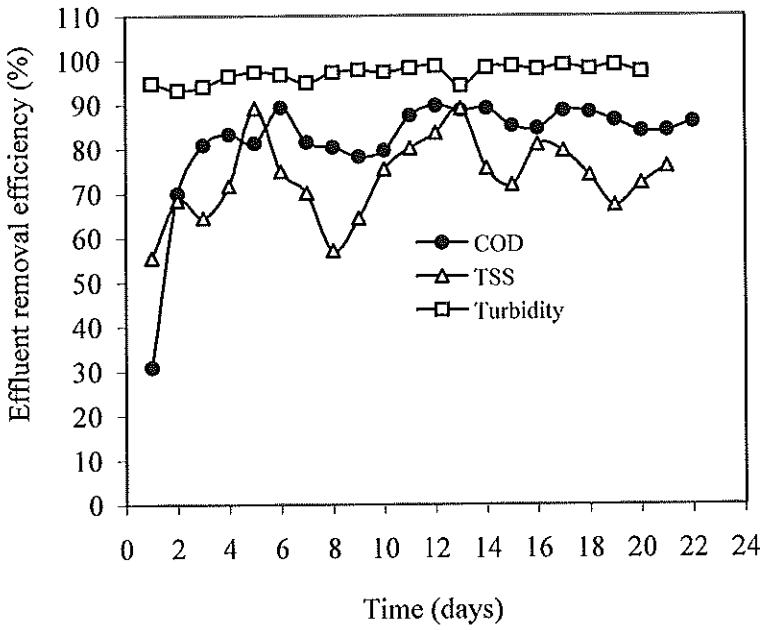

Figure 5.5: Removal efficiency of COD, TSS and turbidity profile in SB-FFBR

5.3.3 Performance Summary at 1 Day HRT

The SB-FFBR system was operated with raw milk industrial wastewater under 1 day HRT. The results shown in Table 5.1 are average of the response parameters under steady condition. This system was operated at 8.2 kg COD/m^3.d and this was selected to be the highest OLR applied to this system. At this high loading rate, the reactor achieved 86.8 % COD, 77.3 % of TSS and 97.8 % turbidity removal efficiencies. Such a high COD removal was similar to that obtained by Yu et al. (2003) using a continuous two stage flexible fibre reactor. In addition, the reactor achieved a good effluent quality with an average of COD effluent concentration 1077 mg/L and 33.1 NTU of turbidity. The suspended bio-mass concentration in the reactor varied and may be affected by the sludge washout during the draw period. It was 2089.2 mg TSS /L and 1970.8 mg VSS/L on average, which falls in the range of biomass concentration recommended in the activated sludge process.

The total amount of biomass concentration does not rely only on suspended biomass but also on attached biomass, which was estimated to be nearly 5000 mg VSS/L, bringing the total biomass up to 6970 mg VSS/L. The increased amount of biomass concentration in the reactor was a key reason for achieving a high COD removal efficiency at the highest OLR. This was due to the packing media providing a very high surface area for microorganisms to grow. The food to microorganism (F/M) ratio can indicate the degree of starvation of the microorganism. In this system, at OLR 8.19 kg COD/m^3.d, the F/M was 1.17, which is high. This means there is an excess food due to increase in the OLR and this may indicate that the microorganisms are in the exponential growth phase. In this condition, not all substrates are utilized by the microorganisms and the remainder will be discharged with the effluent. Sludge age was found to be 14.7 days at 1 day HRT. However, this value is higher than the recommended value to achieve a stable and reliable performance (Metcalf and Eddy, 2003). Consequently, it appears that the F/M ratio is not approximately inversely proportional to SRT.

Table 5.1: Effluent quality and removal efficiency of SB-FFBR system under 1 day HRT

HRT	Influent COD	Organic loading (kg COD/m^3.d)	COD		TSS		Turbidity (NTU)		Suspended bio-mass		Sludge age	F/M
(day)	mg/L		Effluent (mg/L)	Removal (%)	Effluent (mg/L)	% Removal	Effluent (mg/L)	Removal (%)	MLSS (mg/L)	MLVSS (mg/L)	SRT (day)	(day)
1	8,193.3	8.19	1077	86.8	491.6	77.3	33.1	97.8	2089.2	1970.8	14.7	1.17

5.4 Reactor Performance at 1.6 Day HRT

5.4.1 Variation of COD and Solids Concentration

The variation of COD concentrations in the influent and effluent with respect to operation time at 1.6 day HRT are depicted in Figure 5.6. The reactor was run at four different COD concentrations. Firstly, a set of experiments was carried out at low influent COD with an average value of about 610 mg/L (corresponding to an OLR of 0.4 kg COD/m^3.d). At this stage, the reactor attained a very high performance with an average effluent COD concentration of 15.4 mg/L (97.2 % COD removal). In the second trial, influent COD concentration of the reactor was increased to an average 2041 mg/L (corresponding to an OLR of 1.27 kg COD/m^3.d). An average of 70 mg/L of effluent COD (96.6 % removal) was achieved. Thirdly, the influent COD concentration was increased with an average of 4380 mg/L (OLR of 2.74 kg COD/m^3.d). An effluent with a COD concentration of 460 mg/L was obtained. However, COD effluent 1350 mg/L was initially obtained because of the sudden increase in influent COD. In the

fourth trial, the SB-FFBR was tested at an average influent COD concentration of 7636 mg/L (corresponding to an OLR of 4.77 kg COD/m^3.d). The reactor achieved an average effluent COD of 986 mg/L (87% removal), which seems to be high due to a point where the effluent COD concentration rose up to 3130 mg/L. This was because of the increase in the influent COD concentration (8000 mg/L) to beyond the targeted COD concentration.

Therefore, the reactor performance of the SB-FFBR at HRT of 1.6 day was quite satisfactory even when the influent COD concentration increased. The results obtained in this experiment show a similar tendency; the average of 750 mg/L of COD effluent (89.3% removal efficiency) obtained by using the SBR biofilm for treatment of milk industry wastewater at 3 days HRT, showed an effluent concentration decrease with increased HRT Sirianuntapilboon et al.,(2005). About 35 mg/L of effluent COD was obtained with 773 mg/L of a synthetic wastewater treated by a sequencing batch biofilm reactor (SBBR) Rodgers et al., (2004). Findings reported by Bandpi and Bazari (2004) for a SBR system treating dairy wastewater achieved COD removal efficiency around 90% with COD concentrations varying from 400-2500 mg/L.

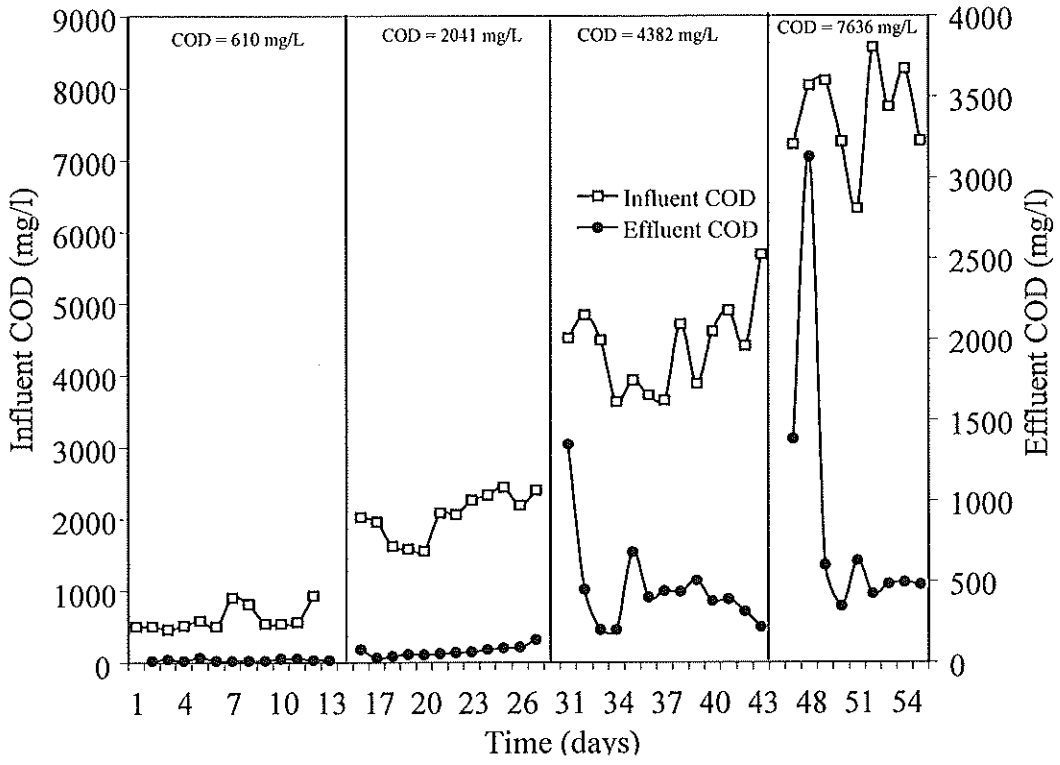

Figure 5.6: Variation of influent and effluent COD in SB-FFBR at 1.6 day HRT

In a biological treatment process, biomass concentration in the bioreactor is an important factor to ensure biological treatment ability. Figure 5.7 shows the VSS concentration variation in SB-FFBR at 1.6 day HRT over the experimental period. It can be seen that with increased influent VSS concentration, the effluent VSS concentration increased correspondingly. In the first and second trials of the experiments, the effluent VSS concentration was low and recorded almost the same levels with an average of 39 and 37 mg/L for first and second trials, respectively. This indicates a high degradation rate of influent VSS and production of new and active microbial cells that have the ability to attach to the fixed support media, resulting in a high VSS removal efficiency of 85% in the first trial and 92% for second trial. In addition, a low level of VSS reflected the reduced amount of sloughed biomass. This is considered as an advantage. In the third trial, the average influent VSS concentration was increased to 1210 mg/L. The reactor effluent VSS reached a steady state within a few days even with increasing of influent VSS. At this set of experiments, the effluent VSS concentration was 235.4 mg/L. This is fairly high compared to previous runs but corresponded to almost similar VSS removal efficiency of 80.5%. This indicates that the SB-FFBR system demonstrated consistent and high clarification efficiency and this also showed in the first and the second experimental trials. These findings were significantly greater than those obtained by Li and Zhang (2002), who obtained about 34.2% of effluent VS at 1 day HRT. Nonetheless, from day 51, the effluent VSS concentration increased and fluctuated with an average effluent VSS concentration of 991 mg/L (corresponding to VSS removal efficiency of 47.1%).

This result confirmed the effect of shock loading on the reactor effluent quality. A good quality effluent was dependent on the amount of solid applied to the reactor as the influent VSS concentration reached 1875.5 mg/L. The high concentration of effluent VSS of SB-FFBR was probably due to low biological conversion and also due to detachment of biomass from the packed support media. As a result, the sludge produced inside the reactor was high. Sludge clogging is often an operational problem in other biofilm reactors. This did not take place in this system due to the flexibility of the fibre.

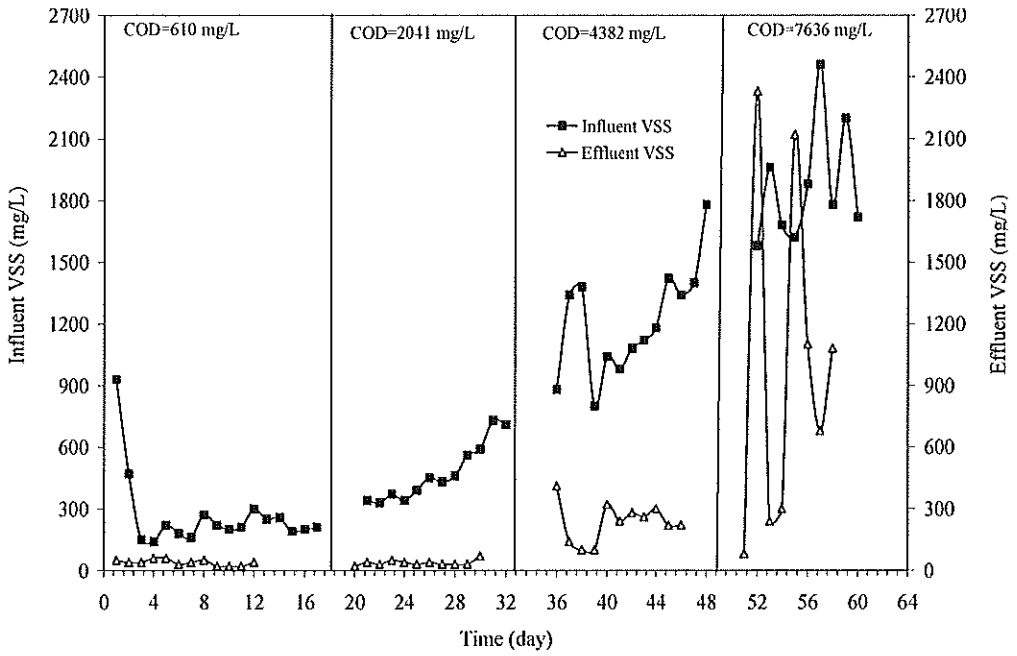

Figure 5.7: Variation of influent and effluent VSS in SB-FFBR at 1.6 day HRT

5.4.2 COD Removal Efficiencies and Effluent Qualities

The overall removal efficiency of the reactor as a function of time (days) at 1.6 HRT is illustrated in Figure 5.8. Generally, the SB-FFBR achieved a high level of COD effectively for all COD concentrations studied. It attained an overall average of 92.6% of COD removal efficiency. Basically, a high COD removal efficiency can be obtained when a reactor is operated at low COD concentration (Metcalf and Eddy, 2003). An average COD removal efficiency of 97% was approached when the reactor operated at average influent COD concentrations of 610 and 2040 mg/L respectively, as shown in Figure 5.8. This was quite consistent up to 14 days. However, the removal efficiency dropped to 89.3% at an influent COD concentration up to 4382 mg/L. The COD removal efficiency showed more variations, and was generally lower, but towards the end of the 14 day period, the removal efficiency was comparable with that at the two lower COD concentrations. The COD removal efficiency decreased to 87.2% at an average influent COD of 7636 mg/L. Initially, the reactor showed a sharp decrease of COD removal efficiency down to 61% before increasing. This illustrates the effect of shock loading on the reactor.

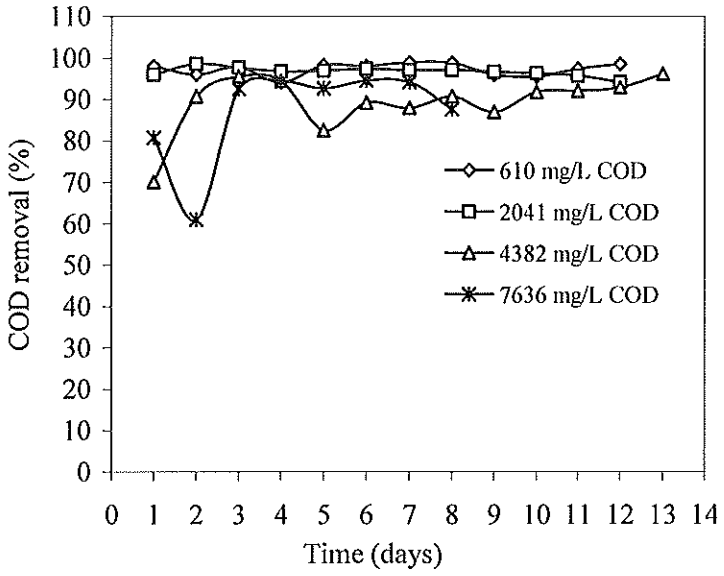

Figure 5.8: COD removal efficiencies of SB-FFBR at 1.6 day HRT

From Figure 5.8, it can also be seen that the reactor reached a steady condition in 8 day cycles. In previous studies conducted with a conventional SBR system for treatment of dairy wastewater, a 90 % COD removal efficiency was achieved with low COD concentration varying from 400-2500 mg/L (Bandpi and Bazari, 2004). This illustrates the capability of SB-FFBR of treating industrial wastewater due to the increase of the biomass concentration by using a high surface area support media.

The performance of the SB-FFBR can also be evaluated by the other effluent quality parameters, indicative of a greater degree of biodegradation. The quality parameters of the reactor effluent are shown in Table 5.2. The amount of COD applied to the system has a significant effect on the reactor performance. The DO level in the treated effluent was decreased by about 75% from 5.9-1.32 mg O_2/L, which is attributed to the increase of the activity of biomass as the substrate concentration increased. The turbidity of the effluent showed an increase with influent COD concentration, which is due to a high solid loading rate into the system. Total suspended solids (TSS) values in the effluent were due to biomass loss in the beginning of the experiment. It was observed that the sloughed biomass from the first run was reattached on the biofilm. When the influent COD concentration increased to 4382 and 7636 mg/L, the performance of the reactor noticeably reduced. This can also be seen in Table 5.2, where effluent TSS increased to 186 and 1030 mg/L due to insufficient time for TSS hydrolysis and increase in biomass growth rate, as well as biomass sloughing, as indicated by the drop in DO levels (5.9 to

0.2 mg/L). Therefore, a high quality effluent which is low in TSS, COD and turbidity under different loading conditions could be obtained.

Table 5.2: SB-FFBR effluent quality at HRT of 1.6 day

Influent waste strength (mg COD/L)	Effluent Characteristics			
	TSS (mg/L)	DO (mg/L)	pH	Turbidity (NTU)
610	10	5.9	6.7	1.6
2041	2	4.55	7.1	1.93
4382	186	2.0	7.4	32.7
7636	1030	1.8	7.3	20.3

5.4.3 Effects of Organic Loading Rate

The effect of OLR on SB-FFBR performance (COD removal) was evaluated and is shown in Figure 5.9. The study was conducted by increasing the influent COD concentration at constant HRT (1.6 day). The experimental runs were started with low COD concentration of 610 mg/L (corresponding OLR of 0.4 kg COD/m^3.d) and ended with a high COD concentration 7636 mg/L (corresponding OLR 4.77 kg COD/m^3.d). It can be seen from Fig. 5.9 that the COD removal percentage exhibited a sharp decrease with increasing organic loading rate. The maximum COD removal efficiency of 97% was noted at an OLR of 0.4 kg COD/m^3.d. The COD removal decreased to 87.2% when OLR increased to an OLR of 4.77 kg COD/m^3.d. The data in Figure 5.9 suggest that the OLR can be higher than 4.77 kg COD/m^3.d in order to achieve a COD removal efficiency of about 80%. An 89 % COD removal efficiency was obtained at an OLR of 2.74 kg COD/m^3.d. Reduction of COD removal efficiency with increasing OLR may be due to the reduction in contact time between substrates and biomass in the reactor. The COD removal efficiency of 87.2% at HRT 1.6 day revealed that suspended microorganisms may also contribute significantly to degradation of organic matter.

A similar finding was reported by Yu et al. (2003) with a removal efficiency of 90% at an OLR of 1.04 kg COD/m^3.d treating food processing wastewater in a comparable reactor. Sirianuntapiboon et al. (2005) also achieved an almost identical performance (89.3%) at OLR of 1.340 g BOD_5/m^3.d. However, a high COD removal (97.4%) was obtained in a rotating biological contactor (RBC) at 18.44 g/m^2.d, indicating relatively high removal rate in such a biofilm reactor (Najafpour et al., 2006). In this RBC reactor, less COD removal efficiency (85.4%) was obtained when the OLR increased to 36.89 g/m^2.d. Raj et al. (1999) observed that the COD removal percentage of 91.4% was

found when the influent COD concentration was 686 mg/L (corresponding hydraulic loading rate of 5 $m^3/m^2.d$).

In contrast, in this SB-FFBR, a different effect of OLR on COD removal rate is shown in Figure 5.9. The rate of COD removal showed an increasing trend, from 0.4 to 4.22 kg COD/m^3.d, with increasing OLR. This implies the productivity of the system, in terms of the amount of COD removed from wastewater, was high when the reactor was loaded with a high OLR. It has also been observed from the experiment that the necessary AFR increased when the OLR increased due to an increase in biomass concentration to consume the DO. A similar trend was observed by Najafpour et al. (2006) while working with food canning wastewater in a three stage aerobic RBC. With an OLR of 4.77 kg COD/m^3.d, the specific substrate utilization rate was calculated to be 0.477 g COD_{rem}/gVSS.d. Note that with increasing COD removal rate, oxygen uptake rate (OUR) was also increased (to the level below 1 mg/L), such that it correlated with the increasing the air flow rate. It is evident from the results obtained and presented that with increase in OLR, the COD removal rate of the system is increased. To achieve steady reactor performance at low concentrations, the reactor required a few days to reach steady state between each operating cycle, as indicated by the COD removal efficiency, typically less than 14 days, but it may require longer at high OLR, as the microorganisms need more time to adjust to the higher loads.

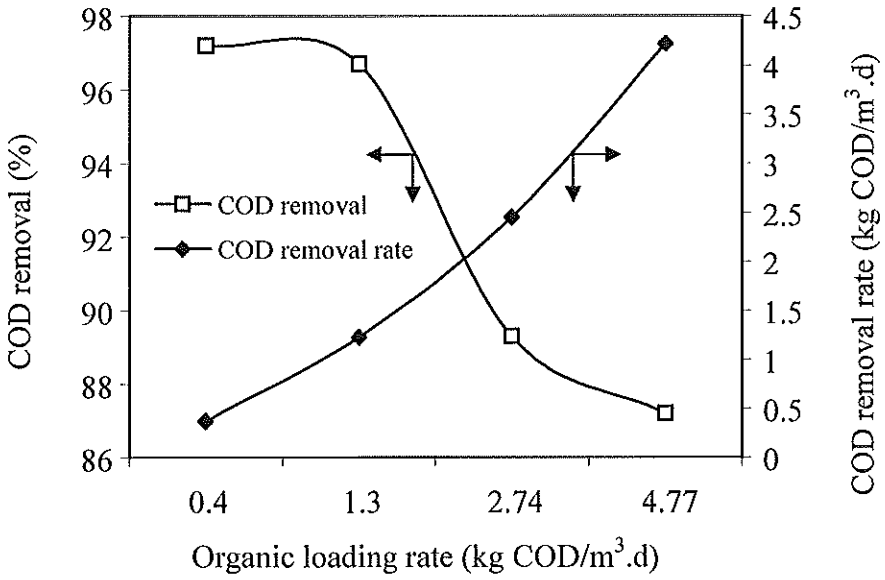

Figure 5.9: Reactor performances at HRT of 1.6 day

The effect of OLR on total suspended solids content in the reactor is illustrated in Figure 5.10. The results clearly show that the SB-FFBR reactor achieved a substantial reduction of TSS with increasing OLR. At low OLR corresponding to 0.4 and 1.3 kg COD/m^3.d, high total suspended solids removal efficiencies of 96.3 and 99%, respectively, were obtained. Good performance may have been enhanced because the concentration of suspended solids in the main wastewater influent was generally low. However, the reactor performance decreased when the organic loading rate increased gradually. At an organic loading rate of 4.77 kg COD/m^3.d, the TSS removal efficiency was 75%. A study conducted by Raj and Murthy (1999) showed a similar effect of organic loading rate on TSS removal and also effluent suspended solids concentration for treatment of synthetic dairy wastewater. In this study, the influence of OLR on TSS removal rate is also illustrated in Figure 5.10. The OLR has a linear relationship with TSS removal rate.

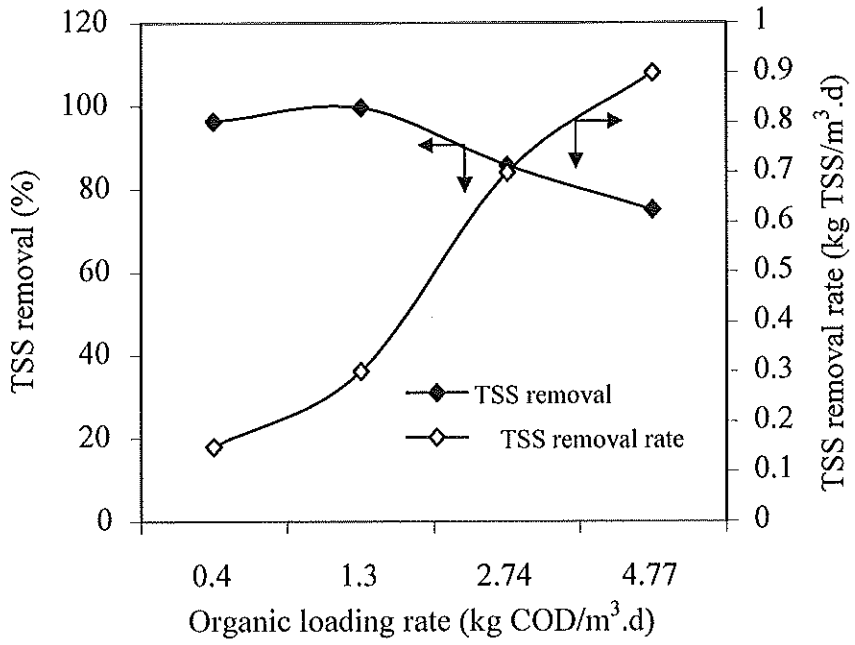

Figure 5.10: Reactor performances at HRT of 1.6 day

Figure 5.11 presents the relationship between the specific substrate utilization rate and organic loading rate. A liner regression was established and shows a high degree of dependence with a correlation coefficient (R^2) of 0.994. The regression analysis applied to the SB-FFBR data indicated that the specific COD utilization rate increased as the OLR increased, indicating that the system had not yet reached its maximum treatment capacity. This shows that the process can utilize more organics at higher OLR. A similar finding was reported for treatment of municipal and industrial wastewaters, so that the

amount of substrate removed increases with an increase of COD concentration (Hamoda, 1989; Hamoda and Al-Sharekh, 1999; Hiras et al., 2004; Izanloo et al., 2006; Su and Ouyang, 1996).

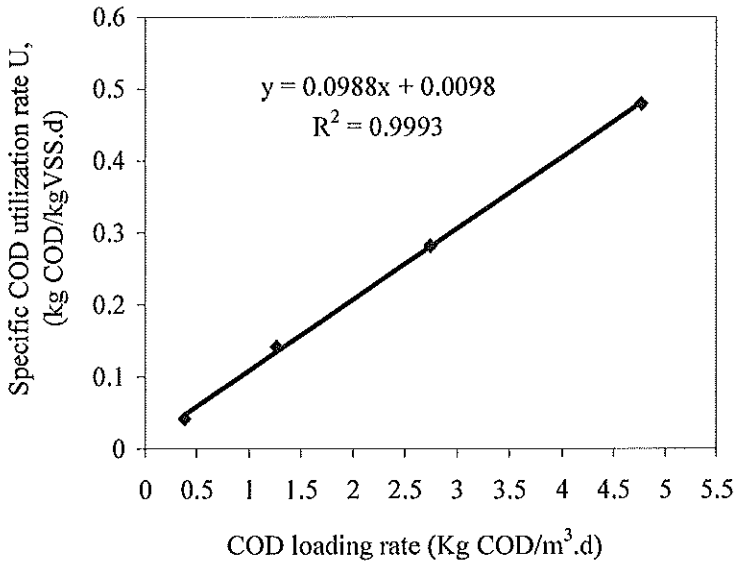

Figure 5.11: Specific substrate utilization rate vs OLR

5.4.4 Effects of Suspended Solid Loading Rate

The influence of the SLR on the SB-FFBR on TSS removal efficiency and TSS removal rate is shown in Figure 5.12. The rate of TSS removal was dependent on the SLR, and rises fairly uniformly over the increase in SLR studied. The percentage of TSS removal is fairly uniform at about 98% in the first and second points of solid loading rate. However, it decreased from 85.7 to 75% while the SLR increased from 0.81 to 1.19 kg SS/m^3.d. It showed that such a SLR needs longer time to be hydrolysed and biologically consumed. These findings were better than those obtained by Najafpour et al. (2005) with 88% of TSS removal efficiency at low SLR. El-Kamah et al. (2010) also obtained 50 mg/L of TSS in batch activated sludge system treating fruit juice industry wastewater. High TSS removal efficiency expresses the reduced amount of sloughed biomass and the increase of attached biomass on the flexible fibre. In addition, the suspended matter could be adsorbed on, or enmeshed into, the biomass and then hydrolysed by extra-cellular enzymes ElKamah et al. (2010)

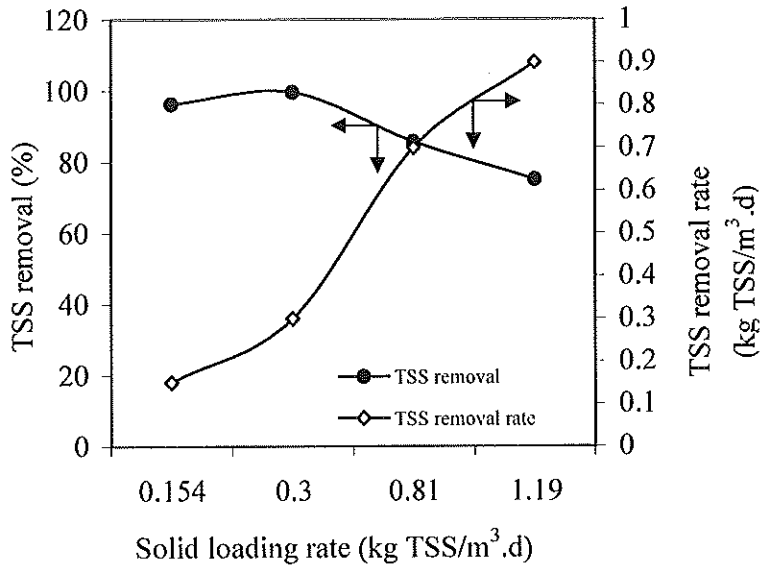

Figure 5.12: TSS removal efficiency and TSS removal rate

The SB-FFBR system achieved a higher COD removal compared with the previous studies, due to the increased amount of biofilm mass in the reactor volume provided by the flexible fibres. This increased biomass concentration was achieved by the combination of two factors. Firstly, the fibre packing media used has a very high specific surface area (in the order of over 2200 m^2/m^3), which provides a much higher support area per unit reactor volume compared with most solid support materials, for which the specific surface area is in the order of lower hundreds, eg. 300 m^2/m^3. Effectively, it is the higher specific surface areas of the fibre that have led to the increased biomass concentration in the reactor. Secondly, the bulk of the biomass in the SB-FFBR system is attached to the fibre support. This is in contrast to the case of a conventional SBR system, where the biomass is suspended in the wastewater medium. The attachment of the biomass to the fibre seemed to have significantly increased the ability of the reactor to retain the biomass in the reactor discharge phase of the operation.

This increased retention of the biomass through the attachment mechanism may, in turn, have further increased the total biomass concentration in the reactor for substrate degradation. Furthermore, the fibre was fixed within the reactor and part of the fibre and its attached biomass was exposed to the air for a short period of time before the reactor was completed filled. The exposure to air may provide some benefits to the microorganisms, for example, increased aeration effects similar to a rotating biological disc. Hence, these combined effects are believed to be the theoretical reasons behind the reactor performance that was observed.

5.5 Reactor Performance at 2 Days HRT

5.5.1 Variation of COD and VSS Concentration

Figure 5.13 shows the influent and effluent COD concentration variation under 2 days HRT. In this experiment, the COD concentration gradually increased in order to study the performance of the SB-FFBR under different substrate concentration, which corresponded to a different OLR. The feeding started at an average influent COD concentration of 945 mg/L, corresponding to 0.47 kg COD/m^3.d of OLR. During the first trial the effluent COD variation was quite constant and the effluent COD concentration was 23.1 mg/L. In the second trial the influent COD concentration was increased to an average of 1913 mg/L, corresponding to 0.96 kg COD/m^3.d of OLR. During this phase of the experiments the influent COD concentrations were varied and kept constant from day 29. Despite the influent COD concentrations variation the reactor showed stability on effluent COD concentration from the beginning of this trial and the average effluent COD concentration was 45.6 mg/L. However, when the influent COD concentration was increased to 3450 mg/L at the third trial, the average effluent COD was also increased to 96.7 mg/L, even though the influent COD concentration was not consistent and it showed a shock loading effect in days 40 and 41 when the effluent COD concentration was 956 and 905 mg/L, respectively. In the fourth trial, the influent COD concentration rose to 5450 mg/L, corresponding to an OLR of 2.72 kg COD /m^3.d.

The variation of the influent COD concentration at this period reflects also on the effluent COD concentration to be varied. But, lately reached stability and obtained an average 255.5 mg/L effluent COD, which corresponded to 95.4 % of COD removal efficiency. The high effluent quality and good performance resulted from the increase of the total biomass concentration inside the reactor that was estimated to be 8700 mg VSS/L as a total biomass concentration. In the last trial, the influent COD concentration rose to 8051 mg/L. The influent COD concentration was significantly varied; however, a good effluent quality was attained with an effluent COD concentration of 403.5 mg/L. Basically, the increase of the influent COD concentration caused the effluent concentration to increase due to a shock loading. The effluent concentration gradually decreased and a low effluent COD concentration achieved, which enhanced COD removal efficiency of the reactor to be able to reach 94.5%. It can be observed that the reactor performance was significantly high and it tolerated high influent COD concentration at this HRT. Subsequently, at high influent COD concentrations, the

effluent COD was largely degraded within short period of time, and it seems that the amount of nonbiodegradable of organic matters in the main influent wastewater was low.

More importantly, because of using a unique packing media that provides a high specific surface area, the reactor retains a high amount of biomass concentration, estimated to be an average of 6970 mgVSS/L of total biomass. This revealed that a high concentration of biomass promoted the SB-FFBR performance on organic removal and, as indicated by Tsang et al. (2007), that the COD removal efficiency was directly proportional to MLSS biomass concentration.

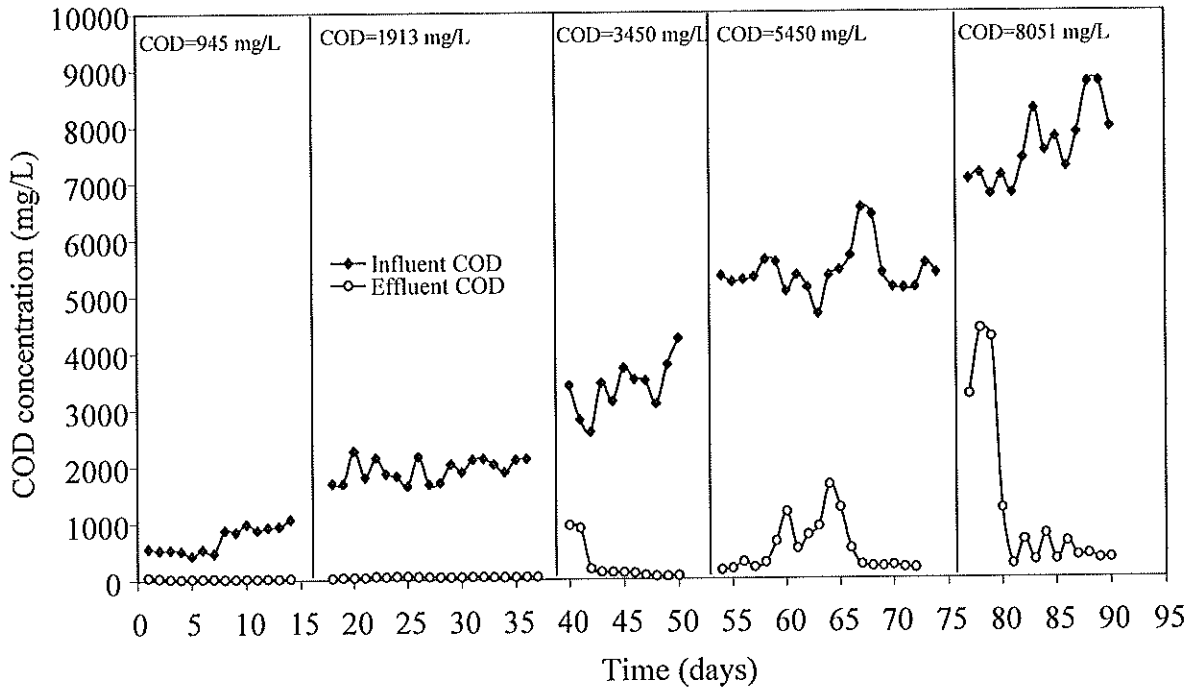

Figure 5.13: Variation of influent and effluent COD in SB-FFBR at 2 days HRT

5.5.2 COD Removal Efficiencies and Effluent Qualities

Figure 5.14 presents the COD removal efficiency of a SB-FFBR as a function of operation time at 2 days HRT for different COD concentrations. It can be seen that the SB-FFBR achieved a different COD removal efficiency and this depends on the applied influent COD wastewater. A high COD removal efficiency obtained for all COD concentrations applied to the system. The COD removal efficiency was above 97 % when the reactor ran at 945, 1913 and 3450 mg/L of influent COD concentration, which correspond to 0.47, 0.96 and 1.72 kg COD/m^3.d of OLR, respectively. This indicates the capability of this reactor, and that it can handle higher organic loading to achieve a good

COD removal efficiency, and there is no significant change on a trend of the COD removal efficiency. However, with an increase of the amount of COD to 5450 mg/L (2.72 kg COD/m^3.d), the reactor approached 95.5 % of COD removal. In this part of the experiments, the reactor COD removal efficiency was quite varied and did not show any stabilization until after 14 days of operation. The SB-FFBR system achieved 94.9% of COD removal when the system operated at 8051 mg/L, corresponding to 4.02 kg COD/m^3.d OLR. It can be seen that the reactor stability was reached approximately after 5 days of reactor operation. Despite the removal efficiency low in the first days of the experiment, which may be due to the increase in the influent concentration, the overall performance was good and the efficiency of COD removal gradually increased. It is evident that the SB-FFBR can tolerate a high organic loading rate at this HRT and can produce a very high quality of treated wastewater.

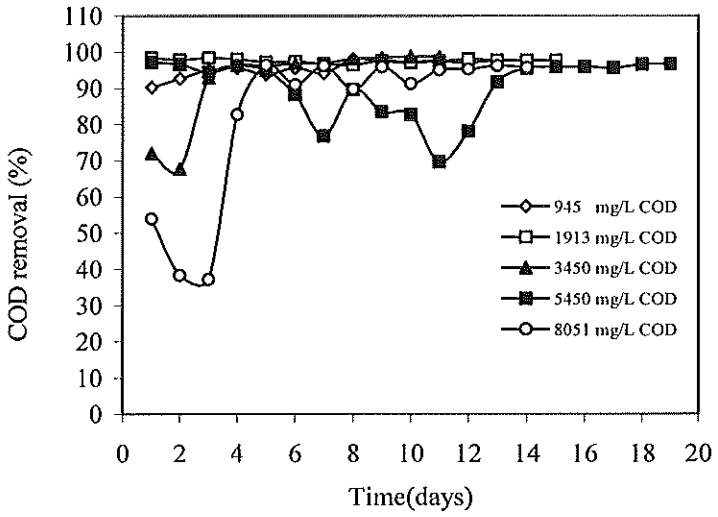

Figure 5.14: COD removal efficiencies of SB-FFBR at 2 days HRT

In an attempt to evaluate the reactor effluent quality of the SB-FFBR, the effluent parameters are shown in Table 5.3. As indicated in this table, an increase of the influent COD concentration, a significant increase on the effluent concentration of TSS, pH, and turbidity can be observed. However, the DO concentration decreased with the increase on the influent COD concentration, which is attributed to increase of the microorganism activity as the substrate concentration increased, and a good range of pH. The effluent turbidity showed remarkable increase as the influent COD concentration increased, and that may be because of the increase in the amount of TSS concentration in the reactor effluent. However, the turbidity decreased to 10.5 NTU when the highest influent COD

concentration increased to 8051 mg/L. TSS effluent concentration noticeably increased with the increase in the influent COD concentration. A 2.8 mg/L of effluent TSS obtained at 945 mg/L of influent COD concentration, while it was 140 mg/L when the influent COD concentration increased to 8051 mg/L. The possible reasons behind these changes were due to an increase of the SLR: the biomass washout that was affected by the increase of the organic loading rate; the insufficient time for the TSS hydrolysis; increase in the biomass growth rate; and increase in the biomass mass sloughing shown by the reduction of the DO level from (3.41 to 1.08 mg/L).

Table 5.3: SB-FFBR effluent quality at HRT of 2 days

Influent waste strength mg COD/L	Effluent Characteristics			
	TSS mg/L	DO mg/L	pH	Turbidity (NTU)
945	2.8	3.41	6.84	1.10
1913	26.6	3.13	7.25	1.09
3450	73.3	3.53	7.55	4.17
5450	85.7	2.47	7.65	17.3
8051	140	1.08	7.68	10.5

5.5.3 Effect of Organic Loading Rate

The performance of the SB-FFBR system at 2 days HRT was investigated for the treatment of milk industrial wastewater. The influence of organic loading rate on the SB-FFBR performance is shown in Figure 5.15. From this Figure it can be observed that the COD removal efficiency decreased with the OLR increase. When the reactor operated at a loading rate of 0.47 and 1.014 kg COD/m^3.d, an excellent COD removal efficiency of 97.5 and 97.8%, respectively, was accomplished. A high performance was obtained due to high biomass concentration inside the reactor, which increased with increase in the influent COD concentration, and this concentration reached 2710 mg VSS/L as suspended biomass only. The removal efficiency started to decrease to 95%, however, when the system loaded with 1.72 kg COD/m^3.d. When the reactor operated at an OLR of 4.02 kg COD/m^3.d, a 94.9 % of COD removal efficiency was achieved. It can be inferred from these results that the system performance and capacity show a slight decline with the increase of OLR. But generally, at the HRT of 2 days, the reactor still can treat high strength wastewater with an OLR more than 4.02 kg COD/m^3.d.

Conversely, the COD removal rate in SB-FFBR at 2 days HRT are presented in Figure 5.15. The COD removal rate increased almost linearly with the increase OLR. The rate of COD removal showed an increasing tendency from 0.46 to 3.7 kg COD/m^3.d with increased OLR. In the literature, Najafpour et al. (2006) reported a similar trend while they were working with seafood wastewater using RBC and Yu et al. (2003) when they used flexible fibre biofilm reactor for treatment of food processing wastewater. The SB-FFBR had a high productivity when it was operated at high OLR. The reactor at this HRT could have the ability to treat a high strength wastewater with high organic loading rate. This reflects that with increasing COD removal rate, the oxygen uptake rate (OUR) was also increased, so that it correlated with the increasing AFR.

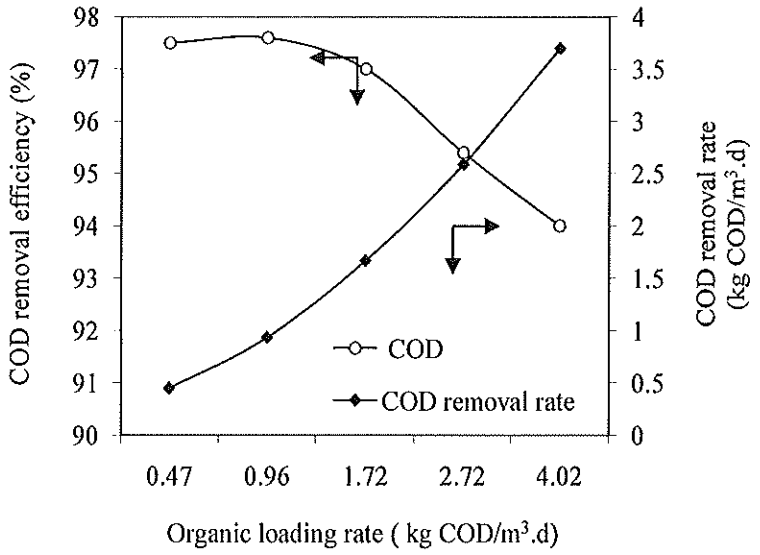

Figure 5.15: Reactor performances at HRT of 2 days

Figure 5.16 shows the effect of the OLR on the TSS removal efficiency and TSS removal rate in the process. As can be seen from this figure, the TSS removal efficiency decreased as the OLR increased. It shows that the system achieved 99.3% reduction of TSS at 0.48 kg COD/m^3.d, and that was mainly due also to low amount of solids applied to the system. By increasing the OLR to 0.96 kg COD/m^3.d, which corresponds to 0.22 kg TSS/m^3.d, a 93.5 % of TSS removal was achieved. The TSS removal efficiency was improved with the increase on the OLR to 2.72 kg COD/m^3.d, which may be due to high consumption rate or degradation rate at such long HRT. However, the TSS removal efficiency deteriorated and decreased to 92.1%, and this was mainly due to an increase of the OLR 4.02 kg COD/m^3.d and also an increase in the amount of solids applied to the reactor.

However, Figure 5.16 also illustrates the relation between the OLR and total suspended solids removal rate. The OLR had a more significant influence on the TSS removed from the system. It can be seen that the TSS removal rate increased dramatically as the OLR increased from 0.47 to 2.72 kg COD/m^3.d. But there was no further removal when the OLR increased to 4.02 kg COD/m^3.d. As a consequence, the increase in the OLR also caused deterioration and increase in the amount of effluent TSS in the system. Nevertheless, the SB-FFBR system displays a good performance on the removal of solids. It can be considered as advantageous when the amount of solids was reduced, and this may confirm that the organic compounds were completely oxidized.

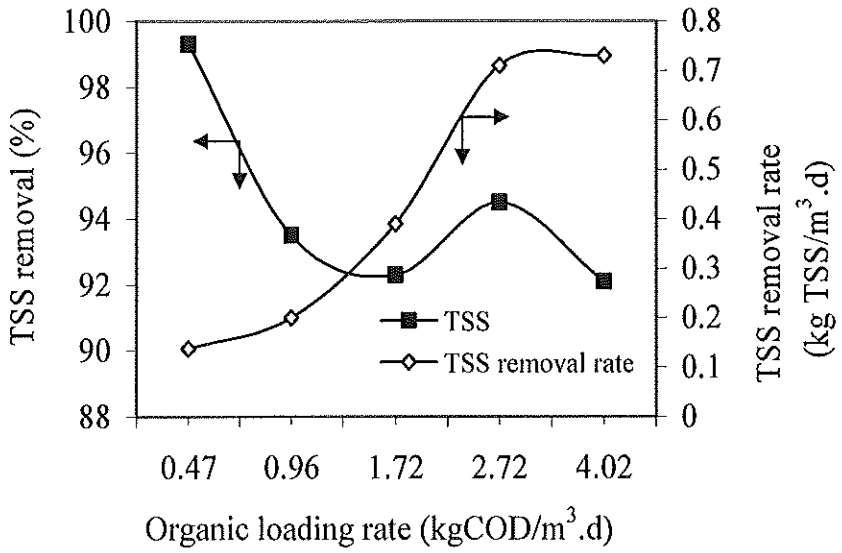

Figure 5.16: Effect of OLR on TSS removal efficiency and TSS removal rate

Figure 5.17 presents the variation of the pH, Turbidity, and dissolved oxygen (DO) concentration with the OLR. As can be seen in Figure 5.17, the pH remained practically constant with value range between 6.8 and 7.7 with the OLR increased from 0.47 to 4.02 kg COD/m^3.d. The pH level in the reactor rose stepwise, but the effect of OLR can be more noticeable if the OLR increase beyond 4.02 kg COD/m^3.d. Generally, though reactor shows good buffering capacity. The OLR also has an effect on the effluent turbidity. The turbidity increased as the OLR increased. At low OLR of 0.47 and 0.96 kg COD/m^3.d, the SB-FFBR produced a high quality effluent with almost constant level of turbidity of 1.1 and 1.09 NTU, respectively. However, the effluent turbidity was increased to 4.14 NTU as the OLR increased to 1.72 kg COD/m^3.d. With increase on the OLR to 2.72 kg COD/m^3.d, the turbidity of the effluent increased to 17.3 NTU, which is attributed to the increase of suspended solids in the effluent which may be due to the loss of biomass or washout out. The turbidity of the effluent decreased again to

10.5 NTU once the OLR increased to 4.02 kg COD/m^3.d. With respect to the level of dissolved oxygen in the reactor, the DO level was nearly stable as the organic loading rate increased. It was estimated to be above 3 mg/L of DO when the OLR increased from 0.47 to 1.72 kg COD/m^3.d; however, the DO level decreased to 2.47 mg/L when the organic loading rate increased to 2.72 kg COD/m^3.d, and it showed a sharp decrease to 1.08 mg/L when the OLR rose to 4.02 kg COD/m^3.d.

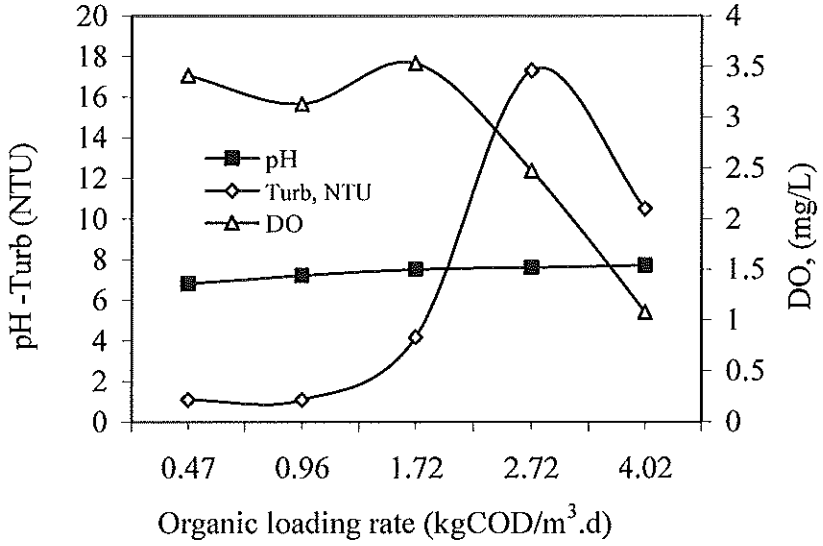

Figure 5.17: Effect of OLR on effluent DO, pH and turbidity of SB-FFBR

5.5.4 Effects of Suspended Solid Loading Rate

Figure 5.18 illustrates the relationship between pH and COD removal efficiency as a function of solid loading rate. The reactor showed varying performance depending on the SLR applied to the system. The COD removal efficiency decrease as the SLR increase. The system achieved nearly a constant COD removal of 97.5 and 97.7% at SLR of 0.146 and 0.22 kg TSS/m^3.d. When the SLR was increased to 0.42 the COD removal efficiency was slightly decreased to 97%. However, at 0.85 kg TSS/m^3.d of SLR the removal efficiency was 94%. The effluent pH was also affected by the increase of SLR. The pH gradually increases as the SLR increase.

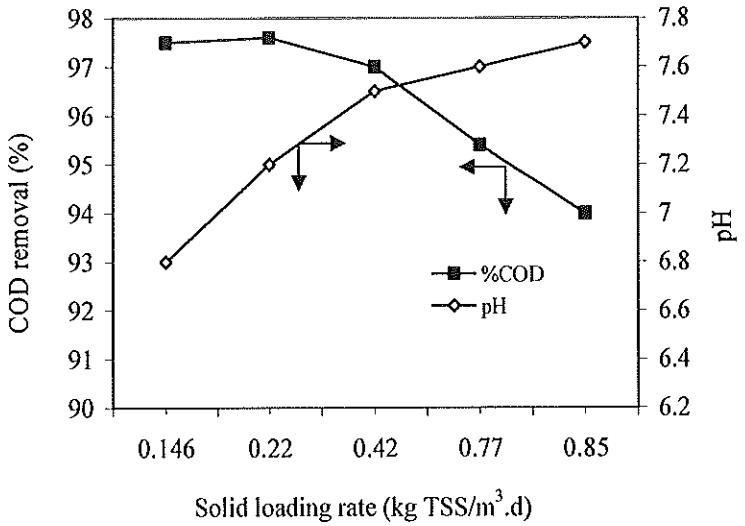

Figure 5.18: Effect of SLR on COD removal and pH

The influence of the solids loading rate on the reactor performance at 2 days HRT is shown in Figure 5.19. The SLR has a similar effect on the process responses to the OLR. It can be noted from this figure that the TSS removal efficiency decreases with increase of the SLR. However, the TSS removal efficiency improved and reached 94.5% at 0.77 kg TSS/m^3.d SLR. At SLR of 0.85 kg TSS/m^3.d the removal efficiency dropped to 92.1%. While the reactor TSS removal rate was increased as the SLR increased, the removal rate has an almost linear relationship with SLR. When the system operated at SLR of 0.146, 0.22 and 0.42 kg TSS/m^3.d, the TSS removal rates of 0.138, 0.2 and 0.39 kg TSS/m^3.d were achieved, respectively. But, at 0.77 and 0.85 kg TSS/m^3.d, the TSS removal rates were almost constant at 0.71 and 0.73, respectively.

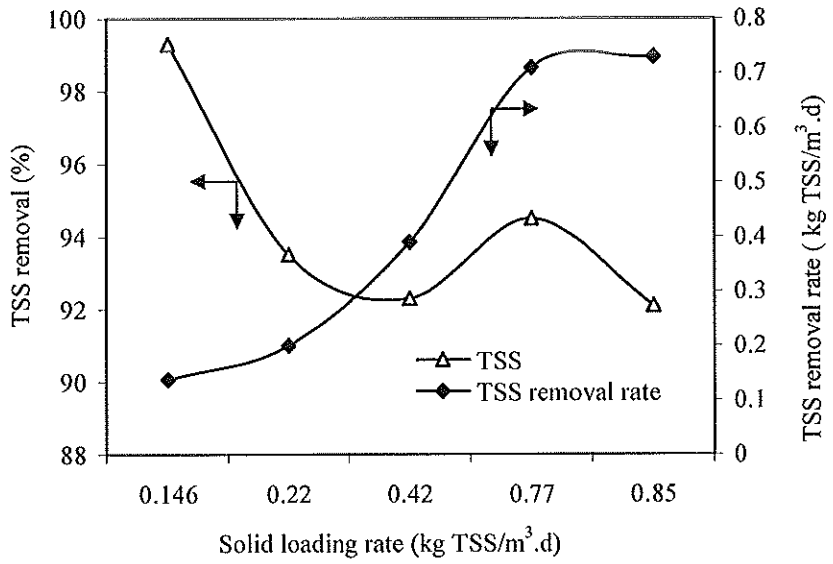

Figure 5.19: TSS removal efficiency and TSS removal rate

5.6 Kinetics Analysis

The analysis of the process kinetics provides a helpful way to evaluate the performance of a reactor and to determine kinetics rate constants. Figures 5.20 (A, B and C), show the kinetics profile of COD in the batch operating phase of the SB-FFBR operated with raw milk processing wastewater at three different influent COD concentrations. The kinetics study was performed at different experiments in which the average of COD concentrations was 500, 810 and 2000 mg/L. In Figure 5.20 (A), the experimental date was obtained when the reactor operated at 500 mg/L at 1.6 day HRT in one of the cycles. Immediately after a new cycle was started a sample was withdrawn from the reactor for determination of initial value of COD in the reactor. Then samples were periodically withdrawn from the reactor every two hours until no further change on the effluent COD concentration was observed. In Figure 5.20 (B) the SB-FFBR system was operated at influent COD concentration of 810 mg/L, and a constant HRT of 1.6 day. The kinetics test was conducted in one of the cycles, a COD concentration was initially measured at time zero, and subsequently, samples withdrawn from the reactor effluent port every two hours to evaluate the kinetics of COD removal as a function of time until COD concentration shows no changes. In addition, the influent COD concentration was gradually increased to 2000 mg/L in Figure 5.20 (C). At this condition, the kinetics study was done on one cycle, and the COD concentration was also measured at intervals of two hours, until a steady value was reached as characterized by the minimum of two hours' interval time.

Several models have been applied to describe the overall kinetics of biological reactors. The plots obtained in Figures 5.20 indicate a first order relationship as commonly observed by (Metcalf and Eddy, 2003). The model was constructed to fulfil the condition that the rate of substrate removal would decrease with time according to the first order kinetics. In the SB-FFBR, the reaction kinetics of the process for substrate utilization can be described as first order kinetics. Hence, the first order model has been applied to determine the kinetics rate constant (k) and half life ($t_{1/2}$) in this study. The substrate removal rate can be expressed by the following equations.

$$\frac{dC}{dt} = -k(C - C_e) \tag{5.1}$$

where t is time, C is initial COD concentration, C_e is the non-biodegradable COD concentration, k is the first order rate constant, which has unit of 1/time.

Integrating Eq. 5.1 yields

$$\int_{C_o}^{C} \frac{dC}{(C - C_e)} = \int_{t_o}^{t} -kdt \tag{5.2}$$

$$\ln(C - C_e) = -kt + \ln(C_o - C_e) \tag{5.3}$$

The half life of a first-order reaction is independent of the initial concentration and is given by

$$t_{1/2} = \frac{\ln 2}{k} \tag{5.4}$$

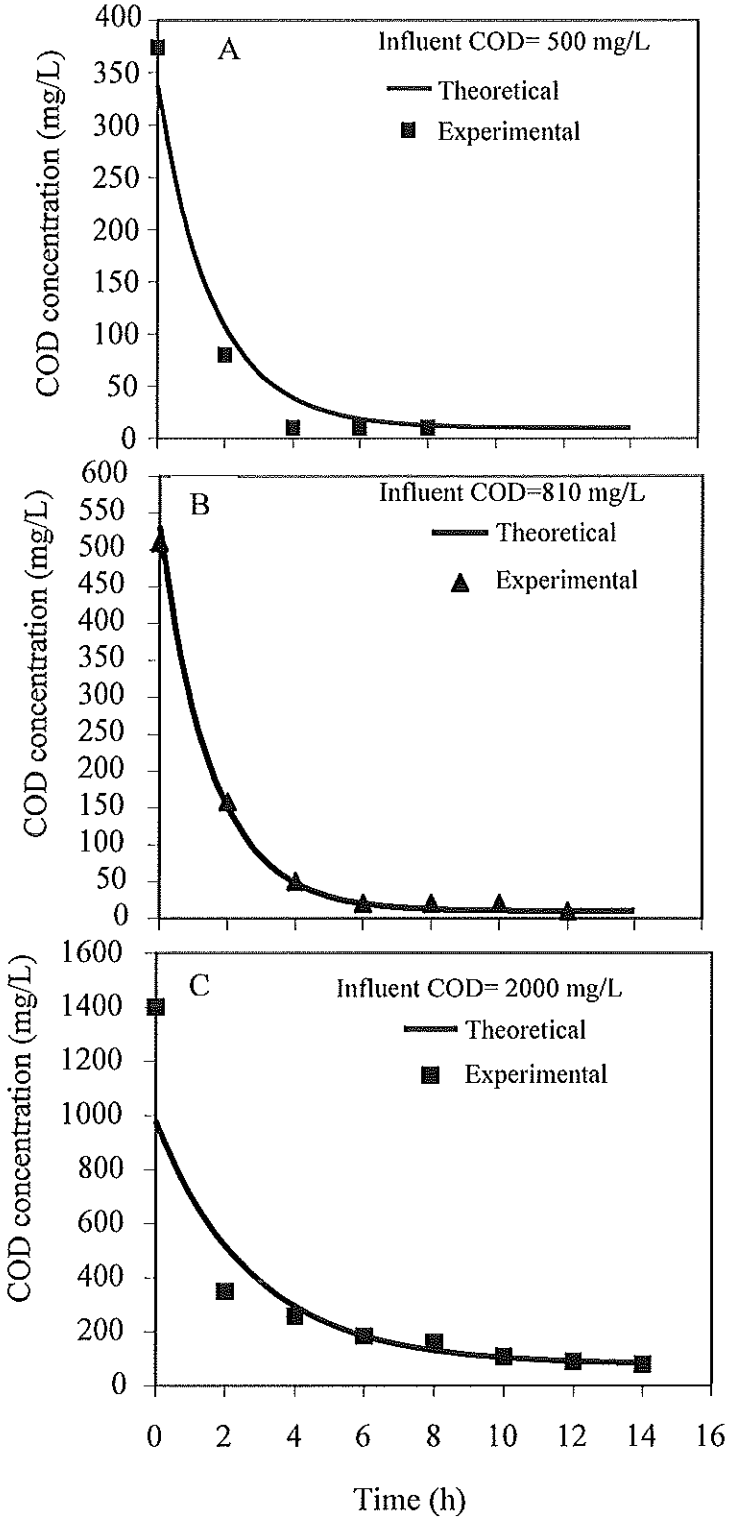

Figure 5.20: Evaluation COD batch removal kinetics

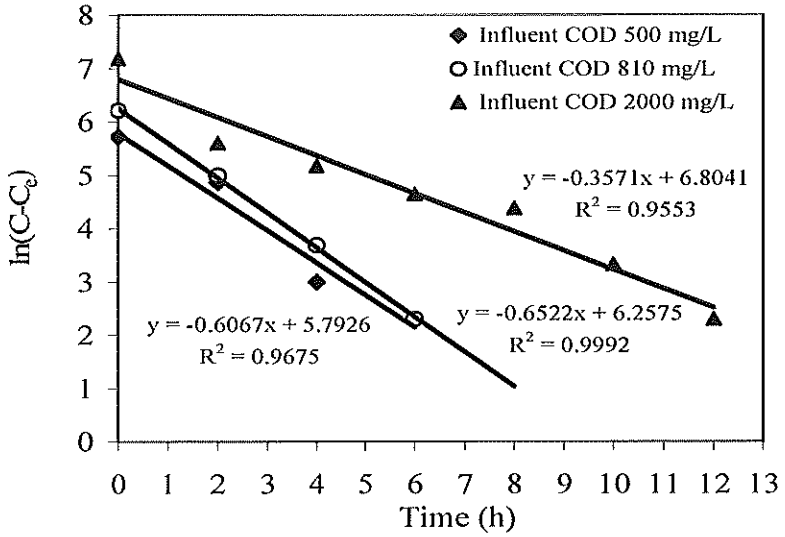

Figure 5.21: Linearized first-order model based on logarithmic transformation

Figure 5.21 illustrates graphically the fit of data from the SB-FFBR system to the first order kinetic model by plotting ln ($C-C_e$) against time (h) for the three different concentrations. It can be seen that the logarithm of substrate concentration decreases with time. The type of kinetics model used to describe the biological process reaction order was confirmed to be first order kinetics model with determination coefficients (R^2) of 0.967, 0.999 and 0.955 respectively for 500, 810 and 2000 mg/L. The kinetic constants (k) for these experimental conditions were obtained to be 0.606, 0.652 and 0.357 h^{-1}, respectively. The value of the k constant at the influent COD concentration of 810 mg/L was found to be the largest when compared with other experimental conditions, implying higher COD degradation rate at COD_{in} of 810 mg/L. The value of the kinetic constants (k) and half life $t_{1/2}$ for the three influent COD concentrations were determined as presented in Table 5.4.

Table 5.4: Kinetic parameters at different concentrations

COD	k	$t_{1/2}$	C_e	C_o	
mg/L	h^{-1}	h^{-1}	mg/L	mg/L	R^2
500	0.606	1.14	10	374	0.967
810	0.652	1.06	10	510	0.999
2000	0.357	1.94	79	1402	0.955

The kinetics of the removal of the organic substrate by a complex mixture of microorganism in the aerobic SB-FFBR system was studied at a limited range of COD concentrations and at a constant HRT of 1.6 day. The above Figures demonstrate that the COD concentrations sharply decreased with time and the removal was accomplished

with the reaction time of less than 6 h, and no further reduction in COD was observed after that for the cases indicated in Figure 5.20 A and B, with the steady COD stabilizing at 10 and 20 mg/L, respectively. The remaining fractions of the COD are considered as non-biodegradable COD. In Figure 5.20 C the COD remaining ranged between 89-79 mg/L. However, the reaction time was also longer when the influent COD concentration in the reactor increased to 2000 mg/L and the initial COD concentration in this stage increased. For COD concentrations of 500 and 810 mg/L, the COD reduction may be due to the limitation of organic mater in these stages, in addition to, high COD consumption occurring in the early stage of the reaction time, which indicates of the availability of biodegradable of COD.

5.7 Biofilm Morphology

Wastewater biofilms are very complex systems consisting of microbial cells and colonies embedded in a polymer matrix with structure and composition as a function of biofilm age and environmental conditions (Lazarova and Manem, 1995). The biofilm samples which were taken from three bundles did not differ significantly in microbial content or overall appearance. The type of packing material and the sample location (top, middle or bottom) has no visible effect on biofilm formation or the diversity of microbial populations. The scanning electron microscopic (SEM) is a suitable tool for investigations of the structure of biofilms. Representative images of SEM photography examination of the biofilm attached to the flexible fibre after the experiments were taken are depicted in Figure 5.22.

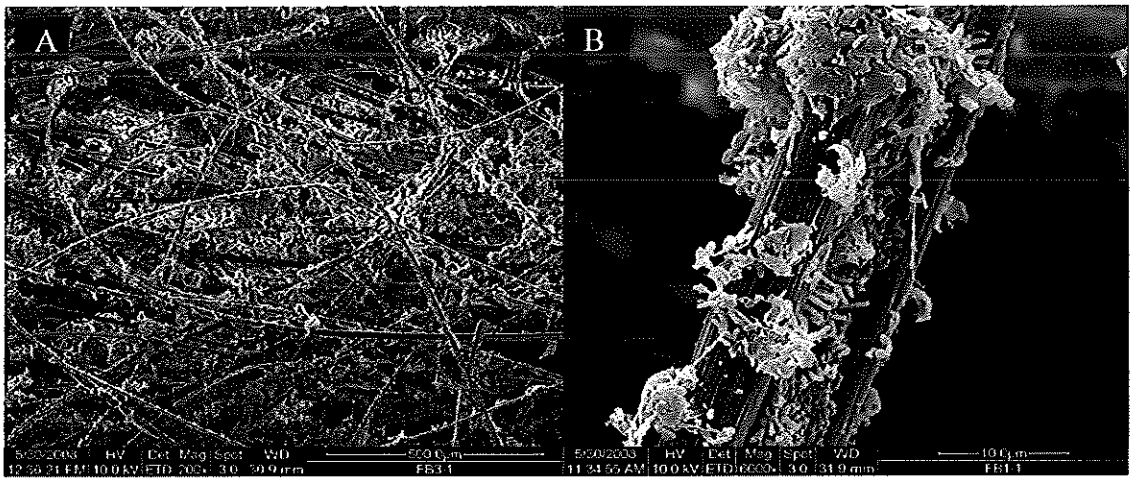

Figure 5.22: Scanning electron microscope images of biofilm on the reactor

Figure 5.22 (A) depicts a typical and uniform distribution over the fibre surface. Although the flexible fibre surface was not entirely covered, the biofilm growth coats the surface of individual fibres and fills the space between closely opposed fibre, seen in a lower magnification of 200X. Further magnification of 6000X of the biofilm surface, as seen in Figure 5.22 (B), shows clumps of bacteria surrounding and closely adherent to the individual fibre, but not completely covering the entire fibre. It appears from the figure that bacterial aggregates are attached to the fibre. In Figure 5.22 (B) clearly shows that there is a high density of extracellular matrix. This is mostly composed of carbohydrate polymers, sometimes called "Glycocalyx or slime layer or capsule". It holds the clumps of bacteria together and acts as an adherent between bacteria and the fibres. It is common for the biofilm to have this kind of material and the images clearly shown fluffy material around the cell and also between the cells. Moreover, such a slime material may be originated from organic solids that existed in the raw wastewater and accumulated inside the bioreactor.

Figure 5.23 shows further high magnification image (C and D) of 10000X of the outer surface of the biofilm. The bacteria were the most abundant organism in the biofilm. A variety of bacterial morphologies were observed in the sample that examined, the shape of the bacteria commonly observed contained rod, coccal, spiral and helical morphologies. In addition, different sizes of bacteria are seen attached to the fibre with some waste debris (e.g organic solids), indicating that a diverse range of species were present. A mixture of straight and comma-shape rods is evident, with approximate dimensions of 0.5 x 3 μm. A grazing nematode species were observed in the (D) zone of Figure 5.23, probably in relation to the availability of dissolved oxygen. Flagella are also seen in this image (5.23 C) and can be easily identified by their tail like structure involved in movement of the bacterial cell.

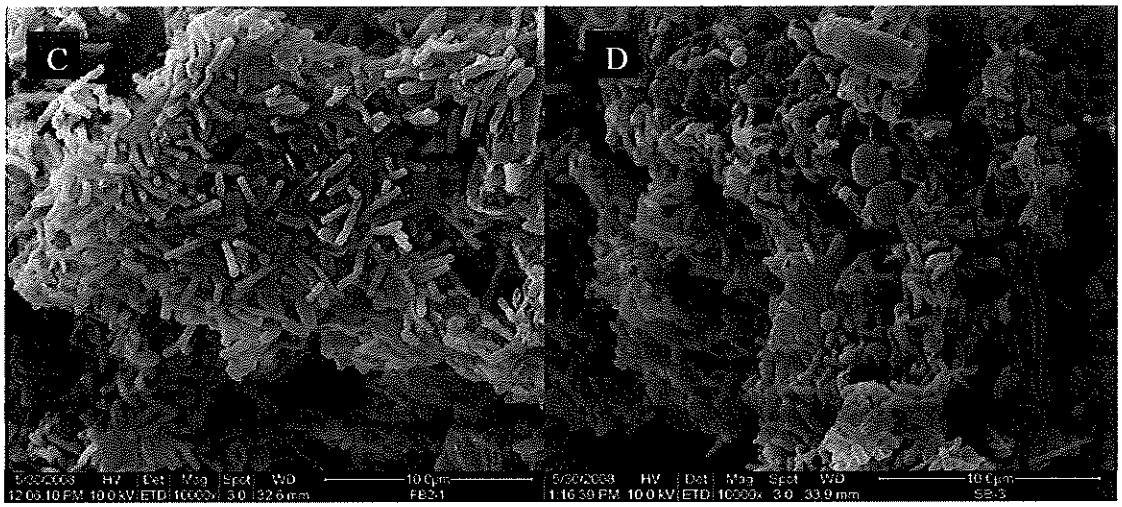

Figure 5.23: High magnification of scanning electron microscope images of biofilm on the reactor

CHAPTER 6 PERFORMANCE OF SINGLE STAGE FLEXIBLE FIBRE BIOFILM REACTOR FOR TREATMENT OF MILK PROCESSING WASTEWATER

6.1 Introduction

This chapter presents and discusses the results on the performance of a single stage flexible fibre biofilm reactor (SS-FFBR) for the treatment of milk processing wastewater. The treatment experiments were carried out over a six-month period. The start-up phase is briefly described and the performance of the reactor during the start-up stage explained in detail. The continuous operation of the SS-FFBR was started after a visible biofilm appeared on the fibre media. The results and the COD removal efficiency and effluent quality are discussed, based on the proposed hydraulic retention times (HRT). The effects of organic loading rate (OLR) on SS-FFBR performance are explained. The results of the SS-FFBR treatment process are carried out by using a response surface methodology (RSM) with respect to the simultaneous effects of two independent operating variables, HRT and influent feed concentration (COD_{in}), where 5 interrelated parameters were evaluated as responses.

6.2 SS-FFBR Start-up Data

The SS-FFBR was initially inoculated with a mixed seed sludge culture in order to start the biofilm development. The reactor was operated in a SBR mode to acclimatize the microorganisms in the reactor. The COD_{in} concentration was gradually increased to the targeted COD concentration. After the acclimatization period, the reactor was run for a couple of days as a SBR mode until the biofilm growth was established, and after that the continuous operation of the reactor was initiated at 12 h HRT and an 11 mL/min feed flow rate. The AFR was not kept constant and varied upon the DO level in the reactor to maintain the DO value at higher than 2 mg/L. The influent pH values were adjusted to the range of 6.5-7.5, and the influent COD concentration were diluted to the desired level by using tap water. The normal investigation of the performance of the SS-FFBR was initiated. During the start-up period, the COD removal, DO, turbidity and volatile suspended solids (VSS) were also monitored daily. Figure 6.1 shows the reactor performance during the start-up period based on COD removal. In the first week, the reactor was fed step-wise with an influent COD concentration varying from 500 to 800 mg/L, at a HRT of 12 h. In this period, the reactor recorded a high COD removal efficiency of approximately 80% despite the decline of the removal efficiency in some

periods. Apparently, the gradual increase of the influent COD concentration resulted in a reduction of the COD removal efficiency that can be observed from day 9 to 18 (Figure 6.1). It illustrated that the reactor was under stress and resulted in organic shocks that may affect the attached microorganisms and cause the washout of biomass. The micro flora then took time to adapt to the new environment before they resumed their pre-shock treatment efficiency. As can be seen in the Figure 6.1, from day 19 the removal efficiency increased as the COD concentration increased and the removal efficiency remained at an almost constant range around 80%, indicating a relatively stable reactor performance.

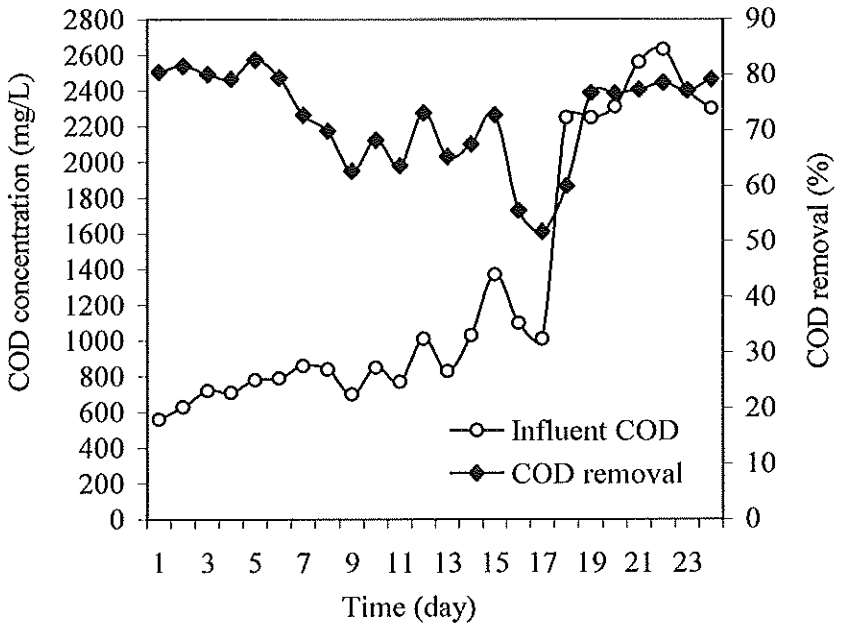

Figure 6.1: COD removal efficiency during start-up period

During the start-up phase, the turbidity and pH of the reactor effluent was monitored regularly. It has been established that pH is an important parameter influencing the performance of biological processes (Metcalf and Eddy, 2003). Figure 6.2 demonstrates the pH variation and effluent turbidity during the start-up period. The pH remained at almost neutral, in the range of 7-7.4, in the first 20 days of the start-up period, but a significant increase in the pH value over 7.5 was observed when the influent COD concentration was increased and reached a value over 2250 mg/L, as indicated in Figure 6.2. However, this range of pH is still in the appropriate range for the biological process involved.

The effluent turbidity has shown a significant variation and fluctuations. In the first week, when the influent COD concentration was below 800 mg/L, the effluent turbidity was stable at a low range between 12.5 to 18 NTU. The effluent turbidity started to increase to more than 30 NTU as the influent COD concentration increased to approximately 1000 mg/L. This was due to the increase of the SLR and OLR in the system. It is also evident that because of the shorter SRT at the start-up stage, there was insufficient time for VSS hydolysis and subsequent digestion of the organic matter. The increase in the amount of total solids in the influent wastewater may also have increased the biomass growth rate in the reactor, which contributes to the effluent turbidity by biomass washout.

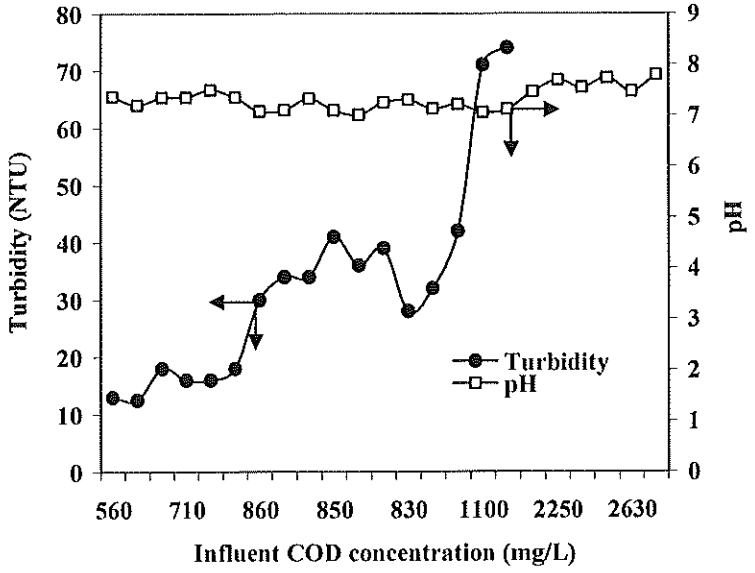

Figure 6.2: pH and turbidity variations during start-up period

The influent and effluent VSS concentration variations during the start-up period are shown in Figure 6.3. It can be seen that the effluent VSS concentration increased gradually with operational time as influent VSS concentration increased. In the first 7 days of the acclimatization, the effluent VSS concentration was low as the biofilm was in the developmental stage. The influent solid concentration applied to the reactor was also low. However, the effluent VSS concentration showed a gradual increase even when there was fluctuation on the influent VSS concentration in the second week. On day 17, the effluent VSS concentration increased significantly even when the influent VSS decreased. This could be due to the detachment of biofilm from the media, or increased growth of suspended growth microorganisms. After day 19, the influent VSS was increased and kept constant, and in this period the effluent VSS concentration was

dropped and fluctuated, which may be attributed to increases in the sloughing rate as well as the rate of hydrolysis.

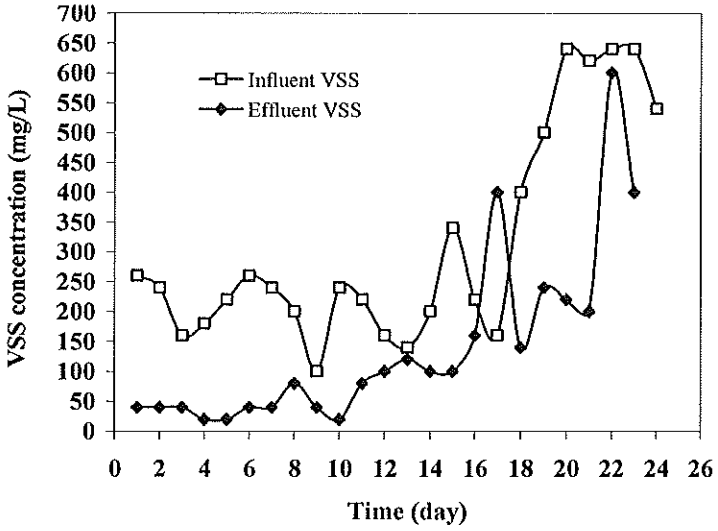

Figure 6.3: Influent and effluent VSS variation during start-up period

Since the treatment process is aerobic, the DO concentration in the reactor was monitored during the start up period. Figure 6.4 presents the variation of DO levels and influent COD concentrations during the start-up time. Figure 6.4 shows that as the influent COD increased, the DO consumption also increased due to higher COD removal at a constant rate of aeration. During the start-up period, the DO level was continuously measured up to day 17, when the DO concentration was significantly decreased to nearly 2 mg/L. Such a decrease may be due to the increase of the biomass growth rate in the reactor, or to the aeration deficiency in the system. In contrast, at high levels of DO (especially on day 12) observed, the DO increased up to 5.8 mg/L. After day 17, the DO was not measured due to a technical difficulty. However, aeration was continued as required.

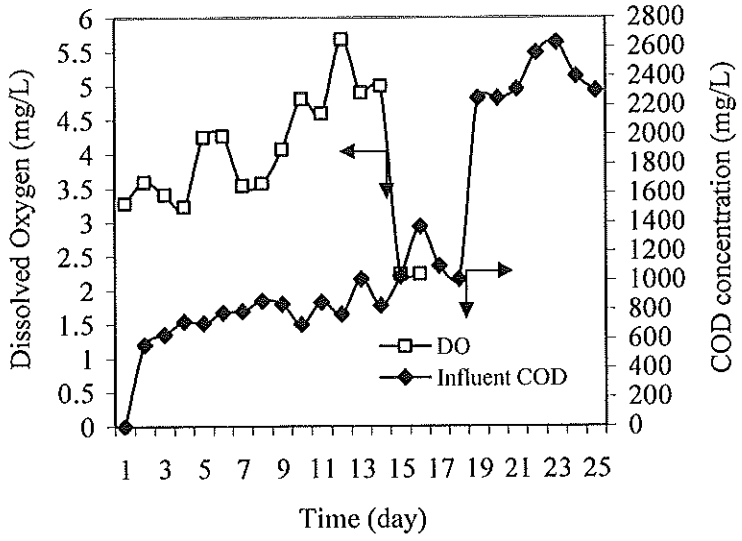

Figure 6.4: Influent COD and DO levels during start-up period

Although the start-up period was run for 23 days, the time needed for the acclimatization was not as long. It was observed that the biofilm appeared quickly on the packing media and that the colour changed on the surface of the media from white to brown, indicating the initial biofilm development process. Nevertheless, the start up period of the SS-FFBR was continued for 23 days to ensure that the biofilm was completely developed and to avoid the consequences of failure of the operation. At the end of the experiment, the system achieved a steady state condition with a removal efficiency of an average 77.6 %, corresponding to an average OLR of 4.8 kg COD/m^3.d and HRT of 12 h. A low turbidity and VSS were also achieved. The results in this period show an improvement in the COD removal for milk processing wastewater treatment by using a SS-FFBR reactor. This can be compared to the work, reported by Xu et al. (2001), which achieved a COD removal efficiency of about 87 % at an OLR of 3.39 kg COD/m^3.d after 8 days of acclimatization period in the first reactor.

6.3 Reactor Performance

6.3.1 COD Removal Efficiencies

The performance of the SS-FFBR for COD removal efficiency was influenced by the influent COD concentration of the wastewater. Figure 6.5 presents the COD removal efficiencies at 8 h HRT for various COD concentrations. It can be observed that the COD removal efficiencies decreased with increase of the influent COD concentration of the wastewater. At the steady condition, the achieved COD removal efficiencies were 95.5, 90.3 and 89.9% when the reactor was operated with an average influent COD concentration of 836, 2480 and 3922 mg/L, respectively. This was a relatively good

performance and even at the highest influent COD of 3922 mg/L, the COD removal efficiency was good (89.9%). There was 9.1% of COD not being removed and this is considered as the non-biodegradable portion of the waste organic. It is evident from the results that the SS-FFBR reactor showed consistently good performance at higher influent COD concentrations and stabilized relatively quickly. This was mainly due to the increased biomass concentration in the reactor, which was nearly 3465 mg VSS/L in the form of suspended biomass.

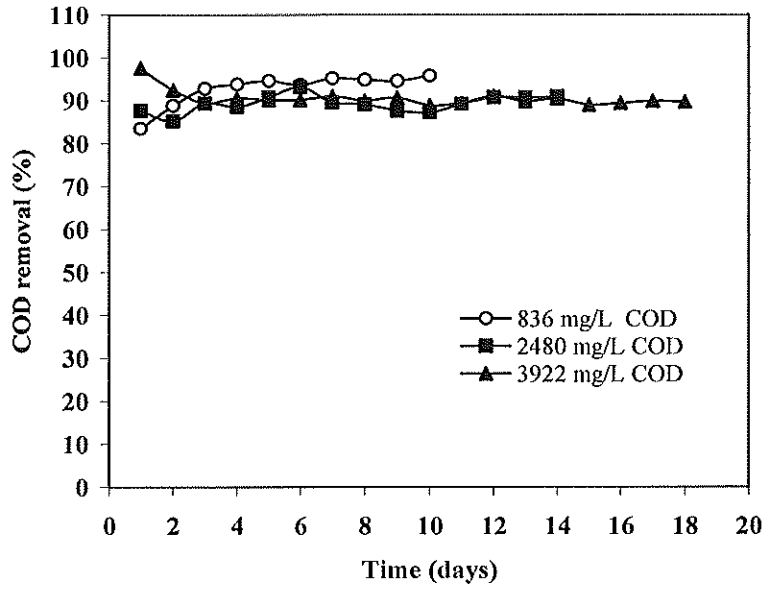

Figure 6.5: COD removal efficiency of SS-FFBR at 8 h HRT

Figure 6.6 illustrates the influence of COD concentration on the COD removal efficiency as a function of time at 12 h HRT. At the steady condition, the reactor achieved 95% of COD removal efficiency at an average influent COD concentration of 830 mg/L, whereas 96.6 % of COD removal was achieved when the influent COD concentration was increased to 2477.3 mg/L. However, the COD removal efficiency decreased to 91% when the influent COD concentration was increased to 4010 mg/L. The experimental results demonstrated that the effect of COD on removal efficiency was significantly related to the influent COD concentration. Therefore, the overall performance of the SS-FFBR was quite satisfactory even with high influent COD concentration of wastewater. Such a high COD removal was achieved because the reactor attained a high concentration of biomass that ranged between 1470 and 3370 mg VSS/L as suspended biomass concentration, while the attached biomass was estimated to be almost 5000 mg VSS/L.

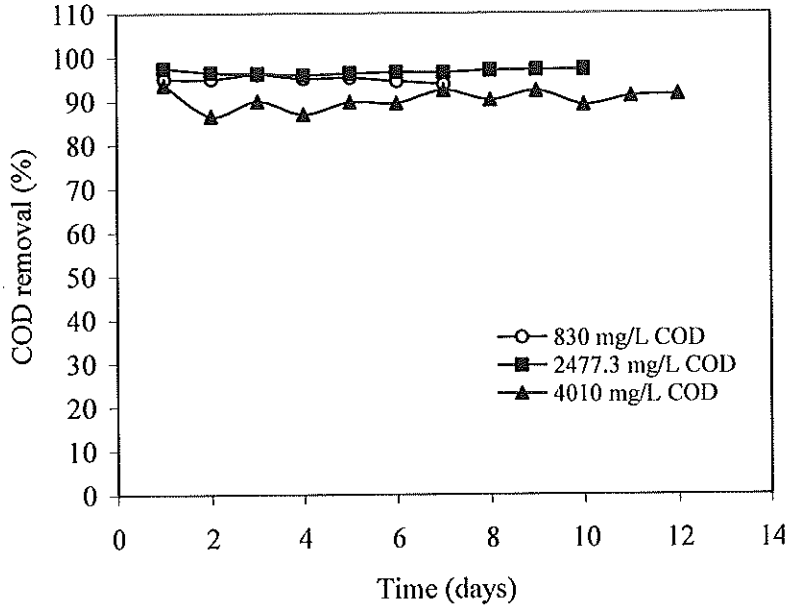

Figure 6.6: COD removal efficiency of SS-FFBR at 12 h HRT

Figure 6.7 shows the COD removal efficiency at 16 h HRT as a function of time for different influent COD concentrations. At the steady condition, the SS-FFBR reactor achieved 94% of COD removal at 763 mg/L of COD influent concentration. While at 2266 mg/L of influent COD, the removal efficiency showed a slight increase to 95%. However, the removal efficiency was slightly lowered to 94.5% when the reactor operated with an influent COD concentration of 3750 mg/L. The reactor exhibited a good COD removal performance even with the increase of the influent COD. It was evident that the reactor has a high capacity to treat high strength wastewater. The above results indicate that the SS-FFBR was able to treat raw milk processing wastewater efficiently. The main reason for such performance was like to be the presence of the flexible fibre packing media, which provided a high surface area for the microorganisms to attach. The total biomass concentration in the reactor was estimated to be approximately 7000 mgVSS/L, with 1392 to 2060 mg VSS/L in the form of suspended biomass.

It can be inferred that the SS-FFBR is readily capable of treating high strength raw milk processing wastewater, which has not undergone any pre-treatment. However, the performance of the SS-FFBR varies with different operating conditions. The reactor's performances are increased with increase of the HRT from 8 to 16 h. This system achieved better performance than the one tested by Yu et al. (2003), treating food

processing wastewater, achieving 76% of COD removal efficiency in one stage even though the technique was similar.

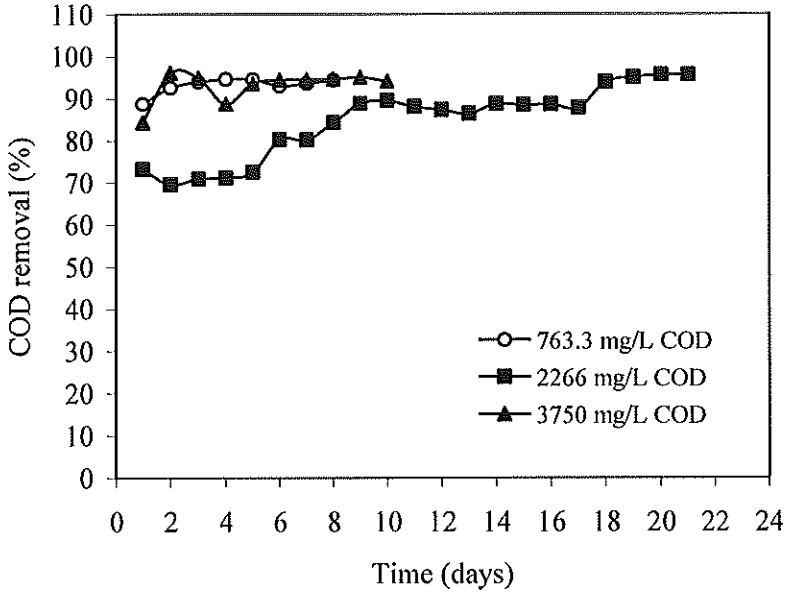

Figure 6.7: COD removal efficiency of SS-FFBR at 16 h HRT

6.3.2 Effluent Qualities

The effects of the operating parameters on the SS-FFBR effluent quality are shown in Table 6.1. It is clearly shown that the qualities of the effluent decreased with increase of the HRT or decrease of the OLR. At a low influent COD concentration of 763 to 836 mg/L, a good effluent quality was obtained with COD concentration ranging between 41 to 47.7 mg/L, and the effluent TSS concentration in the range of 5 to 15 mg/L. In addition, a very low effluent turbidity was obtained, which was in the range of 2.73 to 6.46 NTU. The pH level remained between 7.5 and 7.65 throughout the experiment. At all HRTs, the system was sufficiently aerated, and the DO level was maintained above 5 mg/L, which enhanced the biomass growth. At a HRT of 8 h, the DO level reached 6 mg/L. This may be because of the improved solubility of oxygen and also decreased biomass growth activity.

At an influent concentration between 2266 to 2480 mg/L, the effluent quality decreased with the decrease of HRT as shown in Table 6.1. The effluent COD of the SS-FFBR system increased with the decreased HRT. However, the effluent COD concentration was noticed to be 83.2 mg/L at 12 h HRT while it showed a higher effluent COD concentration of 238.5 mg/L under the lowest operation of 8 h and 7.44 kg COD/m^3.d OLR. As the HRT increased, the effluent TSS concentration decreased except at 12 h

HRT, at which the lowest TSS concentration of 20 mg/L was recorded. With respect to the effluent turbidity, the reactor showed a good effluent turbidity of 6 NTU at 12 h HRT, while it increased to 36.2 NTU when the HRT was to 8 h. The DO level in the reactor was at the recommended level, and ranged between 3 to 3.45 mg/L. However, the pH value was significantly higher and reached 7.9, while it dropped to 7.73 when the HRT decreased to 8 h, which corresponds to an OLR 7.44 kg COD/m^3.d. This indicated that the reactor effluent quality was affected by HRT and as well as the OLR.

When the influent COD concentration increased between 3750 to 4010 mg/L, the variation of SS-FFBR reactor effluent qualities was more obvious. The reactor achieved a good quality effluent despite the high OLR applied to the system. For example, at 16 h HRT, the SS-FFBR reactor achieved 211.6 mg/L of effluent COD, while the effluent COD concentration increased to 352.8 mg/L, and 394.7 mg/L at 12 and 8 h HRT, respectively. It is evident that the reactor effluent quality could also be affected by the other operational parameters such as HRT, as well as influent COD concentration. The effluent turbidity increased from 28.3 to 45.5 NTU when the HRT decreased from 16 h to 8 h. The turbidity of the settled treated wastewater at various HRT was correlated with the level of TSS in the effluent stream. The effluent TSS concentration also increased from 23.3 to 61.2 mg/L when the OLR increased from 5.62 to 11.7 kg COD/m^3.d. The increase of TSS concentration was probably initiated by the higher death rate of microorganisms due to the increase in the organic loading rate. The DO value in the reactor was kept at a satisfactory level and ranged between 2.28 to 3.6 mg/L.

Table 6.1: SS-FFBR effluent quality under various HRT

Influent COD mg/L	HRT (h)	OLR kg COD/m^3.d	pH	DO mg/L	COD mg/L	TSS mg/L	Turbidity NTU
836	8	2.5	7.58	6	41	15	6.46
830	12	1.66	7.5	5.8	41.7	11.4	2.73
763	16	1.145	7.65	5.1	47.7	5	4.64
2480	8	7.44	7.73	3.45	238.5	40	36.2
2477	12	4.95	7.9	3	83.2	20	6
2266	16	3.37	7.9	3.19	111.5	25	18.25
3922	8	11.7	7.8	3.4	394.7	61.2	45.5
4010	12	8.02	7.5	3.6	352.8	51.4	41.7
3750	16	5.62	8.01	2.28	211.6	23.3	28.3

6.3.3 Effect of Organic Loading Rate on Reactor Performance

The effect of OLR on the SS-FFBR performance for COD removal efficiency was evaluated by decreasing the HRT stepwise from 16 to 8 h at different COD concentration. Several experiments using a SS-FFBR were carried out to establish the relationship between the OLR and COD removal efficiency. Figure 6.8 shows the relationship between the COD removal efficiency and OLR at steady condition. The reactor shows varying performance of COD removal efficiency, and that a reverse linear relationship existed between OLR and COD removal efficiency. A better performance was achieved as the OLR decreased to its lowest value and the HRT was lowered to 8 h, whereas at a HRT of 16 h, the COD removal efficiency trend was not pronounced and not reduced at the highest OLR of 5.62 kg COD/m^3.d. This is an indication that the reactor could withstand and remove more substrate at higher OLR. However, a decline in SS-FFBR performance to 89.6 % resulted from increasing the OLR to its high value 11.7 kg COD/m^3.d at the lowest HRT. No other biofilm reactors treating food industrial wastewater have previously obtained such a good performance. The results were higher than those obtained by Yu et al. (2003) when a similar experimental set up was used. In another study, Najafpour et al. (2006) achieved 93.7% of COD removal efficiency at a HRT of 40 h by using a three stage RBC.

Moreover, Resmi and Gopalakrishna (2004) achieved a low COD removal efficiency of 82% at 10.2 kg COD/m^3.d. The SS-FFBR was functioning efficiently up 11.7 kg COD/m^3.d of OLR at 8 h HRT. This good reactor capacity could be due to the high biomass concentration in the reactor, where it reached 7517 mg VSS/L, and due to the high biological conversion, as well as sludge separating in the solids settling tank enhancing the removal efficiency of the system.

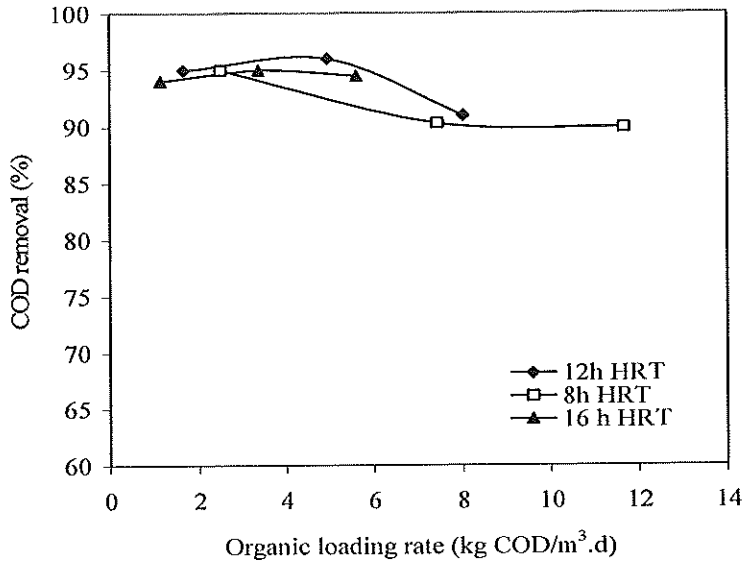

Figure 6.8: Effect of loading rate on COD removal efficiency at different HRT

Conversely, the effect of the OLR in terms of COD removal on the SS-FFBR system performance as indicated by the corresponding removal rates is presented in Figure 6.9. The rates of COD removal increased linearly with increasing OLR at all HRTs studied. This means the productivity of the system, in terms of the amount of COD removed from wastewater, was high when the reactor was loaded at maximum OLR. The rate of COD removal was increased from 1.08 to 10.67 kg COD/m^3.d when the OLR increased from 1.12 to 11.2 kg COD/m^3.d. The figure clearly showed that even when the organic loading exceeded 11.7 kg COD/m^3.d, a high COD removal rate was affected by increasing the organic load, indicating that the system capacity can be higher. A similar trend was reported by Raj and Murthy (1999); Yu et al. (2003) and Najafpour et al., (2006) working with different types of food processing wastewater using biofilm reactors. The higher biomass concentration accumulated in the flexible fibre clearly contributed to achieving a high performance and supports the reactor performance at high organic loading rate. It is also evident from the experimental data that the reactor performance with respect to the COD removal efficiency was found to be primarily influenced by the operating OLR.

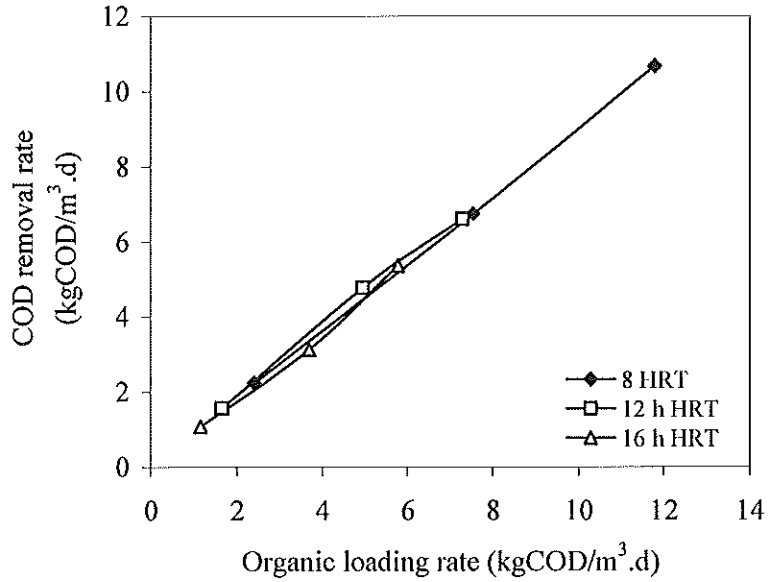

Figure 6.9: Effect of applied loading rate on COD removal rate at different HRT

The influence of OLR on total suspended solids content in the reactor is shown in Figure 6.10. The results clearly show that the SS-FFBR reactor achieved a very good performance in terms of TSS removal efficiency. As noted with an increasing OLR, the TSS removal efficiency decreased. The highest TSS removal efficiency achieved was up to 96.7% at a low OLR corresponding to 1.145 kg COD/m^3.d, and at HRT of 16 h, whereas the TSS removal efficiency slightly decreased to around 93.6% when the OLR increased to 5.62 kg COD/m^3.d at 16 h HRT. Such a good performance may be attributed to the low amount of total suspended solids in the main influent wastewater. Generally, the TSS removal efficiency did not drop down below 92% at both 12 and 16 h HRT, even with the increase in OLR to 8 kg COD/m^3.d. However, the reactor performance slightly dropped, as the TSS removal efficiency linearly decreased with increased OLR. This was clearly observed when the reactor operated at 8 h HRT. Approximately 89.7% of TSS removal efficiency could be achieved at an OLR of 11.67 kg COD/m^3.d, which indicates that the SS-FFBR system was highly effective for the treatment of raw milk processing wastewater at a short HRT. This may be due to high biomass sloughing, and the high amount of food available in the reactor as the OLR increased. Raj and Murthy (1999), while working with synthetic dairy wastewater in a cross flow medium trickling filter, observed a similar trend. Thus, it appears that the performance of this system does not become virtually independent of OLR. The HRT also has a significant effect on the system performance as described in Figure 6.10. Therefore, it would be advantageous to load this system at a high rate, since a high OLR

did not decrease efficiency drastically and resulted in better utilization of reactor capability and efficient use of media for substrate removal.

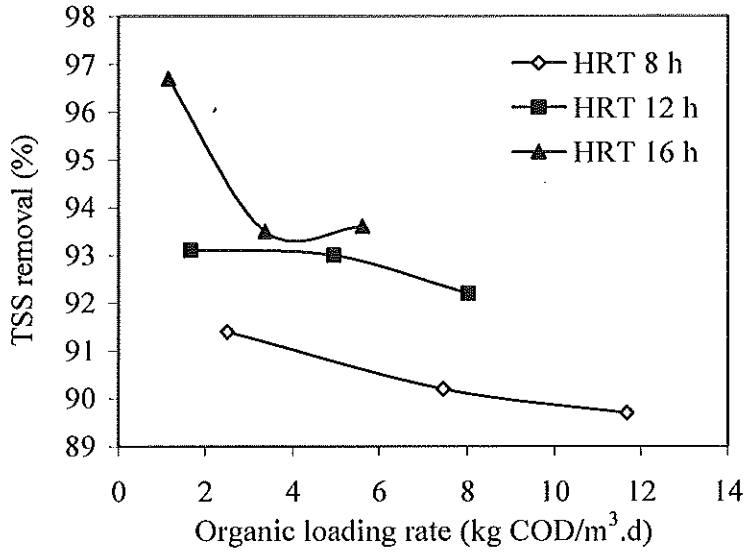

Figure 6.10: Effect of OLR on TSS removal efficiency at different HRT

Figure 6.11 illustrates the effect of the OLR on the TSS removal rate of the SS-FFBR system at different HRT. It can be noted that at all HRTs, the rate of TSS removal increased linearly with increasing OLR up to 11.67 kg COD/m^3.d. From this figure, the TSS removal rate increased from 0.243 kg TSS/m^3.d to 3.00 kg TSS/m^3.d as the OLR increased from 1.145 to 11.67 kg COD/m^3.d. The OLR had a more significant influence on the TSS removed from the system. The reactor seems to have the capacity to treat a wastewater with a high OLR. This indicates that the SS-FFBR is a practical alternative for the treatment of such wastewater compared to other processes, which do not withstand such a high OLR. The SS-FFBR system shows a good performance for the removal of solids. The amount of solids was reduced and this may confirm that the organic compounds were mostly oxidized and removed.

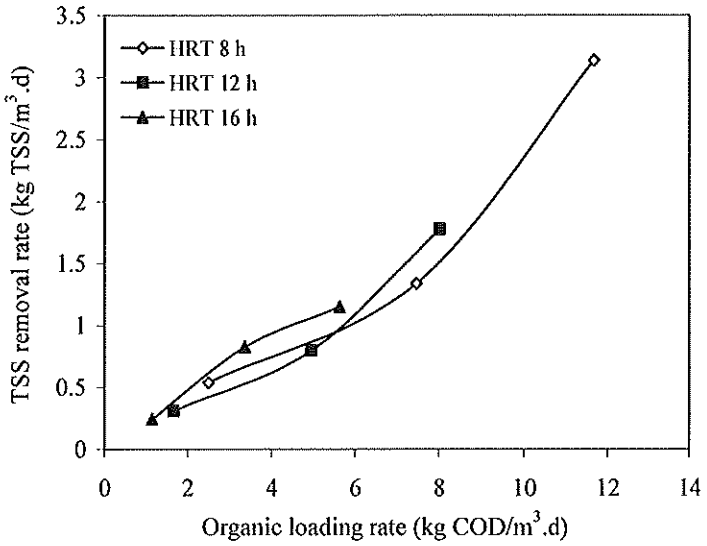

Figure 6.11: Effect of organic loading rate on TSS removal rate at different HRT

The effect of OLR on the effluent turbidity was studied and shown in Figure 6.12. From this figure, it is seen that the effluent turbidity increases with increase in OLR. At an OLR of less than 2.5 kg COD/m^3.d, the SS-FFBR generated a very high effluent turbidity with a level of turbidity ranging from 2.73 to 5.85 NTU. However, the effluent turbidity was increased to 44.6 NTU as the OLR increased to its maximum value of 11.67 kg COD/m^3.d. The increase of effluent turbidity was attributed to the increase of suspended solids in the effluent, which may be due to the loss of biomass or washout. In general, the effluent turbidity achieved in the present work were very much lower than those obtained by Najafpour et al. (2006) in three stage aerobic rotating biological contactor (RBC) treating food canning wastewater where minimum turbidity was 46 NTU achieved at 40 h HRT.

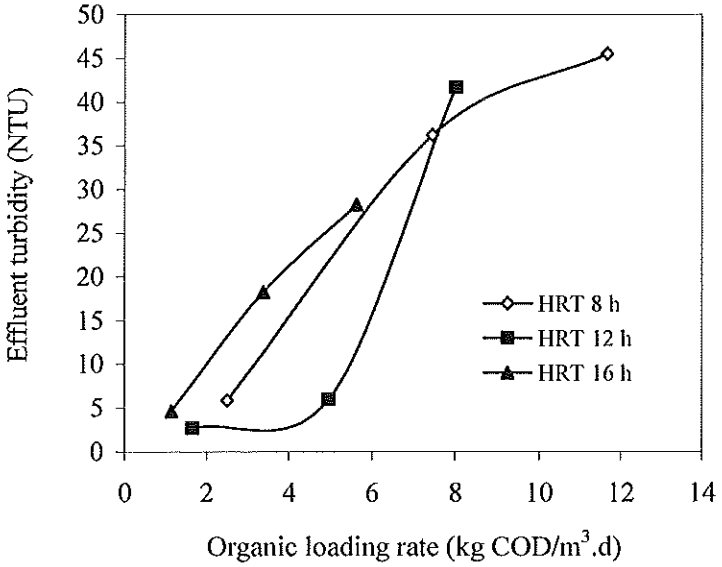

Figure 6.12: Effect of organic loading rate on effluent turbidity at different HRT

The effect of OLR on the level of dissolved oxygen concentration (DO) in the reactor is shown in Figure 6.13. There is a direct relation between the dissolved oxygen concentrations and the OLR, as a higher OLR caused a sharp decrease in DO concentration level. At lower OLRs of 1.145, 1.66 and 2.5 kg COD/m^3.d, the DO concentration in the reactor was 5.18, 5.82 and 6.45 mgO_2/L, respectively, where the DO concentrations were dropped to nearly 3 mg O_2/L, as the OLR increased. The DO level, which was in a realistic range, representing sufficient aeration, does not show that the system had a deficiency for aeration even at high OLR. The reduction in the DO concentration in the reactor was due to the increase of the biomass activities in the reactor that increased the uptake of DO as the substrate concentration increased.

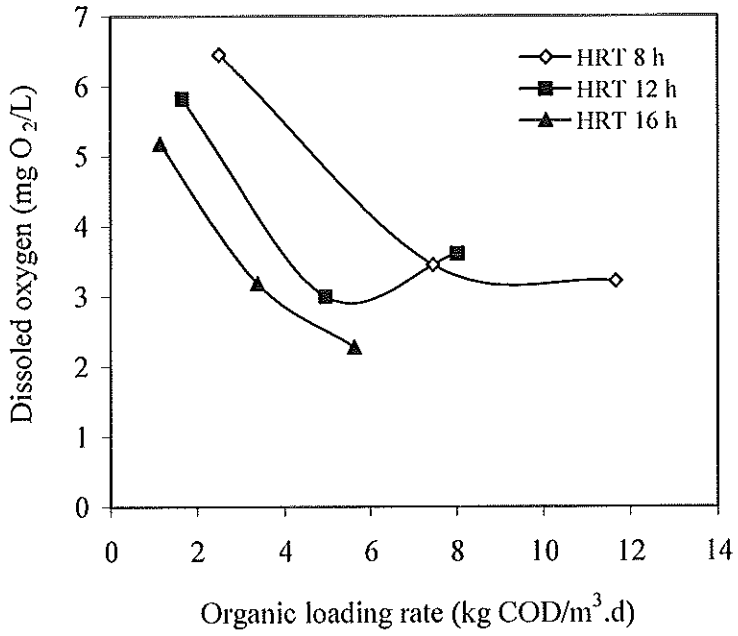

Figure 6.13: Effect of organic loading rate on the dissolved oxygen at different HRT

6.3.4 Effect of Suspended Solids Loading Rate

The effect of the SLR on the SS-FFBR on TSS removal efficiency is presented in Figure 6.14. The TSS removal efficiency was dependent on the SLR, and it decreased with increase of the SLR, and decrease of the HRT. The maximum TSS removal efficiency of 96.7% was obtained at a SLR of 0.25 kg TSS/m^3.d and at 16 h HRT. In addition, the TSS removal efficiency was around 93% when the SLR was in the range of 0.35 to 1.23 kg TSS/m^3.d at HRT 12 and 16 h, respectively. However, there was slightly decreased TSS removal efficiency at HRT of 8 h. The TSS removal efficiency was 91.4, 90.2 and 89.4 % when the SLR increased from 0.54, 1.34 and 3.00 kg TSS/m^3.d, respectively. Such findings were considerably better than that achieved by Najafpour et al. (2006) treating food-processing wastewater with a 3 stage RBC. The

authors achieved only 85% TSS removal efficiency at a low 1 kg TSS/m^3.d SLR and HRT of 48 h, whereas the TSS removal efficiency dropped to 46% at 1.2 SLR when the HRT lowered to 40 h. These results demonstrate that the SS-FFBR achieved a better removal performance and ability to treat high strength organic wastewater.

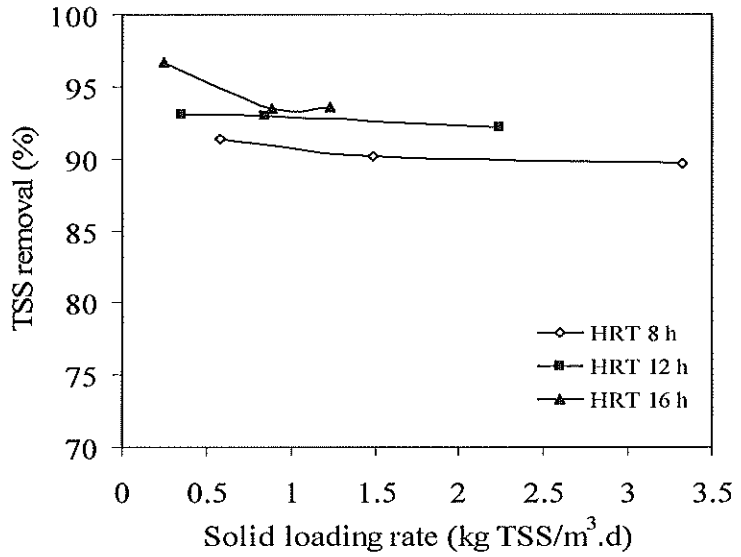

Figure 6.14: Effect of SLR on TSS removal efficiency at different HRT

Figure 6.15 shows the influence of the solids loading rate on the TSS removal rate at different HRTs. The SLR has a similar effect on the process responses to the OLR. It can be noted from this figure that the TSS removal rate increases with increase of the SLR, and there is a strong correlation between these two factors at various HRTs. The TSS removal rate has a linear relationship with SLR. The maximum SLR of 1.23, 2.24, 3.32 kg TSS/m^3.d produced TSS removal rates of 1.15, 1.78 and 3 kg TSS/m^3.d at 16, 12 and 8 h HRT, respectively. It can be deduced from the figure that reactor productivity in terms of TSS removal rate was high and achieved an acceptable level of TSS removal. The reactor should be operated at a SLR more than 3.32 kg TSS/m^3.d.

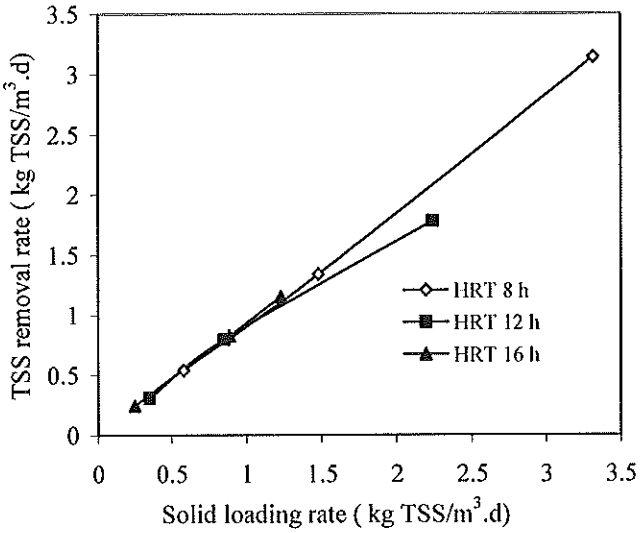

Figure 6.15: Effect of SLR on TSS removal rate at different HRT

Effluent turbidity as a function of SLR for the SS-FFBR at various HRTs is shown in Figure 6.16. An increase in the SLR results in an increase in the effluent turbidity. The minimum effluent turbidity in the range of 2.73 to 6.01 NTU was achieved at a low range of SLR below 1 kg TSS/m^3.d at various HRTs. However, 44.6 and 41.7 NTU was the maximum effluent turbidity obtained when the SLR increased to 3.32 and 2.24 kg TSS/m^3.d when the reactor operated at HRT of 8 and 12 h, respectively. A sudden increase in the effluent turbidity at these conditions was possibly due to the increase of the SLR, which corresponds to the high amount of total suspended solid in the influent wastewater stream. In general, a good effluent turbidity in the present work was much lower than those obtained in a three stage RBC reactor for treatment of food canning wastewater (Najafpour et al., 2006). These findings illustrate that the SS-FFBR could be a suitable alternative to other biofilm reactors, with a high quality effluent produced at short HRT and high SLR and OLR.

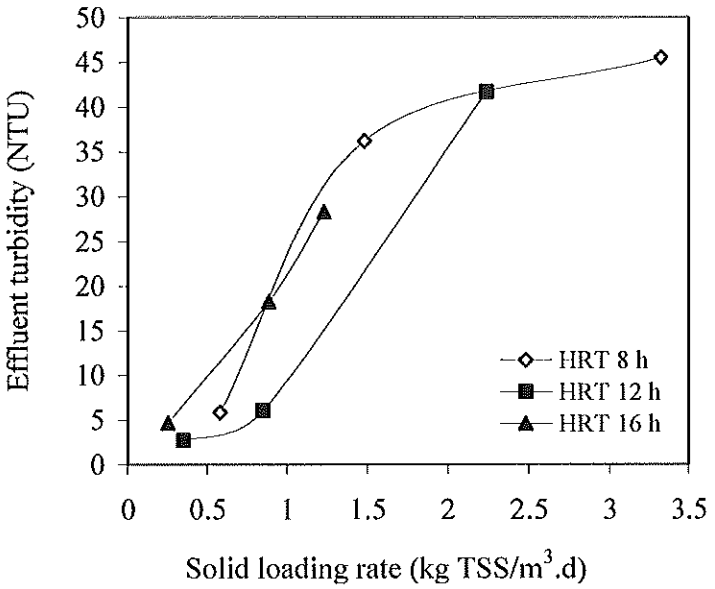

Figure 6.16: Effect of SLR on effluent turbidity at different HRT

6.3.5 Effect of Hydraulic Retention Time on Reactor Performance

The influence of the HRT on the SS-FFBR performance for the effluent COD, TSS, and turbidity at different influent COD concentrations is illustrated in Figure 6.17 (A, B, C). Further explanations of the effects of HRT on the performance of the SS-FFBR are discussed in detail in the following sections.

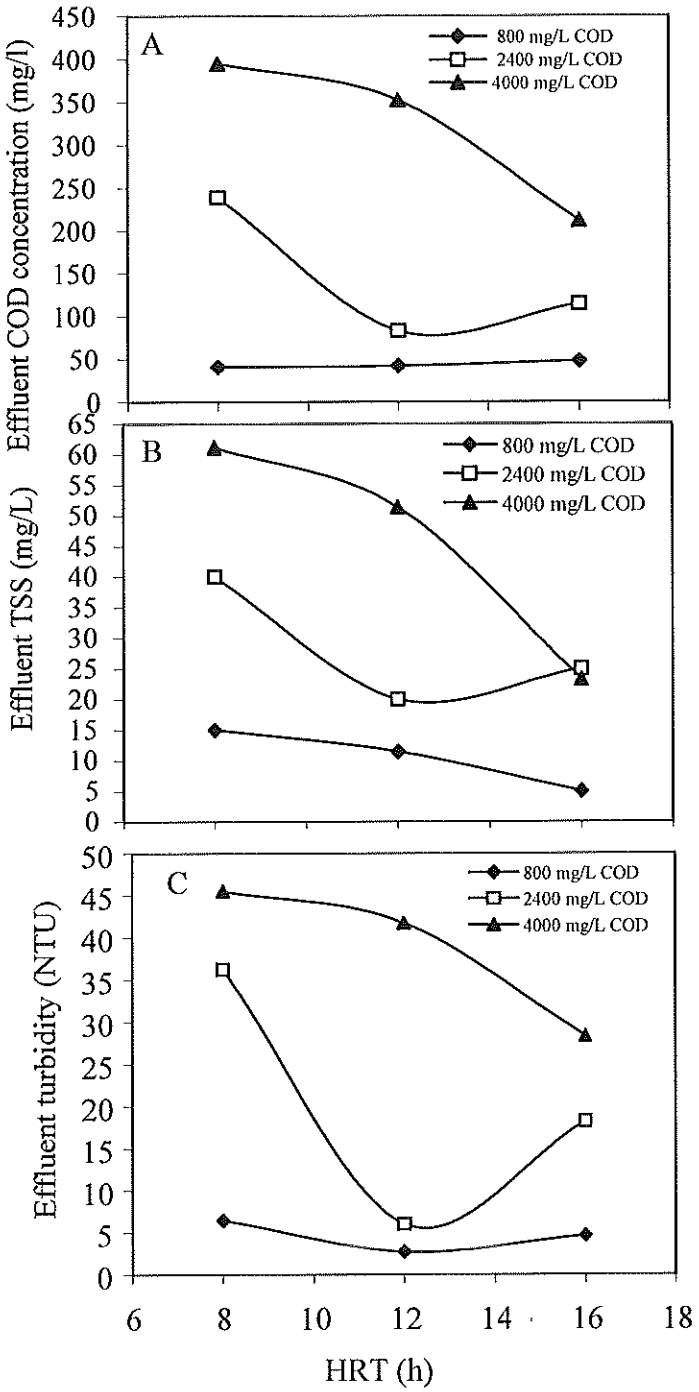

Figure 6.17: Effluent COD, TSS and turbidity vs HRT at different COD concentration

6.4 RSM Analysis of Effect of Hydraulic Retention Time (HRT) and Influent Feed Concentration (COD_{in}) on the Reactor Performance

The SS-FFBR was started up successfully for a period of nearly 20 days. After this period, the reactor was operated continually at different HRTs and COD_{in} concentration. In order to analyse and model the interactive effects of the two independent variables (COD_{in} and HRT) on the reactor responses, Design-Expert software (version 6) was used. In this program, a general factorial design was selected. It allows the user to choose factors with different numbers of level. The responses from the resulting nine runs are shown in Table 6.2.

6.4.1 Statistical Analysis

The ANOVA results for all responses are summarized in Table 6.3. As various responses were investigated in this study, different degree polynomial models were used for data fitting (Table 6.3). In order to quantify the curvature effect, the data from the experimental results were fitted to higher degree polynomial equations, i.e. two factor interaction (2FI), quadratic and so on. In the design expert software, the response data were analysed by default. Some raw data might not be fitted and needs the transformation of data. This transformation applies a mathematical function to all the response data to meet the assumptions that make the ANOVA valid.

Data transformations were needed for the turbidity and SRT as errors (residuals) were a function of the magnitude of the response (predicted values). Therefore, a $\log_{10}$ function was applied for these responses (Ahmad et al., 2005; Chapra and Canale, 2003; Draper and Smith, 1998). The model terms were selected after elimination of insignificant variables and their interactions. The interaction term, i.e. AB, was significant for all equations except the one defining effluent turbidity. Based on the statistical analysis, the models were highly significant with very low probability values (from 0.009 to < 0.0001). It is shown that the model terms of independent variables were significant at 95 % confidence level. The square of correlation coefficient for each response was computed as the coefficient of determination (R^2). A high R^2 coefficient ensures a satisfactory adjustment of the quadratic model to the experimental data. It showed high significant regression at 95 % confidence level.

Adequate precision is a measure of the range in predicted response value at the design points to the average predication error or, in other words, signal to noise ratio, and was

found to be in the range of 8.47-32.42, which indicates an adequate signal. Ratios greater than 4 indicate adequate model discrimination. In this case, the value is well above 4 (Ghafari et al., 2009; Idris et al., 2006; Mason et al., 2003). In addition, the predicated sum of squares (PRESS) is a measure of how a particular model fitted each point in the design (Aghaie et al., 2009). According to data in Table 6.4, the values of adequate precision were found desirable for all models. Simultaneously, low values of the coefficient of variation (CV) (0.26-17.43 %) indicated good accuracy and reliability of the experiments as suggested by Khuri and Cornell (1996); Kuehl (2000); Ahmad et al. (2005) and Zinatizadeh et al. (2006) Detailed analysis of the models is demonstrated in the following section.

Table 6. 2: Experimental results of general factor design

Run	Variable		Response							
	Factor1 A:HRT (h)	Factor2 B:COD_{in} (mg/L)	TCOD removal (%)	TCOD removal rate (g/L.d)	TSS removal, (%)	Specific substrate utilization rate (U), (Q(S0-S)/X.V), g CODrem/g VSS.L.d	SRT (d)	VSS/TSS ratio of biomass (Suspended + Attached) Average	Effluent pH	Effluent Turb, NTU
1	8	2480	90.3	6.72	90.2	0.987	38	0.91	7.73	36.25
2	12	2477	96.6	4.78	93.0	0.772	86	0.92	7.99	6.01
3	12	4010	91	7.31	92.2	0.975	43.7	0.93	7.5	41.6
4	8	836	95.0	2.38	91.4	0.41	76.8	0.93	7.58	5.85
5	16	3750	94.5	5.32	93.6	0.94	104.8	0.91	8.02	28.4
6	12	830	94.9	1.57	93.1	0.218	196.4	0.956	7.5	2.73
7	16	2266	95	3.20	93.5	0.582	91.8	0.94	7.9	18.25
8	16	763.3	94	1.07	96.7	0.213	78.5	0.929	7.65	4.64
9	8	3921.8	89.9	10.5	89.7	1.42	14.9	0.95	7.80	44.6

Table 6.3: ANOVA results for the equations of the Design Expert 6.0.6 for studied responses

Response	Transformation	Modified Equations with Significant Terms	Probability	R^2	Adj. R^2	Adeq. precision	SD	CV	PRESS	Probability for lack of fit
COD removal	-	93.85 +1.48A -1.42B +1.42AB	0.009	0.7073	0.6098	8.478	1.23	1.31	38.86	0.0269
Specific substrate Utilization rate (U)	-	0.75-0.18A+0.42B+0.08 A^2 -0.11 B^2 -0.071AB	<0.0001	0.9843	0.9732	32.421	0.054	7.34	0.15	0.0269
VSS/TSS ratio	-	0.93+2.833E-3B-5.88E-3B^2-5.5E-3AB	<0.0006	0.8410	0.7880	12.370	2.4E-3	0.26	2.17E-4	0.0628
Effluent Turbidity	Base 10 log	0.87+ 0.48B + 0.35A^2	<0.0001	0.8482	0.8179	15.294	0.18	17.43	0.58	0.0295
SRT	Base 10 log	1.95 + 0.23A - 0.21B - 0.17A^2 +0.2AB	<0.0001	0.9416	0.9123	20.40	0.081	4.34	0.35	-

A: first variable, HRT (h), B: second variable, influent COD (mg/L), R^2: determination coefficient, Adj. R^2: adjusted R^2, Adeq. Precision: Adequate precision, SD: standard deviation, CV: coefficient of variation, PRESS: predicted residual error sum of squares.

6.4.2 Effects of Influent COD Concentration and HRT on COD Removal and COD Removal Efficiency

The response surface of COD removal efficiency was described by two reduced quadratic models within the range of the factors. The regression equations (built with codified factors) are as follows:

$$\text{COD removal, \%} = 93.85 + 1.48A - 1.42B + 1.42AB \quad (6.1)$$

where, A is HRT and B is COD_{in}. Diagnostic plots such as the predicted versus values help to judge the model validity. The correlation between the experimental and simulated data of the COD removal efficiency presented in Figure 6.18 with a value of $R^2=0.70$, that indicates a relatively low agreement between the real data and those obtained from the models. Besides, adequate precision (AP) value obtained was higher than 4 (Table 6.4) for COD removal efficiency, which confirms the predicted model can be used to navigate the design space defined by the CCD. For graphical interpretation of the interaction, the use of the three dimensional plots of the regression model is highly recommended. Figure 6.19 presents the simultaneous effects of the two independent variables on the COD removal efficiency obtained from Equation 6.1. It can be seen from the response surface plot, Figure 6.19 that the response increases upon increasing the HRT at higher COD_{in}, whereas the response remained constant by increasing HRT at the lowest COD_{in}, indicating that minimum HRT was sufficient. The interaction showed that the HRT and COD_{in} played an important role in the COD removal efficiency during the process.

The lowest COD removal efficiency of 89.9% was achieved by the SS-FFBR at the highest COD_{in} concentration (corresponding to 11.7 kg COD/m^3.d OLR) at lowest HRT of 8 h. This result is comparable with those results (COD removal efficiency 96.3%) obtained by Rodgers et al. (2006) using a horizontal flow biofilm reactor to treat synthetic dairy wastewater at a lower OLR of 2.3 g COD/m^2.d and longer 36 h HRT. In another study, Najafpour et al. (2006) treated food cannery wastewater using a three stage RBC, and achieved only 93.7% of COD removal efficiency at long HRT of 40 h. An 82.11% COD removal efficiency was achieved at maximum OLR of 10.2 kg COD/m^3.d when dairy wastewater was treated using an aerobic fluidized bed biofilm reactor (FBBR) (Resmi and Gopalakrishna, 2004). The good performance of SS-FFBR may be attributed to the larger amount of biomass accumulated in the reactor due to

large surface area provided by the flexible fibre, and that may increase the substrate consumption in the bioreactor.

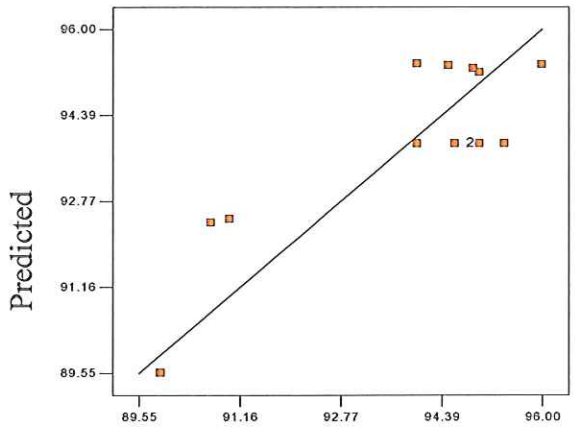

Figure 6.18: Actual versus predicted values of COD removal

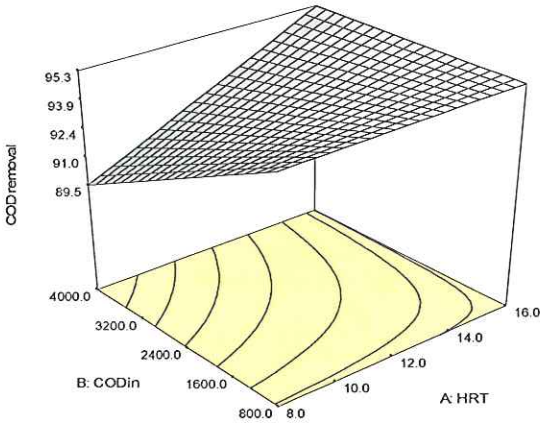

Figure 6.19: Response surface plot for COD removal

6.4.3 Effect of Influent COD Concentration and HRT on Specific Substrate Utilization Rate (U)

The following regression equation is the empirical model in terms of coded factors for specific substrate utilization rate:

$$U= 0.75-0.18A+0.42B+0.08\ A^2\ -0.11\ B^2\ -0.071AB \qquad (6.2)$$

where, U is specific substrate utilization rate, A is HRT and B is COD_{in}. A high correlation was observed between actual and predicted values of specific substrate utilization rate (U) with R^2=0.984 as shown in Figure 6.20. This confirms the adequacy of the model (equations) to predict values for U. The observed points on this plot reveal that the actual values are distributed relatively close to the straight line and show a significant correlation. Figure 6.21 depicts the variation of U as a function of the two variable factors, HRT and influent COD concentration. The Figure shows that a significant mutual interaction occurs between the variables on specific substrate utilization rate as a response. As a general trend, the specific substrate utilization rate (U) increased with increase in COD_{in} and decrease in HRT due to the increase in OLR and biological activity of the microbial population. The maximum value of U was modelled to be 1.39 g COD_{rem}/g VSS.L.d, whereas the actual value was 1.42 g COD_{rem}/g VSS.L.d. However, the modelled minimum value of U was 0.19 g COD_{rem}/g VSS.L.d while the actual value was 0.213 g COD_{rem}/g VSS.L.d. This condition was obtained at 16 h HRT and low COD concentration. Hamoda (1989) found a similar

observation of increase in U with the increase of substrate concentration. It can be observed that as a higher COD is applied to a reactor, the higher specific substrate utilization rate is obtained. This indicates that the influent COD concentration applied to the reactor has not achieved its limiting value and shows the ability of the process to treat a higher range of COD concentration.

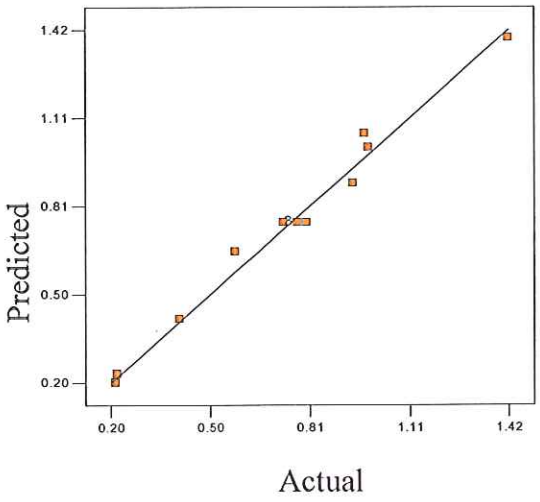

Figure 6.20: Actual versus predicted values of specific substrate utilization rate

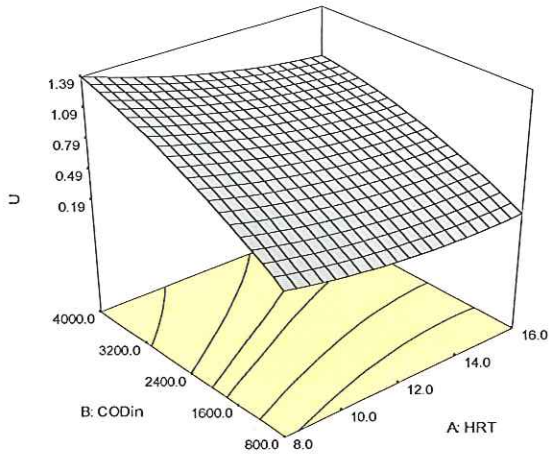

Figure 6.21: Response surface plot for specific substrate utilization rate

6.4.4 Effects of HRT and COD_{in} on Effluent Turbidity

For modelling the interactive effects of the variables (HRT and COD_{in}) on the effluent turbidity as a process response, the following quadratic model is the empirical model (built with codified factors) obtained.

$$\log_{10}(\text{Effluent Turbidity}) = 0.87 + 0.48B + 0.35A^2 \quad (6.3)$$

Figure 6.22 demonstrates a high agreement (R^2=0.8482) between the experimental and modelled data, indicating that 15.18% of the total variation is not explained by the model. The observed points on this plot indicate that the actual value is distributed away from the straight line. The regression model was conducted after transformation of the actual raw data to a function of log base 10, as error is a function of the magnitude of the responses. Figure 6.23 presents the simultaneous effects of the variables on the effluent turbidity. It is clear from the figure that the effluent turbidity has a proportional increase when the influent COD_{in} increased and HRT decreased. This might be attributed to less integrity in the microbial biofilm formed. For example, at the highest COD_{in} of 4000 mg/L, the effluent turbidity declined from 1.649 to 1.45 as the HRT increased from 8 to 16 h. This was expected due to the increase in the biomass growth

rate and the washed out sludge, especially with increase in the influent flow rate. It can be noted from the figure that the maximum value of the effluent turbidity was 1.649 at the higher OLR (corresponding to HRT 8 h and COD 3921.8 mg/L), while the lowest effluent turbidity value was 0.43 which was measured at a HRT of 12 h and COD_{in} of 830 mg/L. At the lower HRT value, a high effluent turbidity was obtained, and this was also affected by the amount of the COD applied to the system. The decrease of the effluent turbidity at 12 h HRT and COD_{in} of 800 and 2400 mg/L was noticeably lower (0.43 and 0.77) than the values obtained at HRT 8 and 16 h. This observation is somewhat in agreement with the findings by Najafpour et al. (2006) for a RBC reactor. Such a low effluent turbidity may be due to a lower range of OLR than the previous run that operated in a similar range of OLR. It suggests that due to low influent TSS contents, which microorganisms can easily degrade, low effluent turbidity is resulted. The low level of turbidity expresses the reduced amount of sloughed biomass and the sludge had good settling property in the settling tank. At a low HRT of 8 h, the reactor effluent turbidity gradually increased from 0.76 to 1.649, which may be due to the increase in the TSS concentration of the influent stream and increase in the OLR that may have an effect on the attached biomass. Despite some variation of the effluent turbidity, particularly at the HRT of 12 h, it can be suggested that HRT is a significant and effective variable amongst the operated variables.

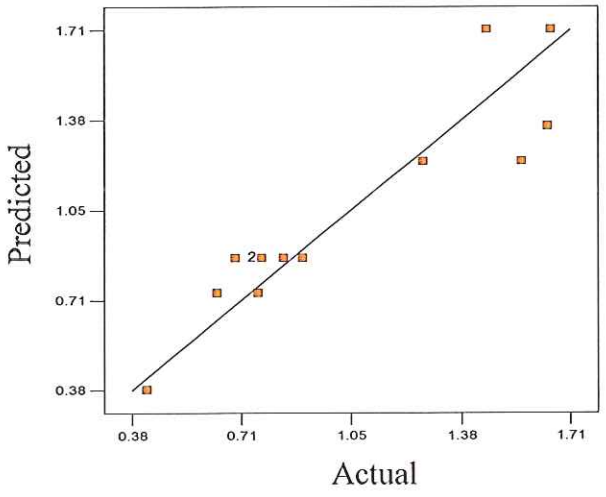

Figure 6.22: Actual versus predicted values of turbidity

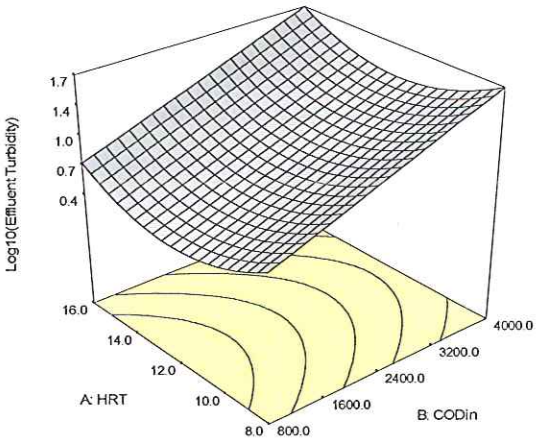

Figure 6.23: Response surface plot for turbidity

6.4.5 *Effect of HRT and COD_{in} on SRT*

SRT, as a process control parameter, was evaluated by measuring VSS in the reactor and in the effluent at various COD_{in} concentrations. The high SRT values denote the effective role of packing media on the process stability due to carrying a high amount of biomass, which allows the microorganisms to resist and survive with changes in OLR. The SRT influences the kinds of microorganisms that can grow in the treatment system and the extent to which various reactions will occur. In order to achieve a desirable SRT in the reactor, the rate of sludge wastage must be controlled at a desired value.

For modelling the interactive effects of the variables (COD_{in} and HRT) on the process control responses, SRT, the following quadratic model (built with codified factors) was obtained.

$$Log_{10}(SRT) = 1.95 + 0.23A - 0.21B - 0.17A^2 + 0.2AB \quad (6.4)$$

Figure 6.24 shows good agreement (R^2=0.941) between the experimental and predicted data of SRT. Figure 6.25 depicts the effect of the two operating variables on SRT. The main effect of HRT (A) and COD_{in} (B) were significant model terms. It should be noted that the ratio of the maximum to minimum SRT was about 13. Therefore, a logarithmic function with base 10 was applied to the SRT model. As can be seen from the 3D figure, the effect of increase in HRT on increase in SRT was more at the higher values of the COD_{in}, implying more effect of HRT relative to COD_{in} at higher values of COD_{in}. As described by the following equation, HRT, as an operating factor, has an effect on SRT (Metcalf and Eddy, 2003):

$$SRT = \frac{X.HRT}{X_e} \quad (6.5)$$

where X is the concentration of sludge in the reactor (g VSS/L) and X_e is the concentration of VSS in the effluent of the reactor (g VSS/L). In order to achieve a high and long SRT, whilst maintaining a short level of HRT, it is necessary to ensure that the biomass in the reactor does not wash out in the effluent. In the SS-FFBR, the provided packing media helps to achieve a high SRT as biofilm attachment on the packing media. In this study, the minimum and the maximum value of SRT were evaluated based on a logarithmic function with base 10 applied in order to fit the data. This curve shows that at HRT of 8 h and COD concentration of 3921 mg/L the reactor achieved a lowest SRT value of 1.17 day. However, the highest SRT (2.29 day) achieved lower COD

concentration of 830 mg/L at 12 h HRT. A general decrease on the SRT at low HRT was expected and that was due to the increase in the feed flow rate. Zinatizadeh et al. (2006) observed a similar trend when treated Palm Oil Mill Effluent (POME) wastewater using an UASB reactor.

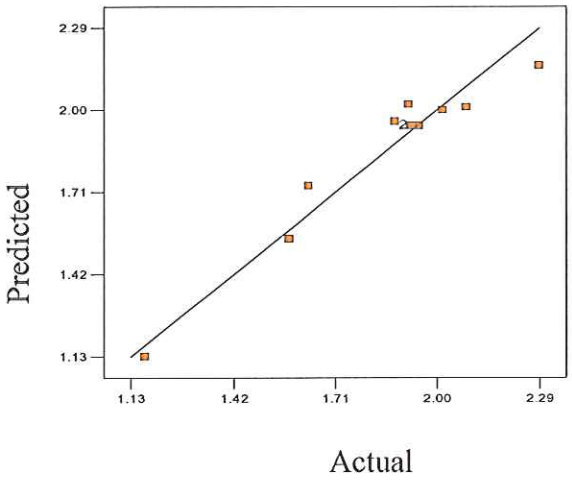

Figure 6.24: Actual versus predicted values of $\log_{10}$ (SRT)

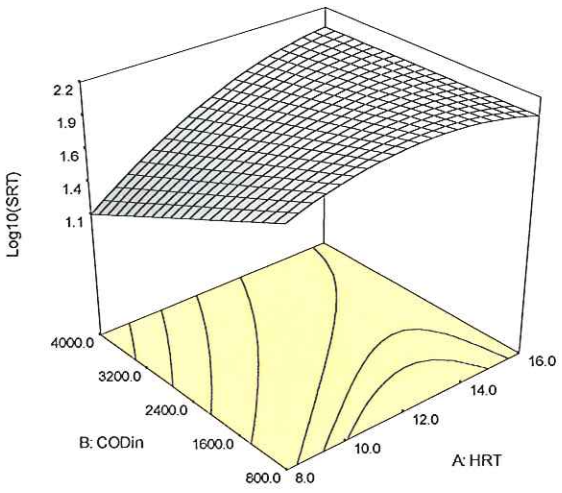

Figure 6.25: Response Surface plote for SRT

6.4.6 Effect of HRT and COD_{in} on VSS/TSS

The VSS to TSS concentration ratio in a biological reactor denotes the organic component in the solids content. The following regression equation (built with codified factors) was obtained for the VSS/TSS ratio:

$$\text{VSS/TSS ratio} = 0.93+2.833E\text{-}3B\text{-}5.88E\text{-}3B^2\text{-}5.5E\text{-}3AB \quad (6.6)$$

Figure 6.26 shows the predicted versus the actual values for VSS/TSS ratio with a correlation coefficient of R^2=0.841. Figure 6.27 demonstrates three-dimensional plots of the model for VSS/TSS ration with respect to COD_{in} and HRT. The figure indicates that the ratio of VSS/TSS sharply dropped as the COD_{in} concentration decreased to 800 mg/L and with increase the in HRT. The typical value of the VSS/TSS ratio should be in the range 0.6-0.8, whereas in this study the ratio was too high and was in the range of 0.91-0.956. This value was beyond the typical value recommended, and this higher value of VSS/TSS ratio indicates the high fraction of organic matter in influent total suspended solids. The COD_{in} was the most effective variable. Hu and Liu, (2002) obtained a similar ratio (0.93) when they treated a synthetic wastewater.

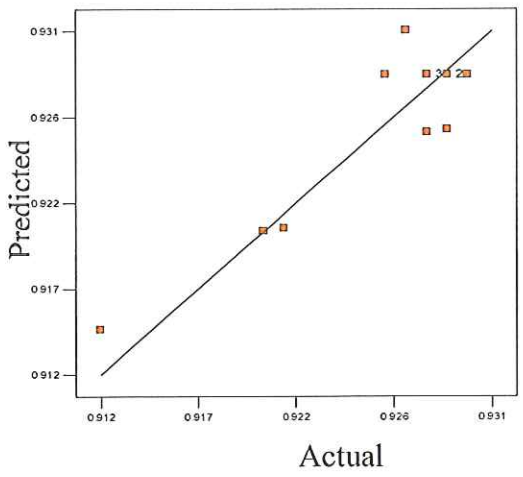

Figure 6.26 : Predicted versus actual values for VSS/TS

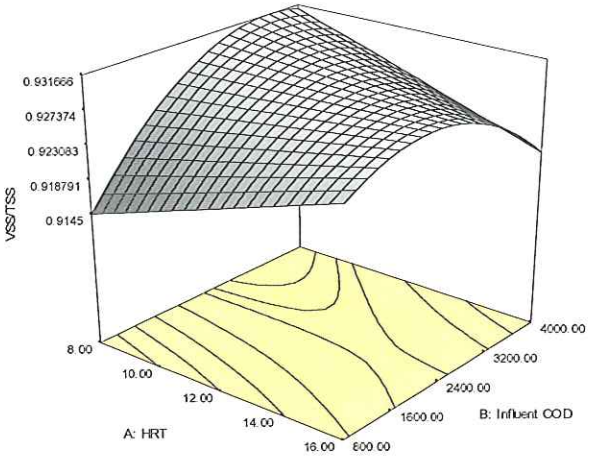

Figure 6.27: Response surface plots for VSS/TSS ratio

6.4.7 Process Optimization Analysis

With multiple responses, the optimum condition where all parameters simultaneously meet the desirable removal criteria could be visualized graphically by superimposing the contours of the response surface in an overlay plot. Graphical optimization displays the area of feasible response values in the factor space. Figure 6.28 shows the graphical optimization, which displays the area of feasible response values (shaded area) in the factors space. The optimum condition was identified based on three critical responses (COD removal, SRT and substrate utilization rate, U). The shaded area in Fig. 6.28 shows the optimum conditions for reactor performance. The optimum removal was obtained at a HRT of 8 h and COD_{in} 3922 mg/L (corresponding to high OLR of 11.67 kg $COD/m^3.d$). The results implied the raw milk processing wastewater could be well treated at a high OLR and Low HRT as indicated above. The results also showed a high treatment capacity of the SS-FFBR.

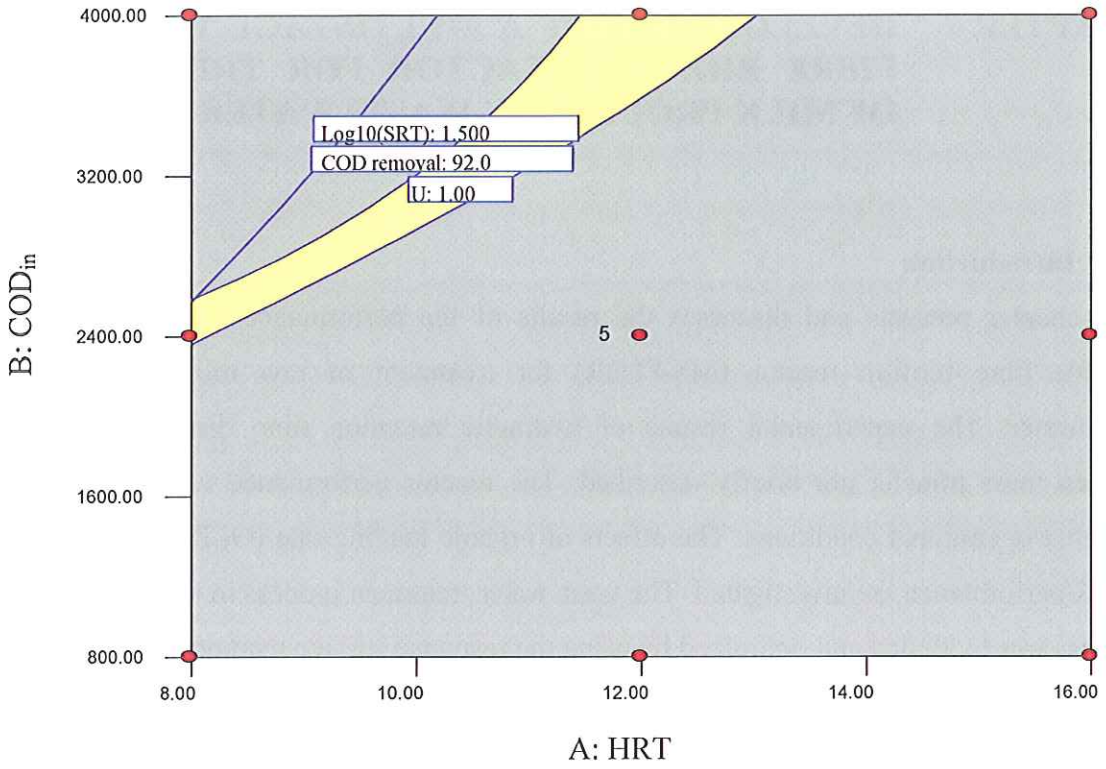

Figure 6.28: Overlay plot for optimal region

CHAPTER 7 DEVELOPMENT OF A MULTISTAGE FLEXIBLE FIBRE BIOFILM REACTOR FOR TREATMENT OF MILK PROCESSING WASTEWATER

7.1 Introduction

This chapter presents and discusses the results of the performance of a multistage flexible fibre biofilm reactor (MS-FFBR) for treatment of raw milk processing wastewater. The experimental results of hydraulic retention time distribution and oxygen mass transfer are briefly described. The reactor performance was studied at different operational conditions. The effects of organic loading rate (OLR) on the MS-FFBR performance are investigated. The wastewater treatment process in the MS-FFBR process was modelled and optimized by using the response surface methodology (RSM) with respect to the simultaneous effects of two independent operating variables, hydraulic retention time (HRT) and influent feed concentration (COD_{in}), where 8 interrelated parameters were assessed as responses. The kinetics evaluation and process optimization of the bioprocess were carried out based on COD removal. This chapter also includes a brief explanation of a morphological study on flexible fibre biofilm using SEM techniques.

7.2 Distribution of Hydraulic Retention Time in the MS-FFBR

The distribution of hydraulic retention time was investigated on the MS-FFBR by the tracer test at 2, 4 and 8 h HRT. The experimental procedures have been described in chapter 4, section 4.9.3.1. This test is usually performed by the measurement of the C-curve and F-curve. In the C-curve method, a tracer is instantaneously added into the first stage of the reactor and the tracer concentration in the effluent is measured as a function of time. The theoretical values were calculated by using Equation 7.1, and all the experimental results and theoretical data for C-curve are shown in Appendix A. Figures 7.1, 7.3 and 7.5 illustrate the experimental and theoretical tracer results for the MS-FFBR as a function of time for 2, 4 and 8 h HRT, respectively. As indicated in chapter 4, the MS-FFBR, the outlet concentration from the nth compartment can be expressed as (Levenspile, 1992; Metcalf and Eddy, 2003):

$$\bar{t}_i E = \left(\frac{t}{\bar{t}_i}\right)^{N-1} \frac{1}{(N-1)!} e^{-t/\bar{t}_i} \tag{7.1}$$

where, $\bar{t}_i$E = mean residence time in on reactor, $\bar{t}_i = N\bar{t}_i$, mean residence time in the N tank system, and N= number of reactors. The data showed almost complete tracer recovery at all conditions studied. It can be seen that the experimental data of HRT obtained in the MS-FFBR in all conditions are in close agreement with those for completely mixed flow reactors. The data of the distribution of HRT in the MS-FFBR at all conditions are close. Hence, HRT of the MS-FFBR is not affected by the flexible fibre packing, and in practice, the reactor can be treated as completely mixed flow reactor under the experimental conditions.

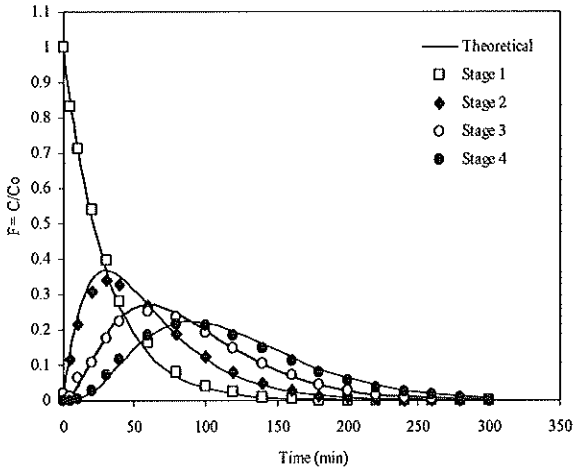

Figure 7.1: Residence time distributions in response to a pulse tracer input for four compartments in series at 2 h HRT C-Curve

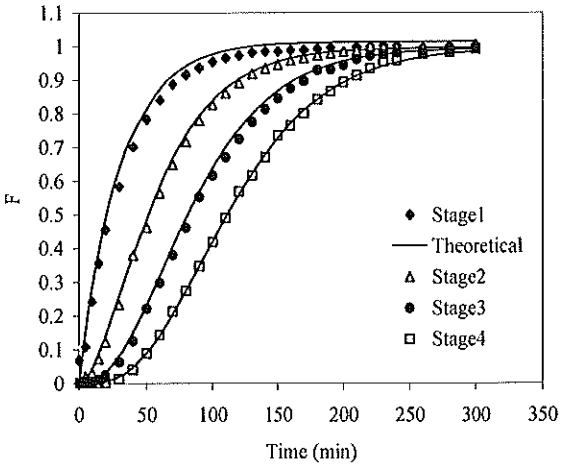

Figure 7.2: Residence time distributions in response to a pulse tracer input for four compartments in series at 2 h HRT F-Curve

The output F curves from a series of number of ideal stirred reactors (MS-FFBR) at different HRT were numerically integrated the corresponding data obtained for C-Curve. The actual F values for the multistage reactor were in the ratio of C/C_o. The actual data for F–curve either experimental results data or calculated theoretical data are listed in Appendix B. Figures 7.2, 4.4 and 7.6 show that F-curve experimental data points of HRT in the all reactor stages are extremely close to that of the theoretical value at HRT of 2 h of complete mixing reactors, while at HRT 4 and 8 h are also close but the points are distributed away from the theoretical value. This is attributed to insufficiency energy resulting from the flow rate applied, so that the portions of the reactor contents may not mix with the incoming water and dead zones develop within the reactor (Levenspile, 1992; Metcalf and Eddy, 2003). Therefore, the HRT of the MS-FFBR slightly affected the residence time distribution of the bioreactor. However, the flexible fibre packing media located in the centre of the stages had no effect on the

regime and exhibited that the reactors can be treated as continuous completely mixed reactor.

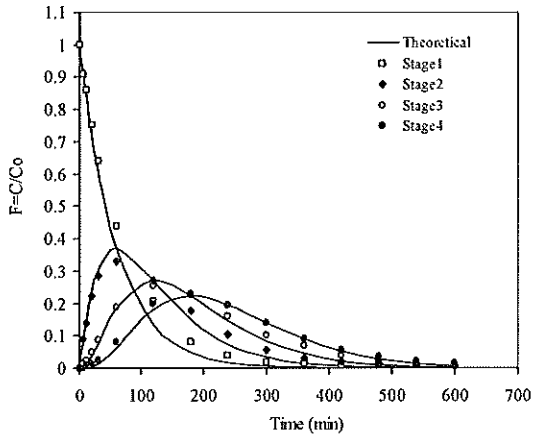

Figure 7.3: Residence time distributions in response to a pulse tracer input for four compartments in series at 4 h HRT C-Curve

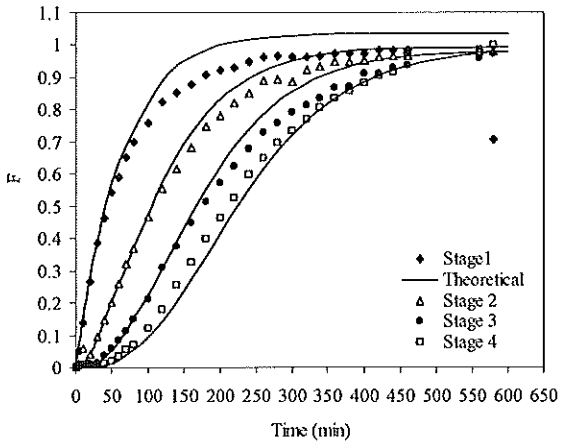

Figure 7.4: Residence time distributions in response to a pulse tracer input for four compartments in series at 4 h HRT F-Curve

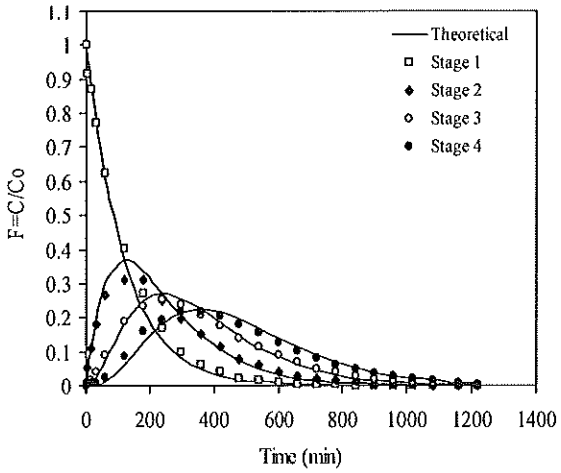

Figure 7.5: Residence time distributions in response to a pulse tracer input for four compartments in series at 8 h HRT C-Curve

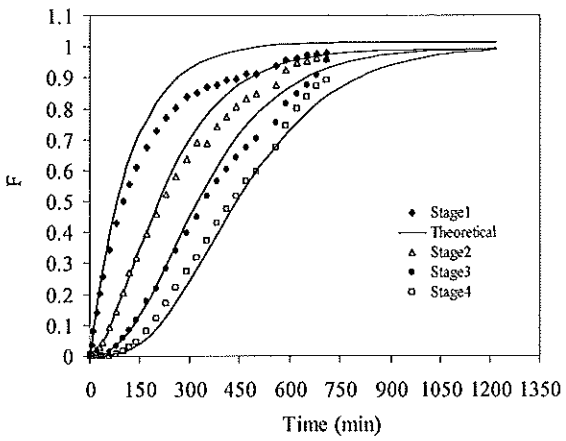

Figure 7.6: Residence time distributions in response to a pulse tracer input for four compartments in series at 8 h HRT F-Curve

7.3 Oxygen Mass Transfer Coefficients

The oxygen transfer coefficient (K_La) is one of the most important parameters in aerobic bioreactors and depends on various factors, such as geometrical and operational characteristics of the reactor, media composition, type, concentration, and microorganisms morphology (Amaral et al., 2008). The oxygen mass transfer coefficient for the MS-FFBR was determined by the gassing out method in the absence of microorganisms. This method was performed by sparging nitrogen gas until the

concentration of DO level in the equilibrium influent tank was zero. The experiments were conducted by pumping the influent water into the reactor at various AFR/WFR ratios. Both HRT and WFR were controlled at 1.0187 L/h and 8 h, respectively. As described in chapter 4, section 4.9.3.2 different air flow rates were used to obtain the above ratio. The data obtained from this experiment and the calculated data for the estimated mass transfer coefficient are given in Appendix C. Figure 7.7 to 7.12 show the regression plots for dissolved oxygen mass transfer coefficients based on $ln(C_s-C_0)/(C_s-C)$ and $(t-t_0)$. All figures have a linear regression relationship with a coefficient ranges between 0.9746 to 0.9975.

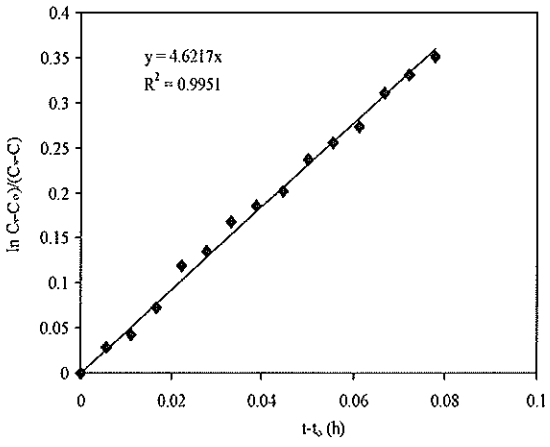

Figure 7.7: Regression plots for oxygen mass transfer coefficient at AFR/WFR =14.4

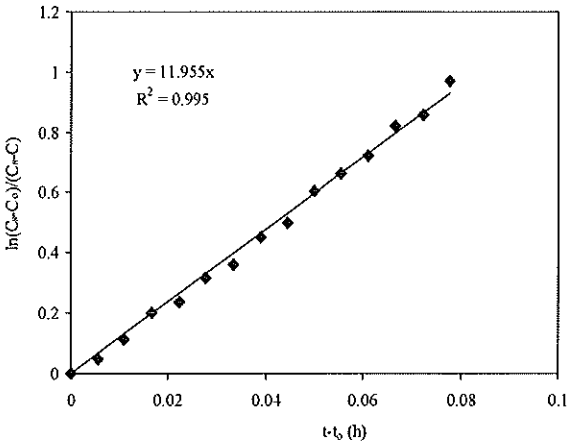

Figure 7.8: Regression plots for oxygen mass transfer coefficient at AFR/WFR=47.5

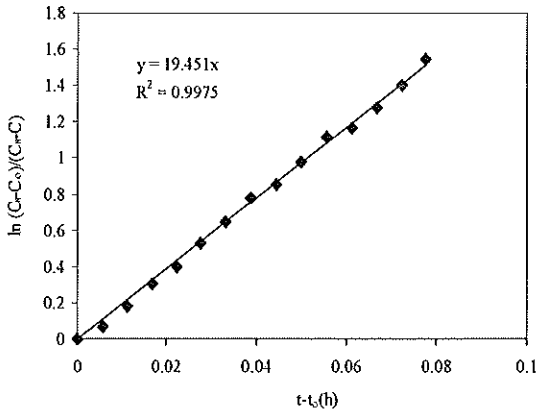

Figure 7.9: Regression plots for oxygen mass transfer coefficient at AFR/WFR =93

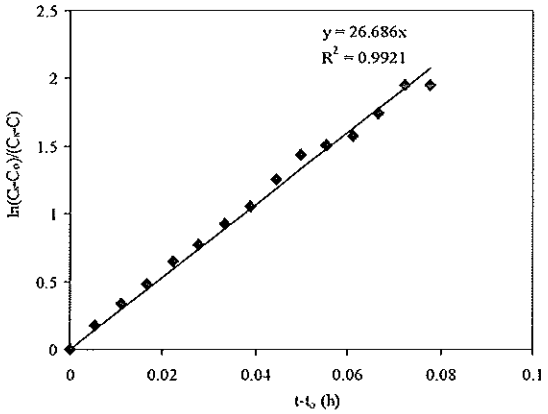

Figure 7.10: Regression plots for oxygen mass transfer coefficient at AFR/WFR= 140

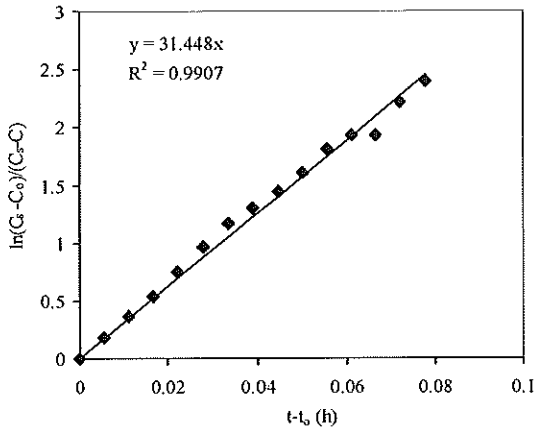

Figure 7.11: Regression plots for oxygen mass transfer coefficient at AFR/WFR =187

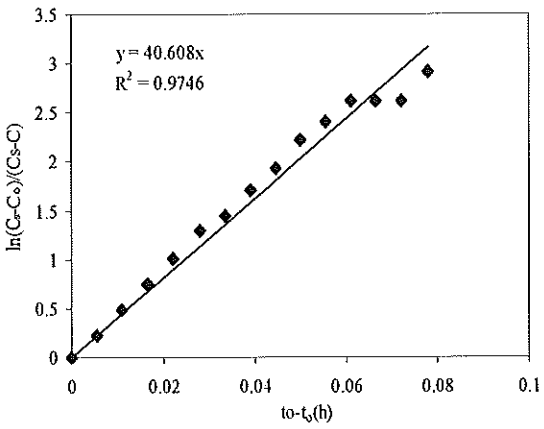

Figure 7.12: Regression plots for oxygen mass transfer coefficient at AFR/WFR =235

The obtained results of $K_{L.a}$ values for MS-FFBR at various AFR/WFR ratios are given in Table 7.1 and are graphically presented in Figure 7.13. The results clearly indicate that the K_{La} notably increased with increasing the ratio of AFR/WFR ratio. The correlation equation obtained for the MS-FFBR is as follows: $K_{L.a}$=0.1533 AFR/WFR = 3.77 with a high regression correlation coefficient, R^2 =0.9919. The results of mass transfer coefficients of the MS-FFBR are slightly lower than those obtained by Chen et al. (2009), and higher than those obtained by (Rodgers et al., 2004) with vertically moving biofilm system used for industrial wastewater treatment. In the new MS-FFBR, the coefficient seemed to be less sensitive to the AFR/WFR ratio variation. Hence, the existence of the flexible fibre packing may slow down the oxygen mass transfer rate of to some degree. This may be attributed to the interference caused by the flexible fibre on the size and the distribution of the air bubbles. Conversely, comparing these results with those obtained by Yu et al. (2006) as the difference in the coefficient is relatively small, and may be neglected in an application that is also due to difference in the reactor shape and geometry. It can be said that the capacities of the oxygen mass transfer in the MS-FFBR are similar to those previously obtained by (Chen et al., 2009; Yu et al., 2006) for a single stage FFBR.

Table 7.1: Relationship between ratio of AFR/WFR and K_{La}

AFR/WFR	$K_{La}(h^{-1})$
15	4.6
47	11.955
93	19
140	26
187	31
235	40

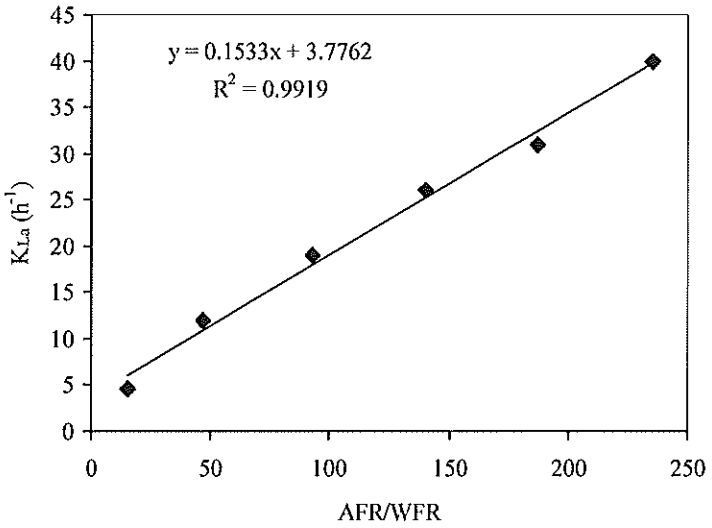

Figure 7.13: Comparison of relationship between oxygen mass transfer coefficient and AFR/WFR for MS-FFBR

7.4 Reactor Performance

7.4.1 Reactor Performance of Intermediate Stages

The performance of the MS-FFBR on the treatment of raw milk processing wastewater was assessed here based on the reduction of some wastewater quality parameters on the final effluent of the whole system and also at intermediate stages at different HRT. Figure 7.14 shows the effluent TCOD reduction with respect to stage numbers at HRT of 16 h, and at different influent COD. As noted, the trend of COD concentration decreased with increasing the number of compartments. As expected, at low influent average TCOD of 1602 and 3947 mg/L, a low amount of TCOD was obtained and most of the degradation occurred in the first stage, corresponding to 170.3 and 494.4 mg/L of TCOD. The TCOD concentrations were stable from stage two to stage four at 1602 and 3947 mg/L of COD_{in}, and reached minimum value of 115.4 and 212.5 mg/L, respectively. However, at an average of influent COD concentration of 5956 mg/L, a 3460 mg/L of effluent TCOD was obtained in the first stage. Therefore, the concentration was reduced to 2683.3, 2186.1 and 1731.6 mg/L for second, third, and

fourth stage, respectively. For the above conditions, it seems that the first stage has the most significant capacity of the TCOD reduction, as the most biodegradable organic COD was apparently removed in this stage.

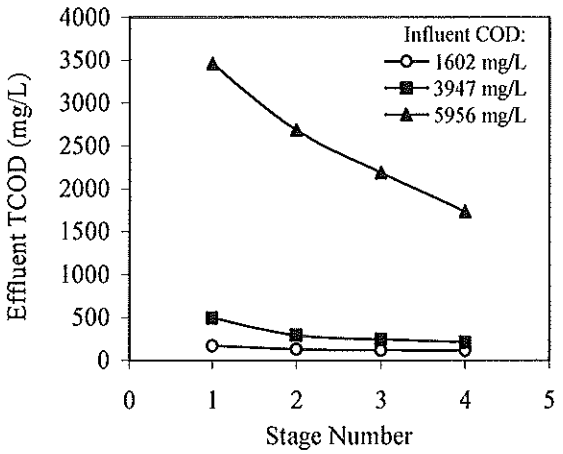

Figure 7.14: TCOD effluent concentration of different stage in MS-FFBR at 16 h HRT

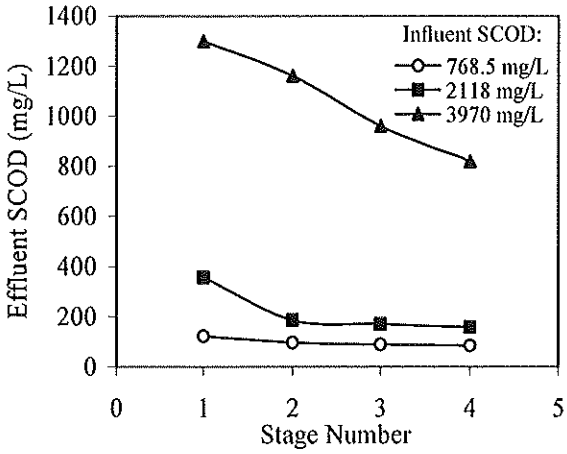

Figure 7.15: SCOD effluent concentration of different stage in MS-FFBR at 16 h HRT

Figure 7.15 presents the average SCOD concentration in the effluent from the four stages of the reactor operating at a constant HRT of 16 h with influent SCOD concentrations of 768.5, 2118 and 3970 mg/L in the first series of experiments. It can be noted that a pronounced decrease of SCOD occurred at all conditions with increased staging. At low average of influent SCOD concentration of 768.5 mg/L, there was not much difference in SCOD concentrations with increase of the stages. At the first stage, a 122.1 mg/L of SCOD concentration was obtained, and it gradually decreased to 97.1, 89.5 and 85.1 mg/L in the second stage, third stage and the fourth stage, respectively. As the influent SCOD concentration increased to an average of 2118 mg/L, a 356.5 mg/L of SCOD concentration were obtained at the first stage; in stages two to four, the SCOD further reduced to 186, 171.1 and 158.7 mg/L, respectively. Analysis of Figure 7.15 shows that SCOD removal was almost entirely achieved in the first stage of the reactor. A sharp decrease on the SCOD was observed when the influent SCOD increased to 3970 mg/L. More than 50% of SCOD was removed in the first stage with a 1298.6 mg/L of effluent SCOD achieved, whilst the concentration decreased to 819.1 mg/L in the fourth stage.

The performance of the MS-FFBR was also evaluated at HRT 12 h for different influent TCOD concentrations. Figure 7.16 displays the TCOD profile of the MS-FFBR system at 12 h HRT, and an average influent TCOD concentrations of 1590, 3843 and 5827 mg/L. As shown in Figure 7.16, the effluent TCOD concentration decreased with increasing stage number. It is obvious from the figure that the effluent concentration was significantly higher when the influent TCOD increased. At a low TCOD concentration of 1590 mg/L, the effluent TCOD concentration varied between 282.1 to 100.7 mg/L for the first to fourth stage, respectively. Higher effluent TCOD was generated as the influent TCOD was increased to 3843 mg/L. At the first stage, an average of 1319 mg/L was achieved. This implied that the majority of TCOD was eliminated in the first stage. The contributions of the later stages were also observed and an average of 856, 772.8 and 582.3 mg/L of TCOD was obtained in the second, third, and fourth stage. However, when the influent TCOD increased to an average of 5827 mg/L, the average TCOD effluent from the first stage was 3128.3 mg/L, which indicated that less than 50% of TCOD content was removed in the first stage, whereas, average TCOD reductions observed in the second, third and fourth stages were 2647, 2390 and 1801.4 mg/L, respectively.

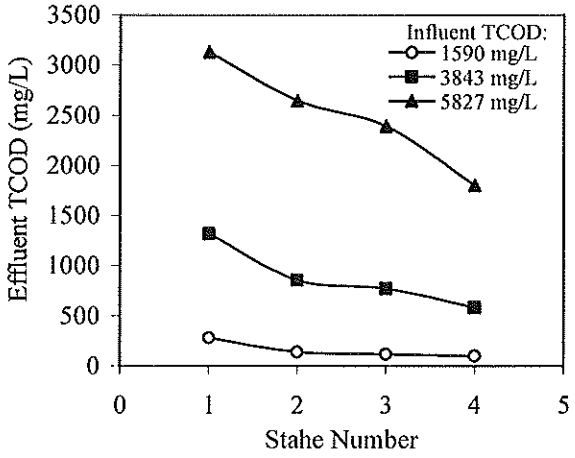

Figure 7.16: TCOD effluent concentration of different stage in MS-FFBR at 12 h HRT

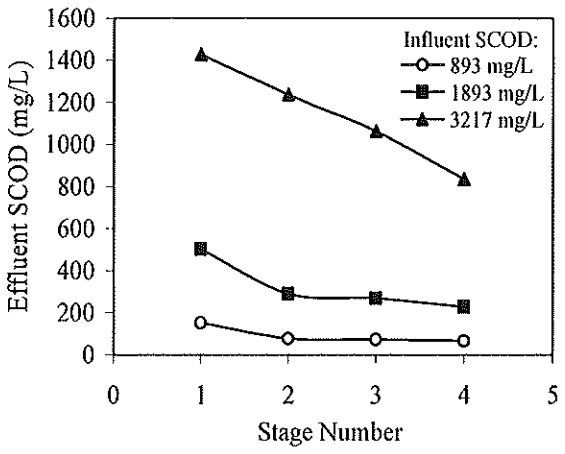

Figure 7.17: SCOD effluent concentration of different stage in MS-FFBR at 12 h HRT

The SCOD concentrations from different stages at HRT of 12 and at different influent SCOD are shown in Figure 7.17. An obvious trend of reducing concentration was observed for this case. With a low influent SCOD of 893 mg/L, about 80% of the SCOD was degraded in the first stage with an SCOD concentration of 152.1 mg/L, while a similar contribution of the stage two to four was identified with SCOD concentration of 77.5, 72 and 66.4 mg/L, respectively. With a higher average influent

SCOD concentration of 1893 mg/L, the effluent concentration increased when compared to the pervious low SCOD concentration run, but it still reduced with the increase of stage number. A 503 mg/L of SCOD was obtained at the first stage, while at the fourth stage was 228.8 mg/L. For the influent SCOD of 3217 mg/L, the effluent SCOD varied between 1427 to 835.4 mg/L, for first to the fourth stage. This indicated that most of the SCOD was removed in the first stage, while a lesser contribution occurred in the later stages.

As the HRT was decreased to 8 h, the MS-FFBR exhibited a different performance. The average effluent TCOD concentration from different stages and at different influent TCOD is shown in Figure 7.18. A low TCOD concentration was observed at an average influent of 1673 mg/L, and the first stage played a most significant role in TCOD reduction. There was about 78% of TCOD removal in this stage with an average effluent TCOD of 364.6 mg/L. Subsequently, the effluent TCOD was decreased with the stage number, and reached its minimum value of 112.8 mg/L in the fourth stage. When the influent TCOD concentration slightly increased to an average of 3955 mg/L, effluent concentrations of 2438.3, 2250, 1906.6 and 1840 mg/L TCOD were observed at the first, second, third, and fourth stages, respectively. The effluent TCOD increased as the initial TCOD increased to 5869 mg/L. The first stage achieved only 4402.5 mg/L, corresponding to about 25% of the initial TCOD reduction. The increase on the influent TCOD also has an impact in the later stages, e.g. a 3403.8 mg/L effluent TCOD was obtained from the second stage, and the concentration was gradually decreased to 2503.8 mg/L from the fourth stage.

Figure 7.19 shows the SCOD reduction with respect to stage numbers at various influents SCOD. At a low SCOD concentration of 724 mg/L, the effluent SCOD was found to vary between 201.8 to 87.5 mg/L, for the first to the fourth stages, respectively. With the increase of influent SCOD to 2455 mg/L, the effluent concentration was only 910 mg/L of SCOD in the first stage, which represents approximately 60% of SCOD removal. However, it can be noted that there was not much reduction on the effluent concentration, and the concentration decreased to 819.8, 720.6 and 573.3 mg/L for the second, third and fourth stage, respectively. A large amount of SCOD was left untreated as the influent SCOD increased to 2963 mg/L. The first stage removed only 50% of SCOD, which corresponds to 1411.2 mg/L effluent SCOD concentration. The effluent

SCOD concentration was gradually reduced and reached to 875.1 mg/L in the fourth stage.

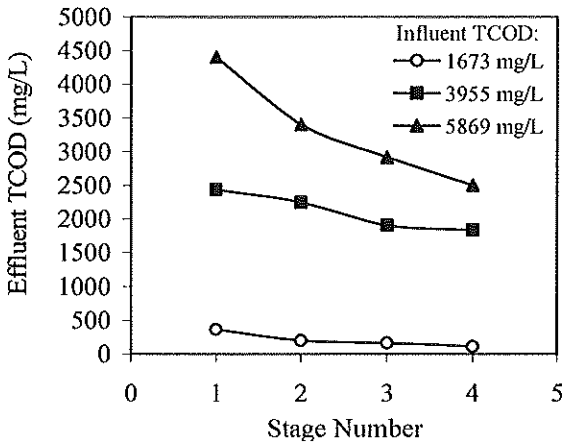

Figure 7.18: TCOD effluent concentration of different stage in MS-FFBR at 8 h HRT

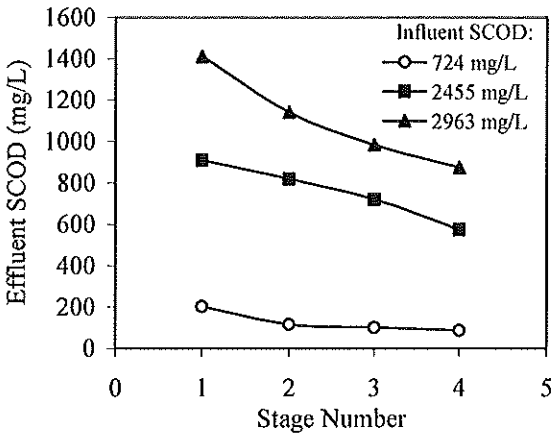

Figure 7.19: SCOD effluent concentration of different stage in MS-FFBR at 8 h HRT

Figures 7.20 (A), (B) and (C) display the average concentrations of TSS from the MS-FFBR basins at various HRT and influent COD concentrations. Generally, the average TSS concentration from the reactor stages showed some variations, especially when a high load was applied to the reactor at all HRTs. It was also observed that the longer HRT, the lower the TSS concentration in all compartments. At a HRT of 16 h, the average TSS concentration decreased with the stage number at an average COD of 1602 and 3947 mg/L, whereas at high COD value of 5956 mg/L, the TSS concentration show a different pattern as it increased suddenly in the third stage to 2050 mg/L, and again the TSS concentration decreased to 1092 mg/L in the fourth stage. For the HRT of 12 h, the experiments were conducted at different influent COD of 1590, 3843 and 5827 mg/L. The TSS concentration at 1590 mg/L of COD decreased with stage, despite an insignificant increase in the third stage, that range from 605 to 288.5 mg/L, whereas a similar pattern attained at an average of COD of 3843 mg/L, with TSS concentration of 1017, 930, 966.6 and 686.6 mg/L for the first, second, third and fourth stage, respectively. As the organic content increased to 5827 mg/L of COD, the TSS concentration in the first stage was 2410 mg/L and showed a decline to 1780 mg/L in the second stage before it increased again in the third stage to 2196.6 mg/L. However, the concentration of TSS reduced again in the fourth stage to 1105 mg/L.

With decrease of the HRT to 8 h, the TSS concentration was slightly different when compared to the previous case for HRT 16 and 12 h. These findings were in agreement with the results obtained by Najafpour et al. (2006) when the TSS concentration increased with decrease of HRT in a three stages RBC reactor. The average TSS concentration smoothly decreased with the increase of stages at lower influent COD concentration of 1673 mg/L, and the concentration ranged from 1363.6 to 403.3 mg/L for first to fourth stage. However, the TSS concentrations showed a similar trend for the case of 3955 and 5869 mg/L. Both cases showed an increase in the TSS concentration in the third stage 1480 and 2083 mg/L, respectively, whereas the concentration falls again to 953.3 and 1285 mg/L in the fourth stage. For all the above experimental conditions, the amount of suspended solids in the third stage was higher but in disagreement with the anticipated results. Such results may be due to the presence of undegraded solids in the wastewater which accumulated in this stage. Also, at high organic loadings applied, the sloughed biomass increased in the first and second stages. Newly generated bacterial cells in the third stage may also contribute to an increase in the amount of TSS in this stage.

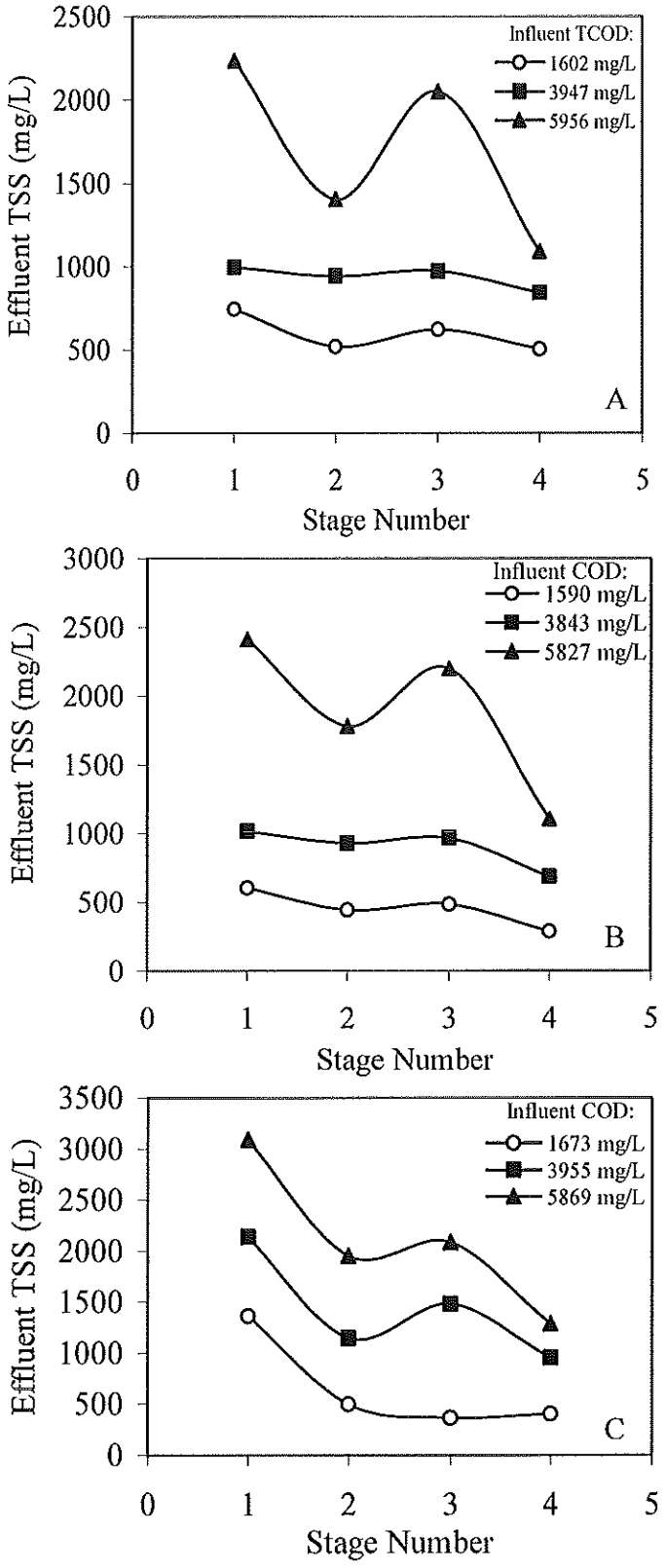

Figure 7.20: TSS effluent concentrations profile of different stages in MS-FFBR at HRT of 16 (A), 12 h (B) and 8 h (C)

To understand the ongoing biochemical processes during the continuous operation, the DO and pH were frequently determined in each stage at all experimental runs. The level of DO concentration in the reactor stages at HRT of 16 h and different COD concentrations is shown in Figure 7.21. As shown in the figure, the DO concentration generally followed a pattern of rapid initial decline in the first stage, and slowly recovered in the later stages. An increase in the COD concentration contributed to the consumption of DO as a low amount of DO in the first stage is an indication of balance between DO consumption and aeration rate. The DO level showed a slight reduction in the third stage at higher influent COD concentration before it showed a recovery again in the fourth stage. Figure 7.22 demonstrates the pH profile at various COD concentrations and HRT of 16 h. The pH at an influent COD of 1602 and 3947 mg/L showed a similar trend and remained in the rage of 7.32-7.61, and also showed an ascending trend from first to fourth stages. However, the pH of high COD concentration of 5956 mg/L was in the range of 7.47-7.80.

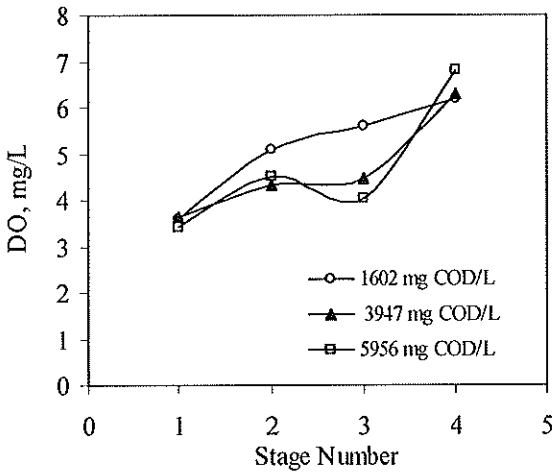

Figure 7.21: Profile of bulk fluid DO in the four stages at 16 h HRT

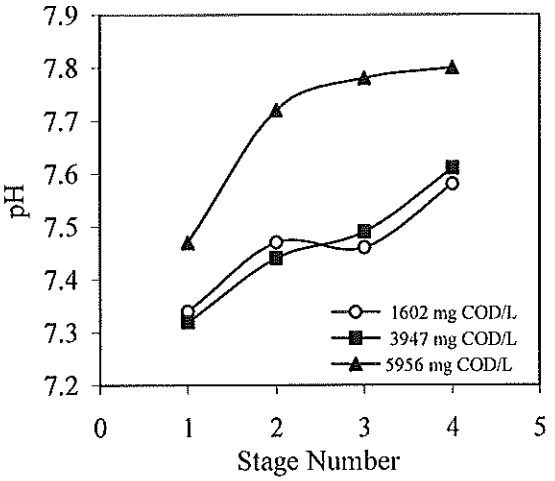

Figure 7.22: Profile of pH in the four stages at 16 h HRT

Figure 7.23 presents the DO levels with respect to the stage numbers at 12 h HRT. In general, the DO level increased with increase of stage number at all conditions. The DO levels were within the range of 3.48-7.21 mg/L for the low influent COD concentration and increased along the flow direction, from stage 1 to 4. When the influent COD increased to an average of 3843 mg/L, the DO trend was increased but it showed a low DO concentration in the range of 3.4 to 6 for the first to fourth stage. Theoretically, the DO concentration should decrease as the incoming substrates concentration increased. But it shows a different pattern where the DO in the first stage and the second stage

decline, and recovered in the third and fourth stages. However, it should not be more than the previous condition (3843 mg/L) where high COD loading caused a sharp decrease in DO. It may be because of less heterotrophic uptake of dissolved oxygen in the later stages. Figure 7.24 shows the pH profile at various COD concentrations and HRT of 12 h. Different ranges of pH were observed at different conditions. The pH obviously increased as the stages increased from the first to fourth stage. It was in the range of 7.07 to 7.51 from the first to fourth stage when the organic load was low. However, it increased from 7.54 to 7.82 from the first to fourth stage with in an average COD level of 3843 mg/L. By increasing the substrate concentration, the pH was increased subsequently from 7.49 to 7.98 for the first and fourth stage, respectively.

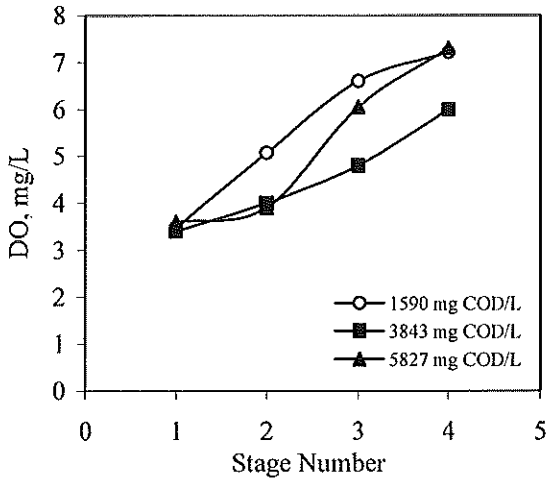

Figure 7.23: Profile of bulk fluid DO in the four stages at 12 h HRT

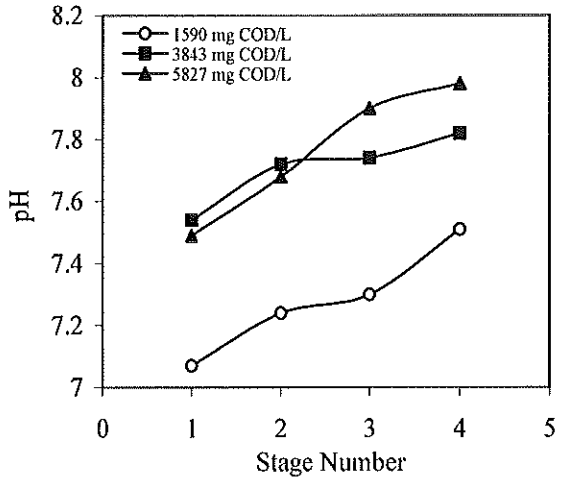

Figure 7.24: Profile of pH in the four stages at 12 h HRT

By decreasing the HRT to 8 h, the DO level concentrations with respect to the stage number at different conditions are illustrated in Figure 7.25. It can be noted that the DO concentration increased subsequently with stages, and decreased as the influent COD increases. Where organic influent COD was low in the average of 1673 mg/L, the DO level was in the range from 2.8 to 6.11 mg/L for the first to the fourth stage, respectively. As the average of the influent COD concentration increased to 3955 mg/L, the average DO concentration (4.1 mg/L) in the first stage was a little higher than in the second stages (3.05 mg/L), while it recovered in successive stages. The DO concentration at the higher influent DO concentration was high when compared to the pervious conditions, which was not compatible with the theoretical value or with pervious studies confirmed by (Al-Ahmady, 2005).

The pH profiles with respect to the stage number at 8 h HRT and at different influent concentrations are shown in Figure 7.26. It can be seen that the pH increased as the substrate loading increase and with increase of stage number. At an average influent COD concentration of 1973 mg/L, the pH value was 7.18, 7.24, 7.01 and 7.35 for the first, second, third and fourth stages, respectively. The pH value was in the range of 7.3-7.58 for the first to fourth stage. However, it apparently increased from 7.38 to 7.8 for high substrate COD concentration of 5869 mg/L for the first to the fourth stage, respectively.

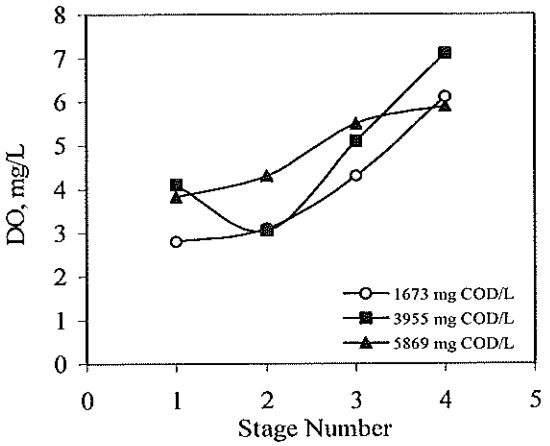

Figure 7.25: Profile of bulk fluid DO in the four stages at 8 h HRT

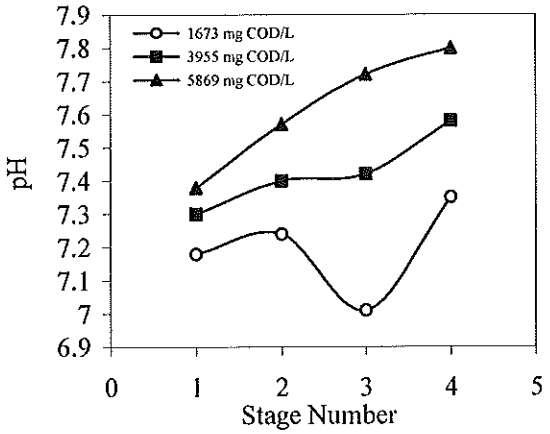

Figure 7.26: Profile of pH in the four stages at 8 h HRT

Therefore, the plots obtained above illustrate that, in general, the longer the HRT the lower the compartmental pH values. Moreover, limited range of pH variations indicates the adequate buffering capacity of the MS-FFBR stages resulted in only a moderate drop in the pH of the reactor's liquid due to the consumption of alkalinity associated with nitrification. Staging of the MS-FFBR reactor proved to be effective in damping excessive loadings, promoting nitrification and eliminating short circuiting of flow streams in the reactor.

Depending upon many factors such as HRT, influent COD, and biomass concentration in each stage, the stages of the MS-FFBR showed varying performance. The cumulative total COD removal at the low COD concentration and HRT of 8, 12 and 16 h is illustrated against stage number in Figure 7.27. The cumulative TCOD removal efficiency refers to removal efficiency in each stage based on the initial influent TCOD. The cumulative TCOD increased as the stage number increases and increase of HRT. At the first stage, about 88.9% was achieved at the average TCOD of 1602 mg/L and HRT

of 16 h. But the cumulative TCOD removal decreased to 82.2% as the HRT decreased to 12 h at 1590 mg/L of average influent COD. Furthermore, a 77.5% of cumulative TCOD was obtained in the first stage at a HRT of 8 h.

The cumulative TCOD removal in the second stage slightly improved and increased to nearly 91.4% for HRT 16 and 12 h, while an 87.5% was achieved at HRT of 8 h and 1673 mg/L. Subsequently, the cumulative TCOD removal gradually increased to about 92.2% at 16 and 12 h HRT. However, it achieved around 89.7% of cumulative TCOD removal at 8 h HRT and an average 1673 mg/L of TCOD. At the fourth stage a similar range of cumulative TCOD removal was obtained. These findings illustrate that with increasing the stage, the cumulative removal efficiency increased. That may be because of a subsequent increase in the reactor volume.

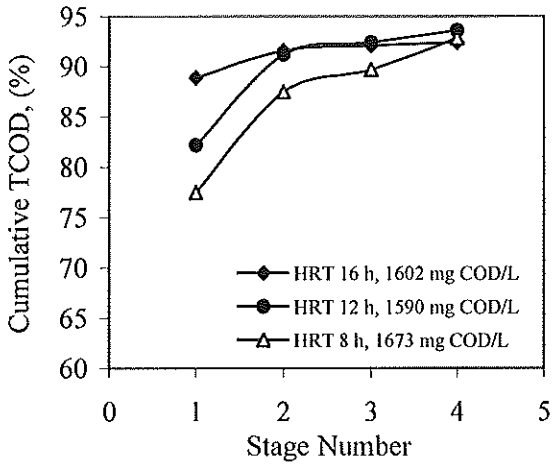

Figure 7.27:Cumulative of TCOD removals at different HRT

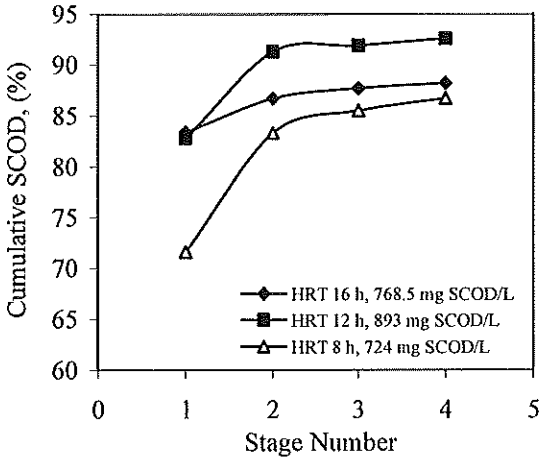

Figure 7.28: Cumulative of SCOD removals at different HRT

Figure 7.28 shows the cumulative SCOD removal efficiency with respect to stage number at different HRT. The figure shows that as the stage number increases the cumulative SCOD removal increases, with decreases the influent substrate concentration. As can be seen in the first stage, 82.8 and 83.4 % removals were obtained at 12 and 16 h HRT, respectively, while about 71.6% removal was achieved at HRT of 8 h. The gradual increase in the cumulative SCOD removal efficiency at the second stage to 91.3%, obtained at 12 h HRT, and 86.7% at 16 h HRT, while an 83.3% accumulative removal was achieved when the reactor operated at 8 h HRT. There was no meaningful increase in the cumulative SCOD removal in the later stages at all HRT. Therefore, it clearly indicated that at the second stage especially for 12 and 16 h HRT, it

was not possible to obtain further removal efficiency as a consequence of the non biodegradable SCOD fraction of the influent COD.

By increasing the influent TCOD concentration to 3947, 3843 and 3955 mg/L for 16, 12 and 8 h HRT, respectively, Figure 7.29 illustrates the cumulative TCOD removal efficiency with respect to the stage numbering at different operation conditions. For all experimental conditions, the cumulative TCOD removal increased gradually with increased stage number. At an average influent TCOD of 3947 and 16 h HRT, 87.4, 92.4, 93.6 and 94.4% of cumulative TCOD achieved as the stage number increased from first, second, third and fourth stage, respectively. The cumulative TCOD removal at an average influent TCOD of 3843 mg/L and 12 h HRT was lower than those obtained at pervious conditions of 16 h HRT. In addition, at HRT of 8 h, the cumulative TCOD removal ranged 37.3 to 52.7% from the first to fourth stage, respectively.

Figure 7.30 presents the cumulative SCOD removal as a function of stage number at 16, 12 and 8 h HRT, and an average of influent SCOD concentration of 2118, 1893 and 2455 mg/L. A clear increase can be seen as the stage number increased from first stage to the fourth stage. At the first stage, where most of the SCOD were degraded, a cumulative SCOD removal was 83, 75.7 and 63% at 16, 12 and 8 h HRT, respectively. However, from the second stage to fourth stage, there was not much further cumulative SCOD removal, which indicates that the most biodegradable SCOD was removed in the first and second stage and that was clearly shown at HRT of 12 and 16 h. But, at 8 h, the cumulative removal of SCOD slightly increased and the trend is evident. The cumulative SCOD removal ranged from 63-76% from the second to fourth stage, respectively.

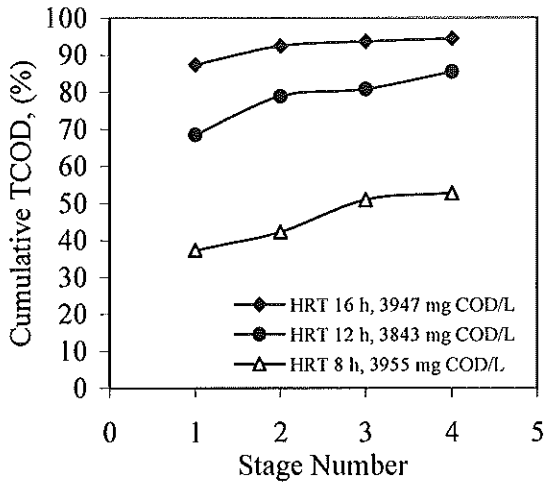

Figure 7.29: Cumulative of TCOD removals at different HRT

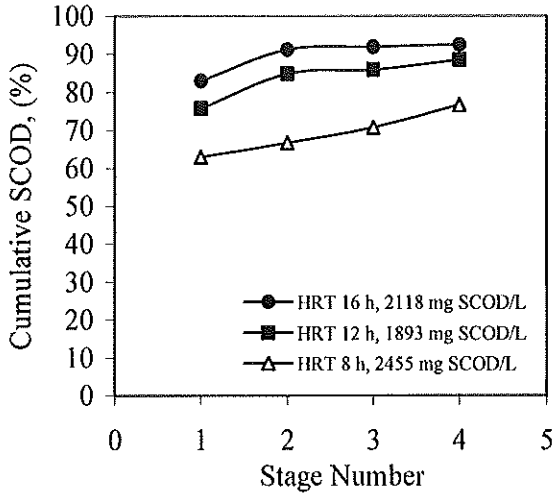

Figure 7.30: Cumulative of SCOD removals at different HRT

For higher influent TCOD concentrations in the MS-FFBR at 16, 12 and 8 h HR, the cumulative TCOD removal efficiency with respect to stage number is shown in Figure 7.31. The cumulative TCOD removal increased with the increase of stage number. The first stage showed the most significant removal of TCOD and it contributed 40.8, 46 and 26.4% at 16, 12 and 8 h HRT, respectively. At both 16 and 12 h HRT it showed almost identical cumulative TCOD removal in the second stage of 53.6 and 54.7% of TCOD, respectively, while a 43% was obtained at 8 h HRT. In the fourth stage, the cumulative TCOD removal was nearly constant at 16 and 12 HRT. However, 58.4% of cumulative of TCOD achieved in stage four at 8 h HRT.

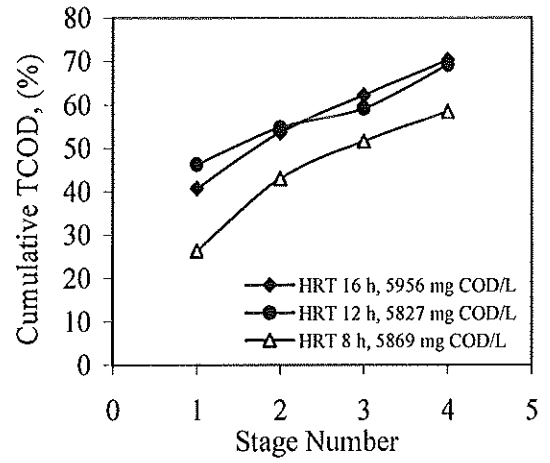

Figure 7.31: Cumulative of TCOD removals at different HRT

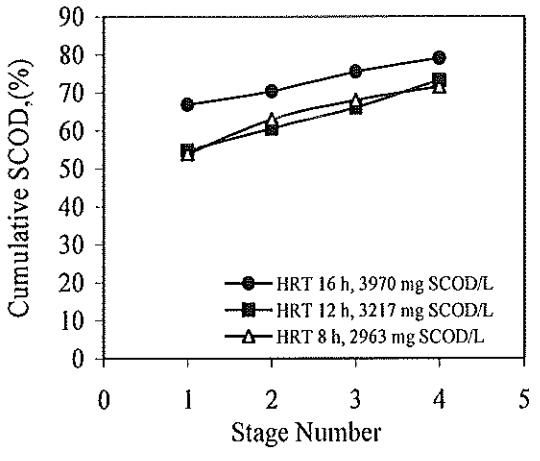

Figure 7.32: Cumulative of SCOD removals at different HRT

Figure 7.32 shows the cumulative removal efficiency of SCOD with respect to stage number at different HRT and influent SCOD concentration. A general increase in the

cumulative SCOD was observed with increased stage number. The first stage has the most contribution to the SCOD removal with a range of 66.6, 54.7 and 53.9% for 16, 12 and 8 h, respectively. The cumulative COD removal increased in the second stage and the third stage, until it reached its maximum of 79.1, 73.3 and 71.5% for 16, 12 and 8 h, respectively. Thus, for all the above experimental results, the performance of the MS-FFBR reactor is basically influenced by the HRT and amount of the COD_{in} applied to the reactor. In addition, the number of stages has a crucial effect on the COD removal from the highly polluted wastewater.

Table 7.2 summarises the average concentration of TCOD, SCOD, TSS, and turbidity obtained for the liquid in each stage of the MS-FFBR in all runs of the experiments. All parameters monitored in all experiments have already been described in detail in section 7.4.1. However, the turbidity was also monitored in some experimental runs. It can be seen from the results that the turbidity decreased as the stages increased and the HRT increased. Generally, at lower influent COD concentrations of 1602, 1590 and 1673 mg/L, low effluent turbidity was obtained, starting from the first stage where the turbidity was 17.6, 50.8 and 62.5 NTU at the HRT of 16, 12 and 8 h. An obvious reduction in the turbidity was obtained in the second and third stages. Furthermore, the turbidity in the fourth stage at this low COD concentration was 9.24, 20 and 16.1 at 16, 12 and 8 h of HRT.

At 12 h HRT, the effluent turbidity of the first stage was 273.3 NTU, while it was 46.6 NTU at 16 h HRT. However, there was no result detected on this stage at 8 h HRT. The turbidity decreased later as the stages increased. Reduced effluent turbidities of 17.5 and 74.8 NTU were obtained at the fourth stages at 16 and 12 h HRT, respectively. No results were obtained for the case of high influent COD concentration at all HRT.

Table 7.2: Summary of average of MS-FFBR stages parameters at various conditions

Stage1					
Influent COD mg/L	HRT (h)	TCOD mg/L	SCOD mg/L	TSS mg/L	Turbidity NTU
1673	8	364.6	201.8	1363.3	62.5
1590	12	282.1	152.1	605	50.8
1602	16	170.3	122.1	745.7	17.6
3955	8	2438.3	910.0	2140	ND
3843	12	1319	503	1833.3	273.3
3947	16	494.4	356.5	997.1	46.6
5869	8	4402.5	1411.2	1904	ND
5827	12	3128.3	1427	3420	ND
5956	16	3460	1298.6	2236	ND

Stage2					
Influent COD mg/L	HRT (h)	TCOD mg/L	SCOD mg/L	TSS mg/L	Turbidity NTU
1673	8	199.5	117	496.6	32.6
1590	12	138.4	77.5	445	22.9
1602	16	129.1	97.1	520	8.95
3955	8	2250	819.8	1146	ND
3843	12	856	290.5	930	158.3
3947	16	293	186	942.8	25.1
5869	8	3403.8	1142.1	1436	ND
5827.5	12	2647	1236.5	1715	ND
5956	16	2683.3	1160.6	1405	ND

Stage 3					
Influent COD mg/L	HRT (h)	TCOD mg/L	SCOD mg/L	TSS mg/L	Turbidity NTU
1673	8	162.5	101.6	363.3	25.8
1590	12	118.5	72	485	20.8
1602	16	118.8	89.5	622.8	9.01
3955	8	1906.6	720.6	1833	ND
3843	12	772.8	269.3	1163.3	133.3
3947	16	245.2	171.1	974	22.9
5869	8	2916.3	984.1	1360	ND
5827	12	2390	1061.8	2545	ND
5956	16	2186.1	960.8	2050	ND

Stage 4					
Influent COD mg/L	HRT (h)	TCOD mg/L	SCOD mg/L	TSS mg/L	Turbidity NTU
1673	8	112.8	87.5	403.3	16.1
1590	12	100.7	66.4	288.5	20
1602	16	115.4	85.1	505.7	9.24
3955	8	1840	573.3	953.3	ND
3843	12	582.3	228.8	686.6	74.8
3947	16	212.5	158.7	842.8	17.5
5869	8	2503.8	875.1	1384	ND
5827.5	12	1801.4	835.4	1105	ND
5956	16	1731.6	819.1	1530	ND

7.4.2 *Overall Total and Soluble COD Removal Efficiency*

The performance of the MS-FFBR was evaluated based on the final effluent total COD and soluble COD removal efficiency at different HRTs. Figures 7.33 and 7.34 show the variations of total and soluble COD removal efficiency with time at constant HRT of 8 h for three different COD_{in}. It can be noted that the TCOD and SCOD removal percentages decreased with increased COD_{in}. In Figure 7.33, the effect of the COD_{in} on the TCOD removal efficiency is more pronounced. At low influent COD_{in} of 1673 mg/L, the MS-FFBR achieved 93.5% of final TCOD removal efficiency, whereas the TCOD removal efficiency of the MS-FFBR was only 76.6% as the COD_{in} increased to 3955 mg/L. A clear impact on removal efficiency of TCOD can be seen when the influent COD_{in} increased to 5869 mg/L, the reactor obtained 69% COD removal efficiency.

With regards to SCOD removal efficiency, the MS-FFBR achieved a good performance. The SCOD removal efficiency of the influent $SCOD_{in}$ of 724 and 2455 mg/L was 88.7 and 86.6%, respectively, whereas the influent $SCOD_{in}$ increased to 2963 mg/L, the removal efficiency of SCOD was 79.1%. All the SCOD removal efficiencies were obtained at steady state conditions.

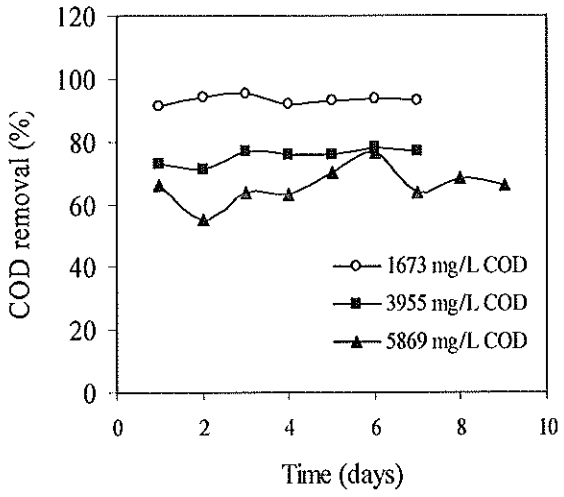

Figure 7.33: TCOD removal efficiency of the MS-FFBR at 8 h HRT

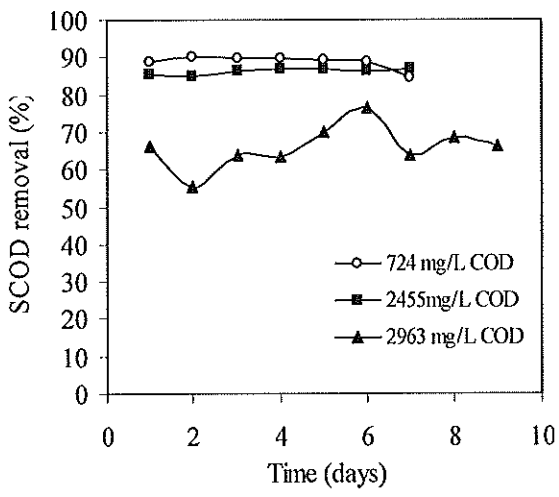

Figure 7.34: SCOD removal efficiency of the MS-FFBR at 8 h HRT

Figures 7.35 and 7.36 illustrate the variations of TCOD and SCOD removal efficiency as a function of time, respectively at 12 h HRT. It can be seen from the figures that the COD removal efficiency at this condition decreased as the COD_{in} increased. At steady state conditions the MS-FFBR achieved a 94.8% of TCOD reduction at an influent

COD_{in} of 1590 mg/L, whereas the TCOD removal decreased to 86.9% when the influent COD_{in} increased to 3843 mg/L. As the influent COD_{in} increased to the high level of 5827 mg/L, corresponding to an OLR of 11.6 kg $COD/m^3.d$, the TCOD removal efficiency was observed to decrease slightly to 85.6%.

With respect to SCOD removal efficiency, Figure 7.36 clearly indicates that a high SCOD removal efficiency was obtained and it was quite similar at all conditions. At these conditions, the reactor achieved 92.9% of SCOD removal at an average influent $SCOD_{in}$ of 892 mg/L. The performance of the reactor was reduced a little to 88 and 88.8% of SCOD removal efficiency at an average influent $SCOD_{in}$ of 1893 mg/L and 3217 mg/L, respectively. Generally, the performances at these conditions were quite similar, which was attributed to the reactor being more efficient in reducing SCOD. In addition, an increase of biomass concentration could also be the key to improve the reactor performance due to the existence of the flexible fibre packing media, which provides a high surface area for microorganisms to grow on.

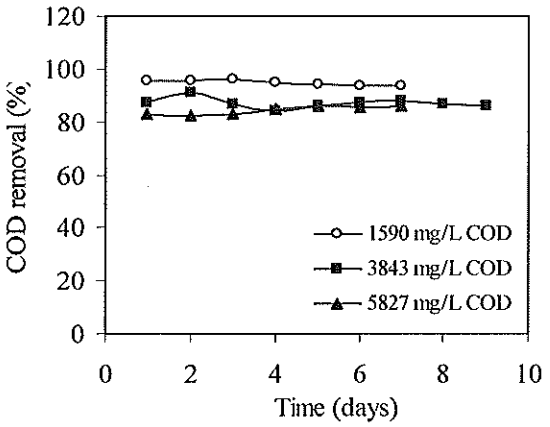

Figure 7.35: TCOD removal efficiency of the MS-FFBR at 12 h HRT

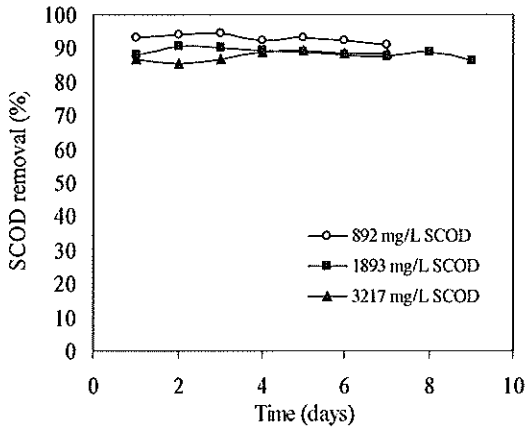

Figure 7.36: SCOD removal efficiency of the MS-FFBR at 12 h HRT

The variation of TCOD removal efficiency as a function of time is depicted in Figure 7.37 at 16 h HRT. At an influent COD_{in} concentration of 1602 and 3947 mg/L, the reactor achieved 93.2 and 93.7 % of TCOD removal efficiency, respectively. However, the TCOD removal efficiency was reduced to 81.8% when the influent COD_{in} concentration was increased to 5956 mg/L. The MS-FFBR exhibited a good TCOD removal at low influent COD_{in}, which reflects a low range of OLR.

The SCOD removal efficiencies as a function of time at HRT of 16 h and different influent concentrations are depicted in Figure 7.38. At this experimental condition, the SCOD removal efficiency showed a different trend when compared to previous experimental conditions at 8 and 12 h HRT. The highest SCOD removal efficiency of 91.8% was attained at an average of influent $SCOD_{in}$ of 2117 mg/L, whereas at lower influent $SCOD_{in}$ of 768 mg/L, the efficiency was decreased to 88.9%. However, in this case the SCOD removal was expected to be higher than this percentage, due to a lower loading to the reactor. An average of 88.3% of SCOD removal efficiency was obtained when the reactor ran at influent $SCOD_{in}$ 3970 mg/L. This result demonstrated the capability of the reactor at a high OLR.

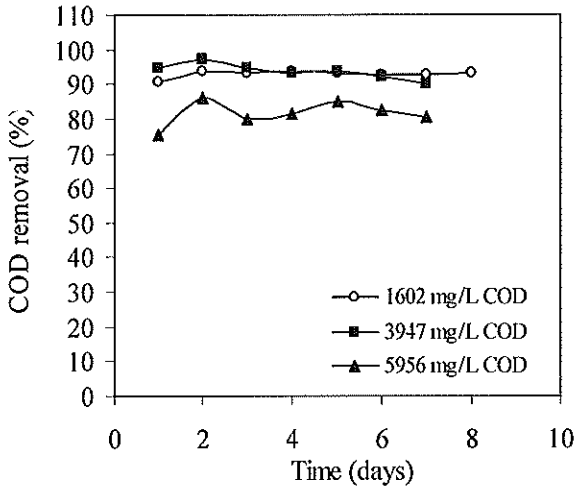

Figure 7. 37: TCOD removal efficiency of the MS-FFBR at 16 h HRT

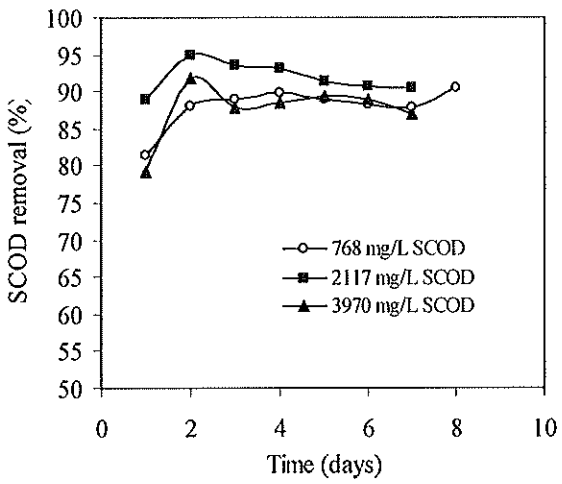

Figure 7.38: SCOD removal efficiency of MS-FFBR at 16 h HRT

7.4.3 Final Effluent Qualities of the MS-FFBR

Table 7.3 presents final effluent quality at various operating conditions. As the table shows, good qualities of the final effluent of MS-FFBR were obtained with increasing the HRT or decreasing OLR. At a low range of influent COD concentration of 1602, 1590 and 1673 mg/L, a good effluent quality was obtained with total effluent COD concentration of 109, 81.7 and 106 mg/L, respectively. While a total BOD_5 was 54.2, 21.5 and 20.5 mg/L at 1602, 1590 and 1673 mg/L, and 16, 12 and 8 h of HRT, respectively. The SCOD and $SBOD_5$ were also determined and low concentrations were achieved as can be seen in Table 7.3. The effluent TSS concentration gradually increased from 8.57, to 31.4, to 96.6 mg/L as the HRT decreased from 16, to 12, to 8 h, respectively. In addition, a very low effluent turbidity was obtained, which 8.38, 17 and 14.5 NTU, respectively. The pH level remained between 7.3 and 7.57 throughout the experiment.

The final effluent quality of MS-FFBR at an influent concentration of 3947, 3843 and 3955 mg/L was assessed and evaluated based on the parameters shown in Table 7.3. The final effluent TCOD of the MS-FFBR system increased with the decreased HRT. It was noted that 239.8, 514.5 and 920.2 mg/L of TCOD was attained at 3947, 3843 and 3955 mg/L TCOD, corresponding to OLR of 5.92, 7.68 and 11.8 kg COD/m^3.d, respectively. A similar trend was observed for SCOD at the same condition. In addition, low BOD_5 and $SBOD_5$ concentrations were observed as the OLR increased from 5.92, to 7.68 and to 11.8 kg COD/m^3.d. The final effluent TSS gradually increased from 51.4, to 196.6 and to 445 mg/L as the OLR increased from 5.92, to 7.68 and to 11.8 kg COD/m^3.d. With respect to the effluent turbidity of MS-FFBR, the reactor showed a good effluent turbidity of 16.1 NTU at 16 h HRT, while it increased to 62.4 NTU when the HRT decreased to 12 h. However, a 253.7 NTU was achieved at 8 h HRT. The pH value showed some variations: a 7.73 was obtained at 12 h HRT, while a lower range of pH of 7.54 and 7.54 was observed at 16 and 8 h HRT.

The final effluent quality deteriorated as the influent TCOD increased to 5956, 5827 and 5869 mg/L corresponding to OLR of 8.93, 11.6 and 17.6 kg COD/m^3.d, respectively. High effluent TCOD concentrations of 1074.5 and 1866.7 mg/L were achieved when the influent COD concentrations were 5956 and 5869 mg/L, respectively. However, at 12 HRT and 5827 mg/L, 838.7 mg/L of effluent TCOD concentration was obtained. At the same time, effluent BOD_5 also increased significantly and ranged between 467.2 to 1038 mg/L. It is evident that the reactor effluent quality could also be affected by the other operational parameters such as HRT, as well as influent COD concentration. The effluent turbidity of MS-FFBR was 169, 145 and 464 NTU at HRT of 16, 12 and 8 h. The final effluent turbidity seems to be high compared to the previous experimental conditions, due to the increase of OLR. The turbidity of the settled treated wastewater at various HRTs was correlated with the amount of TSS concentration in the final effluent stream. In this set of experiments, the effluent TSS concentration was about 456 mg/L at an average TCOD concentration of 5956 mg/L corresponding to OLR of 7.58 kg COD/m^3.d at 16 HRT. However, the TSS concentration decreased to 320 mg/L as the average influent COD concentration decreased to 5827 mg/L corresponding to OLR of 7.6 kg COD/m^3.d and 12 h HRT. As the influent COD increased to 5869 mg/L, a 633.3 mg/L of TSS concentration was obtained. The increase of TSS concentration was probably initiated by the higher death rate of microorganisms due to the increase in the organic loading rate.

Table 7.3 : MS-FFBR effluent quality under various HRT

Influent COD	HRT	OLR	pH	TCOD	SCOD	BOD_5	$SBOD_5$	TSS	Turbidity
mg/L	(h)	kg COD/m^3.d		mg/L	mg/L	mg/L	mg/L	mg/L	NTU
1673	8	5.02	7.33	106	80.1	34.5	20.5	96.6	14.5
1590	12	3.18	7.5	81.7	63.4	21.5	13.0	31.4	17
1602	16	2.4	7.57	109	84.8	54.2	36.1	8.57	8.38
3955	8	11.8	7.53	920.2	327.7	622.5	322.5	445	253.7
3843	12	7.68	7.73	514.5	227.5	236.4	128.4	196.6	62.4
3947	16	5.92	7.54	239.8	172.1	80.9	69.8	51.4	16.1
5869	8	17.6	7.36	1866.7	636.1	1038	387	633.3	464
5827	12	11.6	7.6	838.7	359.7	476.2	210	320	145
5956	16	8.93	7.58	1074.5	463	576	292.5	456	169

7.4.4 Effect of Organic Loading Rate on Reactor Performance

The effect of the OLR on the TCOD removal efficiencies at different range of HRT is plotted in Figure 7.39. As shown in the figure, there is a strong correlation between these two parameters. However, the reactor showed a varying performance as the reactor operational conditions were varied. The results shown in Figure 7.39 indicate that the TCOD removal efficiency decreased as the OLR increased. A reverse linear relationship between the OLR and the TCOD removal was obtained. However, the trend is pronounced for all experimental conditions. It is pointed out that the TCOD removal efficiencies obtained using the MS-FFBR, which ranged between 69-94.8%, are markedly comparably better than those obtained in the literature, as the OLRs applied to MS-FFBR were higher and ranged from 2.4-17.6 kg TCOD/m^3.d. The reduction in the TCOD was possibly caused by some inhibitation of bacterial activity and as well as higher COD loading. Such a high OLR has not been studied in any biofilm reactors treating food processing wastewater. A study conducted by Duarte and Oliveira (1984) observed a similar pattern of TCOD reduction using RBC treating dairy wastewater, but at a low OLR. Treating canning food wastewater using three stages RBC, an 85.4% COD removal was achieved at 36.89 g/m^2.d (Najafpour et al., 2006). Hamoda and Abd-El-Bary (1987) also achieved a COD removal ranging between 88.9-97.0% using a four stages aerated submerged fixed film (ASFF) reactor.

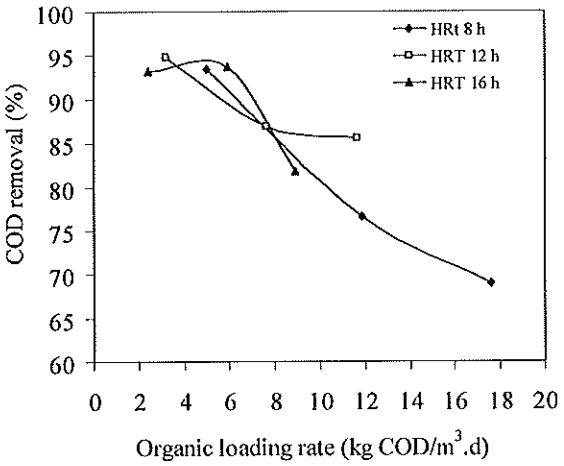

Figure 7.39: Effect of OLR on TCOD removal efficiency at different HRT

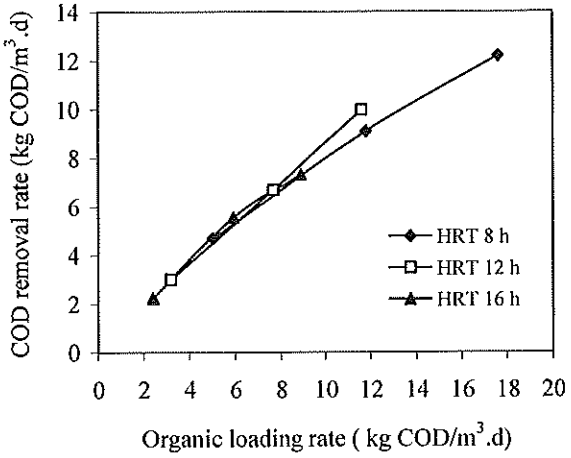

Figure 7.40: Effect of OLR on TCOD removal rate at different HRT

Conversely, the performance of the MS-FFBR system was also estimated in terms of the organic removal (utilization) rates expressed as kg COD/m^3.d. Such a parameter is important in evaluating the effectiveness of the process. Figure 7.40 shows the relationship between the OLR and its removal rate based on TCOD at different HRT, which appears to be linear within the range of OLR studied. It can be seen from Fig.7.40 that the process achieved high COD removal rate as long as the mass transfer limitation for substrate or oxygen were not reached. The TCOD removal rate increased from 2.23 to 12.2 kg TCOD/m^3.d while the OLR increased from 2.4 to 17.6 kg TCOD/m^3.d, which indicated a high reactor capacity. It is clear that no matter how the OLR was varied, the COD removal rate increased with increasing OLR, due to retained high total biomass which increased as the OLR was increased. This coincides with the maximum COD removal attained in the reactor, emphasizing the importance of biomass retention.

Figure 7.41 illustrates the influence of the OLR on the total suspended solid removal efficiency of the final effluent of the MS-FFBR. It was observed that the TSS removal decreased as the OLR increased. The reactor achieved a good performance in terms of total TSS removal efficiency. The figure shows that more than 90% of total TSS removal efficiency was achieved at below OLR of 6 kg TCOD/m^3.d. However, the total TSS removal efficiency deteriorated and decreased significantly with increase OLR. The total TSS removal efficiencies show some variations as the HRT changed. The high total TSS removal efficiency articulated the reduced amount of sloughed biomass, and also was due to low OLR applied to the system, whereas the reduction of TSS removal

efficiency was due to detachment of biomass and increase of the TSS concentration in the final effluent.

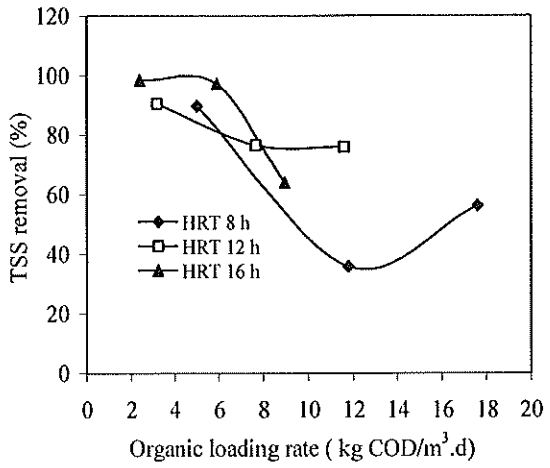

Figure 7.41: Effect of OLR on TSS removal efficiency at different HRT

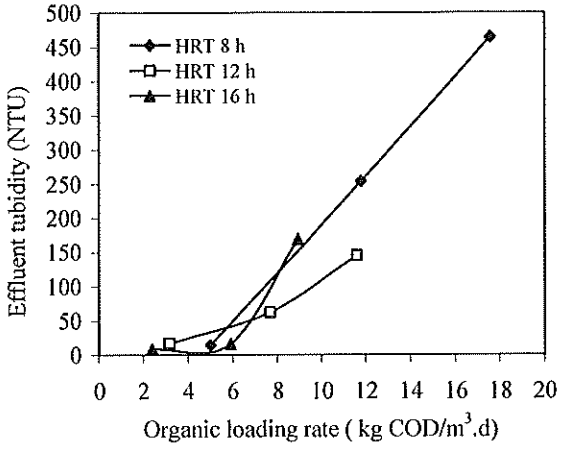

Figure 7.42: Effect of OLR on effluent turbidity at different HRT

Figure 7.42 presents the influence of the OLR on the MS-FFBR effluent turbidity. This turbidity significantly increased as the OLR increased. The reactor achieved low effluent turbidity of ranges from 8.38 to 17 NTU at an OLR of less than 6 kg COD/m^3.d, but increased between 62.4 to 464 NTU as the OLR increased from 7.68 to 17.6 kg COD/m^3.d. It is evident that the increase in the effluent turbidity was attributed to the increase of the suspended solids in the final effluent, which occurred at higher OLRs, and may affect the stability of the attached biomass in the stages. The accumulated biomass on the support media depends on some factors such as oxygen availability which decreased gradually when the OLR increased, substrate nature and concentration, as well as hydraulic shearing and microbial species which influence the attachment of biomass on the flexible fibre. From the figure, it is also clear that the effluent turbidity is affected by the HRT. Low effluent turbidity was produced at 16 h and 12 h HRT, while it increased as HRT decreased to 8 h. Najafpour et al. (2006) confirmed this trend when 46 NTU of effluent turbidity was obtained using a three stage RBC at 40 h HRT.

7.5 Process Analysis and Modelling of the MS-FFBR Treating Raw Milk Processing Wastewater Using Response Surface Methodology

In this part of the study, the performance of the MS-FFBR for the treatment of raw milk processing wastewater was modelled, analysed and optimized with interactive effects of the two independent variables (COD_{in} and HRT) on the reactor responses using Design-Expert software (version 6). In this program, general factorial design was selected. It allows the user to choose factors with different numbers of level. To evaluate the process performance under the above conditions, 8 dependent parameters were either directly measured or calculated as responses. These parameters were total and soluble COD (TCOD and SCOD) removal, total and soluble BOD_5 ($TBOD_5$ and $SBOD_5$) removal, TSS removal, VSS/TSS ratio, effluent pH, effluent turbidity, sludge retention time (SRT) and specific substrate utilization rate (U). The experimental results are shown in Table 7.4.

7.5.1 Statistical Analysis

Table 7.5 shows the obtained analysis of variance (ANOVA) results for all responses. As various responses were investigated in this study, different degrees of a polynomial model were used for data fitting (Table 7.5). In order to quantify the curvature effect, the data from the experimental results were fitted to higher degrees of polynomial equations, i.e. two factor interaction (2FI), quadratic, linear model, etc. In the design expert software, the response data were analysed by default. All raw data are fitted and there was no transformation of data for the responses needed, and applies mathematical functions to all the response data to meet the assumptions, which make the ANOVA to be valid.

Significant model terms are desired to obtain a good fit in a particular model. The selected models terms were those remained after elimination of insignificant variables and their interactions. The interaction term, i.e. AB, was significant for all equations. Based on the statistical analysis, the models were highly significant with very low probability values (from 0.009 to < 0.0001). It is shown that the model terms of independent variables were significant at 95 % confidence level. The quality of the fit polynomial model was expressed by the correlation coefficient R^2. A high R^2 coefficient ensures a satisfactory adjustment of the model to the experimental data. It showed high significant regression at 95 % confidence level.

The model's adequacy was tested through lack of fit F-tests value (Montgomery, 1991). Lack of fit describes the variation of the data around the fitted model. If the model does not fit the data well, this will be significant. It means that if the model shows lack of fit, it should not be used to predict the response (Aghaie et al., 2009). As shown in Table 7.5, the lack of fit results were not statistically significant for all responses as P values were greater than 0.05.

Adequate precision (AP) compares the range of the predicted value at the design points to the average prediction error or, in other words, signal to noise ratio and, was found to be in the range of 7.59-53.30, which indicates an adequate signal. A ratio greater than 4 is generally desirable. In this case, the value is well above 4 (Aghaie et al., 2009; Ghafari et al., 2009; Mason et al., 2003). In addition, the predicted sum of squares (PRESS) is a measure of how a particular model fitted each point in the design (Aghaie et al., 2009). According to data in Table 7.5, the values of adequate precision were found desirable for all models. The coefficient of variance (CV) as the ratio of the standard error of estimates to the mean value of the observed response defines reproducibility of the models. A model normally can be considered reproducible if its CV is not greater than 10% (Ghafari et al., 2009). According to Table 7.5, there were some models which fell short in terms of reproducibility: the models for TSS removal and SRT. Detailed analysis of the models is demonstrated in the following sections.

Table 7.4 : Experimental results of central composite design

Run	Variable		Response										
	Factor 1 A: HRT	Factor 2 B: COD_{in}	COD_{in} average	TCOD removal	SCOD removal	TBOD removal	SBOD removal	TSS removal	Specific substrate utilization rate (U). (Q(S0-S)/X.V)	VSS/TSS ratio of biomass (Suspended + attached) average	Effluent pH	Effluent Turb	SRT
	(h)	(mg/L)	(mg/L)	(%)	(%)	(%)	(%)	(%)	$gCOD_{rem}$/g VSS.L.d			(NTU)	(d)
1	16	3750	3947	93.7	91.8	95	93.9	97.2	0.62	0.94	7.54	16.1	175
2	16	1500	1602	93.2	88.9	94.7	94.4	98.4	0.262	0.94	7.57	8.38	663
3	8	1500	1673	93.5	88.7	95.9	95.8	89.8	0.53	0.8	7.33	14.5	97.5
4	12	1500	1590	94.8	92.9	97.7	97.8	90.5	0.35	0.89	7.5	17	186
5	12	3750	3843	86.9	88	89.3	86.7	76.6	0.72	0.9	7.73	62.4	26.9
6	16	6000	5956	81.8	88.3	84.8	91	64	0.75	0.9	7.58	169	15
7	8	3750	3955	76.6	86.6	75.1	79	35.9	0.95	0.9	7.53	253.7	8
8	12	6000	5827.5	85.6	88.8	89.2	93.8	76	0.97	0.93	7.6	145	16.3
9	8	6000	5869	69	79.1	67.4	78.5	56.2	1.28	0.88	7.36	464	5.49

Table 7.5: ANOVA for response surface models applied

Response	Model type	ANOVA					
		Source	Sum of square	DF	Mean square	F value	Prob>F
TCOD Removal, %	Liner model	Model	485.03	2	242.51	13.78	0.0013
		A	146.03	1	146.03	8.30	0.0164
		B	339.00	1	339.00	19.26	0.0014
		Residual	176.03	10	17.60	-	-
		Lackof fit	156.70	6	26.12	5.40	0.0622
		Pure Error	19.33	4	4.83	-	-
		Cor total	661.06	12	-	-	-
		(R^2=0.7337, Adj. R^2=0.6805, Adeq. Precision=12.354, Std. Dev.=4.20, C.V.=4.86, PRESS=385.63)					
SCOD Removal, %	2FI Model	Model	89.86	3	29.95	7.33	0.0087
		A	35.53	1	35.53	8.69	0.0163
		B	34.08	1	34.08	8.34	0.0180
		AB	20.25	1	20.25	4.95	0.0531
		Residual	36.79	9	4.09	-	-
		Lackof fit	31.99	5	6.40	5.33	0.0650
		Pure Error	7.80	4	1.20	-	-
		Cor total	126.65	12	-	-	-
		(R^2=0.7095, Adj. R^2=0.6127, Adeq. Precision=8.590, Std. Dev.=2.02, C.V.=2.30, PRESS=147.85)					
$TBOD_5$ Removal, %	2FI Model	Model	670.29	3	223.43	9.79	0.0034
		A	217.20	1	217.20	9.52	0.0130
		B	366.60	1	366.60	16.06	0.0031
		AB	86.49	1	86.49	3.79	0.0834
		Residual	205.38	9	22.82	-	-
		Lackof fit	181.26	5	36.25	6.01	.0534
		Pure Error	24.13	4	6.03	-	-
		Cor total	875.68	12	-	-	-
		(R^2=0.7655, Adj. R^2=0.6873, Adeq. Precision=10.441, Std. Dev.=4.78, C.V.= 5.45, PRESS=648.72)					
$SBOD_5$ Removal, %	Reduced quadratic model	Model	363.88	4	90.97	7.07	0.0097
		A	112.67	1	112.67	8.76	0.0182
		B	101.68	1	101.68	7.90	0.0228
		B^2	101.23	1	101.23	7.87	0.0230
		AB	48.30	1	48.30	3.76	0.0886
		Residual	102.91	8	12.86	-	-
		Lackof fit	88.68	4	22.17	6.23	0.0521
		Pure Error	14.23	4	3.56	-	-
		Cor total	466.79	12	-	-	-
		(R^2=0.7795, Adj. R^2=0.6693, Adeq. Precision=7.598, Std. Dev.=3.59, C.V.=4.04, PRESS=622.00)					
TSS Removal, %	Liner model	Model	1829.90	2	914.95	9.36	0.0051
		A	695.53	1	695.53	7.12	0.0236
		B	1134.38	1	1134.38	11.61	0.0067
		Residual	977.31	10	97.73	-	-
		Lackof fit	774.24	6	129.04	2.54	0.1929
		Pure Error	203.07	4	50.77	-	-
		Cor total	2807.21	12	-	-	-
		(R^2=0.6519, Adj. R^2=0.5822, Adeq. Precision=10.325, Std. Dev.=9.89, C.V.=12.84, PRESS=1836.76)					
VSS/TSS Ratio	Reduced 2FI Model	Model	0.010	2	5.133E-003	5.12	0.0294
		A	6.667E-003	1	6.667E-003	6.65	0.0275
		AB	3.600E-003	1	3.600E-003	3.59	0.0873
		Residual	0.010	10	1.003E-003	-	-
			5.026E-003	6	8.376E-004	0.67	0.6856
			5.000E-003	4	1.250E-003	-	-
			0.020	12	-	-	-
		(R^2=0.5059, Adj. R^2=0.4071, Adeq. Precision=8.328, Std. Dev.=0.032, C.V.=3.96, PRESS=0.018)					
Effluent pH	Reduced quadratic model	Model	0.18	3	0.061	12.49	0.0015
		A	0.037	1	0.037	7.58	0.0224
		A^2	0.050	1	0.050	10.36	0.0105
		B^2	0.040	1	0.040	8.18	0.0188
		Residual	0.044	9	4.859E-003	-	-
		Lackof fit	0.027	5	5.371E-003	1.27	0.4195
		Pure Error	0.017	4	4.220E-003	-	-
		Cor total	0.23	12	-	-	-
		(R^2=0.8063, Adj. R^2=0.7418, Adeq. Precision=8.621, Std. Dev.=0.070, C.V.=0.92, PRESS=0.11)					

Table 7.5. (Continued)

Response	Model type	ANOVA					
		Source	Sum of square	DF	Mean square	F value	Prob>F
Effluent Turbidity, NTU	Reduced quadratic model	Model	1.835E+005	4	45879.23	24.85	0.0001
		A	48369.87	1	48369.87	26.20	0.0009
		B	90803.52	1	90803.52	49.18	0.0001
		A^2	23480.60	1	23480.60	12.72	0.0073
		AB	20862.91	1	20862.91	11.30	0.0099
		Residual	14770.83	8	1846.35	-	-
		Lackof fit	14503.44	4	3625.86	54.24	0.0010
		Pure Error	267.39	4	66.85	-	-
		Cor total	1.983E+005	12	-	-	-
		(R^2=0.9131, Adj. R^2=0.9019, Adeq. Precision=28.287, Std. Dev.=1.46, C.V.=1.54, PRESS=102.37)					
SRT, day	2FI Model	Model	3.070E+005	3	1.023E+005	11.78	0.0018
		A	91763.14	1	91763.14	10.56	0.0100
		B	1.379E+005	1	1.379E+005	15.88	0.0032
		AB	77281.22	1	77281.22	8.90	0.0154
		Residual	78181.57	9	8686.84	-	-
		Lack of fit	77479.12	5	15495.82	88.24	0.0004
		Pure Error	702.45	4	175.61	-	-
		Cor total	3.852E+005	12	-	-	-
		(R^2=0.7970, Adj. R^2=0.7294, Adeq. Precision=11.242, Std. Dev.=93.20, C.V.=91.24, PRESS=4.040E+005)					
specific substrate utilization rate (U), g CODrem/g VSS.L.d	Quadratic model	Model	0.82	5	0.16	217.20	< 0.0001
		A	*0.21*	*1*	*0.21*	*280.71*	*< 0.0001*
		B	0.58	1	0.58	761.61	< 0.0001
		A^2	9.181E-003	1	9.181E-003	12.15	0.0102
		B^2	0.013	1	0.013	16.58	0.0047
		AB	0.017	1	0.017	22.72	0.0020
		Residual	5.288E-003	7	7.555E-004	-	-
		Lack of fit	1.968E-003	3	6.561E-004	0.79	0.5591
		Pure Error	3.320E-003	4	8.300E-004	-	-
		Cor total	0.83	12	-	-	-
		(R^2=0.9936, Adj. R^2=0.9890, Adeq. Precision=53.304, Std. Dev.=0.027, C.V.= 3.85, PRESS=0.024)					

7.5.2 Total and Soluble COD Removal Efficiency

A linear model was selected to illustrate the response surface of TCOD removal efficiency within the range of the factors. The following regression equations are the empirical models in terms of coded factors (7.1) for COD removal:

$$\text{COD removal \%} = +86.32 + 4.93\ A - 7.52\ B \qquad (7.1)$$

where A is HRT and B is COD_{in}. The results of ANOVA in Table 7.5 (response: total COD removal) show that the model terms are significant as the model F value was 13.78, which is >4. Other model terms are also significant with a probability value less than 0.05. Figure 7.43 shows the relationship between the experiemental and simulated results of the total COD removal efficiency with relative low value of R^2 = 0.73, indicateing a low agreement between the real data and the data obtained from the model.

The effect of the variables (COD_{in} and HRT) on the TCOD removal efficiency is clearly shown in Figure 7.44 as three-dimensional contour plots for the model with in the design space. It is clear from this figure that the total COD removal decreased

significantly with decreaseing the HRT, and increaseing the COD_{in}. The maximum predicted TCOD removal of 98.77% is achieved at the lowest OLR of 2.40 kg $COD/m^3.d$ (corresponding to the condition of 16 h HRT and the COD_{in} of 1602 mg/L), while the actual value based on the real experimental results was 93.3%. A similar trend was observed by Najafpour et al. (2006). Furthermore, Resmi and Gopalakrishna (2004) achieved 94.58% COD removal efficienct at 2.2 kg $COD/m^3.d$ using aerobic FBBR to treat dairy wastewater.

The lowest TCOD removal efficiency was predicted to be 73.8%, whereas 69% was obtained as an experimental value at the highest OLR of 17.6 kg $TCOD/m^3.d$ (corresponding to HRT of 8 h and COD_{in} of 5869 mg/L). Under these conditions, the OLR applied to the whole system was high, and it caused some organic loading shock in every stage of the reactor. In addition, the potential reason for the poor removal efficiency was perhaps be due to an increase of the OLR, especially in the first stage, which leads to the detachment of many microorganisms from the support media not being able to resist the high load. In the stages two to four, the COD removal at the higher organic loading was much less than in the first stage, and this phenomenon was also found by Hamoda and Abd-Elbary (1987). The interaction shows that both variables (HRT and COD_{in}) were contributing to the reactor TCOD removal efficiency. It is pointed out that the TCOD removal efficiencies obtained at HRT of 16 h using the MS-FFBR (four series of experiments) which range between 83.73-98.77% are similar to the 85.3-97.4% obtained by the three stages RBC system (Najafpour et al., 2006). A similar result was reported by by Hamoda and Abd-Elbary (1987) for treatment of sugar wastewater using aerated submeraged fixed film (ASFF) reactor (88.9-97 %). However, the achieved COD removal of MS-FFBR under the operating conditions described above seemed to be better than those reported in the literature, because the MS-FFBR was using a low HRT and higher OLR.

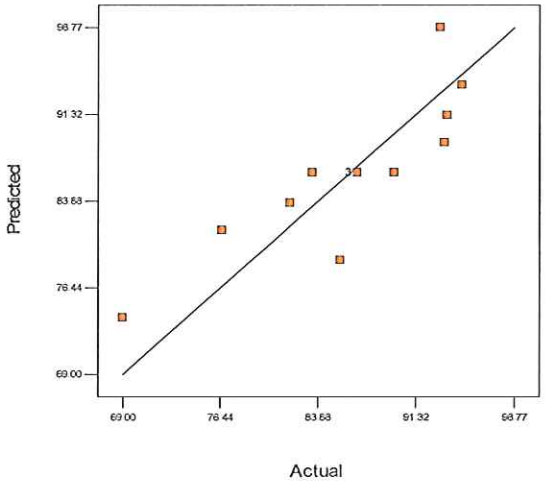

Figure 7.43: Actual versus predicted values of TCOD removal

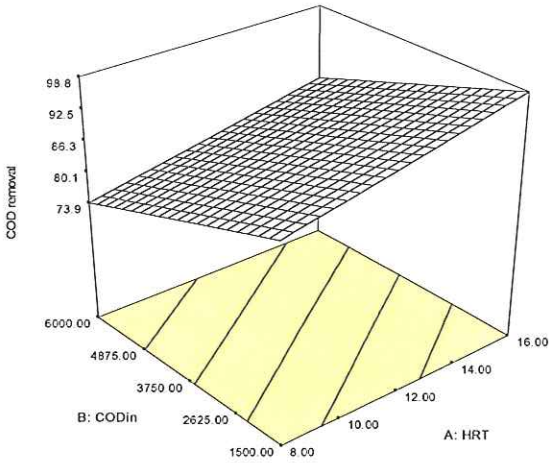

Figure 7.44: Response surface plot for TCOD removal

From the ANOVA (Table 7.5), the two factor interaction models demonstrate that the model was significant as the Fisher F-test (F_{model}, mean square regression / mean square residual = 7.33) with probability value (P=0.0087). The main and two-level interactions of HRT and COD_{in} are significant model terms. The accuracy of the model was checked by the determination coefficient (R^2=0.7095), indicating that 29.05% of the total variation was not described by the model, as R^2 is a ratio of sum square regression to total sum of squares. The value of the adjusted determination coefficienct (adjusted R^2= 0.6127) was moderate. A relatively low value of the coefficienct variation (C.V=2.30) indicated good precision and reliability of the experiments (Kuehl, 2000). The following regression equation is the empirical model in terms of coded factors for SCOD removal and is written as follows:

$$\text{SCOD removal \%} = +88.01 + 2.43A - 2.38\,B + 2.25\,AB \qquad (7.2)$$

Figure 7.45 demonstrates a moderate convergence between the experimental and the predicted values of the SCOD (R^2=0.709). The three dimensional surface and counter plots demonstrate the effect of the variable on SCOD removal efficiency, and are depicted on Figure 7.46. This figure clearly shows that the response increased with increasing HRT and at all COD_{in} studied. At a constant HRT of 16 h, almost constant predicted 90% of SCOD removal efficiency achieved at all range of COD_{in} applied to the system, whereas at a constant HRT of 8 h, the predicted SCOD reduced from 90.21 % to 80.94% as the COD_{in} increased from 1673 to 5869 mg/L. The minimum SCOD removal was modelled to be 80.94%, while its actual value was 79.1%. Such a reduction

was mainly due to the increase in the soluble OLR, which reached 8.88 kg SCOD/m^3.d. During this experiment, the difficulty of reaching high SCOD removal efficiency may be attributed to the nonbiodegrable fraction of COD as the BOD/COD ratio was only 0.58, as two different wastewater samples were collected at two different times, because of a variation of wastewater composition.

In addition, the probable reason is that shorter HRT reduces the time of contact between substrate and biomass, as the liquid residence time inadequacy ultimately affects the SCOD removal percent (Poh and Chong, 2009; Raj and Murthy, 1999). Moreover, low biomass activity also contributed to these results even though a high biomass concentration of 9560 mg/L was obtained. The MS-FFBR achieved a simliar trend at 12 h HRT. In general, the MS-FFBR achieved an excellent 80.94% SCOD removal at high soluble OLR (8.88 kg SCOD/m^3.d) compared with other biofilm reactors, whereas. 90.21% removal was obtained when the soluble OLR reduced to 2.17 kg SCOD/m^3.d. Raj amd Murthy (1999) investigated the treatment of synthetic dairy wastewater using a trickling filter. It was found that SCOD removal decreased with increase in influent COD concentration.

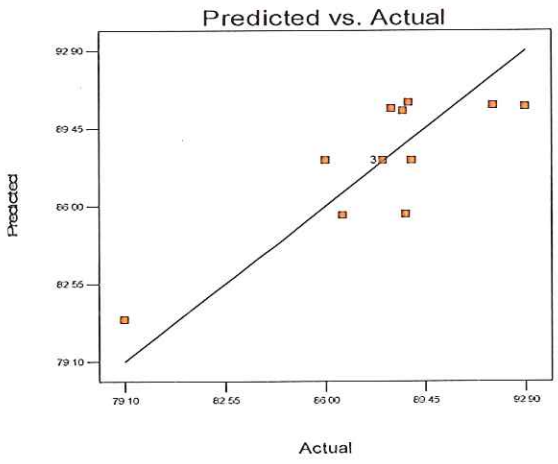

Figure 7. 45: Actual versus predicted values of SCOD removal

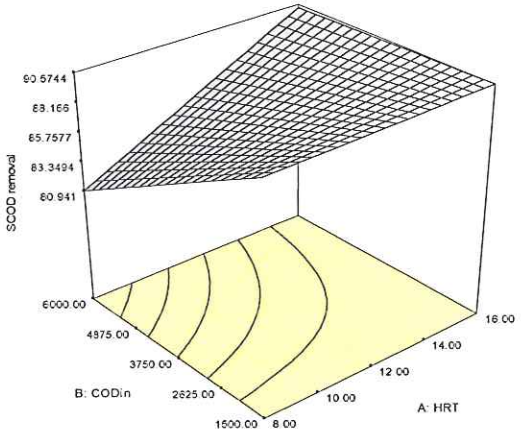

Figure 7.46: Response surface plot for SCOD removal

7.5.3 Total BOD_5 and Soluble BOD_5 Removal Efficiency

A two factor interaction model was selected to describe the response surface for the $TBOD_5$, within the range of factors. The regression equation (built with codified factors) was obtained for the $TBOD_5$ and is written as follows:

Total BOD_5 removal % = +87.68+6.02A -7.82 B + 4.65 AB (7.3)

Two factor interaction models were selected to describe the response surface of removal of $TBOD_5$ within the region (Table 7.5). As seen from the table, the model F-value of 9.79 and a low probability value (Prob> F=0.0034) indicate that the model is significant for $TBOD_5$. The "Adequate Precision" ratio of the model is 10.441, which indicates an adequate signal for the model. The R^2 value of the two fraction interaction model (R^2=0.7655) indicates that only 23.5% of the total variation could not be explained by the empirical model and does not express a good enough fit to navigate the design space, as it should be at least 0.80 for a good fit of a model (Ölmez, 2009).

The correlation between the actual and simulated value of the $TBOD_5$ removal efficiency is shown in Figure 7.47. The R^2 is better compared with other models, therefore, the two-factor interaction model was selected. The observed points on both of these plots reveal that the actual values are distributed relatively near to the straight line. Figure 7.48 illustrates the effect of the factors on the $TBOD_5$ removal efficiency in the original (untransformed) scale. As a general trend, the $TBOD_5$ removal efficiency decreased with decrease in HRT and increase in COD_{in}. Based on the predicted BOD_5 results, it can be seen that there was little variation on the $TBOD_5$ removal efficiency at HRT of 16 h, but it shows a pronounced trend at the HRT of 12 and 8 h. The maximum $TBOD_5$ removal efficiency was predicted to be 96.87 % at HRT of 16 h, while the predicted results at 12 and 8 h HRT showed 95.5 and 94.13%, respectively. However, the actual $TBOD_5$ value shows some fluctuation, and was in the opposite direction of the predicted values. This may due to some experimental errors which may have occurred in the measurement of the $TBOD_5$ test, or it may be due to the way the runs were performed, whereas the experiments of HRT 16 h was conducted at high organic load.

Due to increasing the COD_{in} to 5869 mg/L at HRT of 8 h, the minimum $TBOD_5$ removal efficiency obtained for predicted and actual values were 69.20 and 67.4%, respectively. Low $TBOD_5$ removal efficiency was due to increase of the OLR in each individual stage, which may be caused by an organic load shock loading, and washout of the biomass from the reactor due to the increase of the influent flow rate. Another reason is that at high OLRs with the low BOD_5 to COD ratio, the biomass availability to the biodegradable substrate is restricted, increasing the substrate mass transfer

resistance. From the $TBOD_5$ value in the effluent, it may be concluded that the remaining $TBOD_5$ in the effluent was mostly non-biodegradable.

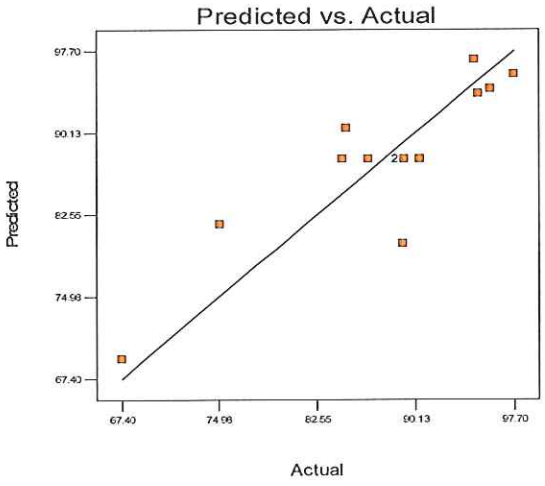

Figure 7.47: Actual versus predicted values of $TBOD_5$ removal

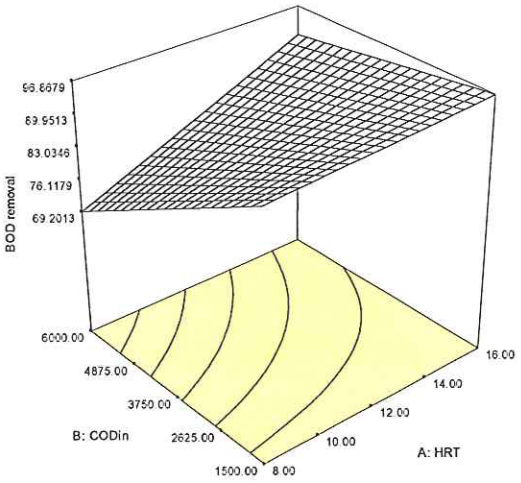

Figure 7.48: Response surface plots for $TBOD_5$ removal

The ANOVA results for $SBOD_5$ response are also presented in Table 7.5. A reduced quadratic regression model was selected to describe the response surface of $SBOD_5$ removal efficiency as a result of changes in the variable factors. The coded regression equation for $SBOD_5$ is presented as follows:

$$SBOD_5 \text{ removal } \% = +86.29+4.33A-4.12B+5.60B^2+3.48AB \quad (7.4)$$

Figure 7.49 shows correlation between predicted and actual values with a correlation coefficient of $R^2=0.7795$. Figure 7.50 shows the response surface graph of model for $SBOD_5$ removal efficiency as a function of HRT (A) and COD_{in} (B). It can be seen from the response plots figure that the predicted responses increase upon increasing the HRT at higher COD_{in} 6000 mg/L. At this influent COD range, the reactor recorded lowest $SBOD_5$ removal efficiency; the reduction $SBOD_5$ is obvious. However, at lower COD_{in} of 1500 mg/L, the trend is showing a slight decrease with increasing HRT. The maximum predicted $SBOD_5$ removal efficiency observed was in the range of 95.14, 96 and 96.86% at HRT of 8, 12 and 16 h, respectively. This indicates that the interaction effect between HRT and COD_{in} played an important role in the reduction of $SBOD_5$, as confirmed by significance test. The high $SBOD_5$ removal efficiency at all HRT revealed that an adequate and stable biofilm was the main reason behind such high removal value and also due to low OLR applied to the reactor, whereas the reactor performance

reduced as the HRT reduced. This may be due to the amount of active biomass being affected by increasing the OLR in the reactor.

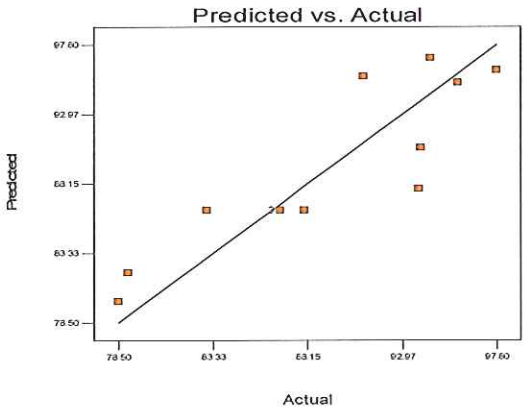

Figure 7.49: Actual versus predicted values of $SBOD_5$ removal

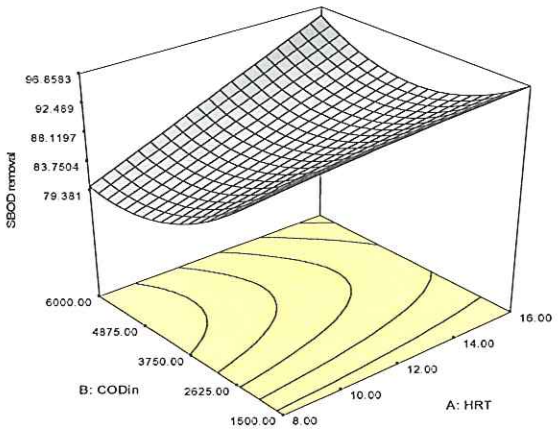

Figure 7.50: Response surface plots for $SBOD_5$ removal

7.5.4 TSS Removal

The ANOVA result of TSS removal efficiency is shown in Table 7.5. A linear model was chosen to show the response surface of TSS removal within the range of the factors. The main effects of the variables HRT (A) and COD_{in} (B) were significant model terms. The accuracy of the model was checked by the determination coefficient (R^2=0.6519), which is low, and indicating that only 34.81 % of the total variation could not be explained by the empirical model and does not show a good fit to the linear model. Adequate precision was found to be 10.325, which is greater than 4, so this model can be used to navigate the design space. The value of the adjusted determination coefficient (Adjusted R^2=0.5822) was low, and this indicates a possible problem with the model or data. The value of coefficient of variation (C.V= 12.84) indicated a moderate precision and reliability of the experiments as it is a bit higher than 10% (Kuehl, 2000). The final regression model in terms of coded factors has been expressed by the following equation (7.5):

$$\text{TSS removal \%} = +76.99+10.77A+13.75B \quad (7.5)$$

The correlation between the predicted versus the actual plot for TSS removal is shown in Figure 7.51. The surface response plot of the linear model for TSS removal efficiency as a function of HRT (A) and COD_{in} (B) is shown in Figure 7.52. A clear influence of the two variables on TSS removal can be seen. A maximum predicted TSS removal was

obtained 101.51%, while the actual value was 98.4% achieved at low COD_{in} of 1602 mg/L and longer HRT of 16 h (corresponding to an OLR of 2.4 kg TCOD/m^3.d). Complete TSS removal could be achieved for lower OLR. However, a minimum predicted 52.48% TSS removal was obtained at shorter HRT of 8 h (corresponding to an OLR of 17.6 kg COD/m^3.d). When the HRT was kept constant at 16 h, TSS removal decreased with increase in the COD_{in}. A similar trend was observed at HRT of 8 h, as the TSS removal efficiency also decreased as the COD_{in} increased, which correspondingly increases the OLR that causes a high amount of food available in the stages and also a high biomass sloughing process. In addition, lower HRT limits the attachment of suspended solids to biofilm. El-Kamah et al. (2010) observed that by increasing the HRT from 30 to 48 h, a high TSS removal can be obtained. The MS-FFBR achieved a better TSS removal than the three stages RBC when canning food wastewater was treated. A maximum of 85.5% was achieved at highest HRT of 48 h, whereas 46% was attained at 40 h (Najafpour et al., 2006). The authors observed that the TSS removal % significantly dropped when the HRT significantly decreased to 30 h. A similar observation was noted by El-Kamah et al. (2010) when fruit juice industry wastewater was treated an using integrated anaerobic and aerobic system.

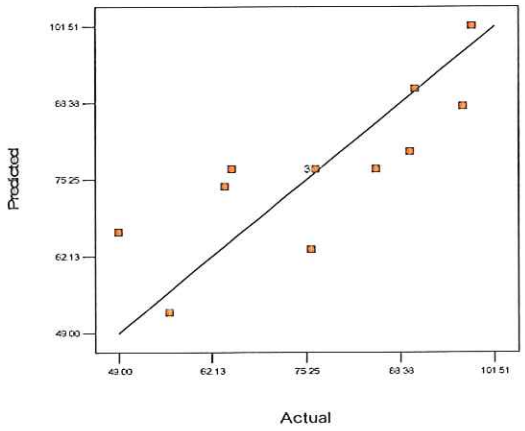

Figure 7.51: Actual versus predicted values of TSS removal

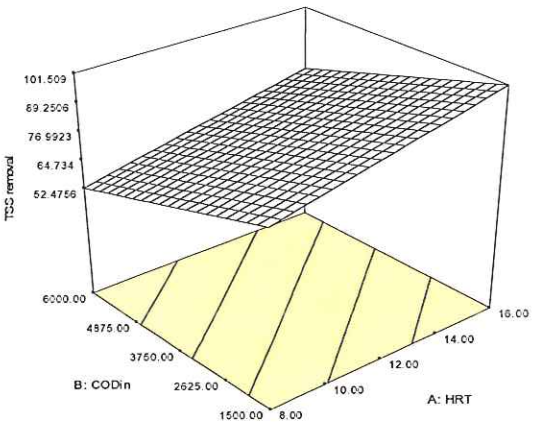

Figure 7.52 : Response surface plot for TSS removal

7.5.5 Effluent pH

As indicated in ANOVA results (Table 7.5), the reduced quadratic regression model was chosen to describe the response surface for effluent pH of MS-FFBR. It demonstrates that the model was highly significant as the Fisher F-test ($F_{model,}$ =12.49) showed very low probability value less than 0.0500. The main and second order effects of COD_{in} and HRT are significant model terms. Other model terms were not significant

with probability value greater than 0.1. The determination of coefficient (R^2= 0.8063) indicates that only 19.37% of the total variation was not explained by the model. For this equation, adequate precision signal–to–noise ratio is greater than 4 (AP=8.621), which is desirable for sound models. A low value of the coefficient of variation (C.V=0.92) pointed out good precision and reliability of the experiments (Kuehl, 2000). The following regression equation (built with codified factors) was obtained for the effluent pH:

$$\text{Effluent pH} = +7.70+0.078A-0.13A^2-0.12B^2 \quad (7.6)$$

The predicted versus the actual plot for effluent pH is illustrated in Figure 7.53. Figure 7.54 demonstrates three-dimensional contour plots of the model for interaction effect of HRT (A) and COD_{in} (B) on the MS-FFBR effluent pH obtained from Equation 7.6. The curvatures of the graph implied that there was a relatively strong interaction between the variables, which was also reflected by the corresponding low P value (0.0015). Both actual and predicated effluent pH at 12 h HRT are nearly similar and observed to be higher pH compared with HRT of 8 and 16 h. The maximum predicted value of effluent pH was 7.70, whereas the actual value was 7.73 observed at 12 h HRT and 3750 mg/L COD_{in}. However, at 3750 mg/L the predicted effluent pH decreased significantly to 7.64 and 7.49 at 16 and 8 h HRT, respectively. The MS-FFBR effluent pH is in the normal range, which indicates the reactor has high buffering capacity.

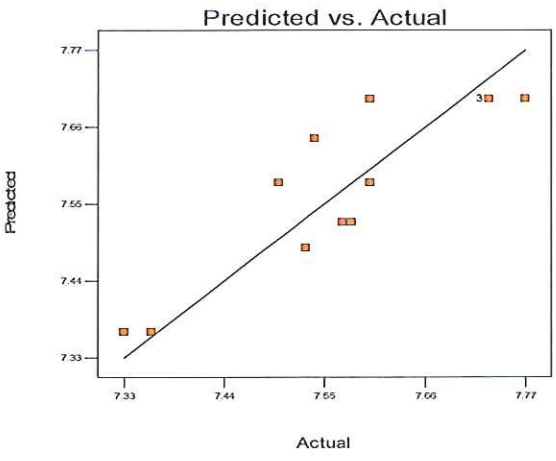

Figure 7.53: Actual versus predicted values of effluent pH

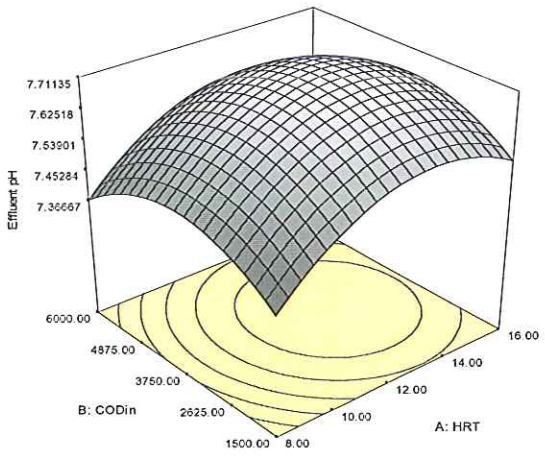

Figure 7.54: Response surface plot for effluent pH

7.5.6 *Effluent Turbidity*

For modelling the interactive effects of the variables (HRT and COD_{in}) on the effluent turbidity as a process response, the following reduced quadratic model (built with codified factors) was obtained:

$$\text{Effluent Turbidity} = +69.03+89.79A+123.02B+85.25A^2+72.22AB \quad (7.7)$$

Figure 7.55 demonstrates a good agreement (R^2=0.9131) between the experimental and predicted values and indicates that 8.69% of the total variation is not explained by the model. The observed points on this plot indicate that the actual values are distributed relatively close to the straight line. Figure 7.56 depicts the effects of the variables on the effluent turbidity. It shows that the effluent turbidity increases with increase of the COD_{in} and decrease of the HRT. It is attributed to the increase in OLR or may also be due to less integrity in the microbial biofilm formed in the reactor. From the figure, it seems that the COD_{in} was the most effective variable on the effluent turbidity as a sharp decrease on the effluent turbidity was observed as the COD_{in} decreased at 8 h HRT. The maximum predicted effluent turbidity of 439.31 NTU was obtained when HRT decreased to 8 h at a high and fixed COD_{in} of 6000 mg/L (corresponding to effluent TSS of 633.3 mg/L), whereas the effluent turbidity was reduced to 192.05 and 115.29 NTU at 12 and 16 h, respectively. This clearly indicates the increase of biomass growth rates at high OLR. The increase of the biomass detachment or biomass washout from the support media was due to increase of the influent flow rate, which led to an increase the suspended solids in the final effluent.

At low range of OLR, a low effluent turbidity produced and it can be seen from the figure as the trend of effluent turbidity at fixed COD_{in} of 1500 mg/L is slightly similar, but increased a little as the HRT was increased to 8 HRT. In the meantime, at this condition the influent TSS content was significantly low where the microorganisms can easily produce a clear effluent, which corresponds to the low effluent turbidity. The low effluent turbidity could be an indication of decrease of the amount of sloughed biomass and that the sludge had good settling property in the settling tank. The results obtained in this study were comparable to and better than the results obtained in literature by Najafpour et al. (2006), where a three stage RBC achieved a minimum effluent turbidity of 46 NTU at 40 h HRT. However, a higher effluent turbidity was achieved at 48 h HRT.

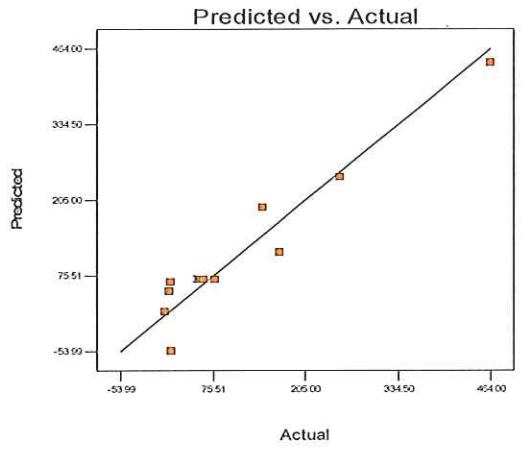

Figure 7.55: Actual versus predicted values of effluent turbidity

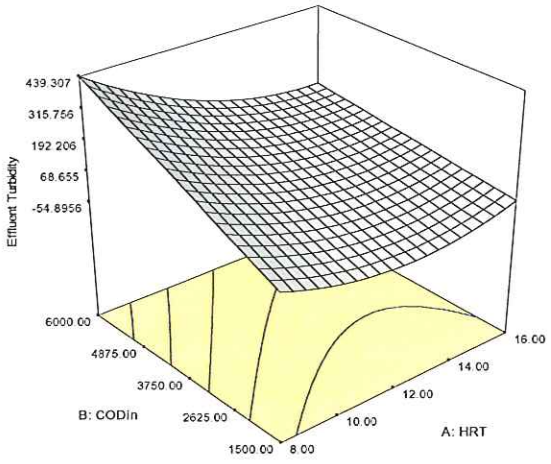

Figure 7.56: Response surface plot for effluent turbidity

7.5.7 SRT

SRT is an important process control parameter, which was evaluated by measuring content of VSS in the reactor and the effluent at various experimental runs. The high SRT values indicate the effective role of packing media on the process stability due to carrying a high amount of biomass, which allows the microorganisms to resist and survive as the OLR changes. The SRT influences the kinds of microorganisms that can grow in the treatment system and the extent to which various reactions will occur. In order to achieve a desirable SRT in the reactor, the rate of sludge wastage must be controlled at a desired value.

The ANOVA results presented in Table 7.5 show that the model was significant. The model was a two factors interaction model (2FI) after elimination of non-significant model terms. The main effect of the variables (A and B), and two-level interactions of HRT and COD_{in} (AB) were also significant model terms. For modelling interactive effects of the variables (HRT and COD_{in}) on the process control response (SRT), the following two factor interaction model (built with codified factors) was obtained:

$$SRT = +102.15+123.67A+151.62B-139.00AB \quad (7.8)$$

A good agreement between the experimental and predicted values of SRT with (R^2=0.7970) was shown in Figure 7.57. The graphical representation of the model Eqs. (7.8) facilitate an examination of the effects of the experimental factors on the responses. The 3D surface graph between the factors was obtained using the Design-Expert software and is presented in Figure 7.58. This figure illustrates that the response

SRT increased with increasing the HRT, and decrease in the COD_{in}. In this situation, it can be clearly observed that the HRT is the most significant variable on SRT. At these conditions, the SRT decreased as the COD_{in} increased to its higher concentration of 6000 mg/L. The actual minimum value of 15 days SRT was obtained, while a predicted negative value of SRT obtained at this condition due to the low actual value of SRT. The maximum actual value of 663 days and predicted value of 516 days were obtained as the COD_{in} reduced to 1500 mg/L. It is essential to guarantee that the biomass in the reactor does not washout with the effluent stream. A longer SRT was maintained due to the attachments of the microorganism into the supported fibre media provided in each stage of the multistage reactor. Conversely, the response was nearly a constant at a constant value of HRT of 8 h with the increase of COD_{in} studied. At an influent COD_{in} of 6000 mg/L, the response is also shown a constant trend as the HRT increased from 8 to 16 h. Therefore, the general decrease on the SRT at low HRT was due to the increase in the feed flow rate. Zinatizadeh et al. (2006) observed a similar trend when treated Palm Oil Mill Effluent (POME) wastewater using an UASB reactor.

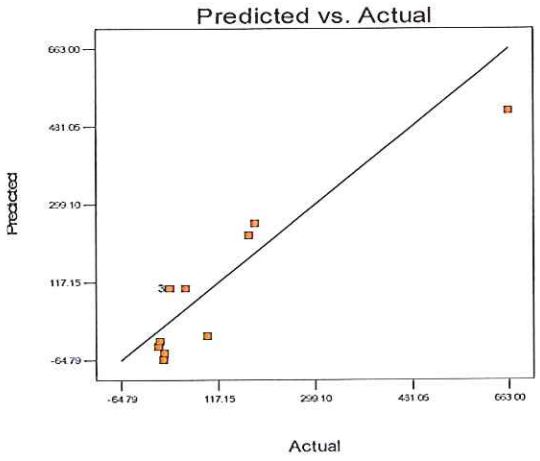

Figure 7.57: Actual versus predicted values of SRT

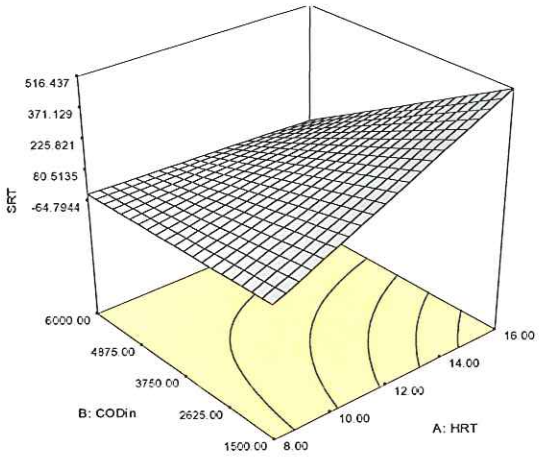

Figure 7.58: Response surface plot for SRT

7.5.8 Specific Substrate Utilization Rate (U)

Analysis of variance (ANOVA) results for the quadratic model are presented in Table 7.5. The quadratic model describes the variation of U as a result of changes in the variables. The following regression equation is the empirical model in terms of coded factors for specific substrate utilization rate:

$$U = +0.72 - 0.19A + 0.31B + 0.058A^2 - 0.067B^2 - 0.065AB \quad (7.9)$$

A good agreement between predicted and actual value of specific substrate utilization rate (U) was obtained with high correlation coefficient (R^2=0.9936) as shown in Figure 6.59. This confirms the adequacy of the model (equations) to predict values for U. The observed points on this plot reveal that the actual values are distributed very close to the straight line and show a significant model. Figure 6.60 illustrates the effect of two variables (HRT and COD_{in}) on the variation of U. It can be seen from the response surface plot that a significant mutual interaction occurs between the variables on specific substrate utilization rate as a response. As noted in the figure, the increase in the specific substrate utilization rate (U) was caused by an increase in COD_{in} and decrease HRT. This may be due to the increase in OLR and biological activity of the microbial population. At HRT of 8 h, the maximum predicted value of U was 1.27 g COD_{rem}/g VSS.L.d, whereas the actual value was 1.28 g COD_{rem}/g VSS.L.d. However, at low COD_{in} and HRT of 16 h, the modelled minimum value of U was 0.28 g COD_{rem}/g VSS.L.d while the actual value was similar at 0.26 g COD_{rem}/g VSS.L.d. Hamoda, (1989) reported a similar observation, as the U increased when substrate concentration significantly increased. It can be observed as a higher COD is applied to the reactor, a higher specific substrate utilization rate is obtained. This indicates that the influent COD concentration applied to the reactor has not achieved its limiting value and shows the ability of the process to handle wide variation in OLR.

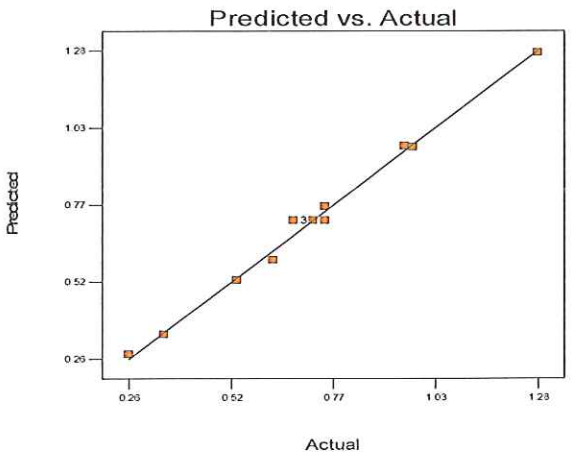

Figure 7. 59: Actual versus predicted values of specific substrate utilization rate

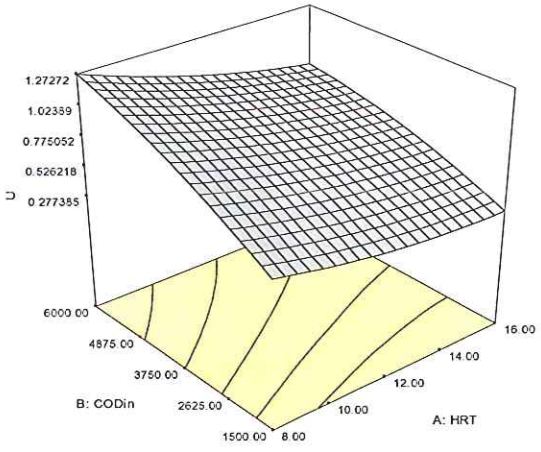

Figure 7.60 : Response surface plot for specific substrate utilization rate

7.5.9 Process Optimization

With multiple responses we need to find regions where requirements simultaneously meet the critical properties, the "sweet spot". The best compromise can be visually searched by superimposing or overlaying critical response contours on a contour plot.

Graphical optimization produces an overlay plot of the contour graphs to display the area of feasible response values in the factor space.

Figure 7.61 shows the graphical optimization which displays the area of feasible response values (shaded portion) in the factors space. The optimum region in this experiment was identified by considering TCOD removal, BOD_5 removal, TSS, pH, SRT, U and safety factor (SF) values greater than those shown in the overlay plot, the adopted criteria of which are shown in Table 7.5. These 6 parameters were chosen as they were considered the most important for reliable representation and optimization of aerobic treatment process. From the plot, as the HRT increases the COD_{in} is also increased, so that, the optimum range of the OLR is found to be between 5.5 and 7.2 kg $COD/m^3.d$.

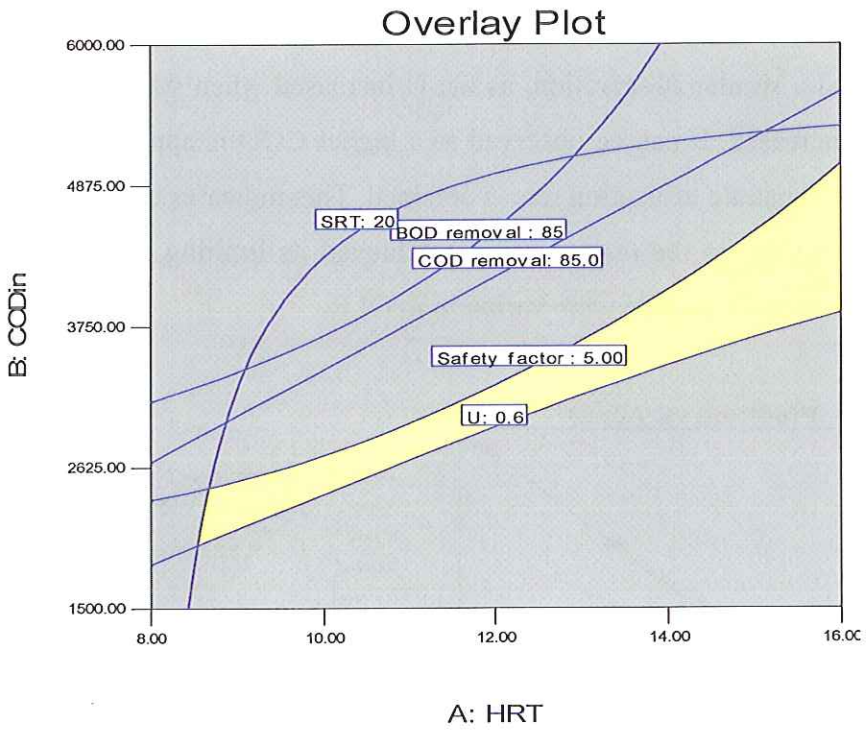

Figure 7.61: Overlay plot for optimal region

For better understanding of the MS-FFBR performance, using the data presented in the previous sections, kinetics evaluation of milk processing wastewater in the MS-FFBR is investigated as described in the following section.

7.6 Kinetics Evaluation of Milk Processing Wastewaters in MS-FFBR

Process kinetics provides a useful technique for predicting the performance of the reactor in order to evaluate COD removal and determine kinetics constants (Raja Priya

et al., 2009). For this purpose the Monod model, first order model, Stover-Kincannon model and others can be used to describe the overall kinetics of biological reactor. The Monod kinetics equation might also be applied for the design of the MS-FFBR. Due to instability of the carbonaceous substrate of the second through to the fourth stages of MS-FFBR, the development of the mathematical model for each stage could be difficult. Therefore, the second through to the fourth stages were considered as one "combined" continuous stirred tank reactor CSTR. This also allowed a comparison of the kinetics coefficient obtained with those obtained in the single stage reactor for treating the milk processing wastewater. The general Monod kinetics model equations which describe the process at steady condition were presented as follows (Metcalf and Eddy, 2003; Zinatizadeh et al., 2009).

The substrate utilization rate in biological systems can be modelled with the following expression for soluble substance:

$$r_{su} = -\frac{dS}{dt} = \frac{kSX}{K_s + S} \tag{7.10}$$

where r_{su} is the rate of change in the substrate concentration due to utilization, g/m^3.d, k is maximum specific substrate utilization rate, g substrate/g microorganisms .d, X is biomass concentration, g/m^3, S is growth-limiting substrate concentration in solution, g/m^3 and K_s is half-velocity constant, substrate concentration at one-half the maximum specific substrate utilization rate, g/m^3.

The biomass growth rate is proportional to the substrate utilization rate by the synthesis yield coefficient, and biomass decay is proportional to the biomass present. When the substrate is being used at its maximum rate, the bacteria are also growing at their maximum rate (Metcalf and Eddy, 2003).

By substituting ($k = \mu_{max}/Y$), Eq. (7.10) becomes:

$$r_{su} = \frac{\mu_{max} XS}{Y(K_s + S)} \tag{7.11}$$

Since the reactor used in this project is an attached biofilm reactor, the equation describing the performance of the system is the mass balance equation for the substrate expressed as COD. The mathematical representation of the substrate mass balance can be written as:

$$\frac{dS}{dt}V = Q_o S_o - QS + r_{su}V \tag{7.12}$$

where Q_o and Q are influent and effluent flow rates, respectively, m^3/d, S_o and S are the influent and effluent substrate concentration, g/m^3, V reactor volume, m^3. By substituting the r_{su} from Eq. 7.11 and assuming steady state conditions ($dS/dt = 0$), Equation 7.13 can be rewritten as:

$$Q_o S_o = QS + \frac{1}{Y}\left(\frac{\mu_{max} SX}{K_s + S}\right) \times V \tag{7.13}$$

where μ_m is maximum specific bacterial growth rate, g new cells/g cells.d, and Y is true yield coefficient, g biomass produced/g substrate consumed.

And also,

$$r_g = \frac{dX}{dt} = -Y\left(\frac{dS}{dt}\right) - K_d X = Y\left(\frac{kSX}{K_s + S}\right) - K_d X \tag{7.14}$$

where K_d, microbial decay rate, d^{-1}. By dividing both sides of Eq. (7.14) by the biomass concentration X, the specific growth rate is defined as follows:

$$\frac{r_g}{X} = \mu = Y\left(\frac{kS}{K_s + S}\right) - K_d \tag{7.15}$$

The specific biomass growth rate (μ, g $VSS_{produced}$/g VSS_{exist}. d) can be defined as the inverse of the solid retention time (SRT) (Metcalf and Eddy, 2003; Zinatizadeh et al., 2009).

$$\frac{1}{SRT} = \frac{(Q - Q_w)X_e + Q_w X_u}{VX} \tag{7.16}$$

Thus, Eq. (6.12) is rearranged as follows:

$$\frac{1}{SRT} = -Y\left(\frac{r_{su}}{X}\right) - K_d = Y\frac{Q(S_o - S)}{VX} - K_d \tag{7.17}$$

where Q and Q_w are influent and waste sludge flow rates, respectively, m^3/d, X, X_e and X_w are biomass concentration in the influent, effluent and settling tank under stream, respectively, g/m^3, V is volume of the reactor, m^3, and $\frac{r_{su}}{X}(U) = Q(S_0 - S)/VX$ is the specific substrate utilization rate, g COD/g VSS.d.

7.6.1 Estimation of the Kinetics Parameters

The experimental data obtained under steady condition on the MS-FFBR system performance in ranges of influent COD concentrations were statically analysed. The experimental data were fitted on a straight line in plot of ($1/SRT$) against specifics substrate utilization rate (U) as in Equation 7.17 and are displayed in Figures 7.62 (A, B and C) to estimates Y and K_d, which was obtained from the slope of the line. In addition, Figure 7.63 (A, B and C) plotted $1/U$ versus $1/S$ to estimate the kinetic coefficients μ_{max}, and K_s based on the average steady-state data. The linear regression analysis of COD data according to the Monod model indicated high corrections at all experimental conditions, thus confirming the applicability of the model. Furthermore, the slopes of the line (K_s/μ_{max}) and the intercepts ($1/\mu_{max}$) were measured to determined the value of K_s and μ_{max}. The results are summarized in Table 7.6. It shows that the yield Y and K_d was lower than those obtained by Bertola et al.,(1999). Other parameters obtained were within the range of the values reported for different industrial wastewaters (Kurian et al., 2006; Orhon et al., 1993).

Table 7.6: Kinetics coefficient estimated COD from MS-FFBR

Model	Kinetics constants	HRT (h)		
		8	12	16
Monod	Y, g VSS/g COD	0.2375	0.0896	0.1083
	μ_{max}, d^{-1}	0.09842	0.0989	0.10021
	K_s, g COD/L	0.13285	0.1588	0.408
	K_d, d^{-1}	0.113	0.0264	0.0341

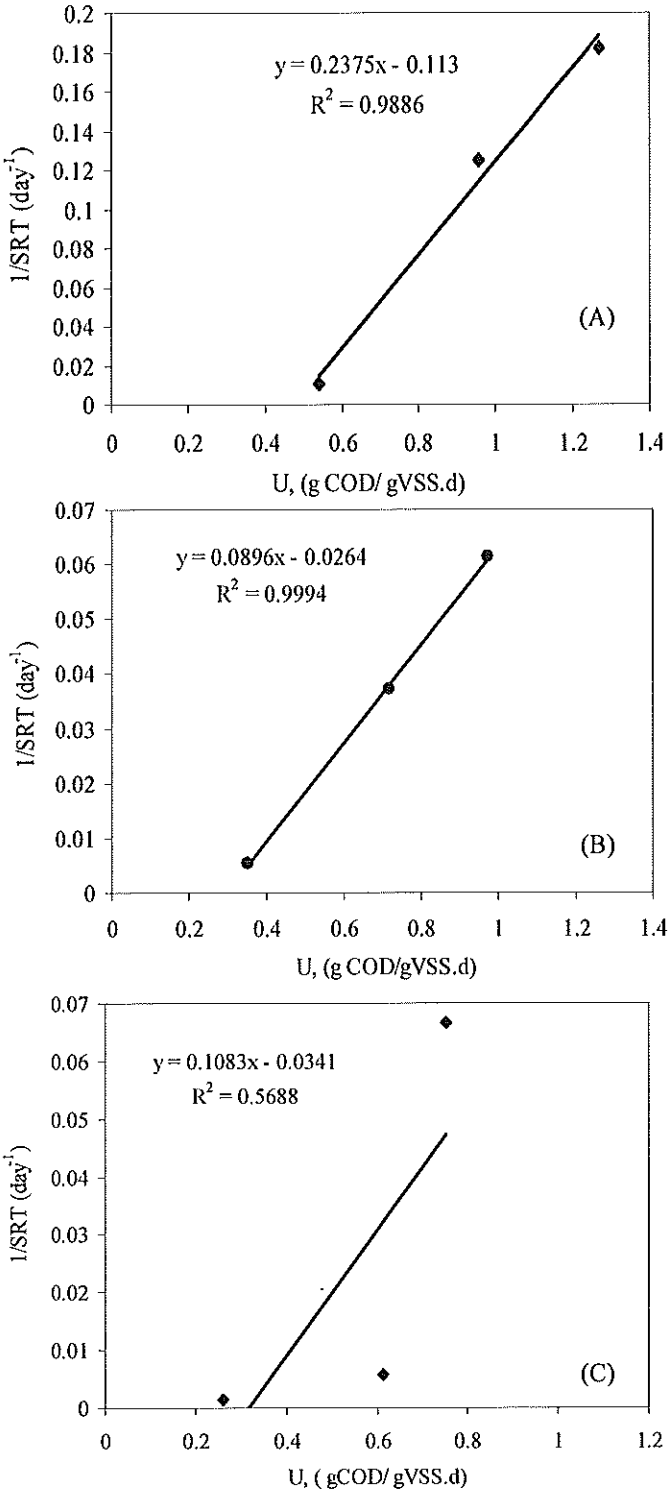

Figure 7.62: Specific microbial growth rate versus at 8 h (A), 12 h (B) and 16 h (C) HRT

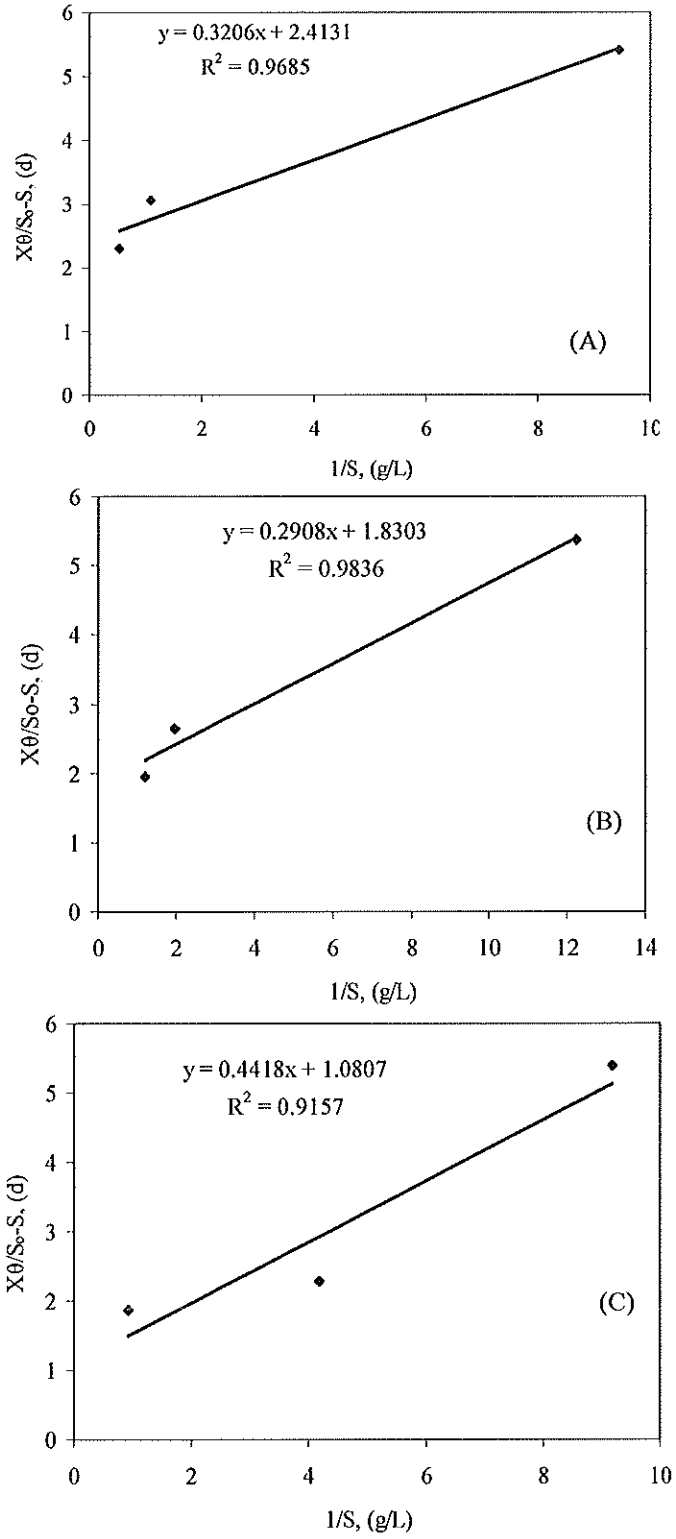

Figure 7.63: Determination of Ks and k based on COD removal at 8 h (A), 12 h (B), and 16 h (C) HRT

7.7 Biofilm Morphology in Reactor Stages

The MS-FFBR unit for wastewater treatment basically assimilates several flexible fibre bundles located on the top, middle and bottom of every stage. These bundles support the growth of the biofilm. However, the wastewater biofilms may be more complex than a simple assemblage of firmly attached bacterial cells. They may posses a thick, overlying, less firmly bound, filamentous bacterial component (Eighmy et al., 1983). Although the biofilms of wastewater treatment systems such as RBC and anaerobic fixed bed reactors has been described by SEM (Alleman et al., 1982; Robinson et al., 1984; Sich and Van Rijn, 1997), examinations of biofilms morphology and structure on flexible fibre biofilm reactors are not present in the literature. Morphological characterizations of biofilm were obtained by SEM technique for the MS-FFBR stages, and are showed in Figures 7.64, 7.65, 7.66 and 7.67 in different magnifications.

In the first stage, scanning electron microscope image of the biofilm is shown in Figure 7.64 (A, B, C and D). Image A depicts a high magnification of 5000X of the biofilm, and a dense biofilm of bacteria cells, seen filling the spaces between fibres. Some fibres are completely encased in the biofilm composed mostly of different type of bacteria, while some fibres show low numbers of adherent bacteria. The bacteria (cocci and short plum rod) were commonly present in this image in different sizes. Image B shows dense clumps of biofilm are seen, mainly between fibres. Most of the fibres in this area show only a few scattered bacteria attached and the fibres are not completely covered by bacteria. Image C clearly showed an extensive growth of visible protozoa (stalked ciliate) organisms with some rod shape bacteria attached to the surface. In addition, as can be seen in the image D, surface grazing nematode species, with a longitudinally furrowed cuticle, and a long fibrous structure with morphology consistent for fungal hyphae, are present within the biofilm.

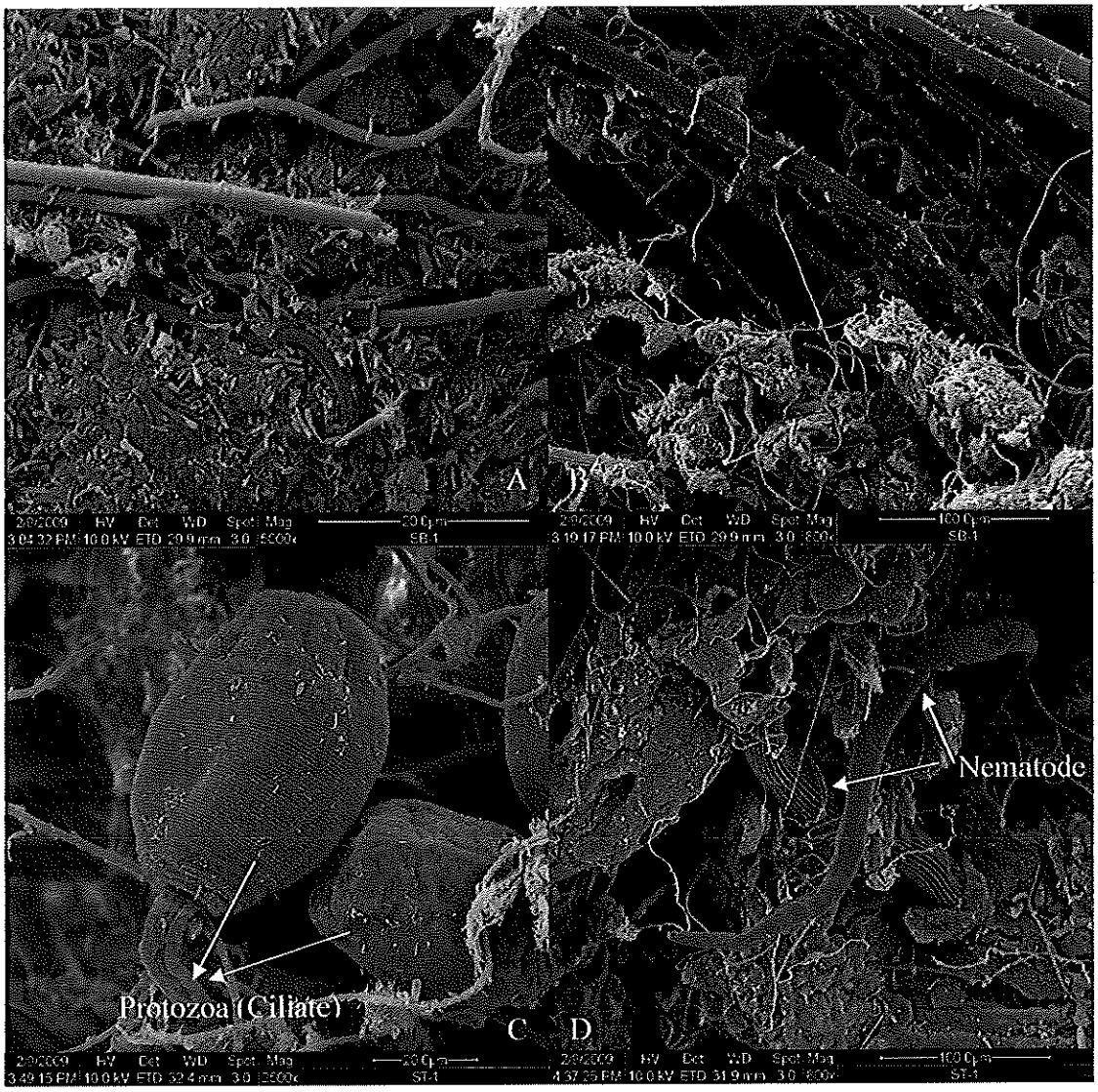

Figure 7.64: Scanning electron microscope images of biofilm in stage 1 of the MS-FFBR

In the second stage, low and high magnifications of the SEM images of biofilm are depicted in Figure 7.65 (A, B, C and D). It can be clearly noted in image A that bacteria are the most dominant organisms with various morphologies (size, shape, cell arrangement) seen in the biofilm, indicating that multiple species/genera of bacteria are present. The large structure seen at the lower right of the image is consistent with the morphology of fungal hyphae. High magnification image B 5000X shows multiple bacterial morphologies, including a long chain of bacilli (centre of field of view). In this region, bacterial cells are seen adhering to the surface of the fibres. In image C, multiple bacterial morphologies are seen, with bacterial cells coating the fibres. The large, smooth walled structure to the right of the image is consistent with the morphology of fungal hyphae. In addition, image D with lower magnification of 400X shows the variability of the biofilm on fibres. Some regions show fibres that are densely coated

with bacterial cells, while in other (adjacent) regions the fibres have very few bacteria attached. Meanwhile, a surface grazing nematode species is also present in this image.

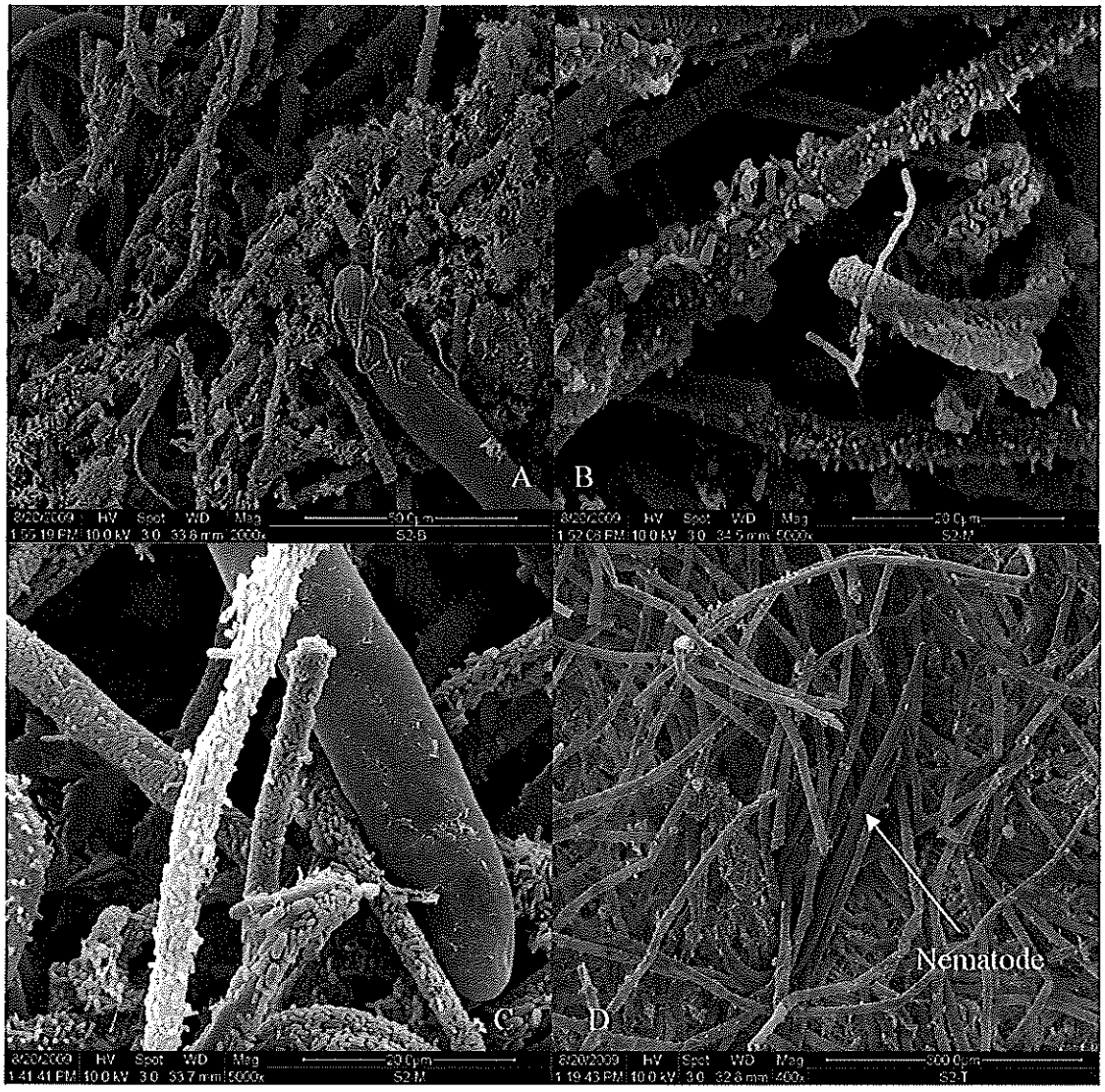

Figure 7.65: Scanning electron microscope images of biofilm in stage 2 of the MS-FFBR

Figure 7.66 (A, B, C, and D) illustrates different magnification range of 1000X to 5000x of the SEM images for flexible fibre biofilm in the third stage of the MS-FFBR. Image A presents a typical distribution of a region dense in biofilm over the flexible fibre surface, with bacteria of different cellular morphology coating the fibres and extending between fibres. Image B shows a very dense population of bacteria, including different sized cells, and different cell shapes, completely coating the fibres, which indicates the uniformity of the distribution of the microorganisms. The different cell morphologies are indicative of a diverse population (different species/genera) of bacteria. Image C shows chains of bacilli (ie. rod-shaped bacterial cells) arranged in a cluster between

fibres. The larger, smooth walled structures are likely to be fungal hyphae. Many bacteria of bacilli species are usually solitary; others associate in characteristic pattern to form diplobacilli and streptobacilli. Image D shows fibres are densely coated with bacteria. Presumptive fungal hyphae have bacteria attached to their surface.

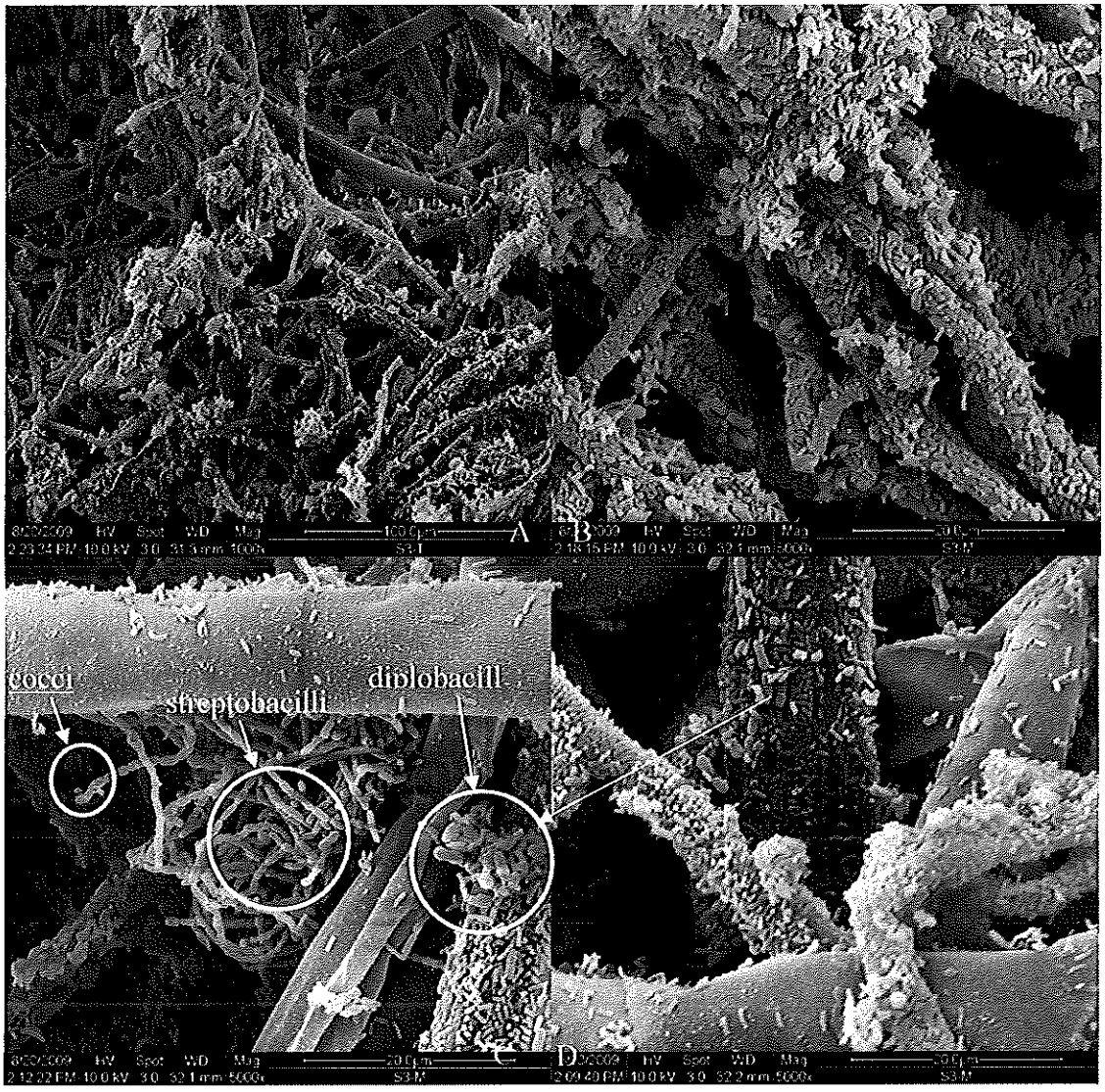

Figure 7.66: Scanning electron microscope images of biofilm in stage 3 of the MS-FFBR

Figure 7.67 depicts the different magnification ranges from 1000x to 10000x of the SEM images for flexible fibre biofilm on the fourth stage of the MS-FFBR. Dense populations of bacteria are seen coating the fibres in image A. Many bacterial cells are arranged in long chains. Image B, a lower magnification image, shows diversity of microorganisms present. Fibres are encased in a dense coating of bacteria, with different bacterial cell morphologies (shape, size, cellular arrangement) indicating different species/genera. Many bacterial cells are arranged in long chains. Smooth walled

structures with rounded ends are consistent with the morphology of fungal hyphae. A nematode with a longitudinally furrowed cuticle is also seen in the middle to upper right of the image. In image C, a region of the sample shows morphology consistent with fungal hyphae, with spores (ovoid structures) at the termini. A high magnification image D shows a diversity of microorganisms in the biofilm: a nematode (upper right), fungal hyphae; and bacterial cells of differing shape, size and cellular arrangement. Bacteria are seen on fibres and on fungal hyphae, as individual cells, in clumps of cells, and in long chains of cells.

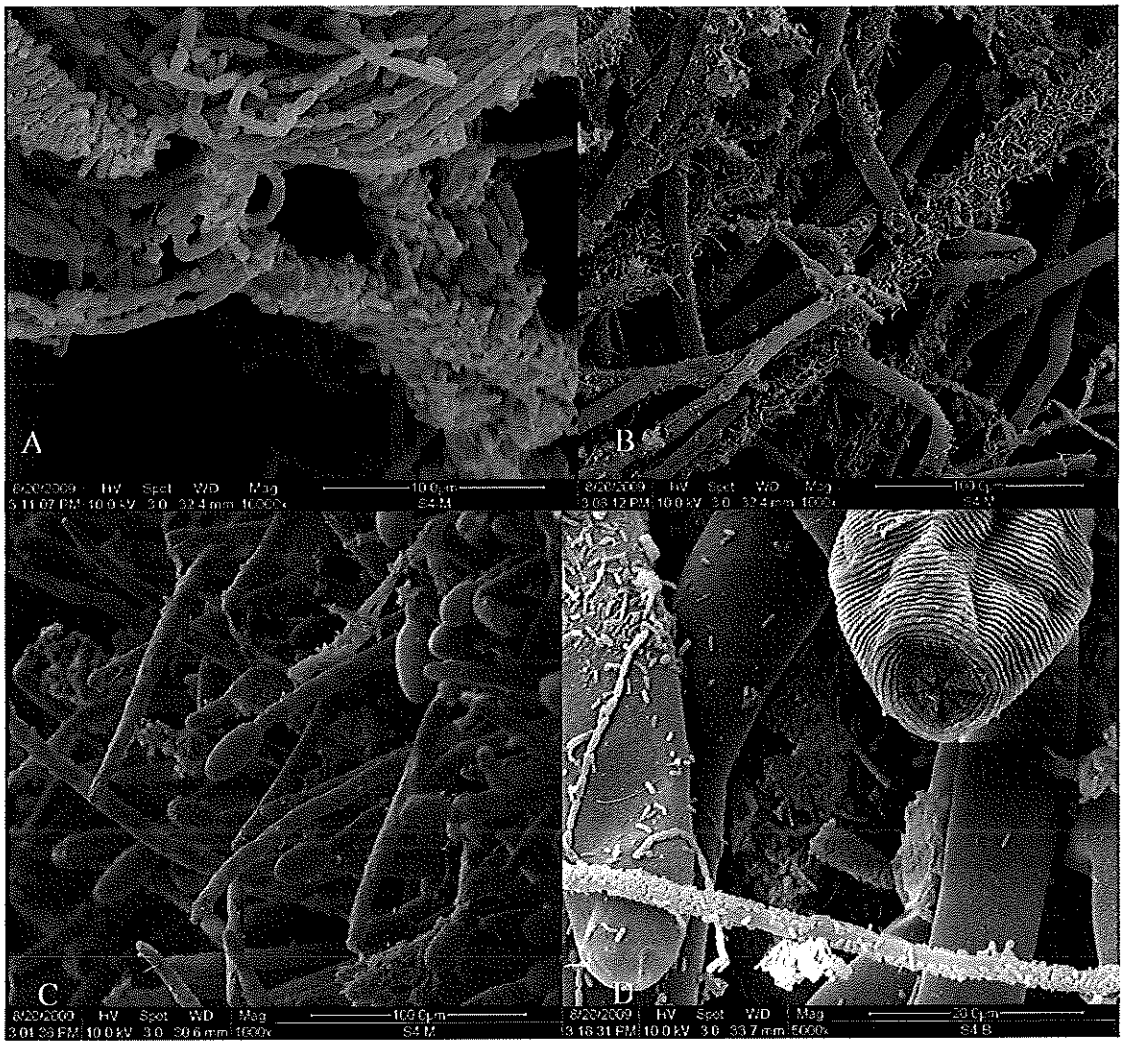

Figure 7.67: Scanning electron microscope images of biofilm in stage 4 of MS-FFBR

The physical structure and formation of the flexible fibre biofilm at different stages were shown above. A comparison can be made and there are no significant differences observed in terms of types of microorganisms attached to the fibre or existing in the biofilm. All stages have similar genes of microorganisms. As regards density of microorganisms, a dramatic increase in biofilm cell density was seen the second, third,

and fourth stages and less in stage one. The fibre in the first stage was not entirely covered by bacteria, but it aggregated in forms of clumps between the fibres which were not observed in the second, third and fourth stages where most of the fibre is covered. As these images were taken from different locations of each stage, it shows that the biofilm in the stage can be uniform. Thus, the above SEM images represent an attempt to define the nature of the flexible fibre biofilm conducted on laboratory environmental condition.

CHAPTER 8 CONCLUSIONS

Laboratory scale flexible fibre biofilm reactors (SB-FFBR, SS-FFBR and MS-FFBR) were successfully developed, fabricated and operated for effective treatment of milk processing wastewater.

The review of different aerobic biological treatment systems conducted in this study showed that both aerobic treatment systems (suspended and attached) are very effective for treatment of various food processing wastewaters. However, attached growth processes are more effective and have better performance with high organic loads. The review concluded that due to the high specific surface area of flexible fibre biofilm reactors (FFBR) there are further advantages when compared with other attached growth biofilm systems. Thus, three types of flexible fibre reactors were experimentally operated for the treatment of milk processing industrial effluent. Based on the results of this study, the following conclusions are drawn.

8.1 Sequencing Batch Flexible Fibre Biofilm Reactor (SB-FFBR)

The use of SB-FFBR was a good strategy and obtained a successful result for the treatment of milk processing wastewater. The reactor incorporated with the novel fibre packing material efficiently achieved a satisfactory performance with high COD and TSS removal efficiency. A maximum of 97.5% and 99.3% of COD and TSS removal efficiency, respectively, were achieved at low OLR of 0.47 kg COD/m^3.d. However, the minimum COD and TSS removal efficiency of 86.8% and 77.3% were achieved with the increase of the OLR to 8.2 kg COD/m^3.d. An inverse relationship was observed between COD and TSS removal efficiencies with respect to OLR. Conversely, a positive relationship was observed between COD and TSS removal rate versus OLR. The influence of SLR on SB-FFBR performance was also evaluated.

The kinetic evaluation of the experimental data of the SB-FFBR was carried out using a first order substrate removal model at different COD concentrations. This model gave a high correlation coefficient, which ranged from 95% to 99%. Therefore, this model could be used in the design of the SB-FFBR. The first order kinetic constant k was 0.60, 0.65 and 0.357 h^{-1} for 500, 810 and 2000 mg COD/L, respectively. The biofilm morphology of the SB-FFBR was studied. The results showed that the use of the flexible fibre as a packing media provided a huge surface area for more microorganism

attachment, so that the used packing media significantly increased the amount of biomass in the reactor, which reached 6970 mg VSS/L.

8.2 Single Stage Flexible Fibre Biofilm Reactor (SS-FFBR)

A good performance of the SS-FFBR was obtained with a high COD removal efficiency of an average 95% at an average low influent COD concentration (809 mg/L). The COD removal was slightly decreased to 91.7% as the influent COD concentration increased to nearly 4000 mg/L. The effect of OLR on the SS-FFBR performance was experimentally studied with some parameters such as TSS removal efficiency, DO and turbidity. The SS-FFBR could increasingly support high OLR, but with a corresponding slight decrease on the COD removal efficiency, even at the highest OLR of 11.7 kg COD/m^3.d, the SS-FFBR achieved a good performance with 89.9% COD removal efficiency. A linear relationship was observed between the OLR and COD removal rate. The rate of COD removal was increased from 1.08 to 10.68 kg COD/m^3.d as the OLR increased from 1.145 to 11.7 kg COD/m^3.d. A 96.7% of TSS removal efficiency obtained at a low OLR of 1.145 kg COD/m^3.d. However, the removal efficiency of TSS declined to 89.7% at maximum OLR of 11.67 kg COD/m^3.d. In addition, both DO and turbidity increased with increase in the OLR.

Response surface methodology was successfully applied to model and analyse the process as well as for determination of the optimum operating conditions. The interactive effects of two studied variables, HRT and COD_{in}, on the process performance were extensively evaluated. The COD removal efficiency increased with increasing the HRT and decreasing the COD_{in}. A significant mutual interaction occurs between the variables and other responses. By applying RSM, the optimum removal was obtained at a HRT of 8 h and COD_{in} 3922 mg/L (corresponding to high OLR of 11.67 kg COD/m^3.d). The experimental findings were in close agreement with model prediction.

8.3 Multistage Flexible Fibre Biofilm Reactor (MS-FFBR)

The residence time distribution characteristics of MS-FFBR for wastewater treatment have been evaluated over a range of HRT involving tracer tests. The results of experiments revealed that the HRT in the MS-FFBR was very close to that of the theoretical value of the C-curve, and also for F-curve especially at 2 h HRT. Therefore, it can be concluded that the flow regime is not affected by the placement of flexible

fibre and the reactor can be described as continuous stirred tank reactor (CSTR) in series model. The oxygen mass transfer coefficient (K_{La}) in the MS-FFBR was obtained using gassing out method correlated with the ratio of air to water flow rate. The results herein showed lower K_{La} compared with those in literature. The presence of the fibre may slow down the oxygen mass transfer due to the interference of the flexible fibre on the size and distribution of the air bubbles.

The performance of the MS-FFBR on the treatment of milk processing wastewater was evaluated based on the contributions of intermediate stages and also final effluent quality of the overall system. The results herein showed that the majority of significant TCOD concentration occurs in the first stage. This stage contributed to remove TCOD up to 89.3, 82.2 and 78 % for HRT of 16, 12, 8 h HRT and COD_{in} of 1602, 1590 and 1673 mg/L, respectively. As the COD_{in} increased and HRT decreased from 16 to 8 h, the first stage contribution significantly decreased from 94.6 to 38.3%. However, the first stage had a lower contribution at high COD_{in} concentrations which were about 42, 46.3 and 25% COD removal at 5956, 5827 and 5869 mg/L, respectively. Conversely, the contribution of the other stages is not as much of the first stage. The results also revealed that there are no significant differences in the TCOD removal efficiency between the second stages to fourth stage. In addition, the TSS effluent concentration was significantly decreased as the stage number increased. The cumulative TCOD and SCOD removal efficiency increased subsequently as the number of stage increased. However, the first and second stages seemed to contribute more efficiently than other stages. The cumulative TCOD improved in the second stage from 91.4 to 87.5% for 16 and 8 h HRT. Increase in the COD_{in} and decreasing the HRT resulted in a gradual increase in the cumulative COD removal, and showed a lower cumulative TCOD removal efficiency of stages. The MS-FFBR was very effective in removing TSS and turbidity.

The overall performance of the MS-FFBR was satisfactory. An inverse relationship between the OLR and the TCOD, TSS, and turbidity was obtained. Conversely, a linear relationship was observed between the OLR and the COD removal rate. A maximum COD removal efficiency of 94.8% obtained at 2.4 kg COD/m^3.d, whereas the COD removal efficiency decreased to 69% at the highest OLR of 17.6 kg COD/m^3.d. Based on the TSS removal, the MS-FFBR achieved more than 90% below OLR of 6 kg COD/m^3.d. However, the TSS removal declined as OLR increased above 6 kg

COD/m^3.d. A similar observation was obtained between the effluent turbidity and OLR. This indicated that the MS-FFBR should be operated at OLR less than 17.6 kg COD/m^3.d in order to have an efficient treatment and good reactor performance.

RSM was also used to evaluate, model and optimize the performance of the MS-FFBR. The effect of variation of the process variables (COD_{in} and HRT) on the system performance was evaluated by measuring different responses (TCOD, SCOD, $TBOD_5$, $SBOD_5$, TSS removal efficiency, turbidity, pH, SRT and U). The predicted TCOD removal efficiency of 98.77% was achieved at 16 h HRT and 1602 mg/L COD_{in}, whereas at COD_{in} of 5869 and HRT of 8 h, the predicted and actual TCOD removal efficiency of 73.8 and 69% was obtained, respectively. At the same time, the removal efficiency of SCOD decreased to 80.94% at soluble OLR of 8.8 kg SCOD/m^3.d. The process performance was also evaluated based on the $TBOD_5$ removal efficiency. A good correlation between the actual and predicted value obtained. The results showed that the $TBOD_5$ removal efficiency decreased with decrease in HRT and increase in COD_{in}. By applying RSM, the optimum range of the OLR was found to be between 5.5 and 7.2 kg COD/m^3.d. The experimental findings were in close agreement with the model prediction.

The Monod kinetic equation was used to determine the performance of the MS-FFBR in the treatment of milk processing wastewater. The kinetic coefficients K_s, K_d, Y and μ_{max}, were found to be 0.133 gCOD/L, 0.113 d^{-1}, 0.237 gVSS/gCOD, 0.098 d^{-1} and 0.158 gCOD/L, 0.026 d^{-1}, 0.089 gVSS/gCOD, 0.098 d^{-1}at 8 h and 0.408 g COD/L, 0.034 d^{-1}, 0.108 gVSS/gCOD, 0.1 d^{-1}, respectively, at 8, 12 and 16 h HRT.

The biofilm morphology of the stages is showed no significant differences in terms of types of microorganisms and the density of microorganism is increased subsequently with stages. Thus, SEM images represent an attempt to define the nature of the flexible fibre biofilm conducted on laboratory environmental condition.

8.4 Comparison of the performance between SB-FFBR, SS-FFBR and MS-FFBR

Generally, SB-FFBR, SS-FFBR and MS-FFBR achieved a high level of performance for the treatment of raw milk processing wastewater. The overall performance of all methods was satisfactory and exhibited a high COD removal efficiency and achieved a high quality effluent particularly at low COD_{in}, despite on the difference on operating

conditions strategies between the flexible fibre reactors such as COD_{in} and HRT. It should be noted that the use of the flexible fibre as a packing media accelerated the time of start-up of the reactors. The SB-FFBR achieved a maximum COD and TSS removal efficiency of 97.5% and 99.3%, respectively, at HRT of 1.6 and 2 days corresponding to OLR of 0.47 kg COD/m^3.d. However, at lowest OLR range between 1.145-2.5 kgCOD/m^3.d, the SS-FFBR achieved a high COD and TSS removal efficiency range between 94-95.5% and 96.7-91.4%. Similarly, MS-FFBR also exhibited a good performance with an overall TCOD and TSS removal efficiency ranges between 93.2-94.8% and 89.8-98.4%, respectively, when the reactor operated at low COD_{in} concentration. The performance of SS-FFBR and MS-FFBR at highest OLR was clearly pronounced and SS-FFBR achieved about 90% of COD removal at 11.7 kgCOD/m^3.d while MS-FFBR achieved only 76.6% at similar OLR of 11.8 kg COD/m^3.d and HRT. Over all performance of MS-FFBR was deteriorated as the OLR increased, and the reactor achieved only 69% of COD removal and low TSS removal efficiency. In terms of the effluent quality, the SS-FFBR and MS-FFBR produced a good effluent quality with low turbidity and TSS concentration compared to SB-FFBR, but at a certain conditions. The microorganism's distributions in all flexible fibre reactors were almost similar, and there was no significant difference between the three reactors in terms of the diversity of microbial species and biomass concentration. The SS-FFBR was easier to operate and monitor than the MS-FFBR.

On the other hand, the SB-FFBR was operated differently from SS-FFBR and MS-FFBR. In the SB-FFBR, it has been observed that during the draw stage, the biomass was separated from the flexible fibre that increases the amount of TSS in the effluent stream, which could be a disadvantage. However, this was not noted at SS-FFBR or MS-FFBR as both were CSTR systems. Both SS-FFBR and MS-FFBR operated with similar HRT but there were large variations in OLRs. Generally, the OLR in each stage of MS-FFBR were 4 times higher than the OLR of SS-FFBR, which may affect the performance of MS-FFBR. The MS-FFBR had a higher performance and more effective in the treatment of wastewater if the reactor was designed into four separate stages.

REFERENCES

Abdulgader, M. E. E., Yu, J., Williams, P., & Zinatizadeh, A. A. L. (2007). *A review of the performance of aerobic bioreactors for treatment of food processing wastewater.* Paper presented at the Proceedings of the International Conference on Environmental Management, Engineering, Planning and Economics, University of Thessaly, Greece.

Achour, M., Khelifi, O., Bouazizi, I., & Hamdi, M. (2000). Design of an integrated bioprocess for the treatment of tuna processing liquid effluents. *Process Biochemistry, 35*, 1013-1017.

Aghaie, E., Pazouki, M., Hosseini, M. R., Ranjbar, M., & Ghavipanjeh, F. (2009). Response surface methodology (RSM) analysis of organic acid production for Kaolin beneficiation by Aspergillus niger. *Chemical Engineering Journal, 147*(2-3), 245-251.

Ahmad, A. L., Ismail, S., & Bhatia, S. (2005). Optimization of Coagulation–Flocculation Process for Palm Oil Mill Effluent Using Response Surface Methodology. *Environmental Science Technology, 39*(8), 2828-2834.

Ahmadi, M., Vahabzadeh, F., Bonakdarpour, B., Mofarrah, E., & Mehranian, M. (2005). Application of the central composite design and response surface methodology to the advanced treatment of olive oil processing wastewater using Fenton's peroxidation. *Journal of Hazardous Materials, 123*(1-3), 187-195.

Ahn, Y.-H., Min, K.-S., & Speece, R. (2001). Pre-acidification in anaerobic sludge bed process treating brewery wastewater. *Water Research, 35*(18), 4267-4276.

Al-Ahmady, K. K. (2005). Effect of Organic Loading on Rotating Biological Contactor Efficiency. *International Journal of Environmental Research and Public Health, 2*(3), 469-477.

Al-Malack, M. H. (2006). Determination of biokinetic coefficients of an immersed membrane bioreactor. *Journal of Membrane Science, 271*(1-2), 47-58.

Alleman, J. E., Veil, J. A., & Canaday, J. T. (1982). Scanning electron microscope evaluation of rotating biological contactor biofilm. *Water Research, 16*(5), 543-550.

Alvarado-Lassman, A., Rustrián, E., García-Alvarado, M. A., Rodríguez-Jiménez, G. C., & Houbron, E. (2008). Brewery wastewater treatment using anaerobic inverse fluidized bed reactors. *Bioresource Technology, 99*(8), 3009-3015.

Amaral, P. F. F., Freire, M. G., Rocha-Leão, M. H. M., Marrucho, I. M., Coutinho, J. A. P., & Coelho, M. A. Z. (2008). Optimization of oxygen mass transfer in a multiphase bioreactor with perfluorodecalin as a second liquid phase. *Biotechnology and Bioengineering, 99*(3), 588-598.

Ana, E., Maurizio, P., Manuela, L., Federico, F., & JoséCardoso, D. (2004). Microbial characterisation of activated sludge in jet-loop bioreactors treating winery wastewaters. *Journal of Industrial Microbiology and Biotechnology, 31*(1), 29-34.

Andreottola, G., ., Foladori, P., Ragazzi, M., & Villa, R. (2002). Dairy wastewater treatment in a moving bed biofilm reactor. *Water Science and Technology, 45*(12), 321-328.

Andreottola, G., Foladori, P., Nardelli, P., & Denicolo, A. (2005). Treatment of winery wastewatre in a full-scale fixed bed biofilm reactor. *Water Science and Technology, 51*(1), 71-79.

Andreottola, G., Foladori, P., Ragazzi, M., & Villa, R. (2002). Treatment of winery wastewater in a sequencing batch biofilm reactor. *Water Science & Technology, 45*(12), 347-354.

Annadurai, G., Ling, L. Y., & Lee, J.-F. (2008). Statistical optimization of medium components and growth conditions by response surface methodology to enhance phenol degradation by Pseudomonas putida. *Journal of Hazardous Materials, 151*(1), 171-178.

APHA. (1995). *Standard methods for the examination of water and wastewater.* Washington, DC.: American public Heath Association.

Apilanez, I., Gutierrez, A., & Diaz, M. (1998). Effect of surface materials on initial biofilm development. *Bioresource Technology, 66*(3), 225-230.

Atkinson, B., Davies, I., & How, S. (1974). The overall rate of substrate uptake by microbial films. *Parts I and II. Trans. Inst. Chem. Eng.*

Australian Dairy. (2007). Australian Dairy Manufacturing Industry Sustainability Report.In http://www.dairyaustralia.com.au/~/media/FEAF16E8D99A4B278544608C11A88300.ashx (Ed.).

Bandpi, A. M., & Bazari, H. (2004). Biological treatment of dairy wastewater by sequencing batch reactor. *Iranian Journal of Environmental Health Science and Engineering, 1*(2), 65-69.

Barr, T. A., taylor, J. M., & Duff, S. J. B. (1996). Effect of HRT, SRT and Temperature on the performance of activated sludge reactors treating bleached kraft mill effluent. *Water Research, 30*(4), 799-810.

Baş, D., & BoyacI, I. H. (2007). Modeling and optimization I: Usability of response surface methodology. *Journal of Food Engineering, 78*(3), 836-845.

Bélanger, D., Bergevin, P., Laperrière, J., & Zaloum, R. (1986). Conception, contrôle et efficacité d'un réacteur biologique séquentiel pour l'épuration des eaux usées d'un abattoir. *Sciences et techniques de l'eau, 19*, 142-156.

Berardino, S. D., Costa, S., & Converti, A. (2000). Semi-continuous anaerobic digestion of a food industry wastewater in an anaerobic filter. *Bioresource Technology, 71*, 261-266.

Bertola, N., Palladino, L., Bevilacqua, A., & Zaritzky, N. (1999). Optimisation of the design parameters in an activated sludge system for the wastewater treatment of a potato processing plant. *Journal of Food Engineering, 40*(1-2), 27-33.

Bloor, J. C., Anderson, G. K., & Willey, A. R. (1995). High rate aeronic treatment of brewery wastewater using the jet loop reactor. *Water Research, 29*(5), 1217-1223.

Borja, R., & Banks, C. J. (1995). Response of an anaerobic fluidized bed reactor treating ice-cream wastewater to organic, hydraulic, temperature and pH shocks. *Journal of Biotechnology, 39*(3), 251-259.

Borja, R., Banks, C. J., & Martin, A. (1995). Influence of the organic volumetric loading rate on soluble chemical oxygen demand removal in a down-flowfixed bed reactor treating abattoir wastewater. *Journal of Chemical Technology and Biotechnology, 64*, 361-366.

Brucculeri, M., Bolzonella, D., Battistoni, P., & Cecchi, F. (2005). Treatment of mixed municipal and winery wastewater in a conventional activated sludge process; a case study. *Water Science & Technology, 51*(1), 89-98.

Bull, M. A., Sterritt, R. M., & Lester, J. N. (1982). The treatment of wastewaters from the meat industry: a review. *Environmental Technology Letters, 3*, 117-126.

Büyükkamaci, N., & Filibeli, A. (2002). Concentrated wastewater treatment studies using an anaerobic hybrid reactor. *Process Biochemistry, 38*, 771-775.

Cassidy, D. P., & Belia, E. (2005). Nitrogen and phosphorus removal from an abattoir wastewater in a SBR with aerobic granular sludge. *Water Research, 39*, 4817-4823.

Cervantes, F. J., Pavlostathis, S. G., & van Haandel, A. C. (2006). *Advanced Biological Treatment Processes for Industrial Wastewaters: Principles and Applications*: IWA Publishing

Chan, Y. J., Chong, M. F., Law, C. L., & Hassell, D. G. (2009). A review on anaerobic-aerobic treatment of industrial and municipal wastewater. *Chemical Engineering Journal, 155*(1-2), 1-18.

Chapra, S. C., & Canale, R. P. (2003). *Numerical Methods for Engineers* (Fourth Ed ed.). New York: McGraw-Hill.

Chen, Y., Yu, J., Xu, H., & Chen, Y. (2009). Oxygen Transfer and Hydrodynamics in a Flexible Fibre Biofilm Reactor for Wastewater Treatment. *Chinese Journal of Chemical Engineering, 17*(5), 879-882.

Chiang, C. F., Lu, C. J., Sung, L. K., & Wu, Y. S. (2001). Full-scale evaluation of heat balance for autothermal thermophilic aerobic treatment of food processing wastewater. *Water Science and Technology, 43*(11), 251-258.

Córdoba, P. R., Riera, F. S., & Siñeriz, F. (1984). Treatment of dairy industry wastewater with an anaerobic filter. *Biotechnology Letters, V6*(11), 753-758.

Crandall, C. J., Kerrigan, J. E., & Rohlich, G. A. (1971). *Nutrient Problem in Meat Industrial wastewater.* Paper presented at the Purdue Industrial Waste Conference Proceeding, Tokyo.

Cronin, C., & Lo, K. V. (1998). Anaerobic treatment of brewery wastewater using UASB reactors seeded with activated sludge. *Bioresource Technology, 64*, 33-38.

Dalzell, J. M. (1994). *Food Industry and the Environment Practical Issues and Cost Implications* (First ed.). London: Blackie Acadamic and Professional, an imprint of Chapman and Hall.

De Oliveira, D. S., Prinholato, A. C., Ratusznei, S. M., Rodrigues, J. A. D., Zaiat, M., & Foresti, E. (2009). AnSBBR applied to the treatment of wastewater from a personal care industry: Effect of organic load and fill time. *Journal of Environmental Management, 90*(10), 3070-3081.

Del Nery, V., de Nardi, I. R., Damianovic, M. H. R. Z., Pozzi, E., Amorim, A. K. B., & Zaiat, M. (2007). Long-term operating performance of a poultry slaughterhouse wastewater treatment plant. *Resources, Conservation and Recycling, 50*(1), 102-114.

Del Pozo, R., Diez, V., & Beltran, S. (2000). Anaerobic pre-treatment of slaughterhouse wastewater using fixed-film reactors. *Bioresource Technology, 71*, 143-149.

Demirel, B., Yenigun, O., & Onay, T. T. (2005). Anaerobic treatment of dairy wastewaters: a review. *Process Biochemistry, 40*, 2583-2595.

Dincer, A. R., & Kargi, F. (2001). Performance of rotating biological disc system treating saline wastewater. *Process Biochemistry, 36*, 901-906.

Dinsdale, R. M., Hawkes, F. R., & Hawkes, D. L. (1996). The mesophilic and thermophilic anaerobic digestion of coffee waste containing coffee grounds. *Water Research, 30*(2), 371-377.

Dinsdale, R. M., Hawkes, F. R., & Hawkes, D. L. (1997). Mesophilic and thermophilic anaerobic digestion with thermophilic pre-acidification of instant-coffee production wastewater. *Water Research, 31*(8), 1931-1938.

Donkin, M. J., & Russell, J. M. (1997). Treatment of a milkpowder/butter wastewater using the AAO activated sludge configuration. *Water Science & Technology, 36*(10), 79-86.

Draper, & Smith. (1998). *Applied Regression Analysis* (Third ed ed.). New York: Wiley.

Droste, R. L. (1997). *Theory and practice of water and wastewater treatment*: John wiley & Sons, Inc.

Duarte, A. C., & Oliveira, F. M. M. (1984). Laboratory study of dairy effluent treatment by the rotating biological disc system. *Environmental Technology, 5*(1), 283 - 288.

Dugba, P. N., & Zhang, R. (1999). Treatment of dairy wastewater with two-stage anaerobic sequencing batch reactor systems -- thermophilic versus mesophilic operations. *Bioresource Technology, 68*(3), 225-233.

Dugba, P. N., Zhang, R., & Dague, R. R. (1997). *Dairy wastewater treatment with a temperature-phased anaerobic sequencing batch reactor system.* Paper presented at the Purdue Industrial waste conference, Chelsea, Michigan.

Eckenfelder, W. W., & Musterman, J. L. (1995). *Activated Sludge Treatment of Industrial Wastewater*. USA: Technomic Publishing Company, Inc.

Eighmy, T. T., Marate, D., & Bishop, P. (1983). Electron Microscopic Examination of Wastewater Biofilm Formation and Structural Components. *Applied and Environmental Microbiology*, 1921-1931.

El-Gohary, F. A., Nasr, F. A., & Aly, H. I. (1999). Cost-effective pre-treatment of food-processing industrial wastewater. *Water Science and Technology, 40*(7), 17-24.

El-Kamah, H., Tawfik, A., Mahmoud, M., & Abdel-Halim, H. (2010). Treatment of high strength wastewater from fruit juice industry using integrated anaerobic/aerobic system. *Desalination, 253*(1-3), 158-163.

El Defrawy, N. M. H., & Shaalan, H. F. (2003). Techno-economic assessment of biological treatment and water reuse of effluent from the food industries. *International Journal of Environmental Studies, 60*(2), 111-122.

Fang, H. H., Jinfu, Z., & Guohua, L. (1989). Anaerobic treatment of brewery effluent. *Biotechnology Letters, II*(9), 673-678.

Fang, H. H. P., & Yeong, C. L. Y. (1993). Biological wastewater treatment in reactors with fibrous packing. *Journal of Environmental Engineering, 119*(5), 946-957.

Frigon, J. C., Breton, J., Bruneau, T., Moletta, R., & Guiot, S. R. (2009). The treatment of cheese whey wastewater by sequential anaerobic and aerobic steps in a single digester at pilot scale. *Bioresource Technology, 100*(18), 4156-4163.

Fumi, M. D., Parodi, G., Parodi, E., Silva, A., & Marchetti, R. (1995). Optimisation of long-term activated-sludge treatment of winery wastewater. *Bioresource Technology, 52*(1), 45-51.

Garrido, J. M., Guerrero, L., Mendez, R., & Lema, J. M. (1998). Nitrification of wastewaters from fish-meal factories. *Water SA, 24*(3), 245-249.

Garrido, J. M., Omil, F., Arrojo, B., Mendez, R., & Lema, J. M. (2001). Carbon and nitrigen removal from a wastewater of an industrial dairy laboratory with a coupled anaerobic filter-sequencing batch reactor system. *Water Science and Technology, 43*(3), 249-256.

Gavala, H. N., Kopsinis, H., Skiadas, I. V., Stamatelatou, K., & Lyberatos, G. (1999). Treatment of dairy wastewater using an Upflow anerobic sludge blanket. *Journal of Agricultural Engineering Research, 73*, 59-63.

Gavrilescu, M., & Macoveanu, M. (1999). Process Engineering in Biological aerobic wastewater treatment. *Acta Biotechnology, 19*(2), 111-145.

Gebara, F. (1999). Activated sludge biofilm wastewater treatment system. *Water Research, 33*(1), 230-238.

Ghafari, S., Aziz, H. A., Isa, M. H., & Zinatizadeh, A. A. (2009). Application of response surface methodology (RSM) to optimize coagulation-flocculation

treatment of leachate using poly-aluminum chloride (PAC) and alum. *Journal of Hazardous Materials, 163*(2-3), 650-656.

Göblös, S., Portöro, P., Bordás, D., Kálmán, M., & Kiss, I. (2008). Comparison of the effectivities of two-phase and single-phase anaerobic sequencing batch reactors during dairy wastewater treatment. *Renewable Energy, 33*(5), 960-965.

Gohil, A., & Nakhla, G. (2006). Performance assessment of a UASB-anoxic-oxic system for the treatment of tomato processing wastes. *Journal of Chemical Technology and Biotechnology, 81*, 927-939.

Gohil, A., & Nakhla, G. (2006). Treatment of tomato processing wastewater by an upflow anaerobic sludge blanket-anoxic-aerobic system. *Bioresource Technology, 97*(16), 2141-2152.

Grabas, M. (2000). Organic matter removal from meat processing wastewater using moving bed biofilm reactors. *Environment Protection Engineering, 26*(1-2), 55-62.

Grady, P. L. J., Daigger, G. T., & Lim, H. C. (1999). *Biological wastewater Treatment* (2nd ed ed.). New York: Marcel Dekker.

Gray, N. F. (2004). *Biology of Wastewater Treatment* (Vol. 4). London: Imperial College Press.

Green, M. G., E.; Beliavski, M.; Lahav, O.; Tarre, S. (2004). Treatment of dairy wastewater using a vertical bed with passive aeration *Environmental Technology, 25*(10), 1123-1129.

Guiot, S. R., & van den Berg, L. (19985). Performance of an Upflow anaerobic reactor combining a sludge blanket and a filter treating sugar waste. *Biotechnology and Bioengineering, 27*, 800-806.

Güven, G., Perendeci, A., & Tanyolaç, A. (2008). Electrochemical treatment of deproteinated whey wastewater and optimization of treatment conditions with response surface methodology. *Journal of Hazardous Materials, 157*(1), 69-78.

Hadjivassilis, I., Gajdos, S., Vanco, D., & Nicolaou, M. (1997). Treatment of wastewater from the potato chips and snacks manufacturing industry. *Water Science and Technology, 36*(2-3), 329-335.

Hamoda, M. F. (1989). Kinetic analysis of aerated submerged fixed-film (ASFF) bioreactor. *Water Research, 23*(9), 1147-1154.

Hamoda, M. F., & Abd-El-Bary, M. F. (1987). Operating characteristics of the aerated submerged fixed film (ASFF) Bioreactor. *Water Research, 21*(8), 939-947.

Hamoda, M. F., & Al-Awadi, S. M. (1995). Wastewater management in a dairy farm. *Water Science and Technology, 32*(11), 1-11.

Hamoda, M. F., & Al-Sharekh, H. A. (1999). Sugar wastewater treatment with aerated fixed-film biological systems. *Water Science and Technology, 40*(1), 313-321.

Hang, Y. D. (2004). Management and Utilization of Food Processing Wastes. *Journal of Food Science, 69*(3), CRH104-CRH107.

Henze, M., Harremoes, P., Jansen, J. C., & Arvin, E. (1995). *Wastewater Treatment: Biological and Chemical Processes*. Germany: Springer-Verlag.

Hiras, D. N., Manariotis, I. D., & Grigoropoulos, S. G. (2004). Organic and nitrogen removal in a two-stage rotating biological contactor treating municipal wastewater. *Bioresource Technology, 93*(1), 91-98.

Hong, C., Hao, H., & Haiyun, W. (2009). Process optimization for PHA production by activated sludge using response surface methodology. *Biomass and Bioenergy, 33*(4), 721-727.

Houbron, E., Torrijos, M., & Moletta, R. (1998). *Application de procede SBR aux effluents vinicoles. Resultats de trois annees de suivi.* Paper presented at the In: 2eme Congres International sur le Traitement des Effluents Vinicoles, Bordeaux, France.

Hu, L.-X., & Liu, Y.-L. (2002). Treatment of wastewater with modified sequencing batch biofilm reactor technology. *Journal of Shanghai University (English Edition), 6*(3), 248-254.

Huang, C. W., & Hung, Y. T. (1987). *Brewery wastewater treatment by contact oxidation process.* Paper presented at the *Procceding of 41st industrial waste conference*, Purdue University, West Lafayette, Indiana.

Huang, J. C., Chang, S. Y., Liu, Y. C., & Jiang, Z. P. (1983). *Growth and activities of fixed films in treating sugar waste.* Paper presented at the *Procceding of 38th industrial waste conference*, Purdue University, West Lafayette.

Idris, A., Kormin, F., & Noordin, M. Y. (2006). Application of response surface methodology in describing the performance of thin film composite membrane. *Separation and Purification Technology, 49*(3), 271-280.

Ince, O. (1998). Performance of a two-phase anaerobic digestion system when treating dairy wastewater. *Water Research, 32*(9), 2707-2713.

Ince, O., Anderson, G. K., & Kasapgil, B. (1994). *Use of the specific methanogenic activity test for controlling the stability and performance in anaerobic digestion of brewery wastewater.* Paper presented at the Proceedings of the 49th Purdue Industrial Waste Conference, Purdue University, Indiana, USA.

Izanloo, H., Mesdaghinia, A., Nabizadeh, R., Nasseri, S., Naddafi, K., Mahvi, A. H., & Nazmara, S. (2006). Effect of organic loading on the performance of aerated submerged fixed-film reactor (ASFFR) for crude oil-containing wastewater treatment. *Iranian Journal of Environmental Health Science and Engineering, 3*(2), 85-90.

Jung, F., Cammarota, M. C., & Freire, D. M. G. (2002). Impact of enzymatic pre-hydrolysis on batch activated sludge systems dealing with oily wastewaters. *Biotechnology Letters, 24*(21), 1797-1802.

Kaewsuk, J., Thorasampan, W., Thanuttamavong, M., & Seo, G. T. (2010). Kinetic development and evaluation of membrane sequencing batch reactor (MSBR) with mixed cultures photosynthetic bacteria for dairy wastewater treatment. *Journal of Environmental Management, 91*(5), 1161-1168.

Kalyuzhnyi, S., Santos, d. l. E., & Martinez, J. R. (1998). Anaerobic treatment for raw and perclarified potato-maize wastewaters in a UASB reactor. *Bioresource Technology, 66*, 195-199.

Kalyuzhnyi, S. V., Martinez, E. P., & Martinez, J. R. (1997). Anaerobic treatment of high-strength cheese-whey wastewater in laboratory and pilot UASB- reactors. *Bioresource Technology, 60*, 59-65.

Kantardjieff, A., & Jones, J. P. (1996). *Aerobic biofilter treatment of slaughterhouse effluent.* Paper presented at the Purdue Industrial Waste Conference, Chelsea, Michigan.

Kargi, F., Dincer, A. R., & Pala, A. (2000). Characterization and biological treatment of pickling industry wastewater. *Bioprocess Engineering, 23*, 371-374.

Ke, S., Shi, Z., & Fang, H. H. P. (2005). Applications of two-phase anaerobic degradation in industrial wastewater treatment. *International Journal of Environmental and pollution, 23*(1), 65-80.

Khuri, A. I., & Cornell, d. J. A. (1996). *response surface: Design and analyses.* New York: Marcel Dekker.

Khuri, A. I., & Cornell, d. J. A. (1996). *Response Surfaces: Design and Analyses* (2nd Edition ed.). New York Marcel Dekker

Kim, B. J., & Molof, A. H. (1982). The scale up and limitation of physical oxygen transfer in rotating biological contactors. *Water Science and Technology, 14*, 569-579.

Körbahti, B. K., Aktas, N., & Tanyolaç, A. (2007). Optimization of electrochemical treatment of industrial paint wastewater with response surface methodology. *Journal of Hazardous Materials, 148*(1-2), 83-90.

Kuehl, R. O. (2000). *Design of Experiments: Statistical Principles of Research Design and Analysis* (second ed ed.). Pacific Grove, CA: Duxbury Press.

Kurian, R., Nakhla, G., & Bassi, A. (2006). Biodegradation kinetics of high strength oily pet food wastewater in a membrane-coupled bioreactor (MBR). *Chemosphere, 65*(7), 1204-1211.

Lazarova, V., & Manem, J. (1995). Biofilm characterization and activity analysis in water and wastewater treatment. *Water Research, 29*(10), 2227-2245.

Lazarova, V., & Manem, J. (2000). Innovative biofilm treatment technologies for water and wastewater treatment. In B. JD (Ed.), *Biofilms II: Process Analysis and Applications* (pp. 159-206). New York: Wiley-Liss.

Leal, K., Chacin, E., Behling, E., Gutierez, E., Fernandez, N., & Forster, C. F. (1998). A mesophilic digestion of brewery wastewater in an unheated anaerobic ilter. *Bioresource Technology, 65*, 51-55.

Lepisto, S. S., & Rintala, J. A. (1997). Start-up operation of Laboratory-scale thermophilic upflow anaerobic sludge blanket reactors treating vegetables processing wastewaters. *Journal of Chemical Technology and Biotechnology, 68*, 331-339.

Lettinga, G., & Hulshoff Pol, L. W. (1991). UASB Process Design for Various Types of Wastewaters. *Water Science and Technology, 24*(8), 87-107.

Levenspile, O. (1992). *Chemical Reaction Engineering*: Jhon Wiley and Sons, Inc.

Li, C. T., Shieh, W. K., Wu, C. S., & Huang, J. S. (1987). Treatment of slaughterhouse wastewater using fluidised bed biofilm reactors. *Water Science & Technology, 19*(1/2), 1-10.

Li, X., & Zhang, R. (2002). Aerobic treatment of dairy wastewater with sequencing batch reactor systems. *Bioprocess Biosystem engineering, 25*, 103-109.

Liu, H., Qin-xue, W., Zhi-qiang, C., & Chun-li, W. (2005). Pilot Test of Jet Loop Bioreactor for Domestic W wastewater Treatment *China Water and Wastewater, 21*(9), 52-53

Liu, V. L., Nakhla, G., & Bassi, A. (2004). Treatability and kinetics studies of mesophilic aerobic biodegradation of high oil and grease pet food wastewater. *Journal of Hazardous Materials, 112*(1-2), 87-94.

Luna-Pabello, V. M., Mayén, R., Olvera-Viascan, V., Saavedra, J., & de Bazúa, c. D. (1990). Ciliated protozoa as indicator of a wastewater treatment system performance. *Biological Waste, 32*, 81-90.

Lunde, S., Feitz, A., Jones, M., Dennien, G., & Morian, M. (2003). Evaluation of the environmental performance of the Australian dairy processing industry using life cycle assessment. *Dairy Research Development Corporation.*

Malina, J. F., & Pohland, F. G. (1992). *Design of anaerobic processes for the treatment of industrial and municipal wastes*. Lancaster: Technomic Pub. Co.

Manjunath, D. L., Mehrotra, I., & Mathur, R. P. (1990). *Treatment of cane sugar mill wastewater in upflow anaerobic sludge blanket (UASB) reactors.* Paper presented at the Procceding of 44st industrial waste conference, Chelsea, Michigan.

Mason , R. L., Gunst Richard F, Hess , J. L., & Hoboken, N. (2003). *Statistical Design and Analysis of Experiments* (2nd ed ed.): Wiley.

Mauldin, A. F., Hemphill, B. W., Soderquist, M. R., Taylor, D. W., & Gerding, E. (1976). *Pilot-scale treatment of brined cherry wastewaters.* Paper presented at the Proceedings of the sixth national symposium on food processing waste.

Mendez, R., Lema, J. M., & Soto, M. (1995). Treatment of seafood processing wastewaters in mesophilic and thermophilic anaerobic filters. *Water Environment Research, 67*(1), 33-45.

Menon, R., & Grames, L. M. (1995). *Pilot testing and development of a full scale carrousel activated sludge system for treating potato processing wastewaters.* Paper presented at the Purdue Industrial Waste Conference Proceedings, Chelsea, Michigan

Metcalf, & Eddy. (1991). *Wastewater Engineering: Treatment, Disposal, Reuse* (Fourth Edition ed.). USA: McGraw-Hill Book Company.

Metcalf, & Eddy. (2003). *Wastewater engineering: Treatment and reuse* (4th ed ed.). New York: McGraw-Hill

Mikkleson, K. A., & Lowery, K. W. (1992). *Designing A sequencing Batch Reractor System for the Treatment of High Strenght Meat processing wastewater.* Paper presented at the Prudue Industrial Waste Conference Processing, Tokyo.

Mittal, G. S. (2006). Treatment of wastewater from abattoirs before land application a review. *Bioresource Technology, 97*, 1119-1135.

Mohan, S., & Sunny, N. (2008). Study on biomethonization of waste water from jam industries. *Bioresource Technology, 99*(1), 210-213.

Montgomery, D. C. (1991). *Design and Analysis of Experiments* (Third Edition ed.). New York: Wiley.

Montgomery, D. C. (2005). *Design and Analysis of Experiments*. New York: Wiley.

Mulkerrins, D., O'Connor, E., Lawlee, B., Barton, P., & Dobson, A. (2004). Assessing the feasibility of achieving biological nutrient removal from wastewater at an Irish food processing factory. *Bioresource Technology, 91*(2), 207-214.

Muthukumar, M., Sargunamani, D., Selvakumar, N., & Venkata Rao, J. (2004). Optimisation of ozone treatment for colour and COD removal of acid dye effluent using central composite design experiment. *Dyes and Pigments, 63*(2), 127-134.

Myers, R. H., & Montgomery, D. C. (1995). *Response surface methodology, process and product optimization using designed experiments* (2nd ed ed.): John Wiley and Sons.

Nadais, H., Capela, I., Arroja, L., & Duarte, A. (2005). Optimim cycle time for intermittent UASB reactors treating dairy wastewater. *Water Research, 39*, 1511-1518.

Najafpour, G., Yieng, H. A., Younesi, H., & Zinatizadeh, A. (2005). Effect of organic loading on performance of rotating biological contactors using Palm Oil Mill effluents. *Process Biochemistry, 40*(8), 2879-2884.

Najafpour, G. D., Naidu, P. N., & Kamaruddin, A. H. (2002). *Rotating biological contactor for biological treatment of poultry processing plant wastewater using Saccharomyces Cerevisiae.* Paper presented at the AJCHE, Malaysia.

Najafpour, G. D., Zinatizadeh, A. A. L., & Lee, L. K. (2006). Performance of a three-stage aerobic RBC reactor in food canning wastewater treatment. *Biochemical Engineering Journal, 30*(3), 297-302.

Nakhla, G., Liu, V., & Bassi, A. (2006). Kinetic modeling of aerobic biodegradation of high oil and grease rendering wastewater. *Bioresource Technology, 97*, 131-139.

Naundorf, E. A., Subramanian, D., Räbiger, N., & Vogelpohl, A. (1985). Biological treatment of waste water in the compact reactor. *Chemical Engineering and processing, 19*(5), 229-233.

Neczaj, E., Kacprzak, M., Kamizela, T., Lach, J., & Okoniewska, E. (2008). Sequencing batch reactor system for the co-treatment of landfill leachate and dairy wastewater. *Desalination, 222*(1-3), 404-409.

Nicolella, C., Loosdrecht, M. C. M. v., & Heijnen, J. J. (2000). Wastewater treatment with particulate biofilm reactors. *Journal of Biotechnology, 80*, 1-33.

Nikolavcic, B., & Svardal, K. (2000). Biological treatment of potato-starch wastewater-design and application of an aerobic selector. *Water Science and Technology, 41*(9), 251-258.

Ochieng, A., Odiyo, J. O., & Mutsago, M. (2003). Biological treatment of mixed industrial wastewater in a fluidised bed reactor. *Journal Hazardous Materials, B96*, 79-90.

Ochieng, A., Ogada, T., Sisenda, W., & Wambua, P. (2002). Brewery wastewater treatment in a fluidised bed bioreactor. *Journal of Hazardous Materials, B90*, 311-321.

Ødegaard, H., Rusten, B., & Westrum, T. (1994). A new moving bed biofilm reactor-application and Results. *Water Science and Technology, 29*(10-11), 157-165.

Oh, S. E., & Logan, B. E. (2005). Hydrogen and electricity production from a food processing wastewater using fermentation and microbial fuel cell technology. *Water Research, 39*, 4673-4682.

Oliva, L. C. H. V., Zaiat, M., & Foresti, E. (1995). Anaerobic reactors for food processing wastewater treatment: established technology and new developments. *Water Science and Technology, 32*(12), 157-163.

Oliveira, G. M., Nogami, E., & Nozaki, J. (2000). Biokinectic parameter investigation and biological treatment of coffee berry effluent. *Bulletin Environmental Contamination and Toxicology, 64*, 771-779.

Ölmez, T. (2009). The optimization of Cr(VI) reduction and removal by electrocoagulation using response surface methodology. *Journal of Hazardous Materials, 162*(2-3), 1371-1378.

Omil, F., Garrido, J. M., Arrojo, B., & Mendez, R. (2003). Anaerobic filter reactor performance for the treatment of complex dairy wastewater at industrial scale. *Water Research, 37*(17), 4099-4108.

Onken, U., & Liefke, E. (1989). Effect of total and partial pressure (oxygen and carbon dioxide) on aerobic microbial processes *Bioprocesses and Engineering* (pp. 137-169).

Orhon, D., Görgün, E., Germirli, F., & Artan, N. (1993). Biological treatability of dairy wastewaters. *Water Research, 27*(4), 625-633.

Palenzuela-Rollon, A., Zeeman, G., Lubberding, H. J., Lettinga, G., & Alaerts, G. J. (2002). Treatment of fish processing wastewater in a one-or two-step upflow anaerobic sludge blanket (UASB) reactor. *Water Science and Technology, 45*(10), 207-212.

Parawira, W., Kudita, I., Nyandoroh, M. G., & Zvauya, R. (2005). A study of industrial anaerobic treatment of opaqe beer brewery wastewater in a tropical climate using a full-scall UASB reactor seeded with activated sludge. *Process Biochemistry, 40*, 593-599.

Petruccioli, M., Duarte, J. C., Eusebio, A., & Federici, F. (2002). Aerobic treatment of winery wastewater using a jet-loop activated sludge reactor. *Process Biochemistry, 37*, 821-829.

Pirsaheb, M., Mesdaghinia, A.-R., Shahtaheri, S. J., & Zinatizadeh, A. A. (2009). Kinetic evaluation and process performance of a fixed film bioreactor removing phthalic acid and dimethyl phthalate. *Journal of Hazardous Materials, 167*(1-3), 500-506.

Poh, P. E., & Chong, M. F. (2009). Development of anaerobic digestion methods for palm oil mill effluent (POME) treatment. *Bioresource Technology, 100*(1), 1-9.

Prasad, P., Pagan, R. J., Kauter, M. D., & Price, N. (2005). Eco-efficiency for the Dairy Processing Industry. *Southbank, Victoria Dairy Australia* 1-153.

Prasertsan, P., Jung, S., & Buckle, K. A. (1994). Anaerobic filter treatment of fishery wastewater. *World Journal of Microbiology and Biotechnology, V10*(1), 11-13.

Punal, A., Mendez, R., & Lema, J. M. (1998). Mutli-fed upflow anaerobic filter: development and features. *Journal of Environmental Engineering, 124*(12), 1188-1192.

Raj, A. S., & Murthy, D. V. S. (1999). Carbon oxidation and nitrification of dairy wastewater in a trickling filter. *Journal of Environmental Science and Health, A34*(6), 1317-1327.

Raj, A. S., & Murthy, D. V. S. (1999). Comparsion of the trickling filter models for the treatment of synthetic dairy wastewater. *Bioprocess Engineering, 21*, 51-55.

Raj, A. S., & Murthy, D. V. S. (1999). Synthetic dairy wastewater treatment using cross flow medium trickling filter. *Journal of Environmental Science and Health, A34*(2), 357-369.

Raja Priya, K., Sandhya, S., & Swaminathan, K. (2009). Kinetic analysis of treatment of formaldehyde containing wastewater in UAFB reactor. *Chemical Engineering Journal, 148*(2-3), 212-216.

Ramasamy, E. V., Gajalakshmi, S., Sanjeevi, R., Jithesh, M. N., & Abbasi, S. A. (2004). Feasibility studies on the treatment of dairy wastewaters with upflow anaerobic sludge blanket reactors. *Bioresource Technology, 93*, 209-212.

Resmi, G., & Gopalakrishna, K. (2004). *Performance studies of aerobic FBBR for the treatment of dairy wastewater.* Paper presented at the 30th WEDC International Conference, Vientiane, Lao PDR.

Rintala, J. A., & Lepisto, S. S. (1997). Pilot-scale thermophilic anaerobic treatment of wastewaters from seasonal vegetable processing industry. *Water Science and Technology, 36*(2-3), 279-285.

Rittman, B. E., & McCarty, P. L. (2001). *Environmental biotechnology : principles and applications* New York: McGraw-Hill.

Robinson, R. W., Akin, D. E., Nordstedt, R. A., Thomas, M. V., & Aldrich, H. C. (1984). Light and Electron Microscopic Examinations of Methane-Producing Biofilms from Anaerobic Fixed-Bed Reactors. *Applied and Environmental Microbiology, 48*(1), 127-136.

Rodgers, M. (1999). Organic carbon removal using a new biofilm reactor. *Water Research, 33*(6), 1495-1499.

Rodgers, M., & Burke, D. (2001). Carbonaceous oxidation using a new vertically moving biofilm system. *Environmental Technology, 22*(6), 673-678.

Rodgers, M., Xiao, L. W., & Mulqueen, J. (2006). Synthetic dairy wastewater treatment using a new horizontal-flow biofilm reactor. *Journal of Environmental Science and Health Part A, 41*, 751-761.

Rodgers, M., Xin-Min, Z., & Angela, C. (2004). Oxygen Transfer and Industrial Wastewater Treatment Efficiency of a Vertically Moving Biofilm System. *Water, Air, & Soil Pollution, V151*(1), 165-178.

Rodgers, M., Zhan, M., & Burke, M. D. (2004). Nutrient removal in a sequencing batch biofilm reactor (SBBR) using a vertically moving biofilm system. *Environmental Technology, 25*, 211-218.

Rodgers, M., & Zhan, X. M. (2003). Moving-Medium Biofilm Reactors. *Reviews in Environmental Science and Biotechnology, V2*(2), 213-224.

Rodgers, M., Zhan, X. M., & Prendergast, J. (2005). Wastewater treatment using a vertically moving biofilm system followed by a sand filter. *Process Biochemistry, 40*(9), 3132-3136.

Ruiz, C., Torrijos, M., Sousbie, P., Martinez, J. L., Moletta, R., & Delgenes, J. P. (2002). Treatment of winery wastewater by an anaerobic sequencing batch reactor. *Water Science and Technology, 45*(10), 219-224.

Rusten, B., Lundar, A., & Thune, L. (1992). *Reliable and high efficiency treatment of potato processing wastewater in cold climate using aerated lagoons with combined precipitation.* Paper presented at the Purdue Industrial Waste Conference Proceedings, Chelsea, Michigan

Rusten, B., Ødegaard, H., & Lundar, A. (1992). Treatment of dairy wastewater in a novel moving bed biofilm reactor. *Water Science and Technology, 26*(3-4), 703-711.

Rusten, B., Siljudalen, J. G., & Strand, H. (1996). Upgrading of a biological--chemical treatment plant for cheese factory wastewater. *Water Science and Technology, 34*(11), 41-49.

Rusten, B., Siljudalen, J. G., Wien, A., & Eidem, D. (1998). Biological pretreatment of poultry processing wastewater. *Water Science and Technology, 38*(4-5), 19-28.

Rusten, B., & Thorvaldsen, G. (1983). Treatment of food industry effluents- Avtivated Sludge versus aerated submerged biological filters. *Environmental Technology Letters, 4*, 441-450.

Saravanane, R., & Murthy, D. V. S. (2000). Application of anaerobic fluidized bed reactors in wastewater treatment : a review. *Environmental Management and Health, 11*(2), 97-117.

Schnell, S., & Mendoza, C. (2004). The condition for pseudo-first-order kinetics in enzymatic reactions is independent of the initial enzyme concentration. *Biophysical Chemistry, 107*(2), 165-174.

Shao, X., Peng, D., Teng, Z., & Ju, X. (2008). Treatment of brewery wastewater using anaerobic sequencing batch reactor (ASBR). *Bioresource Technology, 99*(8), 3182-3186.

Sich, H., & Van Rijn, J. (1997). Scanning electron microscopy of biofilm formation in denitrifying, fluidised bed reactors. *Water Research, 31*(4), 733-742.

Sirianuntapiboon, S., & Prasertsong, K. (2008). Treatment of molasses wastewater by acetogenic bacteria BP103 in sequencing batch reactor (SBR) system. *Bioresource Technology, 99*(6), 1806-1815.

Sirianuntapiboon, S., & Yommee, S. (2006). Application of a new type of moving bio-film in aerobic sequencing batch reactor (aerobic-SBR). *Journal of Environmental Management, 78*(2), 149-156.

Sirianuntapilboon, S., Jeeyachok, N., & Larplai, R. (2005). Sequencing batch reactor biofilm system for treatment of milky industry wastewater. *Journal of Environmental Management, 76*, 177-183.

Sklyar, V., A. Epov, M. Gladchenko, D. Danilovich, & S. Kalyuzhnyi. (2003). Combined biologic (anaerobic–aerobic) and chemical treatment of starch industry wastewater. *Applied Biochemistry and Biotechnology 109* pp. 253–262.

Sokol, W. (2001). Operating parameters for a gas-liquid-solid fluidised bed bioreactor with a low density biomass support. *Biochemical Engineering Journal, 8*(3), 203-212.

Soloman, P. A., Ahmed Basha, C., Velan, M., Balasubramanian, N., & Marimuthu, P. (2009). Augmentation of biodegradability of pulp and paper industry wastewater by electrochemical pre-treatment and optimization by RSM. *Separation and Purification Technology, 69*(1), 109-117.

Sötemann, S. W., Ristow, N. E., Wentzel, M. C., & Ekama, G. A. (2005). A steady state model for anaerobic digestion of sewage sludge. *Water SA, 31*(4), 511-527.

Souza, R. R., Bresolin, I. T. L., Bioni, T. L., Gimenes, M. L., & Dias-Filho, B. P. (2004). The performance of a three-phase fluidized reactor in treatment of wastewater with high organic load. *Brazilian Journal of Chemical Engineering, 21*(2), 1-13.

Su, J. L., & Ouyang, C. F. (1996). Nutrient removal using a combined process with activated sludge and fixed biofilm. *Water Science and Technology, 34*(1-2), 477-486.

Tam, P. C., Lo, K. V., & Bulley, N. R. (1986). Treatment of milking centre waste using sequencing batch reactors. . *Canadian Agricultural Engineering 28* 125-130.

Tawfik, A., Klapwijk, B., El-Gohary, F. A., & Lettinga, G. (2002). Treatment of anaerobically pre-treated domestic sewage by a rotating biological contactor. *Water Research, 36*, 147-155.

Tawfik, A., Sobhey, M., & Badawy, M. (2008). Treatment of a combined dairy and domestic wastewater in an up-flow anaerobic sludge blanket (UASB) reactor followed by activated sludge (AS system). *Desalination, 227*(1-3), 167-177.

Tay, J.-H., & Zhang, X. (2000). A fast predicting neural fuzzy model for high-rate anaerobic wastewater treatment systems. *Water Research, 34*(11), 2849-2860.

Torkian, A., Hashemian, S. J., & Alinejad, K. (2003). Posttreatment of upflow anaerobic sludge blanket-treated industrial wastewater by a rotating biological contactor. *Water Environment Research, 75*(3).

Torrijos, M., & Moletta, R. (1997). Winery wastewater depollution by Sequencing Batch Reactor. *Water Science and Technology, 35*(1), 249-257.

Torrijos, M., Sousbie, P., Moletta, R., & Delgenes, J. P. (2004). High COD wastewater treatment in an aerobic SBR: treatment of effluent from a samll farm goat's cheese dairy. *Water Science and Technology, 50*(10), 259-267.

Tsang, Y. F., Hua, F. L., Chua, H., Sin, S. N., & Wang, Y. J. (2007). Optimization of biological treatment of paper mill effluent in a sequencing batch reactor. *Biochemical Engineering Journal, 34*(3), 193-199.

Tyagi, R., & Vembu, K. (1990). *Wastewater Treatment by Immobilized Cells*: CRC, Boca Raton.

USEPA. (1993). Nitrogen removal. Pennsylvania, USA: Technomic Publishing Company.

van Haandel, A. C., & Lettinga, G. (1994). *Anaerobic sewage treatment: a practical guide for regions with a hot climate*. Chichester: John Wiley and Sons.

Vanhooren, H., Yuan, Z., & Vanrolleghem, P. A. (2002). Benchmarking nitrogen removal suspended-carrier biofilm systems using dynamic simulation. *Water Science and Technology, 46*(1-2), 327-332.

Vegt, A. d., & Vereijken, T. (1992). *Eight year full-scale experience with anaerobic treatment of potato processing effluent.* Paper presented at the Purdue Industrial Waste Conference Proceedings, Chelsea, Michigan

Veiga, M. C., Mendez, R., & Lema, J. M. (1992). *Treatment of tuna oricessing wastewater laboratory and pilot scale DSFF anaerobic reactors.* Paper presented at the Purdue Industrial Waste Conference Proceedings, Chelsea, Michigan.

Veiga, M. C., Mendez, R., & Lema, J. M. (1992). *Treatment of tuna processing wastewater laboratory and pilot scale DSFF anaerobic reactors.* Paper presented at the Purdue Industrial Waste Conference Proceedings, Chelsea, Michigan.

Veiga, M. C., Pan, M., Blazquez, R., Mendez, R., & Lema, J. M. (1994). A double-feed anaerobic filter for the treatment of high strength wastewaters. *Biotechnology Techniques, 8*(2), 77-82.

Vriens, L., Eynde, E., Van den., & Verachtert, H. (1983). Parameters affecting protein production from wrewrey wastewater in a multi-channel laboratory scale activated sludge system. *European Journal of Applied Microbiology and Biotechnology, 18*, 52-59.

Wallis, D., Brook, P., & Thompson, C. (2007). Water sustainability in the Australian food processing industry. *Australian Food Statistics*, 27-34.

Wang, S.-G., Liu, X.-W., Gong, W.-X., Gao, B.-Y., Zhang, D.-H., & Yu, H.-Q. (2007). Aerobic granulation with brewery wastewater in a sequencing batch reactor. *Bioresource Technology, 98*(11), 2142-2147.

Wang, S., Chandrasekhara Rao, N., Qiu, R., & Moletta, R. (2009). Performance and kinetic evaluation of anaerobic moving bed biofilm reactor for treating milk permeate from dairy industry. *Bioresource Technology, 100*(23), 5641-5647.

Wilson, F. (1997). Total organic carbon as a predictor of biological wastewater treatment efficiency and kinetic reaction rates. *Water Science and Technology, 35*(8), 119-126.

Wilson, F., Hamoda, M. F., Islam, H., & Buranasin, P. (1988). The treatment of high strength vegetable pickling waste using the RBC process. *Environmental Technology Letters, 9*, 1201-1212.

Witherow, J. L. (1973). *Small meat- packing waste treatment systems.* Paper presented at the Purdue industrial waste, Tokyo.

Wu, S., Yu, X., Hu, Z., Zhang, L., & Chen, J. (2009). Optimizing aerobic biodegradation of dichloromethane using response surface methodology. *Journal of Environmental Sciences, 21*(9), 1276-1283.

Xu, H., Yu, J., & Williams, P. (2001). *A comparative study of flexible fibre biofilm reactors with conventional activated sludge process for wastewater treatment.* Paper presented at the Proc. of AWA Qld. Regional Conference.

Xu, H., & Yu, Q. (2000, July 9-12). *Review of methods of biological treatment of food processing wastewater.* Paper presented at the Australian Chemical Engineering Conference (chemeca'2000), Perth, Australia.

Xue, Q., Zhi-qiang, W., & Bing-nan, L. C. (2004). Sanitary Sewage Treatment with Jet Inner-loop Bioreactor. *WUHAN UNIVERSITY JOURNAL OF NATURAL SCIENCES, 9*(3), 388-394

Xue, Q. W., Chen, Z., Lu, B.-N., & Yan, W. (2004). Treatment of synthetic brewery wastewater in j et inner-loop reactor *Journal of Harbin Industrial University.*

Yang, K., Yu, Y., & Hwang, S. (2003). Selective optimization in thermophilic acidogenesis of cheese-whey wastewater to acetic and butyric acids: partial acidification and methanation. *Water Research, 37*(10), 2467-2477.

Yu, H.-Q., Zhao, Q.-B., & Tang, Y. (2006). Anaerobic treatment of winery wastewater using laboratory-scale multi- and single-fed filters at ambient temperature. *Process Biochemistry.*

Yu, H. Q., Hu, Z. H., Hong, T. Q., & Gu, G. W. (2002). Performance of an anaerobic filter treating soybean processing wastewater with and without effluent recycle. *Process Biochemistry, 38*, 507-513.

Yu, H. Q., Zhao, Q.-B., & Tang, Y. (2006). Anaerobic treatment of winery wastewater using laboratory-scale multi- and single-fed filters at ambient temperature. *Process Biochemistry.*

Yu, J., Xu, H., & Chen, Y. (2006). *Hydrodynamics and oxygen mass transfer in a flexible fibre biofilm reactor for wastewater treatment.* Paper presented at the Proceedings of 11th Asian Pacific Confederation of Chemical Engineering Congress.

Yu, Q. J., Xu, H., & Williams, P. (2003). Development of Flexible Fibre Biofilm Reactor for Treatment of Food Processing Wastewater *Environmental Technology, 24*(4), 429-434.

Yu, Q. J., Xu, H., Yao, D., & Williams, P. (2003). Development of a two-stage flexible fiber biofilm reactor for treatment of food processing wastewater. *Water Science and Technology, 47*(11), 189-194.

Zhao, H.-Z., Cheng, P., Zhao, B., & Ni, J.-R. (2008). Yellow ginger processing wastewater treatment by a hybrid biological process. *Process Biochemistry, 43*(12), 1427-1431.

Zinatizadeh, A. A. L., Mohamed, A. R., Abdullah, A. Z., Mashitah, M. D., Hasnain Isa, M., & Najafpour, G. D. (2006). Process modeling and analysis of palm oil mill effluent treatment in an up-flow anaerobic sludge fixed film bioreactor using response surface methodology (RSM). *Water Research, 40*(17), 3193-3208.

Zinatizadeh, A. A. L., Younesi, H., Bonakdari, H., Pirsaheb, M., Pazouki, M., Najafpour, G. D., & Hasnain Isa, M. (2009). Effects of process factors on biological activity of granular sludge grown in an UASFF bioreactor. *Renewable Energy, 34*(5), 1245-1251.

Zoutberg, G. R., & Eker, Z. (1999). Anaerobic treatment of potato processing wastewater. *Water Science and Technology, 40*(1), 297-304.

APPENDICS

Appendix A: Theoretical Data for C-curve

Q=271 mL/min **Ratio=2** **C-Curve 20/08/2007**

HRT =2 h **Co=0.820** $F=\exp^{-t/t}$

AFR=564 mL/min

Time (min)	S1 (ABS)	S2 (ABS)	S3 (ABS)	S4 (ABS)	Theoretical value1	F=C1/Co	F=C2/Co	F=C3/Co	F=C4/Co	Theoretical 2	Theoretical 3	Theoretical 4
0	0.82	0.014	0.017	0	1	1	0.017073	0.020732	0	0	0	0
5	0.681	0.094	0.01	0	0.846481725	0.830488	0.114634	0.012195	0	0.141080287	0.011756691	0.000653149
10	0.585	0.177	0.054	0.004	0.716531311	0.713415	0.215854	0.065854	0.004878	0.23884377	0.039807295	0.004423033
20	0.443	0.251	0.088	0.024	0.513417119	0.540244	0.306098	0.107317	0.029268	0.342278079	0.114092693	0.025353932
30	0.325	0.278	0.144	0.059	0.367879441	0.396341	0.339024	0.17561	0.071951	0.367879441	0.183939721	0.06131324
40	0.23	0.268	0.185	0.094	0.263597138	0.280488	0.326829	0.22561	0.114634	0.351462851	0.234308567	0.104137141
60	0.134	0.219	0.206	0.152	0.135335283	0.163415	0.267073	0.25122	0.185366	0.270670566	0.270670566	0.180447044
80	0.067	0.154	0.192	0.177	0.069483451	0.081707	0.187805	0.234146	0.215854	0.185289203	0.247052271	0.219602019
100	0.033	0.102	0.159	0.173	0.035673993	0.040244	0.12439	0.193902	0.210976	0.118913311	0.198188852	0.220209835
120	0.019	0.065	0.122	0.152	0.018315639	0.023171	0.079268	0.14878	0.185366	0.073262556	0.146525111	0.195366815
140	0.008	0.04	0.085	0.122	0.009403563	0.009756	0.04878	0.103659	0.14878	0.043883292	0.102394348	0.159280097
160	0.003	0.023	0.058	0.091	0.00482795	0.003659	0.028049	0.070732	0.110976	0.025749067	0.068664178	0.122069649
180	0	0.011	0.036	0.066	0.002478752	0	0.013415	0.043902	0.080488	0.014872513	0.044617539	0.089235078
200	0	0.007	0.023	0.045	0.001272634	0	0.008537	0.028049	0.054878	0.008484225	0.028280751	0.062846114
220	0	0.002	0.013	0.03	0.000653392	0	0.002439	0.015854	0.036585	0.004791541	0.017568984	0.042946406
240	0	0	0.008	0.019	0.000335463	0	0	0.009756	0.023171	0.002683701	0.010734804	0.028626144
260	0	0	0.004	0.012	0.000172232	0	0	0.004878	0.014634	0.00149268	0.006468278	0.018686137
280	0	0	0.002	0.007	8.8427E-05	0	0	0.002439	0.008537	0.000825319	0.003851487	0.011982403
300	0	0	0	0.001	4.53999E-05	0	0	0	0.00122	0.000453999	0.002269996	0.007566655

Appendix A (Continued)

Q=135 mL/min **Ratio=2** **C-Curve 22/08/2007**

HRT =4 h **Co=0.820**

AFR=270 mL/min 250-300 mL/min

Time (min)	S1 (ABS)	S2 (ABS)	S3 (ABS)	S4 (ABS)	Theoretical value	F=C1/Co	F=C2/Co	F=C3/Co	F=C4/Co	Theoretical 2	Theoretical 3	Theoretical 4
0	0.82	0	0	0	1	1	0	0	0	0	0	0
5	0.744	0.075	0.01	0.001	0.920044415	0.907317	0.091463	0.012195	0.00122	0.076670368	0.003194599	8.87389E-05
10	0.706	0.114	0.019	0.009	0.846481725	0.860976	0.139024	0.023171	0.010976	0.141080287	0.011756691	0.000653149
20	0.617	0.182	0.04	0.011	0.716531311	0.752439	0.221951	0.04878	0.013415	0.23884377	0.039807295	0.004423033
30	0.526	0.233	0.071	0.021	0.60653066	0.641463	0.284146	0.086585	0.02561	0.30326533	0.075816332	0.012636055
60	0.359	0.271	0.153	0.066	0.367879441	0.437805	0.330488	0.186585	0.080488	0.367879441	0.183939721	0.06131324
120	0.169	0.224	0.208	0.163	0.135335283	0.206098	0.273171	0.253659	0.19878	0.270670566	0.270670566	0.180447044
180	0.065	0.147	0.186	0.187	0.049787068	0.079268	0.179268	0.226829	0.228049	0.149361205	0.224041808	0.224041808
240	0.03	0.085	0.13	0.161	0.018315639	0.036585	0.103659	0.158537	0.196341	0.073262556	0.146525111	0.195366815
300	0.015	0.047	0.082	0.115	0.006737947	0.018293	0.057317	0.1	0.140244	0.033689735	0.084224337	0.140373896
360	0.012	0.027	0.056	0.075	0.002478752	0.014634	0.032927	0.068293	0.091463	0.014872513	0.044617539	0.089235078
420	0.006	0.016	0.03	0.047	0.000911882	0.007317	0.019512	0.036585	0.057317	0.006383174	0.022341108	0.052129252
480	0.006	0.01	0.018	0.028	0.000335463	0.007317	0.012195	0.021951	0.034146	0.002683701	0.010734804	0.028626144
540	0.005	0.008	0.01	0.018	0.00012341	0.006098	0.009756	0.012195	0.021951	0.001110688	0.004998097	0.014994291
600	0.005	0.006	0.007	0.01	4.53999E-05	0.006098	0.007317	0.008537	0.012195	0.000453999	0.002269996	0.007566655

Appendix A (Continued)

Q=68ml/min Ratio=2 C-Curve 24/08/2007
HRT =8h Co=0.820
AFR=135 mL/min 250-300 mL/min

Time (min)	S1 (ABS)	S2 (ABS)	S3 (ABS)	S4 (ABS)	Theoretical value	F=C1/Co	F=C2/Co	F=C3/Co	F=C4/Co	Theoretical 2	Theoretical 3	Theoretical 4
0	0.82	0	0	0	1	1	0	0	0	0	0	0
5	0.751	0.045	0.008	0.006	0.959189457	0.915854	0.054878	0.009756	0.007317	0.039966227	0.00083263	1.15643E-05
15	0.714	0.091	0.014	0.006	0.882496903	0.870732	0.110976	0.017073	0.007317	0.110312113	0.006894507	0.000287271
30	0.633	0.149	0.032	0.008	0.778800783	0.771951	0.181707	0.039024	0.009756	0.194700196	0.024337524	0.002028127
60	0.511	0.218	0.075	0.021	0.60653066	0.623171	0.265854	0.091463	0.02561	0.30326533	0.075816332	0.012636055
120	0.331	0.257	0.156	0.072	0.367879441	0.403659	0.313415	0.190244	0.087805	0.367879441	0.183939721	0.06131324
180	0.222	0.255	0.192	0.132	0.22313016	0.270732	0.310976	0.234146	0.160976	0.33469524	0.25102143	0.125510715
240	0.137	0.206	0.208	0.159	0.135335283	0.167073	0.25122	0.253659	0.193902	0.270670566	0.270670566	0.180447044
300	0.082	0.162	0.196	0.179	0.082084999	0.1	0.197561	0.239024	0.218293	0.205212497	0.256515621	0.213763017
360	0.052	0.125	0.171	0.18	0.049787068	0.063415	0.152439	0.208537	0.219512	0.149361205	0.224041808	0.224041808
420	0.034	0.093	0.144	0.168	0.030197383	0.041463	0.113415	0.17561	0.204878	0.105690842	0.184958973	0.215785469
480	0.018	0.064	0.114	0.149	0.018315639	0.021951	0.078049	0.139024	0.181707	0.073262556	0.146525111	0.195366815
540	0.014	0.05	0.094	0.129	0.011108997	0.017073	0.060976	0.114634	0.157317	0.049990484	0.11247859	0.168717885
600	0.008	0.035	0.075	0.106	0.006737947	0.009756	0.042683	0.091463	0.129268	0.033689735	0.084224337	0.140373896
660	0.005	0.025	0.056	0.085	0.004086771	0.006098	0.030488	0.068293	0.103659	0.022477243	0.061812418	0.113322766
720	0.003	0.018	0.042	0.067	0.002478752	0.003659	0.021951	0.05122	0.081707	0.014872513	0.044617539	0.089235078
780	0.002	0.013	0.032	0.052	0.001503439	0.002439	0.015854	0.039024	0.063415	0.009772355	0.031760153	0.068813665
840	0	0.009	0.023	0.04	0.000911882	0	0.010976	0.028049	0.04878	0.006383174	0.022341108	0.052129252
900	0	0.005	0.016	0.029	0.000553084	0	0.006098	0.019512	0.035366	0.004148133	0.015555498	0.038888745
960	0	0.003	0.012	0.023	0.000335463	0	0.003659	0.014634	0.028049	0.002683701	0.010734804	0.028626144
1020	0	0.002	0.009	0.016	0.000203468	0	0.002439	0.010976	0.019512	0.001729481	0.007350295	0.020825835
1080	0	0.001	0.007	0.012	0.00012341	0	0.00122	0.008537	0.014634	0.001110688	0.004998097	0.014994291
1160	0	0	0.003	0.007	6.33607E-05	0	0	0.003659	0.008537	0.000612487	0.002960353	0.009538915
1220	0	0	0.002	0.005	3.84302E-05	0	0	0.002439	0.006098	0.000390707	0.001986095	0.006730654

Appendix B: Theoretical Integrated Data for F-curve

Numerically Integrated value of C-Curve at 2 h HRT

Int Theore 1	Int Theore 2	Int Theore 3	Int Theore 4	Int Theore 1 divided by 30	Int Theore 2 divided by 30	Int Theore 3 divided by 30	Int Theore 4 divided by 30
0	0	0	0	0	0	0	0
4.616204312	0.352700719	0.029391727	0.001632874	0.153873477	0.011756691	0.000979724	5.44291E-05
8.523736901	1.302510863	0.158301691	0.014323329	0.284124563	0.043417029	0.005276723	0.000477444
14.67347905	4.208120111	0.927801631	0.163208152	0.489115968	0.14027067	0.030926721	0.005440272
19.07996185	7.758907713	2.4179637	0.596544012	0.635998728	0.258630257	0.08059879	0.0198848
22.23734475	11.35561917	4.509205139	1.423795918	0.741244825	0.378520639	0.150306838	0.047459864
26.22666896	17.57695335	9.558996476	4.269637771	0.874222299	0.585898445	0.318633216	0.142321259
28.2748563	22.13655104	14.73622485	8.270128401	0.94249521	0.737885035	0.491207495	0.275670947
29.32643075	25.17857619	19.18863608	12.66824694	0.977547692	0.839285873	0.639621203	0.422274898
29.86632707	27.10033485	22.63577571	16.82401345	0.995544236	0.903344495	0.754525857	0.560800448
30.14351909	28.27179333	25.1249703	20.37048256	1.00478397	0.942393111	0.83749901	0.679016085
30.28583421	28.96811691	26.83555555	23.18398002	1.009527807	0.965603897	0.894518518	0.772799334
30.35890123	29.37433271	27.96837272	25.29702729	1.011963374	0.979144424	0.932279091	0.843234243
30.39641509	29.6079001	28.69735563	26.81783921	1.013213836	0.986930003	0.956578521	0.893927974
30.41567535	29.74065776	29.15585298	27.87576441	1.013855845	0.991355259	0.971861766	0.929192147
30.4255639	29.81541018	29.43889087	28.59148992	1.014185463	0.993847006	0.981296362	0.953049664
30.43064085	29.85717399	29.61092169	29.06461272	1.014354695	0.995239133	0.987030723	0.968820424
30.43324744	29.88035397	29.71411933	29.37129812	1.014441581	0.996011799	0.990470644	0.979043271
30.43458571	29.89314715	29.77533416	29.5667887	1.01448619	0.996438238	0.992511139	0.985559623

Appendix B: Theoretical Integrated Data for F-curve (Continued)
Numerically Integrated Value of C-Curve at 4 h HRT

Int Theore 1	Int Theore 2	Int Theore 3	Int Theore 4	Int Theore 1 divided by 60	Int Theore 2 divided by 60	Int Theore 3 divided by 60	Int Theore 4 divided by 60
0	0	0	0	0	0	0	0
4.800111037	0.19167592	0.007986497	0.000221847	0.080001851	0.003194599	0.000133108	3.69745E-06
9.216426385	0.736052558	0.04536472	0.002076568	0.153607106	0.012267543	0.000756079	3.46095E-05
17.03149156	2.635672846	0.303184648	0.027457479	0.283858193	0.043927881	0.005053077	0.000457625
23.64680141	5.346218347	0.881302786	0.11275292	0.394113357	0.089103639	0.01468838	0.001879215
38.26295293	15.41338991	4.777643581	1.221992354	0.637715882	0.256889832	0.079627393	0.020366539
53.35939466	34.56989014	18.41595219	8.47480089	0.889323244	0.576164836	0.306932537	0.141246681
58.91306521	47.17084329	33.25732342	20.60946645	0.98188442	0.786180721	0.554288724	0.343491107
60.95614643	53.84955611	44.37433098	33.19172512	1.015935774	0.897492602	0.739572183	0.553195419
61.707754	57.05812483	51.29681444	43.26394644	1.028462567	0.950968747	0.854946907	0.721065774
61.98425498	58.51499227	55.16207074	50.15221567	1.033070916	0.975249871	0.919367846	0.835870261
62.085974	59.15266287	57.17083016	54.39314559	1.034766233	0.985877715	0.952847169	0.906552426
62.12339434	59.42466911	58.16310753	56.81580749	1.035389906	0.990411152	0.969385125	0.946930125
62.13716051	59.53850079	58.63509456	58.12442055	1.035619342	0.992308347	0.977251576	0.968740343
62.1422248	59.58544142	58.85313737	58.80124893	1.035703747	0.99309069	0.980885623	0.980020816

Appendix B: Theoretical Integrated Data for F-curve (Continued)
Numerically Integrated Value of C-Curve at 8 h HRT

Int Theore 1	Int Theore 2	Int Theore 3	Int Theore 4	Int Theore 1 divided by 120	Int Theore 2 divided by 120	Int Theore 3 divided by 120	Int Theore 4 divided by120
0	0	0	0	0	0	0	0
4.897973643	0.099915568	0.002081574	2.89108E-05	0.040816447	0.00083263	1.73465E-05	2.40923E-07
14.10640544	0.851307269	0.040717258	0.001523088	0.117553379	0.007094227	0.00033931	1.26924E-05
26.56613808	3.138899584	0.274957495	0.018888574	0.221384484	0.026157497	0.002291312	0.000157405
47.34610973	10.60838247	1.777265349	0.238851311	0.394550914	0.088403187	0.014810545	0.001990428
76.57841275	30.7427256	9.56994694	2.457330179	0.63815344	0.25618938	0.079749558	0.020477751
94.30870079	51.81996604	22.61878146	8.062048837	0.78590584	0.43183305	0.188489846	0.06718374
105.0626641	69.98094024	38.26954136	17.24078162	0.875522201	0.583174502	0.318912845	0.14367318
111.5852725	84.25743213	54.08512698	29.06708347	0.929877271	0.702145268	0.450709391	0.242225696
115.5414346	94.89464318	68.50184983	42.20122821	0.962845288	0.790788693	0.570848749	0.351676902
117.9409681	102.5462046	80.77187326	55.39604651	0.982841401	0.854551705	0.673098944	0.461633721
119.3963588	107.9148065	90.7163958	67.73061503	0.994969657	0.899290054	0.755969965	0.564421792
120.2790978	111.6123977	98.48650683	78.65315602	1.002325815	0.930103314	0.82072089	0.655442967
120.8145062	114.1228043	104.3875947	87.92590944	1.006787551	0.951023369	0.869896622	0.732715912
121.1392477	115.8078136	108.7686973	95.53680931	1.009493731	0.965065114	0.906405811	0.796140078
121.3362134	116.9283063	111.961596	101.6135447	1.011135112	0.974402553	0.9330133	0.846779539
121.4556792	117.6676524	114.2529268	106.3550069	1.01213066	0.98056377	0.952107723	0.886291725
121.5281388	118.1523182	115.8759646	109.9832945	1.01273449	0.984602652	0.965633039	0.916527454
121.5720878	118.4682574	117.0128628	112.7138344	1.013100731	0.987235478	0.97510719	0.939281953
121.5987442	118.6732124	117.8015719	114.739281	1.013322868	0.988943437	0.981679766	0.956160675
121.6149121	118.8056079	118.3441248	116.2228404	1.013457601	0.990046732	0.98620104	0.96852367
121.6247185	118.890813	118.7145766	117.2974442	1.013539321	0.990756775	0.989288138	0.977478702
121.6321893	118.95974	119.0329146	118.2787725	1.013601577	0.991331166	0.991940955	0.985656437
121.635243	118.9898358	119.181308	118.7668596	1.013627025	0.991581965	0.993177567	0.98972383

Appendix B-1: Experimental and Theoretical Data for F-curve

F-curve experiment (Step input Curve)----15/08/2007

HRT=2 h Q=271.4mL/min Co=0.553 AFR=564mL/min Ratio=2

Time (min)	Theroritical value	Stage1 (ABS)	Stage 2 (ABS)	Stage3 (ABS)	Stage4 (ABS)	F1=C/Co	F2=C/Co	F3=C/Co	F4=C/Co
0	0	0.038	0	0.002	0	0.068716094	0	0.003617	0
5	0.040811	0.06	0.011	0	0.003	0.108499096	0.019892	0	0.005425
10	0.079956	0.134	0.017	0.001	0	0.242314647	0.030741	0.001808	0
15	0.117503	0.197	0.04	0.006	0	0.356238698	0.072333	0.01085	0
20	0.153518	0.252	0.068	0.013	0	0.455696203	0.122966	0.023508	0
30	0.221199	0.323	0.129	0.035	0.007	0.584086799	0.233273	0.063291	0.012658
40	0.283469	0.388	0.21	0.07	0.022	0.701627486	0.379747	0.126582	0.039783
50	0.340759	0.433	0.256	0.123	0.049	0.783001808	0.462929	0.222423	0.088608
60	0.393469	0.465	0.312	0.165	0.079	0.840867993	0.564195	0.298373	0.142857
70	0.441965	0.491	0.359	0.211	0.118	0.887884268	0.649186	0.381555	0.213382
80	0.486583	0.507	0.396	0.255	0.152	0.91681736	0.716094	0.461121	0.274864
90	0.527633	0.518	0.431	0.306	0.192	0.936708861	0.779385	0.553345	0.347197
100	0.565402	0.528	0.457	0.341	0.232	0.954792043	0.826401	0.616637	0.41953
110	0.60015	0.534	0.476	0.371	0.271	0.965641953	0.860759	0.670886	0.490054
120	0.632121	0.538	0.493	0.401	0.315	0.972875226	0.891501	0.725136	0.56962
130	0.661535	0.543	0.508	0.429	0.341	0.981916817	0.918626	0.775769	0.616637
140	0.688597	0.545	0.517	0.45	0.371	0.985533454	0.934901	0.813743	0.670886
150	0.713495	0.545	0.523	0.468	0.407	0.985533454	0.94575	0.846293	0.735986
160	0.736403	0.547	0.53	0.484	0.423	0.98915009	0.958409	0.875226	0.764919
170	0.757479	0.547	0.534	0.496	0.443	0.98915009	0.965642	0.896926	0.801085
180	0.77687	0.549	0.538	0.514	0.466	0.992766727	0.972875	0.929476	0.842676
190	0.79471	0.551	0.541	0.515	0.479	0.996383363	0.9783	0.931284	0.866184
200	0.811124	0.544	0.544	0.522	0.494	0.983725136	0.983725	0.943942	0.893309
210	0.826226	0.552	0.546	0.532	0.505	0.998191682	0.987342	0.962025	0.913201
220	0.84012	0.553	0.553	0.38	0.517	1	1	0.687161	0.934901
230	0.852904	0.554	0.552	0.54	0.528	1.001808318	0.998192	0.976492	0.954792
240	0.864665	0.554	0.552	0.543	0.53	1.001808318	0.998192	0.981917	0.958409
260	0.885441	0.551	0.551	0.543	0.541	0.996383363	0.996383	0.981917	0.9783
280	0.903028	0.553	0.553	0.547	0.544	1	1	0.98915	0.983725
300	0.917915	0.555	0.556	0.551	0.549	1.003616637	1.005425	0.996383	0.992767

Appendix B-1: Theoretical data for F-curve (continued)

F-curve experiment (Step input Curve)----09/08/2007
HRT=4h, Q=135 mL/min Ratio=6 AFR=807mL/min Co=0.329

Time (min)	Theoretical Value	Stage1 (ABS)	Stage 2 (ABS)	Stage3 (ABS)	Stage4 (ABS)	F1=C/Co	F2=C/Co	F3=C/Co	F4=C/Co
0	0	0.001	0	0	0	0.003039514	0	0	0
5	0.020618	0.017	0.003	0.002	0.001	0.051671733	0.009119	0.006079	0.003125
10	0.040811	0.046	0.019	0.002	0.002	0.139817629	0.057751	0.006079	0.00625
20	0.079956	0.088	0.013	0.003	0.002	0.267477204	0.039514	0.009119	0.00625
30	0.117503	0.127	0.031	0.005	0.002	0.386018237	0.094225	0.015198	0.00625
40	0.153518	0.152	0.048	0.012	0.003	0.462006079	0.145897	0.036474	0.009375
50	0.188064	0.178	0.066	0.019	0.006	0.541033435	0.200608	0.057751	0.01875
60	0.221199	0.194	0.085	0.027	0.011	0.589665653	0.258359	0.082067	0.034375
70	0.252982	0.214	0.105	0.037	0.017	0.650455927	0.319149	0.112462	0.053125
80	0.283469	0.23	0.121	0.049	0.022	0.699088146	0.367781	0.148936	0.06875
100	0.340759	0.249	0.153	0.07	0.038	0.756838906	0.465046	0.212766	0.11875
120	0.393469	0.271	0.182	0.102	0.057	0.823708207	0.553191	0.31003	0.178125
140	0.441965	0.281	0.203	0.123	0.082	0.854103343	0.617021	0.37386	0.25625
160	0.486583	0.289	0.224	0.147	0.104	0.878419453	0.680851	0.446809	0.325
180	0.527633	0.298	0.246	0.169	0.127	0.905775076	0.74772	0.513678	0.396875
200	0.565402	0.303	0.257	0.188	0.148	0.920972644	0.781155	0.571429	0.4625
220	0.60015	0.306	0.27	0.205	0.168	0.930091185	0.820669	0.6231	0.525
240	0.632121	0.312	0.279	0.223	0.191	0.948328267	0.848024	0.677812	0.596875
260	0.661535	0.316	0.292	0.24	0.207	0.960486322	0.887538	0.729483	0.646875
280	0.688597	0.318	0.294	0.249	0.223	0.96656535	0.893617	0.756839	0.696875
300	0.713495	0.316	0.291	0.26	0.234	0.960486322	0.884498	0.790274	0.73125
320	0.736403	0.316	0.303	0.267	0.246	0.960486322	0.920973	0.81155	0.76875
340	0.757479	0.318	0.307	0.274	0.258	0.96656535	0.933131	0.832827	0.80625
360	0.77687	0.32	0.312	0.285	0.267	0.972644377	0.948328	0.866261	0.834375
380	0.79471	0.32	0.311	0.287	0.274	0.972644377	0.945289	0.87234	0.85625
400	0.811124	0.32	0.313	0.299	0.282	0.972644377	0.951368	0.908815	0.88125
420	0.826226	0.323	0.316	0.3	0.289	0.981762918	0.960486	0.911854	0.903125
440	0.84012	0.323	0.317	0.306	0.293	0.981762918	0.963526	0.930091	0.915625
460	0.852904	0.323	0.317	0.308	0.311	0.981762918	0.963526	0.93617	0.971875
560	0.903028	0.324	0.322	0.315	0.315	0.984802432	0.978723	0.957447	0.984375
580	0.910781	0.232	0.322	0.32	0.319	0.705167173	0.978723	0.972644	0.996875

F-curve experiment (Step input Curve)----13/08/2007									
HRT=8h			Co=0.439						
Q=68 mL/min		Ratio=11.86	AFR=807 mL/min						
Time (min)	Theoretical Value	Stage1 (ABS)	Stage 2 (ABS)	Stage3 (ABS)	Stage4 (ABS)	F=C1/Co	F=C2/Co	F=C3/Co	F=C4/Co
0	0	0.002	0.002	0.003	0.002	0.004555809	0.004556	0.006834	0.004556
5	0.010363	0.016	0.002	0.003	0.002	0.036446469	0.004556	0.006834	0.004556
10	0.020618	0.035	0.003	0.003	0.001	0.079726651	0.006834	0.006834	0.002278
20	0.040811	0.062	0.006	0.008	0.004	0.141230068	0.013667	0.018223	0.009112
30	0.060587	0.089	0.013	0.001	0	0.202733485	0.029613	0.002278	0
40	0.079956	0.113	0.02	0.002	0	0.257403189	0.045558	0.004556	0
60	0.117503	0.15	0.041	0.006	0	0.341685649	0.093394	0.013667	0
80	0.153518	0.189	0.064	0.014	0.003	0.430523918	0.145786	0.031891	0.006834
100	0.188064	0.219	0.09	0.025	0.007	0.498861048	0.205011	0.056948	0.015945
120	0.221199	0.244	0.118	0.036	0.013	0.555808656	0.268793	0.082005	0.029613
140	0.252982	0.268	0.14	0.05	0.02	0.61047836	0.318907	0.113895	0.045558
170	0.298242	0.295	0.173	0.077	0.035	0.671981777	0.394077	0.175399	0.079727
200	0.340759	0.32	0.201	0.096	0.054	0.728929385	0.457859	0.218679	0.123007
230	0.380701	0.338	0.23	0.124	0.074	0.769931663	0.523918	0.28246	0.168565
260	0.418222	0.352	0.255	0.149	0.097	0.801822323	0.580866	0.339408	0.220957
290	0.45347	0.367	0.279	0.174	0.119	0.835990888	0.635535	0.396355	0.271071
320	0.486583	0.373	0.303	0.197	0.14	0.849658314	0.690205	0.448747	0.318907
350	0.517689	0.381	0.301	0.227	0.163	0.867881549	0.685649	0.517084	0.371298
380	0.546911	0.385	0.325	0.248	0.188	0.876993166	0.740319	0.56492	0.428246
410	0.574362	0.391	0.339	0.265	0.208	0.890660592	0.77221	0.603645	0.473804
440	0.60015	0.393	0.353	0.282	0.227	0.895216401	0.8041	0.642369	0.517084
470	0.624376	0.4	0.364	0.295	0.248	0.911161731	0.829157	0.671982	0.56492
500	0.647134	0.4	0.372	0.309	0.262	0.911161731	0.84738	0.703872	0.596811
560	0.688597	0.411	0.385	0.331	0.295	0.936218679	0.876993	0.753986	0.671982
590	0.707464	0.419	0.405	0.357	0.327	0.954441913	0.922551	0.813212	0.744875
620	0.725188	0.423	0.415	0.372	0.351	0.963553531	0.94533	0.84738	0.799544
650	0.741838	0.427	0.418	0.385	0.368	0.972665148	0.952164	0.876993	0.838269
680	0.757479	0.428	0.423	0.399	0.383	0.974943052	0.963554	0.908884	0.872437
710	0.772173	0.429	0.423	0.419	0.392	0.977220957	0.963554	0.954442	0.892938

Appendix C: Oxygen Mass transfer Coefficient Data

1- Oxygen mass transfer Experiments 6/09/2007
Q=1.0178 L/h = 17 mL/min AFR=250 mL/min=15 L/h
HRT=8h AFR/WFR=14.7
Cs20=8.6 mg/L
C influent=1.1 mg/L,,, Cat 1st stage=1.1 mg/L

Time (sec)	$t-t_o$ (h)	C= DO mg/L	C_s -Co	C_s -C	$(C_s - Co)/(C_s - C)$	$\ln(C_s-Co)/(C_s-C)$
20	0	1.5	7.1	7.1	1	0
40	0.005556	1.7	7.1	6.9	1.028985507	0.028573372
60	0.011111	1.8	7.1	6.8	1.044117647	0.043172172
80	0.016667	2	7.1	6.6	1.075757576	0.073025135
100	0.022222	2.3	7.1	6.3	1.126984127	0.119545151
120	0.027778	2.4	7.1	6.2	1.14516129	0.135545492
140	0.033333	2.6	7.1	6	1.183333333	0.168335315
160	0.038889	2.7	7.1	5.9	1.203389831	0.185142433
180	0.044444	2.8	7.1	5.8	1.224137931	0.202236866
200	0.05	3	7.1	5.6	1.267857143	0.237328186
220	0.055556	3.1	7.1	5.5	1.290909091	0.255346692
240	0.061111	3.2	7.1	5.4	1.314814815	0.27369583
260	0.066667	3.4	7.1	5.2	1.365384615	0.311436158
280	0.072222	3.5	7.1	5.1	1.392156863	0.330854244
300	0.077778	3.6	7.1	5	1.42	0.350656872

(Continued)

2- Oxygen Mass Transfer Experiments **6/09/2007**

Q=1.0178 L/h = 17 mL/min **AFR=807mL/min=48.2l/h**

HRT=8h **AFR/WFR=47.5**

Cs20=8.6 mg/L

C influent=2.1 mg/L,,, Cat 1st stage=1.4 mg/L

Time (sec)	$t-t_o$ (h)	C= DO mg/L	C_s -Co	C_s -C	$(C_s - Co)/(C_s - C)$	$\ln(C_s - Co)/(C_s - C)$
20	0	2	6.6	6.6	1	0
40	0.005556	2.3	6.6	6.3	1.047619048	0.046520016
60	0.011111	2.7	6.6	5.9	1.118644068	0.112117298
80	0.016667	3.2	6.6	5.4	1.222222222	0.200670695
100	0.022222	3.4	6.6	5.2	1.269230769	0.238411023
120	0.027778	3.8	6.6	4.8	1.375	0.318453731
140	0.033333	4	6.6	4.6	1.434782609	0.361013346
160	0.038889	4.4	6.6	4.2	1.571428571	0.451985124
180	0.044444	4.6	6.6	4	1.65	0.500775288
200	0.05	5	6.6	3.6	1.833333333	0.606135804
220	0.055556	5.2	6.6	3.4	1.941176471	0.663294217
240	0.061111	5.4	6.6	3.2	2.0625	0.723918839
260	0.066667	5.7	6.6	2.9	2.275862069	0.822358912
280	0.072222	5.8	6.6	2.8	2.357142857	0.857450232
300	0.077778	6.1	6.6	2.5	2.64	0.970778917

(Continued)

3- Oxygen Mass Transfer Experiments		6/09/2007				
Q=1.0178 L/hr = 17 mL/min		AFR=1.576 L/min=94.5 l/h				
HRT=8h	AFR/WFR=93					
Cs20=8.6 mg/L						
C influent=2 mg/L, „ C	at 1st stage=1.2 mg/L					
Time (sec)	**t-t_o (h)**	**C= DO mg/L**	**C_s -Co**	**C_s -C**	**(C_s -Co)/(C_s -C)**	**ln(C_s -Co)/(C_s -C)**
20	0	2.5	6.1	6.1	1	0
40	0.005556	2.9	6.1	5.7	1.070175439	0.067822596
60	0.011111	3.5	6.1	5.1	1.196078431	0.179048231
80	0.016667	4.1	6.1	4.5	1.355555556	0.304211374
100	0.022222	4.5	6.1	4.1	1.487804878	0.397301797
120	0.027778	5	6.1	3.6	1.694444444	0.527354926
140	0.033333	5.4	6.1	3.2	1.90625	0.645137961
160	0.038889	5.8	6.1	2.8	2.178571429	0.778669354
180	0.044444	6	6.1	2.6	2.346153846	0.852777326
200	0.05	6.3	6.1	2.3	2.652173913	0.975379648
220	0.055556	6.6	6.1	2	3.05	1.115141591
240	0.061111	6.7	6.1	1.9	3.210526316	1.166434885
260	0.066667	6.9	6.1	1.7	3.588235294	1.27766052
280	0.072222	7.1	6.1	1.5	4.066666667	1.402823663
300	0.077778	7.3	6.1	1.3	4.692307692	1.545924507

(Continued)

4- Oxygen Mass Transfer Experiments **6/09/2007**
Q=1.0178 L/h = 17 mL/min **AFR=2.374 L/min=142.4 L/h**
HRT=8h **AFR/WFR=139.9**
Cs20=8.6 mg/L
C influent=2.5 mg/L,,, C at 1st stage=1.2 mg/L

Time (min)	$t-t_o$ (h)	C= DO mg/L	C_s -Co	C_s -C	$(C_s - Co)/(C_s - C)$	$\ln(C_s - Co)/(C_s - C)$
20	0	2.3	6.3	6.3	1	0
40	0.005556	3.3	6.3	5.3	1.188679245	0.172842813
60	0.011111	4.1	6.3	4.5	1.4	0.336472237
80	0.016667	4.7	6.3	3.9	1.615384615	0.47957308
100	0.022222	5.3	6.3	3.3	1.909090909	0.646627165
120	0.027778	5.7	6.3	2.9	2.172413793	0.775838896
140	0.033333	6.1	6.3	2.5	2.52	0.924258902
160	0.038889	6.4	6.3	2.2	2.863636364	1.052092273
180	0.044444	6.8	6.3	1.8	3.5	1.252762968
200	0.05	7.1	6.3	1.5	4.2	1.435084525
220	0.055556	7.2	6.3	1.4	4.5	1.504077397
240	0.061111	7.3	6.3	1.3	4.846153846	1.578185369
260	0.066667	7.5	6.3	1.1	5.727272727	1.745239454
280	0.072222	7.7	6.3	0.9	7	1.945910149
300	0.077778	7.7	6.3	0.9	7	1.945910149

(Continued)

5- Oxygen Mass Transfer Experiments **6/09/2007**

Q=1.0178 L/h = 17 mL/min **AFR=3.176 L/min=190.5 l/h**

HRT=8 h **AFR/WFR=187.2**

Cs20=9.09 mg/L

C influent=2.5 mg/L, C at 1st stage= 1.5 mg/L

Time (min)	$t-t_o$ (h)	C= DO mg/L	C_s -Co	C_s -C	$(C_s - Co)/(C_s - C)$	$\ln(C_s - Co)/(C_s - C)$
20	0	3.1	5.5	5.5	1	0
40	0.005556	4	5.5	4.6	1.195652174	0.178691789
60	0.011111	4.8	5.5	3.8	1.447368421	0.369747026
80	0.016667	5.4	5.5	3.2	1.71875	0.541597282
100	0.022222	6	5.5	2.6	2.115384615	0.749236647
120	0.027778	6.5	5.5	2.1	2.619047619	0.962810748
140	0.033333	6.9	5.5	1.7	3.235294118	1.174119841
160	0.038889	7.1	5.5	1.5	3.666666667	1.299282984
180	0.044444	7.3	5.5	1.3	4.230769231	1.442383828
200	0.05	7.5	5.5	1.1	5	1.609437912
220	0.055556	7.7	5.5	0.9	6.111111111	1.810108608
240	0.061111	7.8	5.5	0.8	6.875	1.927891644
260	0.066667	7.8	5.5	0.8	6.875	1.927891644
280	0.072222	8	5.5	0.6	9.166666667	2.215573716
300	0.077778	8.1	5.5	0.5	11	2.397895273

(Continued)

6- Oxygen mass transfer Experiments 6/09/2007

Q=1.0178l/h = 17 mL/min AFR=3.997 L/min=239.8 l/h

HRT=8h AFR/WFR=235.6

Cs20=9.08 mg/L

C influent=2.3 mg/L,- C at 1st stage=1 mg/L

Time (min)	$t-t_o$ (h)	C= DO mg/L	C_s -Co	C_s -C	$(C_s$ -Co)/(C_s-C)	ln(C_s -Co)/(C_s -C)
20	0	3.1	5.5	5.5	1	0
40	0.005556	4.2	5.5	4.4	1.25	0.223143551
60	0.011111	5.2	5.5	3.4	1.617647059	0.480972661
80	0.016667	6	5.5	2.6	2.115384615	0.749236647
100	0.022222	6.6	5.5	2	2.75	1.011600912
120	0.027778	7.1	5.5	1.5	3.666666667	1.299282984
140	0.033333	7.3	5.5	1.3	4.230769231	1.442383828
160	0.038889	7.6	5.5	1	5.5	1.704748092
180	0.044444	7.8	5.5	0.8	6.875	1.927891644
200	0.05	8	5.5	0.6	9.166666667	2.215573716
220	0.055556	8.1	5.5	0.5	11	2.397895273
240	0.061111	8.2	5.5	0.4	13.75	2.621038824
260	0.066667	8.2	5.5	0.4	13.75	2.621038824
280	0.072222	8.2	5.5	0.4	13.75	2.621038824
300	0.077778	8.3	5.5	0.3	18.33333333	2.908720897